



Netherlands Enterprise Agency

Wind Resource Assessment

Hollandse Kust (west) Wind Farm Zone

Update February 2022

*>> Sustainable. Agricultural. Innovative.
International.*





RVO Approval for Publication

Document Characteristics

Version	Title	Date of Publication	Reference Contractor	Reference RVO
Update	Wind Resource Assessment Hollandse Kust (west) Wind Farm Zone	December 13 th , 2021	Tractebel Engie	WOZ2190166

Approval

Approval for public disclosure	Position
Joep Bronkhorst	Project Coordinator RVO Offshore Wind Energy
Peter-Paul Lebbink	Senior Advisor RVO Offshore Wind Energy

HOLLANDSE KUST (WEST) WIND FARM ZONE

Certification Report

Site Conditions Wind

Netherlands Enterprise Agency

Report No.: CR-SC-DNVGL-SE-0190-05500-1_Wind

Date: 2022-02-15



Project name: Hollandse Kust (west) Wind Farm Zone
 Report title: Certification Report
 Site Conditions Wind
 Customer: Netherlands Enterprise Agency,
 Croeselaan 15
 3521 BJ Utrecht The Netherlands
 Customer contact: Hygen van Steen (RVO)
 Date of issue: 2022-02-15
 Project No.: 10151362
 Report No.: CR-SC-DNVGL-SE-0190-05500-1_Wind
 Applicable contract(s) governing the provision of this Report:

Objective: To confirm that the wind speed at Hollandse Kust (west) Wind Farm Zone has been derived in line with the requirements as stated in section 2.3.2 of the DNVGL-SE-0190:2020 for site conditions. The wind speeds are to be used for design for Hollandse Kust (west) Wind Farm Zone.

Prepared by:	Verified by:	Approved by:
Hunt, Helena Jane 2022.02.15 15:25:37 +01'00'	Simón-Donaire, José 2022.02.15 19:15:49 +01'00'	Redanz, Pia Digitally signed by Redanz, Pia Date: 2022.02.16 09:24:53 +01'00'
Helena Hunt Principal Engineer	José Simón-Donaire Senior Engineer	Pia Redanz Project Sponsor, Head of Section

Copyright © DNV 2022. All rights reserved. Unless otherwise agreed in writing: (i) This publication or parts thereof may not be copied, reproduced or transmitted in any form, or by any means, whether digitally or otherwise; (ii) The content of this publication shall be kept confidential by the customer; (iii) No third party may rely on its contents; and (iv) DNV undertakes no duty of care toward any third party. Reference to part of this publication which may lead to misinterpretation is prohibited.

DNV Distribution:

- OPEN. Unrestricted distribution, internal and external.
- INTERNAL use only. Internal DNV document.
- CONFIDENTIAL. Distribution within DNV according to applicable contract.*
- SECRET. Authorized access only.

Keywords:

HKW Site Conditions Wind

*Specify distribution: DNV Renewables Certification

Rev. No.	Date	Reason for Issue	Prepared by	Verified by	Approved by
0	2020-11-25	First issue	IPL	HEHU	PR
1	2022-02-15	Update for 24 months data campaign	HEHU	JSIMON	PR



Table of contents

1	EXECUTIVE SUMMARY.....	1
2	CERTIFICATION SCHEME	1
3	SCOPE OF EVALUATION.....	1
4	CONDITIONS.....	1
5	OUTSTANDING ISSUES.....	1
6	CONCLUSION	1

Appendix A Wind Resource Assessment

1 EXECUTIVE SUMMARY

The Hollandse Kust (west) Wind Farm Zone is located in the Dutch Sector of the North Sea, approximately 51 km from the coastline. As part of the tender preparations, the Netherlands Enterprise Agency (Rijksdienst voor Ondernemend Nederland, RVO) has requested a wind resource assessment of the Hollandse Kust (west) Wind Farm Zone.

DNV was assigned to validate this wind study and its use within a Design Basis for Offshore Wind Turbine Structures in accordance with DNVGL-ST-0437 and DNVGL-ST-0126.

2 CERTIFICATION SCHEME

Document No.	Title
DNVGL-SE-0190:2020-09	Project certification of wind power plants

3 SCOPE OF EVALUATION

The scope and interface of the evaluation covered by the report is the wind assessment part of the site conditions assessment of the rotor-nacelle assembly, tower, substructure, foundation, topside and support structure and array power cable.

The Appendix to this report comprises the detailed DNV evaluation which include references to standards, list of documentation and the conclusion of the DNV evaluation.

4 CONDITIONS

No conditions have been identified.

5 OUTSTANDING ISSUES

No outstanding issues have been identified.

6 CONCLUSION

DNV finds that the wind properties as defined in the documents listed in section A4 are derived in line with the requirements following section 2.3.2 of the DNVGL-SE-0190 and the basis for the evaluation listed in Section A3 for establishing site assessment.

The properties estimated are:

- Annual average wind speed (at 100 m MSL): 9.74 m/s
- Wind roses
- Wind distributions:
 - Weibull A-parameter (at 100 m MSL): 11.00 m/s
 - Weibull k-parameter (at 100 m MSL): 2.30

APPENDIX A

Wind Resource Assessment

Evaluation of Wind Resource Assessment for Hollandse Kust (west) Wind Farm Zone

A1 Description of verified component, system or item

Within the Wind Farm Zone the wind conditions have been estimated. The resulting site conditions are documented by the customer and build the basis for the verification described in the current report.

A2 Interface to other systems/components:

No interfaces to other systems/components are present.

A3 Basis for the evaluation

Applied codes and standards:

Document No.	Revision	Title
DNVGL-ST-0437	2016-11	Loads and site conditions for wind turbines
IEC 61400-3	2009-02	Wind Turbines – Part 3: Design requirements for offshore wind turbines

A4 Documentation from customer

List of reports:

Document No.	Revision	Title
/1/ HKWWRA/4NT/0704127/000/03	03 2021-12-13	Site Studies Wind Farm Zone Hollandse Kust Wind Resource Assessment (West)
/2/	V03_D	HKW_20200807_TracTebel_DeliverablesAsTables_V03_D.xlsx

List of reports taken for information only:

Document No.	Revision	Title
/A/ Proj. ID: 11822658	Final 0.6 Dated 2021-05-31	MetOcean Study and database for Dutch Wind Farm Zones Hollandse Kust (west)

A5 Evaluation Work

/1/ presents the wind resource assessment for the planned Hollandse Kust (west) Offshore Wind Farm Zone. The assessment has been based on combined use of offshore wind measurements and mesoscale model data. The main outcome of /1/: The long-term mean wind speed at a hub height of 100 m MSL at the center of the zone has been determined to be 9.74 ± 0.31 m/s (\pm standard deviation) based on 24 months of measurements covering 05/02/2019 – 11/02/2021. The variation in the wind speed as predicted by Tractebel within the zone when evaluated against the mesoscale model DOWA was found to be about ± 0.01 m/s.

A wake analysis has been undertaken which is not part of the certification of this report. However, the report /1/ concludes that the stated losses are uncertain, and that the inclusion of wake loss is left open to the designers. DNV agree to this conclusion.

The wind speed was measured in an on-site floating LiDAR campaign initially with three independent lidars HKW A, HKW B and HKW C at measurement heights of 30, 40, 60, 80, 100, 120, 140, 160, 180, 200 and 250 m MSL. The data from the period 11/02/2019-10/02/2020 was initially used in the assessment. The data campaign was extended to a total of 24 months with the addition of a fourth on-site floating LiDAR measurement point HKWA-2 at measurement heights of 30, 40, 60, 80, 100, 120, 140, 160, 180, 200 and 250 m MSL covering the period 09/05/2020 – 11/02/2021.

The on-site measurements are supported by the following other Dutch North Sea offshore wind measurements taken at

- Europlatform met mast and LiDAR
- Lichteiland Goeree (LEG) met mast and LiDAR
- Offshore Wind Farm Egmond aan Zee (OWEZ) met mast
- K13 lidar
- Met mast IJmuiden (MMIJ)
- Floating LiDAR at HKZ Wind Farm Zone
- Floating LiDAR at HKN Wind Farm Zone

In /1/ data from three different reanalysis datasets

- ERA5 reanalysis data
- MERRA2 reanalysis data
- CFSv2 reanalysis data (extended CFSR data)

have been compared with the measurements.

It was found that ERA5 was the best data source and therefore chosen to be used as long-term reference data source for the MCP routine.

For the horizontal extrapolation, data from five different mesoscale models

- KNW mesoscale data
- DOWA mesoscale data
- NEWA mesoscale data
- 3TIER-ERA5
- EMD-WRF-ERA5

have been compared with the measurements.

It was found that DOWA was the best data source and therefore chosen to be used for the horizontal extrapolation at the site.

DNV has reviewed

- Measurements
- Long-term correction
- Horizontal extrapolation

The results of the wind climate calculation including

- Air temperature
- Air pressure
- Relative humidity
- Air density Correction
- Time Series presented in /2/

and has found the documentation to be correct.

Furthermore, DNV has compared the wind speeds presented in /1/ with in-house knowledge about the ‘Design’ and ‘Measured Wind’ on existing Belgian and Dutch offshore wind farms and has found that 9.74 m/s long-term mean wind speed including ± 0.31 m/s (\pm standard deviation) can be agreed on.

The wind speeds are to be used for design of future the Hollandse Kust (west) offshore wind farm.

It has been checked that the ‘wind distribution and wind roses’ used in the metocean desk study presented in /A/ are aligned.

A6 Conditions to be considered in other certification phases

No conditions have been identified.

A7 Outstanding issues

There are no outstanding issues.

A8 Conclusion

DNV finds that the wind properties as defined in the documents listed in section A4 are derived in line with the requirements following section 2.3.2 of the DNVGL-SE-0190 and the basis for the evaluation listed in Section A3 for establishing site assessment.

The properties estimated are:

- Annual average wind speed (at 100 m MSL): 9.74 m/s
- Wind roses
- Wind distributions:
 - Weibull A-parameter (at 100 m MSL): 11.00 m/s
 - Weibull k-parameter (at 100 m MSL): 2.30



About DNV

DNV is the independent expert in risk management and assurance, operating in more than 100 countries. Through its broad experience and deep expertise DNV advances safety and sustainable performance, sets industry benchmarks, and inspires and invents solutions.

Whether assessing a new ship design, optimizing the performance of a wind farm, analyzing sensor data from a gas pipeline or certifying a food company's supply chain, DNV enables its customers and their stakeholders to make critical decisions with confidence.

Driven by its purpose, to safeguard life, property, and the environment, DNV helps tackle the challenges and global transformations facing its customers and the world today and is a trusted voice for many of the world's most successful and forward-thinking companies.

TRACTEBEL ENGINEERING S.A.
 boulevard Simon Bolivar 34-36
 1000 - Bruxelles - Belgium

engineering@tractebel.engie.com
 tractebel-engie.com

TECHNICAL DOCUMENT

Our ref.: **HKWWRA/4NT/0704127/000/03**

TS:

Imputation: P.014997/0004

RESTRICTED

Client:

Project: **WRA - Hollandse Kust West wind farm Zone**

Subject: Site Studies Hollandse Kust: Wind Resource Assessment Wind Farm Zone Hollandse Kust (west)

Comments:

Keywords: Layout, Offshore wind power, Renewable energy, Wind, Wind farm, Wind measurement, Wind power, Wind resource, Wind shear

03	2021 12 13	PRL	*J. Heinen *C. Abiven	*C. Abiven *J. Vermeir	*J. Vermeir	*C. Abiven
02	2021 11 15	PRL	J. Heinen C. Abiven	C. Abiven	J. Vermeir	C. Abiven
REV.	YY/MM/DD	STAT.	WRITTEN	VERIFIED	APPROVED	VALIDATED

* This document is completely signed on 2021 12 13.

TRACTEBEL ENGINEERING S.A. - Registered office: Boulevard Simón Bolívar 34-36, 1000 Brussels - BELGIUM
 VAT: BE 0412 639 681 - RPM/RPR Brussels: 0412 639 681 - Bank account IBAN: BE74375100843707 - BIC/SWIFT: BBRUBEBB

HOLLANDSE KUST (WEST) WIND FARM ZONE – THE NETHERLANDS – RVO

Wind Resource Assessment

GLOSSARY.....	7
1. EXECUTIVE SUMMARY.....	9
2. SAMENVATTING.....	11
3. INTRODUCTION	13
3.1. Offshore Wind in the Dutch North Sea	13
3.2. Assessment of the Wind Resource at the Hollandse Kust (west) Wind Farm Zone	13
3.3. Hollandse Kust (west)1.....	15
3.4. Structure of the Report.....	16
3.5. Differences with the 12 months report	16
4. ON-SITE WIND MEASUREMENTS	17
4.1. On-site Wind Measurements Locations.....	17
4.2. Measurement Equipment	18
4.3. Data Evaluation.....	21
4.3.1. Data Quality Assessment and Filtering.....	21
4.3.2. HKW Main Data Source.....	26
4.3.3. Data Substitution	32
4.3.4. Data Availability after Filtering and Substitution.....	32
4.3.5. HKW reference measurement location.....	33
4.4. Measured Data.....	34
4.4.1. Measured Wind Speed	34
4.4.2. Weibull Distribution.....	34
4.4.3. Measured Wind Direction.....	36
4.4.4. Measured Wind Shear	37
4.4.5. Diurnal and Monthly Profiles	38
4.4.6. Environmental Measurements.....	39

5. OTHER WIND DATA	41
5.1. Wind Measurements.....	41
5.1.1. HKN Floating LiDARs	42
5.1.2. HKZ Floating LiDARs.....	42
5.1.3. IJmuiden met mast	43
5.1.4. Offshore Wind Farm Egmond aan Zee (OWEZ) Met Mast.....	44
5.1.5. Lichteiland Goeree (LEG)	46
5.1.6. Europlatform (EPL).....	47
5.1.7. K13	48
5.2. Wind Flow Models	49
5.2.1. Reanalysis datasets.....	49
5.2.2. Mesoscale datasets.....	50
6. WIND CLIMATE ASSESSMENT	54
6.1. Main Source Selection.....	54
6.1.1. Methodology	54
6.1.2. Results	57
6.2. Vertical Extrapolation	57
6.2.1. Wind Shear Calculation	58
6.2.2. Short Term Wind Climates at 100 m MSL	59
6.3. Long-Term Correction	60
6.3.1. Long-term evaluation	60
6.3.2. Long-Term Wind Climate	65
6.4. Horizontal Extrapolation.....	69
6.4.1. Mesoscale Model Selection	69
6.4.2. Extrapolation to nodes	72
6.5. Uncertainty Assessment	75
7. WIND FARM ZONE WIND CLIMATE	77
7.1. Wind Climate.....	77
7.1.1. Wind Speed.....	77
7.1.2. Weibull Distribution.....	78
7.1.3. Wind Direction.....	80
7.1.4. Wind Shear	81
7.1.5. Diurnal and Monthly Profiles	82
7.2. Stability Conditions	84
7.2.1. Stability classification.....	84
7.2.2. Link with shear values	86

7.3.	Comparison with other Sources	87
7.3.1.	Alignment with MetOcean Desk Study	88
7.3.2.	Previous Studies.....	88
7.3.3.	Wind Atlases	90
7.3.4.	Conclusion	93
8.	WAKE ASSESSMENT	94
8.1.	Preliminary Turbine Layouts.....	94
8.2.	Wake Modelling	95
8.2.1.	Industry-standard wake modelling.....	95
8.2.2.	Three-layer model	97
8.2.3.	Combined wake losses	99
9.	CONCLUSIONS.....	100
10.	REFERENCES	101
11.	APPENDICES.....	105
HKW.....	134	
MMIJ	136	
OWEZ	138	
Dataset.....	158	
Analysis.....	161	
Conclusions.....	169	
1. Introduction.....	176	
2. Methodology	176	
3. Results	178	
4. Conclusions	183	
5. References	184	

GLOSSARY

AEP	: Annual Energy Production
DOWA	: Dutch Offshore Wind Atlas
ECN	: Energy Research Centre of Netherlands
EPL	: Europlatform
FLS	: Floating Lidar System
HKN	: Hollandse Kust (noord)
HKW	: Hollandse Kust (west)
HKZ	: Hollandse Kust (zuid)
HKWWFZ	: Hollandse Kust (west) Wind Farm Zone
KNMI	: Koninklijk Nederlands Meteorologisch Instituut
KNW	: KNMI North sea Wind atlas
KPI	: Key Performance Indicator
KUL	: KU Leuven
LAT	: Lowest Astronomical Tide
LEG	: Lichteiland Goeree
LIDAR	: Light Detection And Ranging
LTC	: Long-term Correction
MCP	: Measure Correlate Predict
MMIJ	: IJmuiden Offshore Met Mast
MSL	: Mean Sea Level
OWEZ	: Offshore Wind Farm Egmond aan Zee
RSD	: Remote Sensing Device (e.g. LIDAR or SODAR)
RVO	: Netherlands Enterprise Agency ("Rijksdienst voor Ondernemend Nederland")
SWLB	: Seawatch Wind LiDAR Buoy
TLM	: Three-layer model
TNO	: Netherlands Organisation for Applied Scientific Research
VKI	: von Karman Institute
WAsP	: Wind Atlas analysis and application Program

WFSD : Wind Farm Site Decision
WFS : Wind Farm Sites
WFZ : Wind Farm Zones
WRA : Wind Resource Assessment
WRG : Wind Resource Grid
WTG : Wind Turbine Generator

1. EXECUTIVE SUMMARY

Tractebel was assigned by RVO to carry out an independent assessment of the wind resources at the Hollandse Kust (west) Wind Farm Zone (HKWWFZ). This study makes part of a more broad metocean study in which the waves, current and wind climate within the Wind Farm Zone (WFZ) are assessed. The aim of both studies is to align on the estimated wind resources at 6 pre-defined site nodes, which enables wind farm developers to prepare their bid and evaluate the yield and load assessments as well as business case calculations. The present report produced by Tractebel is intended for wind farm modelling, yield assessment and business case calculation. On the other side, the metocean report by DHI described the normal and extreme wind conditions. This includes wind speed turbulence intensity, extreme wind speeds and wind shear, all of which are intended for wind farm design.

In the context of this assignment, RVO has contracted FUGRO to install, monitor and eventually decommission 3 SEAWATCH LIDAR Buoys, at four different measurement locations across the Wind Farm Zone (WFZ). The on-site measurement campaign was started in February 2019 and the current report includes an analysis of 24 months of data. Differences with a previous report based on 12 months of data are detailed in the present report. In order to avoid a seasonal bias in the estimated wind resources, those data have been long-term corrected with ERA-5 reanalysis data using a Measure-Correlate-Predict approach based on Neural Networks.

As several high quality measurement campaigns were performed in the Dutch North Sea, and to lower the overall uncertainties of the assessed wind climate, these on-site measurements have been merged with two other wind data sets. In this analysis, the met mast campaigns of IJmuiden and Offshore Wind farm Egmond aan Zee (OWEZ) have been selected as they result in the lowest overall uncertainty. These short-term measurements have been corrected to the long-term in the same way as the on-site measurements described above.

To merge those measurements with the on-site measured data, and to allow horizontal extrapolation of the resulting wind climate throughout the Wind Farm Zone (WFZ), a suitable mesoscale data set was selected. An extensive validation process, backed up by the expertise of the von Karman Institute, has pointed the Dutch Offshore Wind Atlas (DOWA) as the most suitable data set.

To give more weight to high quality data and data closer to the HKWWFZ, time-series resulting from the three selected measurement sources (Hkw buoys, OWEZ and IJmuiden met masts) were weighted based on the inverse of the uncertainty of each individual data set. The accuracy of the resulting wind climate was confirmed by the alignment with the independent metocean desk study, leading to an alignment within 0.1 m/s at 6 pre-defined locations (nodes). Finally, an overall evaluation of the uncertainties associated with the resulting wind climate has been performed.

The resulting long-term wind speed at the HKWWFZ centre (which is close to the three buoy locations) has been estimated to be **9.74 +/- 0.31 m/s at 100 m MSL**.

Based on this wind climate, a wake assessment study has been performed considering latest (theoretical derived) offshore wind turbine models in the >10 MW class. To ensure the latest evolutions in wake modelling are taken into account in the wake assessment, an industry best practice approach (including the impact of variating stability conditions) has been benchmarked against a state-of-the-art “3-layer” model developed at the KU Leuven (KUL). This latest model enables the evaluation of self-induced AEP loss due to blockage and long distance cluster wake effects. From all the tested models, an ensemble model has been created which lead to an expected wake loss of 18.6 and 18.4 % for respectively a wind farm layout considering 10 MW and 13 MW wind turbines. While these figures suggest that wake effects should be a subject of attention, they are associated with a large uncertainty and it is recommended for users of this document to satisfy themselves of the influence of neighbouring farms.

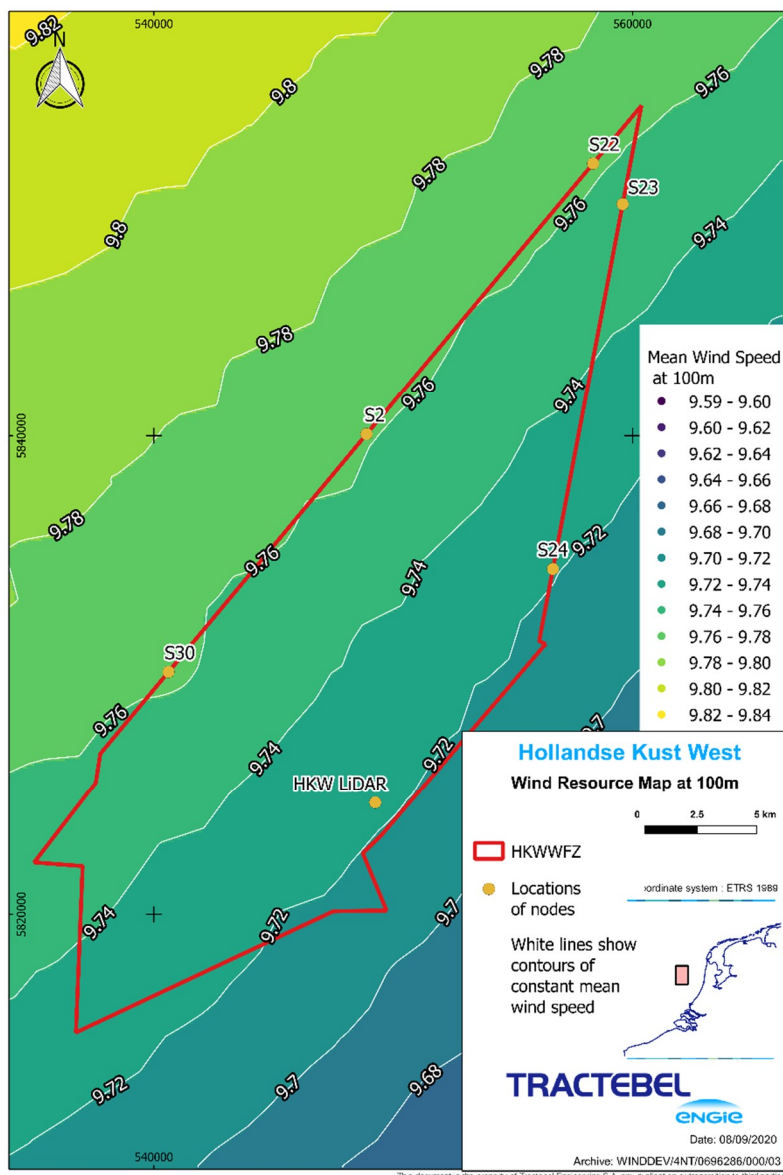


Figure 1: Wind Resource map of HKWWFZ at 100 m. Coordinates are in UTM31N, ETRS89

2. SAMENVATTING

In opdracht van RVO heeft Tractebel het windklimaat in het windenergiegebied Hollandse Kust (west) bestudeerd. Deze studie maakt deel uit van een bredere metocean studie waarin zowel de golf-, stromings- alsook de windcondities binnen het windenergiegebied eerst worden gemeten en nadien worden geanalyseerd. Het doel van beide studies is om het ingeschatte windklimaat op zes overeengekomen locaties te aligneren met elkaar. Zodoende hebben projectontwikkelaars voldoende informatie om een financiële analyse uit te voeren met bijhorende belastings- en productieberekeningen en op die manier hun bod, om het windpark te bouwen, voor te bereiden. Terwijl deze studie voornamelijk zal gebruikt worden voor zowel het modelleren van het windturbinepark, productie inschattingen als een financiële analyse, zal de metocean studie op zijn beurt eerder gebruikt worden voor de evaluatie van de normale en extreme windcondities. Deze condities worden dan gebruikt voor het effectieve ontwerp van het windturbinepark.

In deze context heeft RVO, Fugro aangesteld om drie drijvende LIDAR's te installeren, monitoren en uiteindelijk te ontmantelen op vier locaties in het windenergiegebied. Deze metingen zijn gestart in Februari 2019 en de huidige studie omvat een analyse van de data over een periode van 24 maanden. Dit rapport detailleert de verschillen met de vorige versie die gebaseerd was op 12 maanden data. Om een mogelijk deviatie in het ingeschatte windklimaat, als gevolg van seizoensvariatie te voorkomen, zijn de metingen gecorrigeerd naar een langere termijn op basis van ERA5 data. Hiervoor is een zogenaamde MCP procedure gebruikt.

Aangezien er kwalitatieve data van verschillende meetcampagnes beschikbaar zijn en om ook de totale onzekerheid van de studie te verlagen, zijn de lokale windmetingen gecombineerd met twee andere wind datasets. In deze analyse zijn meetmast data van IJmuiden en Offshore Windpark Egmond aan Zee (OWEZ) geselecteerd op basis van hun lage onzekerheid. Net zoals bij de lokale windmetingen zijn deze korte termijn datasets nadien gecorrigeerd naar een langere termijn op basis van de Neuraal netwerk MCP methode en ERA5 data.

Om deze metingen te combineren en ook het ingeschatte windklimaat horizontaal te extrapoleren door het windenergiegebied heen, is een geschikte model nodig die de horizontale gradiënt tussen land en zee weergeeft. Het Dutch Offshore Wind Atlas (DOWA) model is geselecteerd op basis van een validatieproces dat gemeten en gemodelleerde data op verschillende locaties in het Nederlandse deel van de Noordzee vergelijkt. Dit validatieproces is samen met het Von Karman Instituut ontwikkeld.

Meetcampagnes die dichtbij het windenergiegebied Hollandse Kust (west) zijn uitgevoerd en waarvoor kwalitatieve data is verzameld, hebben in de combinatie van de verschillende datasets een zwaarder gewicht gekregen. Deze combinatie is dan ook gebaseerd op de inverse van de onzekerheid. De nauwkeurigheid van dit resulterende windklimaat is nadien eveneens bevestigd op basis van een vergelijking met de onafhankelijk uitgevoerde metocean studie. Deze vergelijking resulteerde in een beperkte afwijking van 0.1 m/s tussen beide ingeschatte windklimaten op de zes overeengekomen locaties. Tenslotte, is er een onzekerheidsanalyse uitgevoerd die de algemene onzekerheid op dit ingeschatte windklimaat heeft bepaald.

Het resulterend windklimaat in het windenergiegebied Hollandse Kust (west) is ingeschat op **9.74 +/- 0.31 m/s** op **100 m MSL**.

Op basis van dit windklimaat is eveneens een studie uitgevoerd naar de mogelijke zogeffecten van het windpark. Hiervoor is gebruik gemaakt van (theoretische) windturbine modellen met een vermogen hoger dan 10 MW. Om er voor te zorgen dat de laatste evoluties in het modelleren van zogeffecten werden meegenomen, is gebruik gemaakt van de expertise van KU Leuven (KUL). De resultaten van het "3-layer" model ontwikkeld door KUL zijn vergeleken met de resultaten van meer conventionele industrie modellen. Het voordeel van het "3-layer" model is dat het toelaat om zowel de zogeffecten van de windturbineparken op grote afstand te bepalen als ook de zelf-geïnduceerde blokkering van de wind stromen langsheel en doorheen het park. Deze verschillende modellen zijn nadien gecombineerd en de zogeffecten bedragen 18.6 en 18.4 % voor respectievelijk een scenario met 10 MW en 13 MW wind turbine modellen. De inschatting van de zogeffecten zijn louter toegevoegd ter illustratie om aandacht te vestigen op de invloed van de naburig gelegen windturbine parken en zijn geassocieerd met een hoge onzekerheid.

3. INTRODUCTION

3.1. Offshore Wind in the Dutch North Sea

The Dutch North Sea plays a significant role in achieving its national contribution towards a global sustainable development of energy supply. Therefore, the Dutch government has set out ambitious roadmaps to further develop offshore wind energy in the Dutch North Sea. The initial target was set based on the Energy Agreement for Sustainable Development (developed in 2013) and aimed to construct a wind farm capacity of 4.45 GW by 2023 (1). To follow this roadmap, the Ministry of Economic Affairs and Climate Policy has designated three areas for the construction of (offshore) wind farms: Borssele, Hollandse Kust (zuid) and Hollandse Kust (Noord). This roadmap was further extended in the Offshore Wind Energy Roadmap 2030 for the development of 7 GW of additional offshore wind capacity during the 2024-2030 period (2). To support this extension, three additional areas were designated: Hollandse Kust (west), IJmuiden Ver and Ten noorden van de Waddeneilanden.

The Netherlands Enterprise Agency (RVO) is the agency operating under the Ministry of Economic Affairs and Climate Policy which coordinates site investigations within these designated areas. These site investigations, described in the so-called Wind Farm Site Decision (WFSD), identify the Wind Farm Site within the designated area that enables a suitable construction of the (offshore) wind farm. Each of these areas are divided into several tenders for which wind farm developers are allowed to bid. The winning bid then obtains a permit to construct the (offshore) wind farm and is allowed to apply for an SDE+ (3) (Stimulation of Sustainable Energy Production) grant if required. In order to lower the risks for wind farm developers RVO provides all relevant site data to allow bidders to properly prepare their bid. This includes the provision of an independent assessment of the wind resource at the Wind Farm Zone which is the subject of the current report.

3.2. Assessment of the Wind Resource at the Hollandse Kust (west) Wind Farm Zone

In line with the Offshore Wind Energy Roadmap 2030, The Netherlands Enterprise Agency (RVO) has been requested to prepare site data required for wind farm developers to prepare a competitive bid for a permit to build a wind farm within the Hollandse Kust (west) Wind Farm Zone (HKWWFZ). This includes an independent assessment of the wind resource at the HKWWFZ. This information is to be used as an input for wind farm modelling, yield assessments and business case calculations for the (offshore) wind farm to be developed within the HKWWFZ.

To support this assessment, RVO has deployed three metocean buoys with LiDAR devices at the HKWWFZ. The metocean campaign lasted 24 months, from February 2019 until February 2021. Besides this specific metocean campaign additional wind measurement sources are available in the area to support the assessment (e.g. metocean campaigns at Borssele, Hollandse Kust (noord) and Hollandse Kust (zuid) as well as other data sources).

In order to analyse the data from the measurement campaign and to perform the independent assessment, RVO has awarded Tractebel the assignment of the following tasks:

- The detailed analysis of available wind measurement data;
- The evaluation and selection of appropriate wind flow model(s) and measurement stations for horizontal and long-term extrapolations;
- The prediction of the long-term wind climate across the site;
- The estimation of the uncertainty associated with the predicted wind climate;
- The alignment of the predicted wind resource with the metocean desk study (awarded to DHI) at 6 specific locations (nodes) within the HKWWFZ; and
- The evaluation of potential wake effects within the wind farm and from existing and future neighbouring wind farms.

For this assignment, Tractebel leads a collaboration of industry and research partners with the von Karman Institute (VKI) and KUL. This allows to couple the strengths of Tractebel in Project Management and state-of-the-art offshore wind resource assessments with the strengths of research institutes with world-renowned expertise in the field of wind flow models.

In the current framework, Tractebel is the leading party and the expertise of research partners is specifically used on two aspects of the assessment:

- Expert advice on the selection and validation of the available mesoscale models by the team of Professor Jeroen Van Beeck from the von Karman Institute (VKI) (Head of Environmental and Applied Fluid Dynamics Department); and
- State-of-the-art wake modelling approach (as defined in 8.2.2) to evaluate self-induced Annual Energy Production (AEP) loss due to blockage and long-distance cluster wake effects by the team of Professor Johan Meyers from KUL.

The expertise of our partner research institutes is highlighted in the report wherever it was used.

3.3. Hollandse Kust (west)

The Hollandse Kust (west) Wind Farm Zone (HKWWFZ) (4) is situated approximately 60 km off the Dutch coast and located in the Dutch shelf of the North Sea, where several wind farms have already been constructed or are under development. A detailed list of these wind farms and of related wind turbines can be found in **Annex A**.

As for previous Wind Farm Zones, RVO has provided the coordinates of the Wind Farm Sites (WFS) which will be designated to accommodate an installed wind capacity of 1.4 GW. The Hollandse Kust (west) Wind Farm Zone and Hollandse Kust (west) Wind Farm Site are presented in Figure 2.

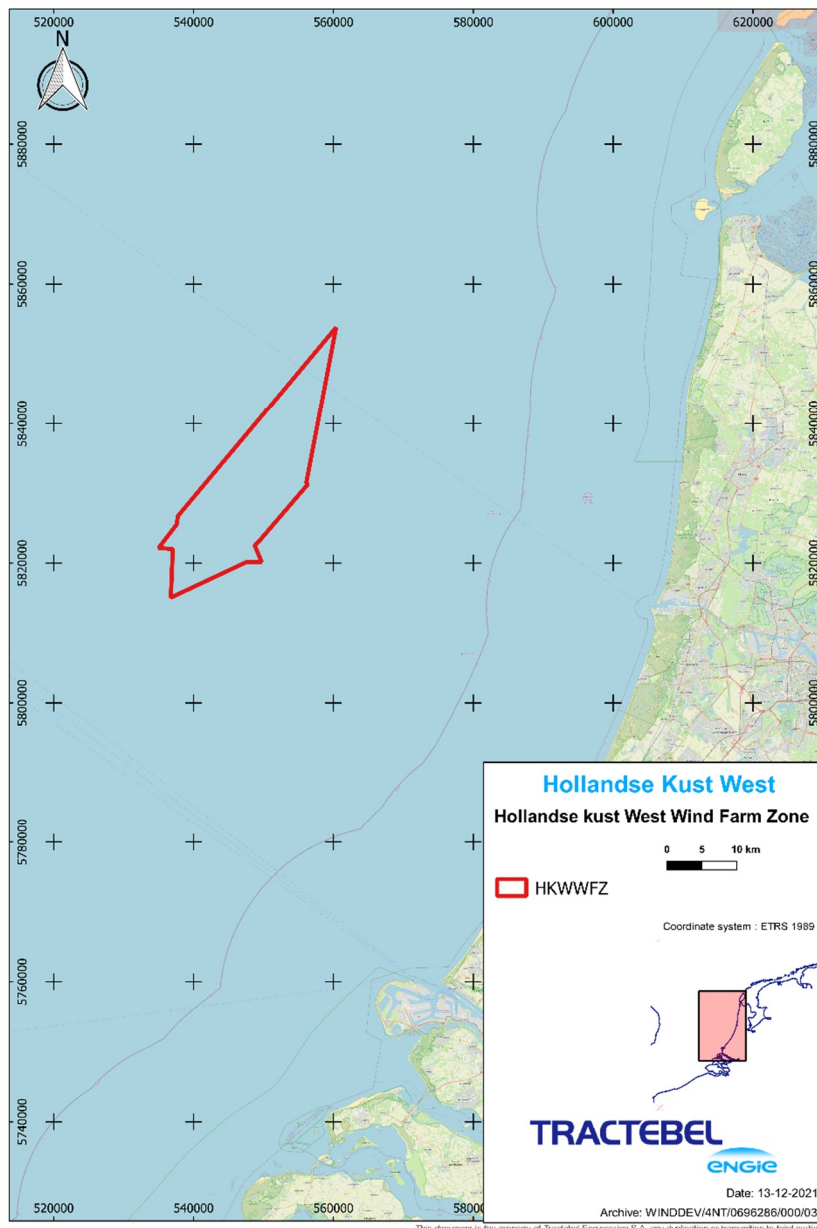


Figure 2: Location of the HKWWFZ (red polygon) and of the HKW WFS (black polygon within the HKWWFZ). Coordinates are in UTM31N, ETRS89

3.4. Structure of the Report

This report is divided in 9 sections. The following paragraphs give an overview of the structure and the content of each sections.

Section 4 of this report presents the analysis of the on-site measurements at the HKWWFZ performed by the FUGRO SEAWATCH Lidar buoys.

Section 5 provides an overview of all available wind data in the vicinity of the HKWWFZ including measured and modelled data (reanalysis and mesoscale data).

Section 6 details the combination of data sets used to generate the predicted wind climate, vertical and horizontal extrapolation and associated uncertainties.

Section 7 describes the combination of several datasets used to lower uncertainties and the resulting wind climate and associated uncertainties, as well as the outcomes of the alignment with the metocean desk study.

Section 8 describes the methodology used to assess wake losses in the Wind Farm Zone combining the expertise of Tractebel and KUL.

Section 9 provides the conclusions of this assessment.

3.5. Differences with the 12 months report

This report makes use of 24 months of data. A previous report (5) made use of 12 months of data. The sections which were subject to the most important modifications are listed below:

- Executive summary (Section 1)
- Samenvatting (Section 2)
- Differences with the 12 months report (Section 3.5)
- On-site wind measurements (Section 4)
- Wind climate assessment (Section 6)
- Wind farm zone wind climate (Section 7)
- Conclusions (Section 9)
- References
- Annexes B to J in the Appendix

4. ON-SITE WIND MEASUREMENTS

In the context of the development of wind farm projects in the Dutch shelf of the North Sea RVO contracted Fugro to perform a metocean measurement campaign. Part of this assignment consisted in measuring the wind resource at the Wind Farm Zone by means of a ZX Lidar mounted on top of dedicated buoys. Several buoys were deployed on four locations close to one another, alternatively and in parallel. The results and configuration of these measurements are described in the following sections.

4.1. On-site Wind Measurements Locations

On-site wind measurements locations are illustrated by Figure 3 below; note that in reality buoys are free to float around their mooring point within a radius of 110 m. Information about wind measurements is provided in Table 1.

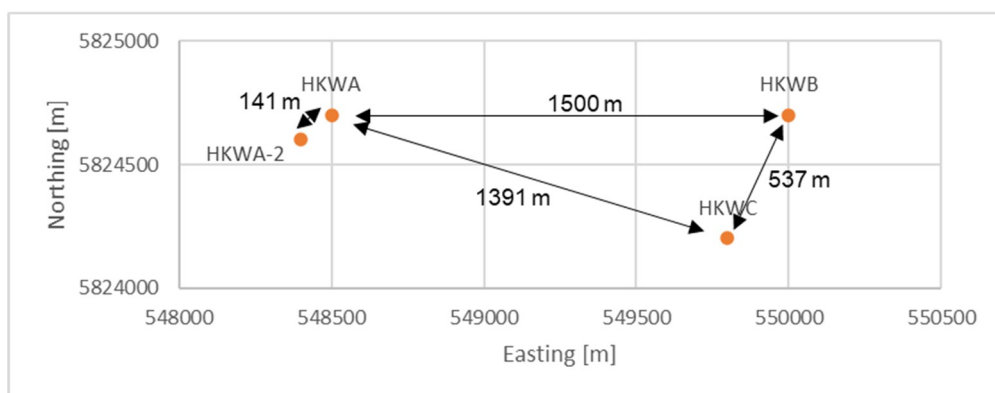


Figure 3: Illustration of the locations of HKWA, HKWA-2, HKWB and HKWC measurement locations (orange dots). Coordinates are in UTM31N, ETRS89

TABLE 1: WIND MEASUREMENTS CONFIGURATION

Wind measurements	Locations [EPSG 25831]		Measurement period	Measurement heights	
-	Easting [m]	Northing [m]	-	Wind speed [m] MSL	Wind direction [m] MSL
HKWA	548 500	5 824 700	05/02/2019 – 24/04/2020		
HKWA-2	548 400	5 824 600	09/05/2020 – 11/02/2021		
HKWB	550 000	5 824 700	10/02/2019 – 11/02/2021	4 ¹ , 30, 40, 60, 80, 100, 120, 140, 160, 180, 200, 250	
HKWC	549 799	5 824 202	01/08/2019 – 07/02/2020		

4.2. Measurement Equipment

During the measurement campaign Fugro used three different Seawatch Wind LiDAR Buoys (SWLBs), the basic shape and principle of which are illustrated by Figure 4. For the purpose of this assessment, SWLBs can be viewed as floating buoys based on the original Seawatch Wavescan buoy on top of which are mounted a marinized version of the ZX 300 LiDAR, a Gill Windsonic M acoustic wind sensor as well as Vaisala pressure, temperature and humidity sensors. Table 3 provides some details about these instruments. Additional details about instrument configuration can be found in Fugro's report (6).

Fugro's SWLBs are considered by DNV GL to be in the pre-commercial stage according to the Carbon Trust's requirements (7), after a 6 months trial involving comparisons with the IJmuiden met mast data (8). Additionally, the performance of two of these SWLBs, WS187 and WS188, was verified by DNV GL before their installation on site. These verifications were performed against a ground based LiDAR located on the island of Frøya in Norway and resulted in an excellent performance of both devices in terms of wind speed and wind direction. The results of these tests were summarized in specific reports (9), (10) and were used in Section 6.5 in order to assess the uncertainty of the devices. It is important to note that buoy WS170, as opposed to the other buoys, was not validated against a fixed based LiDAR prior to installation on site but was verified in-situ against buoy WS188 (11). This resulted in an excellent performance as well. Moreover, WS170 was validated after the measurements against a fixed LiDAR at LEG, passing wind speed and direction best practice criteria for heights up to 200 m (12).

The 3 SWLBs were deployed and rotated between locations as indicated on the timeline of

¹ Measured by the ultrasonic Wind Sensor

Table 2 with the aim of having 2 SWLBs active at all times in order to minimize chances for data loss.

The LiDARs were set to measure at heights of 30, 40, 60, 80, 100, 120, 140, 160, 180, 200 and 250 m using a frequency of 1 Hz. Wind direction measurements from the LiDAR could be shifted by 180°, a well-known limitation of continuous wave LiDARs to identify the exact orientation of the wind vector. Indeed, the device is able to sense the magnitude, but not the sign of the Doppler shift which leads to a 180° uncertainty on measured wind direction (13), (14). The Gill sensor was used as a reference for the LiDAR in order to resolve this ambiguity. However note that when wind direction measured at the ground differs significantly from measured wind direction aloft, directions outputted by the device can still be shifted by 180° as discussed in Section 4.3.1. On SWLB WS188 the Gill sensor was mounted with an offset of 9°, which was corrected for. Similarly, the Gill sensor was mounted with a 8° offset on WS170 in 2020.

Buoy reference direction (compass and DGPS) as well as wind direction from the Gill sensor were stored at a frequency of 1 Hz and were combined with LiDAR data before the calculation of 10-min averages, which were stored in the on-board memory system. The data was sent via satellite to allow for near real-time performance checks, before being downloaded manually whenever a buoy was serviced. Data originating from manual downloads was used here in order to circumvent any data loss due to potential transmission issues.

The data of each buoy have been processed and filtered by Fugro and were delivered as “ready to use” datasets. Indeed, processing from raw 1 Hz data to 10 min averages, corrections with respect to direction and tilting of the buoy were performed by Fugro and are not part of the scope of this study.

Deltares was subcontracted by Fugro to perform an independent validation (15) of the data performing consistency checks and validation against various existing sources (measurements in the vicinity of the HKWWFZ, as well as model data). The report highlighted high correlations in terms of wind speeds and directions between concurrent deployments. A few issues in resolving the 180° ambiguity were noted. The report concluded that the accuracy of wind speed and directional data was high and suitable for wind resource assessment.

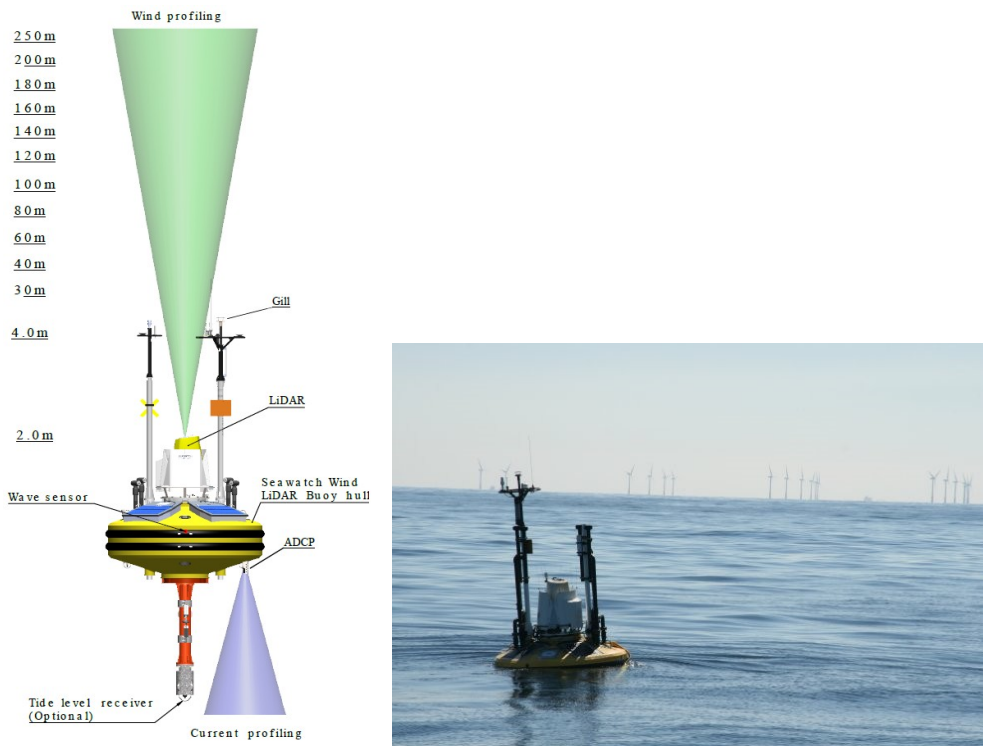


Figure 4: Left: Illustration of the SWLB from Fugro's data provision report (6). Right: Illustration of the type of Lidar deployed at the HKZ, HKN and HKW sites, from RVO (7)

TABLE 2: BUOY DEPLOYMENT PER LOCATION. GREEN, BLUE AND ORANGE COLOURS ARE USED TO DENOTE WS187, WS188 AND WS170 BUOYS, RESPECTIVELY

	02/19	03/19	04/19	05/19	06/19	07/19	08/19	09/19	10/19	11/19	12/19	01/20	02/20
HKWA	05/Feb			WS187				21/Sep	WS188	24/Nov		WS187	
HKWA-2													
HKWB	10/Feb			WS188				19/Sep					
HKWC					16/Jun		WS170			24/Nov	18/Dec	WS188	07/Feb
(continued)	03/20	04/20	05/20	06/20	07/20	08/20	09/20	10/20	11/20	12/20	01/21	02/21	
HKWA		24/Apr											
HKWA-2			09/May		WS187			06/Nov		WS188		11/Feb	
HKWB			24/Apr		WS188		15/Sep	WS170	14/Nov		26/Nov	WS170	11/Feb
HKWC					WS187 : 14/Nov - 23/Nov								

TABLE 3: BUOY EQUIPMENT

Buoy Id	LiDAR	Ultrasonic	Air Pressure	Air Temperature & Pressure	Comments
WS187	ZX818M, Firmware 2.2020	Gill Windsonic 18320062	Vaisala PTB N5230736	Vaisala HMP P1730335	Primary buoy for HKWA location. Validated against Frøya, certified by DNV- GL
WS188	ZX802M, Firmware 2.2020	Gill Windsonic 18320035	Vaisala PTB N5230739	Vaisala HMP P1730334	Primary buoy for HKWB location. Validated against Frøya, certified by DNV- GL
WS170	ZP585M, Firmware 2.2020	Gill Windsonic 18320033	Vaisala PTB M5220804	Vaisala HMP P4050602 2018	Spare buoy for HKW project. In-situ verified against WS188 and WS187, validation certified by DNV GL. Post- validated against LEG, certified by DNV-GL

4.3. Data Evaluation

4.3.1. Data Quality Assessment and Filtering

The main focus of the data analysis was on LiDAR data. The ultrasonic measurements were solely used (together with a set of reanalysis data) to correct/adapt the wind direction measurements of the LiDAR that could be shifted by 180°. This issue is solved by relying on a wind vane located next to the device. When wind direction measured at the ground differs significantly from measured wind direction aloft directions outputted by the device can be shifted by 180°. Wherever possible 180° shifts were corrected for based on ERA5 re-analysis data. Fortunately such instances mostly coincides with low wind speed events. For the remainder of the assessment, the results of the ultrasonic anemometer measurements will not be presented.

The data of each buoy have been processed and filtered by Fugro and were delivered as “ready to use” datasets. However, an additional quality assessment of the measured data has been carried out according to standard practice (16). Erroneous data were rejected from the analysis. A brief overview of the filtering procedures is summarized below:

- Low availability in the number of packets;
- Suspicious data such as freezes (data continuously fixed on one specific value) and unphysical peaks; and
- Outliers in wind speed and direction between different heights.

A first indication of the quality of the data is data availability which is presented in Table 4 and Table 5. In these tables, data is considered available when both wind speed and wind direction are available. The figures are given as a percentage of availability with respect to full months, potentially leading to low availability values when the deployment of a buoy does not occur at the beginning of the month for example. While measurements at location HKWA (together with A-2) span the complete measurement period, data availability is significantly higher at locations HKWB and HKWC from February to November 2019. These differences in availability are discussed for each location in the following sections. It should be noted that during the two weeks period ranging from the 24/04/2020 until the 09/05/2020 wind direction data is unavailable while wind speed data is available and usable.

TABLE 4: AVAILABILITY PER LOCATION, BEFORE FILTERING. THE COLOURS IN THE TABLE GIVE AN INDICATION OF THE QUALITY OF THE DATA WITH RESPECT TO AVAILABILITY: BELOW 50 % THE COLOUR IS RED, FROM 50 TO 80 % THE COLOUR GRADUALLY CHANGES FROM RED TO ORANGE, AND ABOVE 80 % THE COLOUR CHANGES GRADUALLY FROM ORANGE TO GREEN.

	2019												2020		
	Feb	Mar	Apr	May	Jun	Jul	Aug	Sep	Oct	Nov	Dec	Jan			
HKWA @100 m	84.7	82.5	91.1	78.2	84.3	82.7	84.3	88.2	94.3	22.6	99	97.2			
HKWA-2 @100 m															
HKWB @100 m	98.4	95.4	94.8	91.3	91.5	92.1	50.9	6.2							
HKWC @100 m							99.4	98.6	99.3	72.3	40.7	3			
	2020												2021		
	Feb	Mar	Apr	May	Jun	Jul	Aug	Sep	Oct	Nov	Dec	Jan	Feb	Average	
HKWA @100 m	99.7	99.3	98.8												85.8
HKWA-2 @100 m				99.8	95.9	99.9	97.2	97.1	99.9	90.3	85.8	93.5	92		95.1
HKWB @100 m				72.3	95.8	99.9	97.8	99.5	99.9	87.5	98	86.9	73.3		85.1
HKWC @100 m	0														59
Colour thresholds	0	50	60	70	80	90	100								

TABLE 5: AVAILABILITY PER LOCATION, AFTER FILTERING

	2019												2020
	Feb	Mar	Apr	May	Jun	Jul	Aug	Sep	Oct	Nov	Dec	Jan	
HKWA @100 m	74.5	74.2	83.8	72.1	72.8	74.5	76	83.2	89.8	21	92	86.2	
HKWA-2 @100 m													
HKWB @100 m	89.5	87.9	88	83.8	81.4	84.3	44.3	5.8					
HKWC @100 m							96.2	94.7	94.9	69.4	38.8	2.2	
	2020												2021
	Feb	Mar	Apr	May	Jun	Jul	Aug	Sep	Oct	Nov	Dec	Jan	Average
HKWA @100 m	96.6	94.4	95.7										79
HKWA-2 @100 m				98.5	91.8	97.3	92.3	92.6	96.8	88.2	78.9	86.3	78.7
HKWB @100 m				71.8	93	98.3	93.2	96.4	98.1	85.1	90.9	76.9	64.5
HKWC @100 m	0												56.6
Colour thresholds	0	50	60	70	80	90	100						

4.3.1.1. HKWA

At location HKWA, two different buoys were deployed: WS187 was first deployed on site, before being replaced by WS188; WS187 was subsequently deployed on site a second time. Both buoys had been previously validated against a fixed/land based industry accepted LiDAR by DNV GL (9) (10).

The provided documentation (validation reports (9) (10), LiDAR validation reports (17) (18), installation reports and maintenance reports) is satisfactory.

Several gaps were observed in the data. The longest gaps are mentioned hereunder:

- from the 15/02/2019 until the 16/02/2019;
- from the 20/05/2019 until the 22/05/2019;
- from the 28/07/2019 until the 29/07/2019; and
- from the 02/11/2019 until the 23/11/2019.

These main gaps represent a data loss of approximately 7 % over the total period of measurement.

In their report (6), Fugro lists the following issues during the first deployment of the buoy at HKWA, from February to September 2019: DGPS malfunction “affecting transmitted LiDAR wind direction” and a met station on the LiDAR not working resulting in missing data (ca. 1.4 %). It is also specified that after this deployment the LiDAR was sent back to the manufacturer for power regulator replacement.

The measurement duration at this location is 14 months and 20 days. The overall availability for wind speed and direction measurements at HKWA is of 78.8 % at 100 m MSL after filtering. Several months (February, March, May to August and November – all in 2019) show an availability below 80 %. Therefore, the measurements of HKWA alone do not strictly fulfil the Carbon Trust’s criteria for Stage 2 Floating LiDARs which require a monthly availability of 80 % or more and 85 % overall availability (16). However, these criteria will be fulfilled through the use of a combination of HKWA, HKWA-2, HKWB and HKWC, as shown in paragraph 4.3.4.

4.3.1.2. [HKWA-2](#)

At location HKWA-2, two different buoys were deployed: WS187 followed by WS188. As for HKWA, both LiDARs and buoys were validated against fixed Lidar data as presented in various reports (9), (10), (17) and (18).

The provided documentation is the same as for HKWA and is deemed satisfactory.

Some minor gaps were observed during the first deployment, from May to October 2020. They were not listed in this report but can be found in (19).

In November and December, several short gaps were found, explaining the slightly lower availability before filtering compared to other months. Fugro mentions communication issues between the LiDAR unit of buoys WS188 and the datalogger in their report (19).

The overall measurement duration at this location is of 9 months. The overall availability for wind speed and direction measurements at HKWA-2 is of 90.0 % at 100 m MSL after filtering. The months of December 2020 and February 2021 show an availability below 80 %. Apart from these months, the criterion of a monthly data availability of 80 % or more is fulfilled (20). The 9 months of measurements of HKWA-2 fulfil the Carbon Trust’s criterion for Stage 2 for floating LiDARs which requires an overall availability of 85 % or more. By using a combination of the HKWA, HKWA-2, HKWB and HKWC datasets, a period of 24 months of measurements fulfilling the Carbon Trust’s criteria (20) is obtained, as shown in paragraph 4.3.4.

4.3.1.3. [HKWB](#)

For location HKWB, all three buoys (WS170, 187 and 188) were used. As mentioned above in 4.3.1.1, WS187 and 188 were validated against a fixed/land based LiDAR and certified by DNV GL. Unlike the two other buoys, WS170 was not validated against a fixed/land based Lidar prior to on-site installation but was verified in-situ against buoy WS188 (11). The buoy had been validated against a land-based LiDAR in 2017 (21), however this validation is deemed to be outdated. Both validation reports mentioned hereabove have been certified by DNV GL.

For WS187 and WS188, the same documentation as for HKWA was provided and is deemed satisfactory. The provided documentation for WS170 (in-situ validation report (11), LiDAR validation report (22), installation reports and maintenance reports) is satisfactory.

Several gaps were observed in the data, the most important ones are listed below:

- from the 12th of August 2019 until the demobilisation of the buoy on the 19th of September;
- from the 24/04/2020 until the 9/05/2020;
- from the 23/11/2020 until the 26/11/2020; and
- several short gaps throughout January 2021.

These gaps lead a data loss of approximately 10 % compared to the total measurement time.

In their reports (19), (6), Fugro mention an issue with power starting in August and September 2019 and leading to a drop in LiDAR data. Additionally, the buoy deployed in April 2020 was not transmitting data and had to be restarted on the 9th of May. On the 23rd of November 2020, the buoy located at HKWB drifted away from its position. The measurement duration at this location can be split into two: 7.3 months before the 19th of September 2019; and 9.6 months after the 24th of April 2020. The overall availability for wind speed and direction measurements at HKWB is of 80.3 % at 100 m MSL after filtering. The months of August and September 2019 as well as April-May 2020 and January-February 2021 show an availability below 80 %. The measurements of HKWB alone do not strictly fulfil Carbon Trust's criterion for Stage 2 Floating LiDARs which require an overall availability of 85 % or more, mainly because of low availability during the months of August and September. However, this criterion will be fulfilled through the use of a combination of HKWA, HKWA-2, HKWB and HKWC, as shown in paragraph 4.3.4. Apart from the months mentioned above, the criterion of a monthly availability of 80 % or more is fulfilled (20).

4.3.1.4. HKWC

For location HKWC two buoys were used: WS170 and WS188. The documentation and validation for these buoys have been discussed above in 4.3.1.1 and 4.3.1.3.

Several gaps were observed in the data:

- from the 23/11/2019 until the 18/12/2019; and
- from the 01/01/2020 until the 07/02/2020.

These gaps lead to a data loss of approximately 33 % compared to the total measurement time.

In their reports (6), (19), Fugro mention a faulty power cable within the LiDAR leading to missing data after the 23/11/2019, a corrupted disk resulting in missing data from the 01/01/2020, and the loosening of keel weight leading to the unit drifting out of position from the 07/02/2020.

The measurement duration at this location is of 5.7 months. The overall availability for wind speed and direction measurements at HKWC is of 63.4 % at 100 m MSL after filtering. The months of November until February show an availability below 80 %. The measurements of HKWC alone do not strictly fulfil the Carbon Trust's criterion for Stage 2 Floating LiDARs which requires an overall availability of 85 % or more, but do fulfil the criterion of a monthly availability of 80 % or more (20) from August to October. However, the Carbon Trust's criteria will be fulfilled through the use of a combination of HKWA, HKWA-2, HKWB and HKWC, as shown in paragraph 4.3.4.

4.3.2. HKW Main Data Source

As none of the datasets described above provided a measurement period of sufficient quality over the length of the measurement campaign, Tractebel further investigated how an optimal dataset could be retrieved from the four measurement campaigns to be used as one of the main sources of measurement in the remainder of this Wind Resource Assessment (WRA).

4.3.2.1. ELEMENTS OF CHOICE

4.3.2.1.1. Distance between buoys

The distance between the different measurement locations is shown in Table 6. The smallest distance between buoys is found between HKWA and HKWA-2 (141 m), followed by the distance between HKWB and HKWC (537 m), while other distances are two to three times larger. Distances between buoys are relatively limited in comparison to distance to shore.

TABLE 6: DISTANCES BETWEEN BUOY LOCATIONS AT HKW

Distances [m]	HKWA	HKWB	HKWC
HKWA	-	-	-
HKWB	1500	-	-
HKWC	1391	537	-
HKWA-2	141	1603	1455

4.3.2.1.2. Difference in wind speed between buoys

In order to combine these data sets, a first step is to validate if the difference in the expected wind resource at each location is sufficiently limited, to allow for direct filling. Mesoscale data sets available in the area (see Section 5.2.2) indicate a maximum difference of 0.1 % in wind speed between the four buoy locations, well below measurement uncertainty (2.6%, see Table 26).

To determine which data set is to be used, the analysis focused on concurrent measurement periods between the various pairs of buoys. The time lag that occurs due to the distance between data sets is considered to be negligible, as it amounts to 2 minutes and 40 seconds for a 10 m/s wind speed between HKWA-2 and B while 10-minute averages have been used. The results of the comparison are detailed below.

Table 7 indicates average wind speed, bias and relative bias for the concurrent measurements between the various buoys. Differences between buoys are significantly lower than expected measurement uncertainties.

TABLE 7: WIND SPEED BIAS BETWEEN HKW A, A2, B, C (CONCURRENT DATA BETWEEN PAIRS OF BUOYS)

HKW Buoys compared	Wind speed bias, concurrent data				
	Wind speed at buoys location		Count	Bias [m/s]	Rel. Bias
	Y-X	X [m/s]			
B-A	8.94	8.96	19544	0.02	0.3 %
C-A	9.87	9.87	12513	0.00	0.0 %
C-B	9.95	9.96	2160	0.02	0.2 %
B-A2	9.48	9.47	34659	-0.01	-0.1 %

4.3.2.1.3. Wind speed and direction correlations

Correlations on wind speeds and direction between the four datasets was analysed. Coefficients of determination (R^2) and slopes of these correlations are provided in Table 8 and Table 9. The correlations are also illustrated by Figure 5 to Figure 8. Note that raw values of directions were modified in order to ensure a maximum difference between two directions of 180° ; this resulted in values larger than 360° (e.g. if directions of 330° and 5° were measured, 330° and 365° were plotted). All values of correlation and slopes are close to 1. Although R^2 values for wind direction are close to 1 the plots below exhibit differences between devices. They can be attributed to the inherent LiDAR's uncertainty on direction discussed above, which remains for some points even after correction with ERA5 data.

TABLE 8: R^2 VALUES FOR CONCURRENT VALUES OF WIND SPEED AND WIND DIRECTION MEASURED AT HKWA, HKWA2, HKWB AND HKWC

R^2 (wind speed)	HKWA	HKWB	R^2 (direction)	HKWA	HKWB
HKWA	-	-	HKWA	-	-
HKWB	0.998	-	HKWB	0.999	-
HKWC	0.998	0.999	HKWC	0.998	1.000
HKWA-2	-	0.998	HKWA-2	-	0.999

TABLE 9: SLOPES OF REGRESSION LINES FOR CONCURRENT VALUES OF WIND SPEED AND WIND DIRECTION AT HKWA, HKWA-2, HKWB AND HKWC

Slope (wind speed)	HKWA	HKWB	Slope (direction)	HKWA	HKWB
HKWA	-	-	HKWA	-	-
HKWB	1.002	-	HKWB	0.996	-
HKWC	0.999	1.002	HKWC	0.997	1.001
HKWA-2	-	0.997	HKWA-2	-	1.000

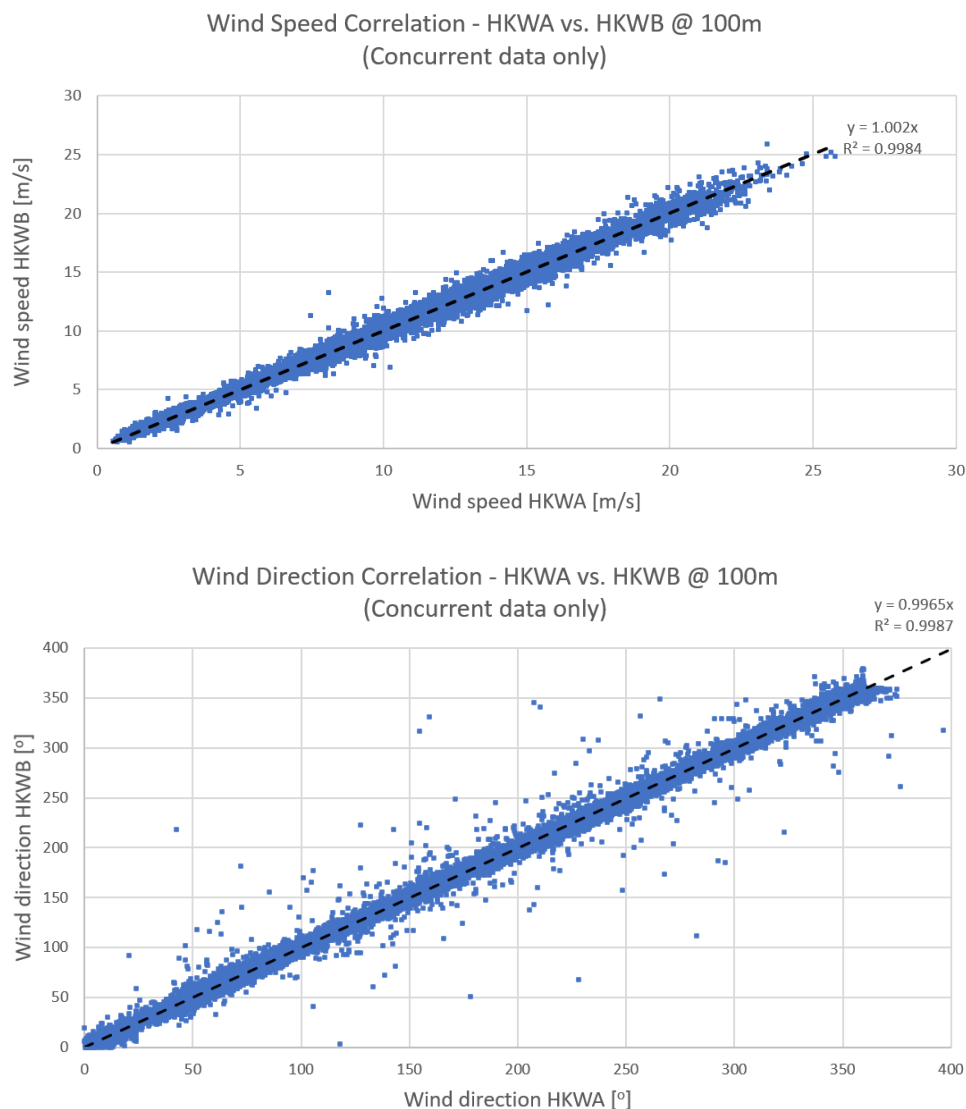


Figure 5: Concurrent wind speed/wind direction of HKWB as a function of HKWA

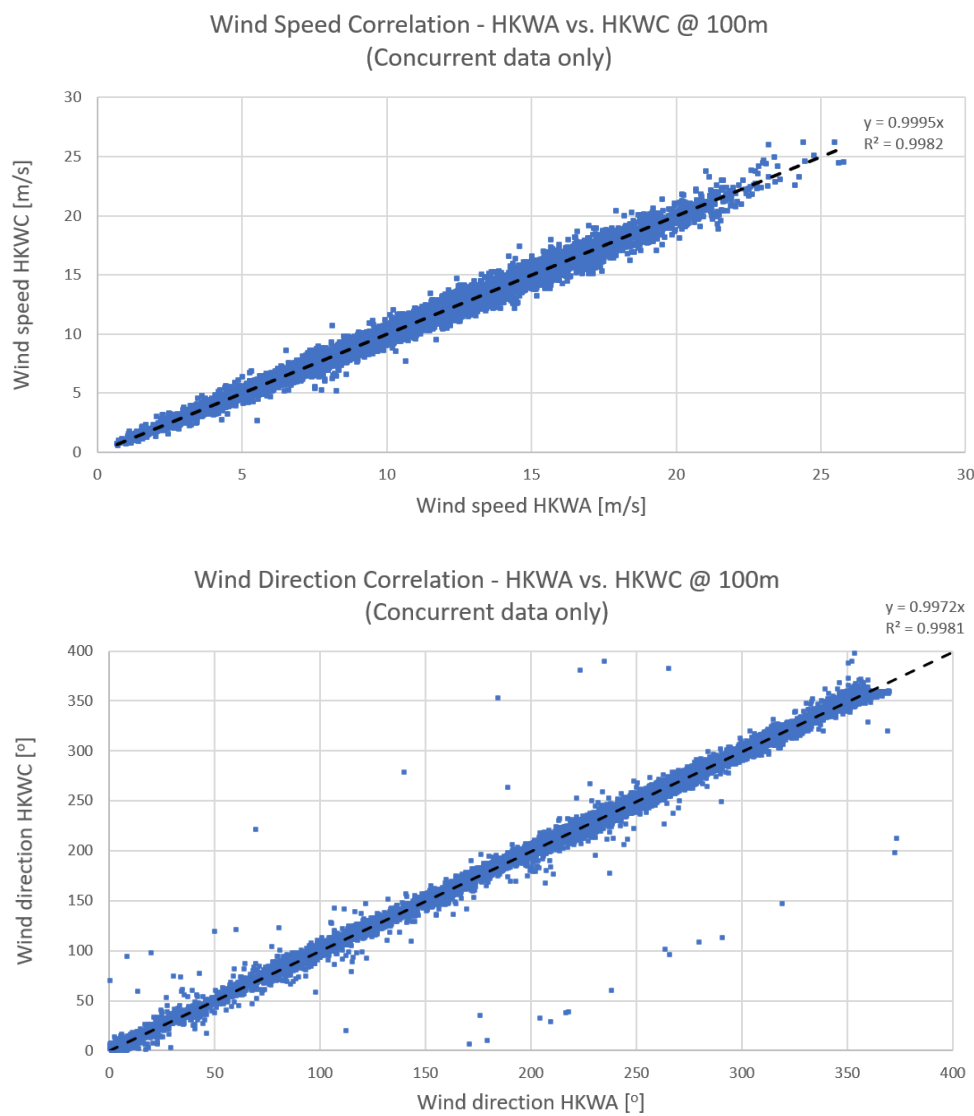


Figure 6: Concurrent wind speed/wind direction of HKWC as a function of HKWA

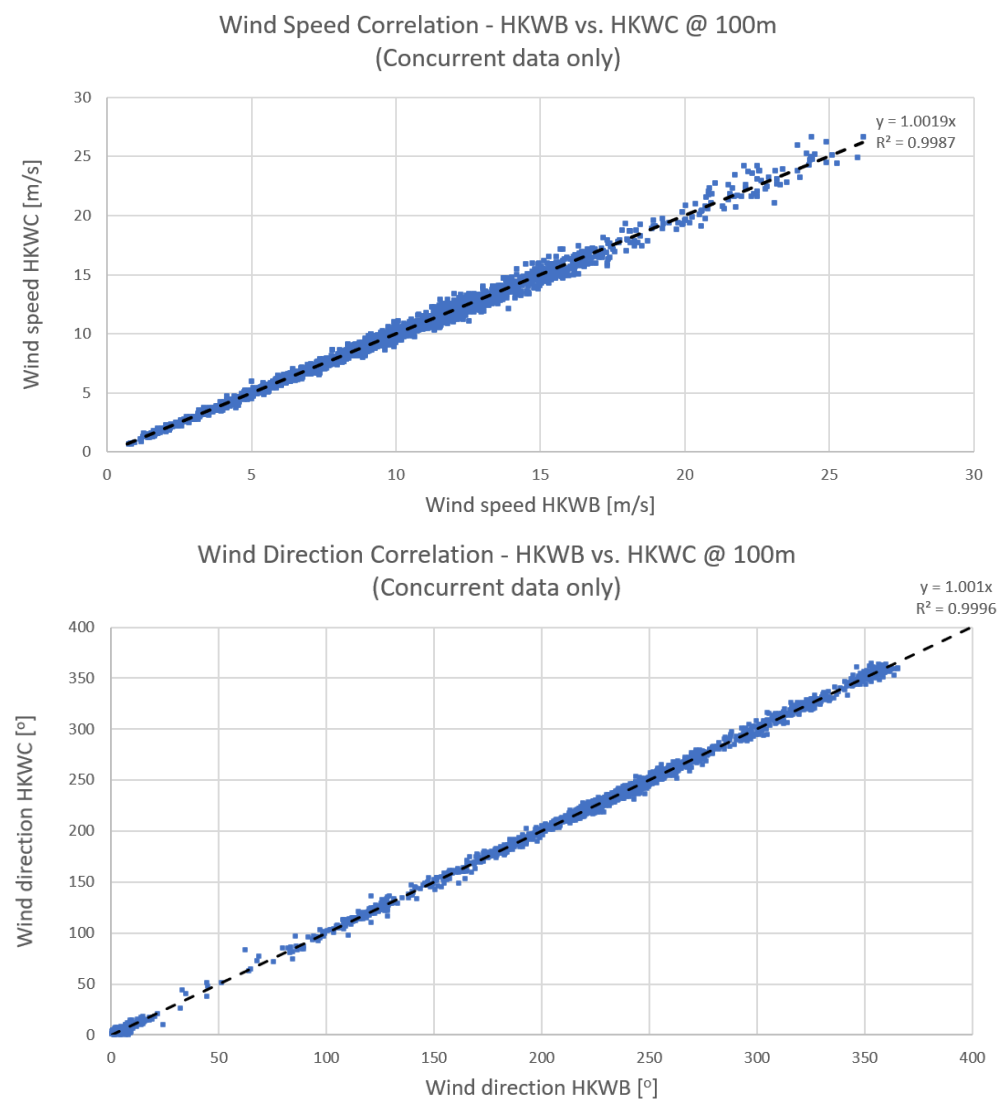


Figure 7: Concurrent wind speed/wind direction of HKWC as a function of HKWB

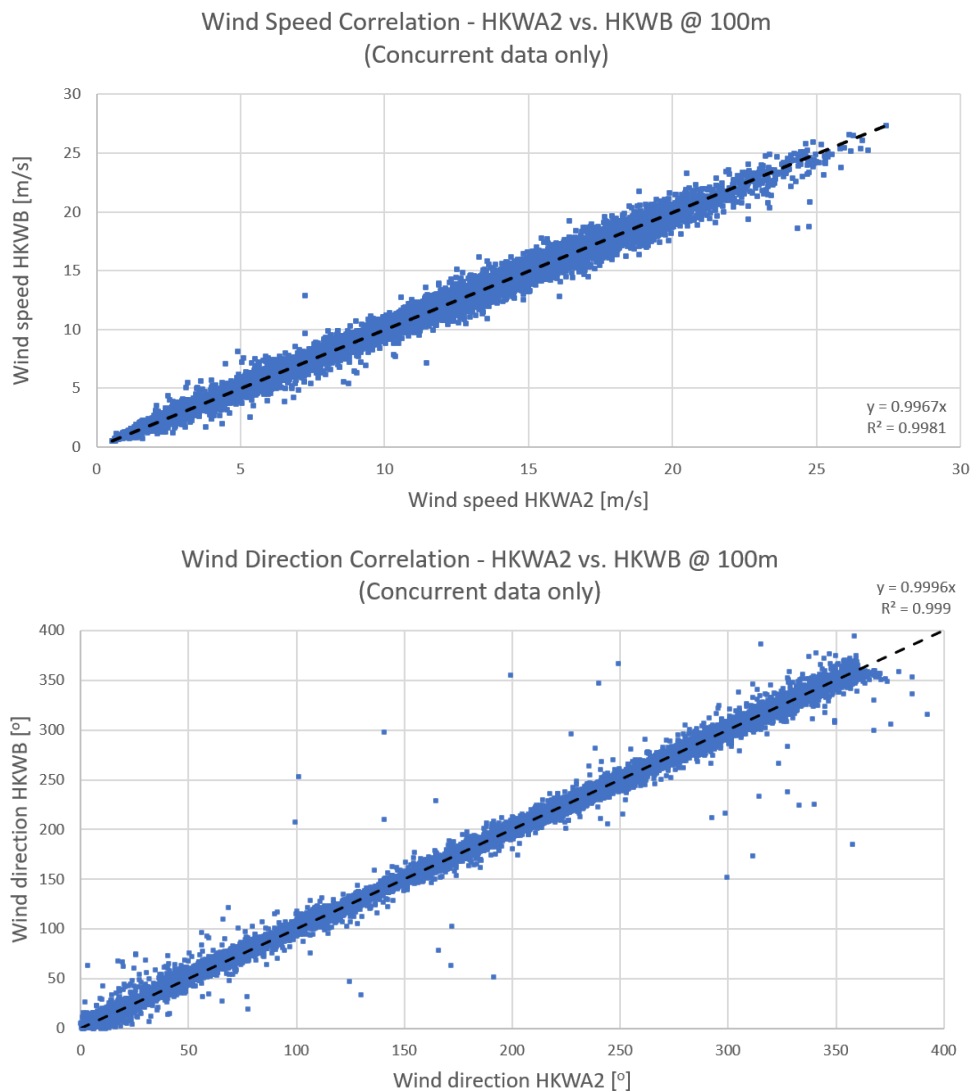


Figure 8: Concurrent wind speed/wind direction of HKWB as a function of HKWA-2

4.3.2.2. DATA SOURCE SELECTION

As indicated in Table 6, the distance between HKWA and HKWA-2 is one order of magnitude smaller than distances between HKWA and HKWB and HKWC, which still show very high levels of correlations and differences in concurrent wind speeds smaller than 0.3 %. Additionally, the area associated with measurements at HKWA overlaps with the area associated with measurements at HKWA-2 (given the possibility for buoys to circle around their anchoring point). Therefore, HKWA and HKWA-2 were considered as a single dataset. Since this dataset spans the 24 months of the campaign it was decided to use it as the main source of measurements and to use HKWB and HKWC to fill the gaps of missing data.

4.3.3. Data Substitution

Data substitution was performed on the 24 months of data measured at HKWA and HKWA-2 to replace disabled or missing data and fill data gaps. This yielded a 24 months time-series.

As a variant, MCPs were performed using the HKWB and HKWC measurements as reference measurements to obtain datasets that cover the HKWB and HKWC measurement periods, but scaled by the HKWB and HKWC measurements. These datasets were merged into a single dataset and compared with the time series obtained above. This comparison showed a difference on mean wind speed of 0.02 % between the two time series, with coefficients of determination of 1.000 for both wind speed and wind direction.

Since a MCP could introduce artificial variations in the resulting dataset it was decided to fill the gaps in the HKWA/A-2 dataset by replacing them directly with available data coming from the original HKWB and HKWC datasets.

In the remainder of this report, this compiled data set will be referred to as HKW.

4.3.4. Data Availability after Filtering and Substitution

Table 10 summarises the availability of the measurements during the period of available measurements after filtering and substitution. The corresponding monthly data availability is provided in Table 11.

The monthly data availability for the considered period after substitution ranges between 72 and 99 % for an overall availability of 92.4 %. The final dataset therefore does not fully fulfil the Carbon Trust's criteria for Stage 2 Floating LiDARs which require a monthly availability larger than 80 % and an overall availability larger than 85 % (20). The two months showing an availability of less than 80 % are due to a period of two weeks of missing wind direction at HKWB which was highlighted above. The impact of these two weeks of data was investigated on the long-term-corrected dataset as follows: the dataset with the two weeks of missing data was first long-term corrected (as detailed in Section 6.3). A second dataset was then generated using the same long-term correction procedure but using MERRA-2 reanalysis data to fill the two weeks of missing directional data. A comparison between the two datasets showed an impact of 0.01% on wind speed, with coefficients of determination of 1.000 for both wind speed and direction. The impact of this two weeks of missing data on the long-term dataset was therefore quantified as negligible.

TABLE 10: MEASUREMENTS PERIOD AND AVAILABILITY AFTER FILTERING AND DATA SUBSTITUTION

Instrument	Instrument height	Total period	Start date	End date	Availability
-	[m MSL]	[months]	-	-	[% of the total period]
HKW - Final	100	24	07/02/2019	06/02/2021	92.4 %

TABLE 11: AVAILABILITY OF FINAL DATASET AFTER FILTERING AND DATA SUBSTITUTION

Availability [%] (final dataset)	2019												2020		
	Feb	Mar	Apr	May	Jun	Jul	Aug	Sep	Oct	Nov	Dec	Jan	Feb		
HKW @100 m MSL	92	92	94	87	86	90	99	98	99	90	95	87	97		
Availability [%] (final dataset)	2020												2021		All
(continued)	Mar	Apr	May	Jun	Jul	Aug	Sep	Oct	Nov	Dec	Jan	Feb			All
HKW @100 m MSL	94	76	73	95	99	96	98	99	96	94	91	93	92		

4.3.5. HKW reference measurement location

As HKW is a combination of data sets performed at different locations, a central point has to be derived to serve as a geographic reference for the final data set. This point will be hereunder referred as HKW reference measurement location.

Several methods can be used to derive a central point:

- Point minimising the total distance to buoys;
- Centre of extreme points; and
- The barycentre.

These different locations are illustrated by Figure 9. A decision concerning the location of the reference measurement had to be made before completing the analysis of the datasets. Tractebel selected the point minimising the distance to the different buoys to select a location that would fit best any outcome of the analysis. In order for this report to be more easily comparable with the 12 months report, and given the proximity (and overlap) between HKWA & A-2 locations, the A-2 location was considered to be the same as A. The coordinates of the different calculated centres are provided in Table 12. The selected one is shown in bold. Note that taking into account HKWA-2 independently of HKWA would have led to a central point located 50 m away from the one proposed here, which would have led to negligible differences in wind climate.

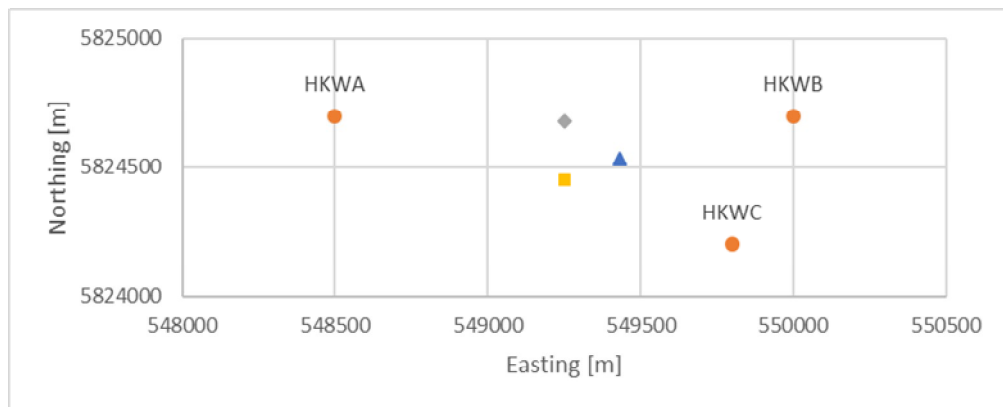


Figure 9: Illustration of the possible central points for HKW: minimizing distances to buoys (grey diamond), using the centre of extreme points (yellow square), and using the barycentre (blue triangle)

TABLE 12: LOCATION OF HKW REFERENCE MEASUREMENT LOCATION

Location	Locations [EPSG 25831]	
	Easting [m]	Northing [m]
Min dist(x,y)	549 250	5 824 678
Centre of extreme Points	549 250	5 824 451
Barycentre	549 433	5 824 534

4.4. Measured Data

4.4.1. Measured Wind Speed

The short-term wind climate at the HKW reference measurement location is characterised by the following parameters at 100 m MSL:

TABLE 13: MEASURED WIND SPEED AT 100 M

Measurement	Height [m MSL]	Considered period	Statistical mean wind speed [m/s]	Availability [%]
HKW	100	07/02/19 – 06/02/21	10.06	92.4

4.4.2. Weibull Distribution

The short-term wind climate at the HKW reference measurement location is characterised by the following Weibull parameters at 100 m MSL:

TABLE 14: WEIBULL PARAMETERS AT 100 M

Measurement	Height [m MSL]	Weibull fitted wind speed [m/s]	A parameter [m/s]	k parameter
HKW	100	10.10	11.41	2.23

Detailed Weibull parameters and frequency by sector, at a height of 100 m MSL, are presented in Table 15.

Weibull parameters presented in this report were computed using Windpro, which uses a method based on energy weighting (23) as described in the European Wind Atlas (24). Other methods and assumptions could possibly be chosen for Weibull fitting which would lead to different values of A and k.

TABLE 15: WEIBULL PARAMETERS BY SECTOR AT 100 M MSL

Sector	A parameter [m/s]	k parameter	Frequency [%]	Mean wind speed [m/s]
N	9.10	1.90	5.71	8.08
NNE	9.13	1.91	4.40	8.10
ENE	10.35	3.14	6.89	9.26
E	9.86	2.78	6.67	8.78
ESE	9.10	2.74	4.21	8.09
SSE	9.54	2.25	5.09	8.45
S	12.50	2.46	8.80	11.09
SSW	13.80	2.48	15.98	12.24
WSW	13.15	2.59	17.18	11.68
W	11.96	2.32	11.39	10.59
WNW	9.85	2.04	7.76	8.73
NNW	8.91	2.06	5.91	7.89

Figure 10 below shows the Weibull fit overlaid on the frequency distribution of the wind speed at the selected measuring height.

The Weibull distribution fits relatively well with the measured frequency data even though the fit seems to slightly underestimate the frequency from about 6 to 8 m/s, and overestimate the frequency from 9 to 11 m/s. Statistical mean wind speed (Table 13) is also found to match well with Weibull mean wind speed (Table 14).

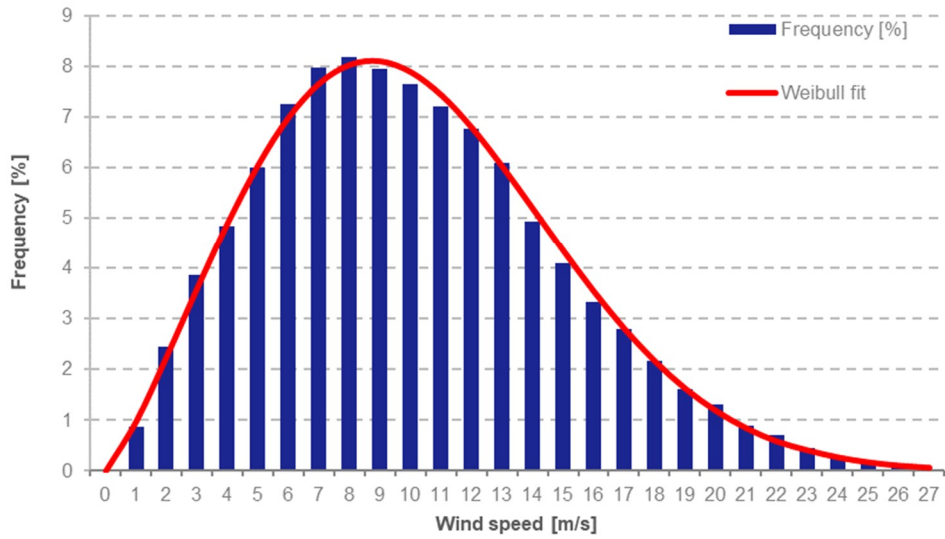
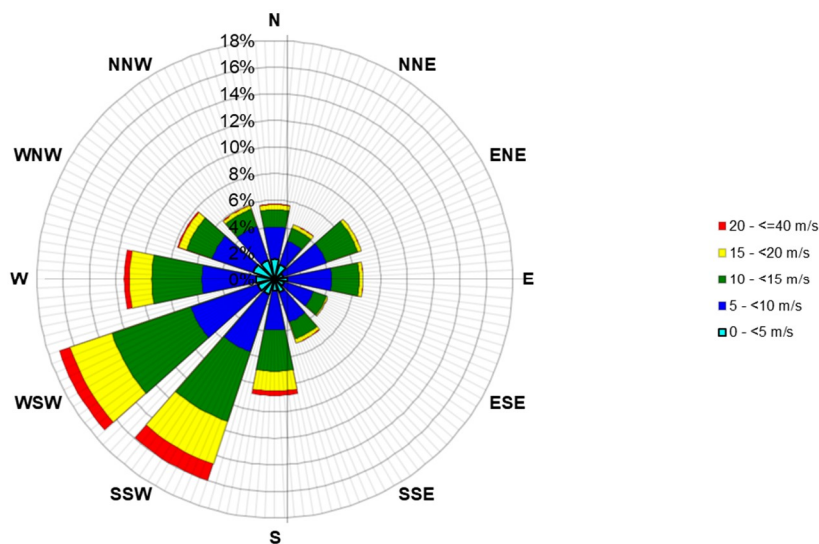


Figure 10: Frequency distribution and Weibull fit

4.4.3. Measured Wind Direction

The following figures show the frequency and energy roses. The WSW and SSW wind directions are anticipated to provide the largest amount of wind energy (21.2 % and 20.1 % respectively).



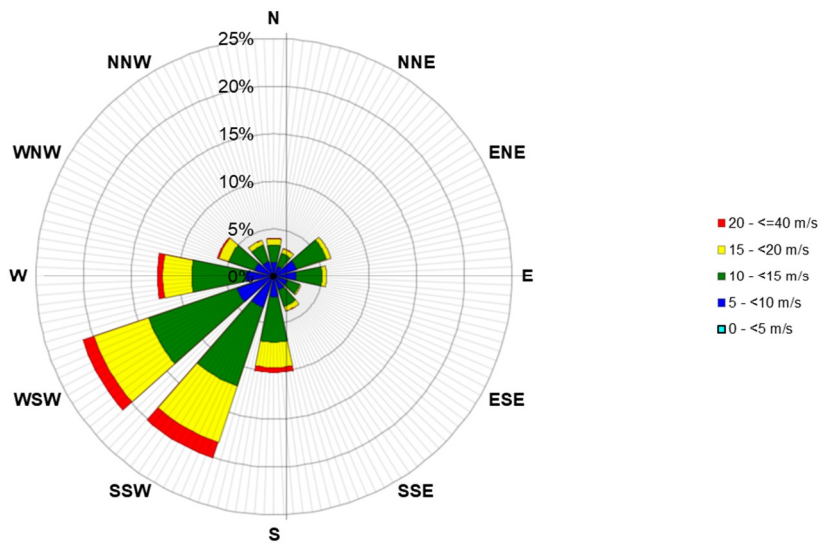


Figure 11: Frequency (top) and energy (bottom) roses at 100 m MSL (HKW)

4.4.4. Measured Wind Shear

To analyse the vertical wind shear at 100 m MSL at HKW, measurements at 80, 100 and 120 m have been used. The measured wind shear exponent (defined by the power law) is presented in Table 16.

Directional values of wind shear are provided in Table 17 and presented graphically in Figure 12.

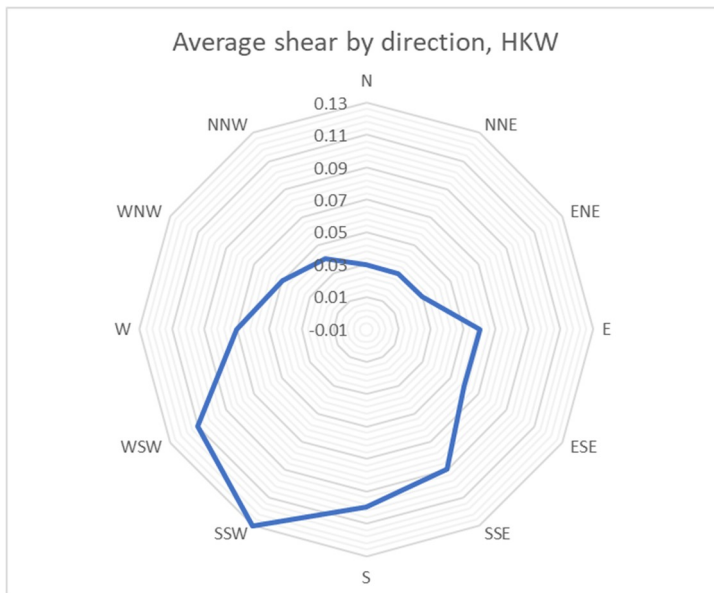


Figure 12: Directional shear at 100 m MSL at HKW, based on measurements

TABLE 16: MEASURED WIND SHEAR POWER LAW EXPONENT AT 100 M

Measurement Location	Considered period	Considered heights [m MSL]	α
HKW	07/02/2019 - 06/02/2021	80, 100 & 120	0.09

TABLE 17: DIRECTIONAL WIND SHEAR COEFFICIENTS FOR HKW AT 100 M MSL

Sector	Shear value	# of datapoint
N	0.03	5 440
NNE	0.03	4 134
ENE	0.03	6 787
E	0.06	6 602
ESE	0.06	4 091
SSE	0.09	4 836
S	0.1	8 337
SSW	0.13	15 222
WSW	0.11	16 439
W	0.07	10 962
WNW	0.05	7 422
NNW	0.04	5 646
Average / Total	0.09	95918

4.4.5. Diurnal and Monthly Profiles

The following figures show the daily and monthly profile of wind speed versus wind direction at 100 m MSL.

The wind speed varies slightly during the day, ranging from 9.8 m/s to 10.2 m/s, with higher values during the night from 7 pm until midnight. The lowest values can be found during the day between 5 am and 2 pm.

The variation in wind direction are more visible during the day, the lowest value at 9 am (228°) and the highest value in the afternoon at around 4pm (245°). During the night, the direction varies very slightly between 230° and 235°.

Highest wind speeds occur during the winter (from October to March), while lowest wind speeds are recorded during the summer (May to July). July shows wind speeds 5 m/s lower than February.

Tractebel notes a particular behaviour in April and May (2019 and 2020) where the mean wind direction shifts from Easterly (100°) to North-Westerly (330°) winds. It was also noticed that the month of February 2020 was very windy. These results were confirmed by an analysis of available long-term data which showed the same patterns for 2019 and 2020. An analysis of long-term data shows that wind direction varies the most for the months of April and May (a standard deviation of 90° over the course of 20 years of data versus 60° on average for other months).

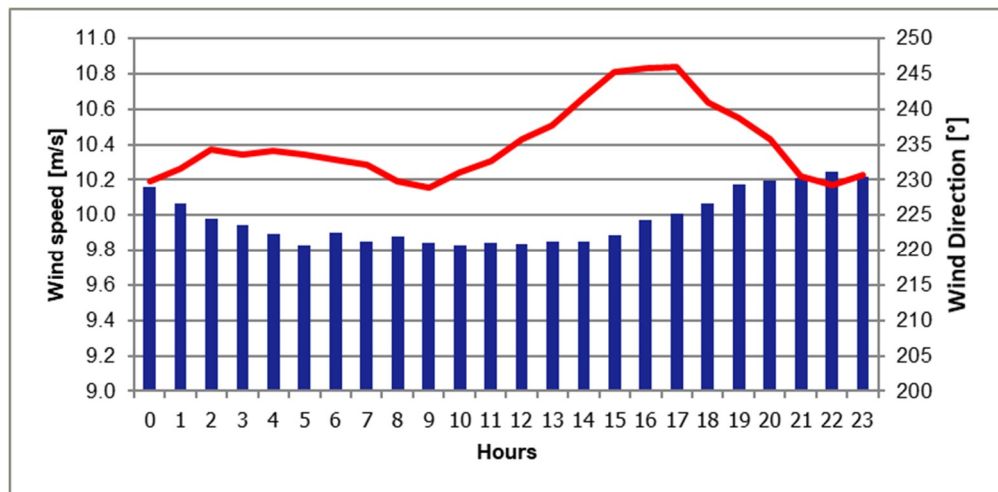


Figure 13: Diurnal profile of wind speed (blue) and wind direction (red) at HKW at 100 m MSL

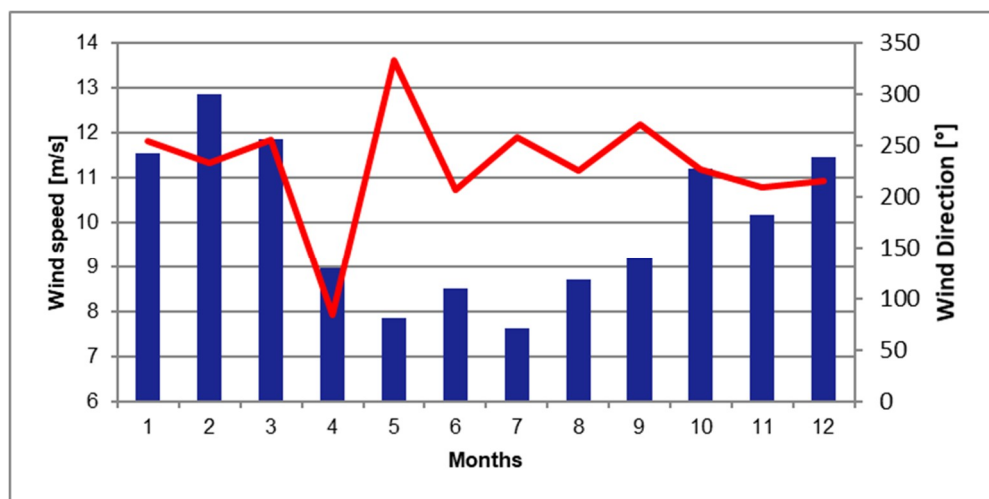


Figure 14: Monthly profile of wind speed (blue) and wind direction (red) at 100 m MSL

4.4.6. Environmental Measurements

This paragraph summarizes the remaining environmental measurements, measured by the equipment described in 4.2:

- Relative humidity (measured at 4.0 m MSL);

- Air temperature (measured at 4.0 m MSL); and
- Air pressure (measured at 4.0 m MSL).

The data has been filtered for freezes, spikes and any data which seemed unrealistic.

Monthly averages for each sensor are provided in the following table.

TABLE 18: MONTHLY RESULTS OF ENVIRONMENTAL MEASUREMENTS

		Relative humidity [%]	Air temperature [°C]	Air pressure [hPa]
	Channel	H1	T1	P1
	Height [m MSL]	4	4	4
2019	February	86.2	7.7	1022
	March	83.7	7.9	1014.5
	April	80.2	9.1	1015.4
	May	80.8	10.6	1016.5
	June	86.6	14.9	1015.2
	July	83.5	16.9	1015.8
	August	81.2	18.6	1014.2
	September	75.4	16.5	1016.8
	October	78.4	13.5	1010.8
	November	78.4	9.7	1001.4
	December	81.2	8.8	1008.6
	January	85.6	8.1	1018.8
2020	February	79.9	7.8	1008.9
	March	76.7	7.4	1016.5
	April	79	9	1021.2
	May	80.6	11.8	1023.6
	June	86.2	14.5	1012.7
	July	82.4	16.2	1015.8
	August	83.5	18.8	1012
	September	78.8	16.8	1015.5
	October	78.2	13.5	1007.8
	November	80.4	11.4	1019.6
	December	82.4	8.2	1003.3
	January	78.3	5.9	1009.9
2021	February	90	5.8	1003.1
	Average	81.2	11.9	1013.7

5. OTHER WIND DATA

Besides wind data from direct measurements at the Hollandse Kust (west) Wind Farm Zone, additional measurements in the vicinity of the site were considered for the synthesis of the wind climate, long-term corrections, and the validation of mesoscale models. Additionally, data from wind flow models were also used for long-term corrections and horizontal extrapolations. This section first describes additional measurements and then presents a set of available wind flow models.

5.1. Wind Measurements

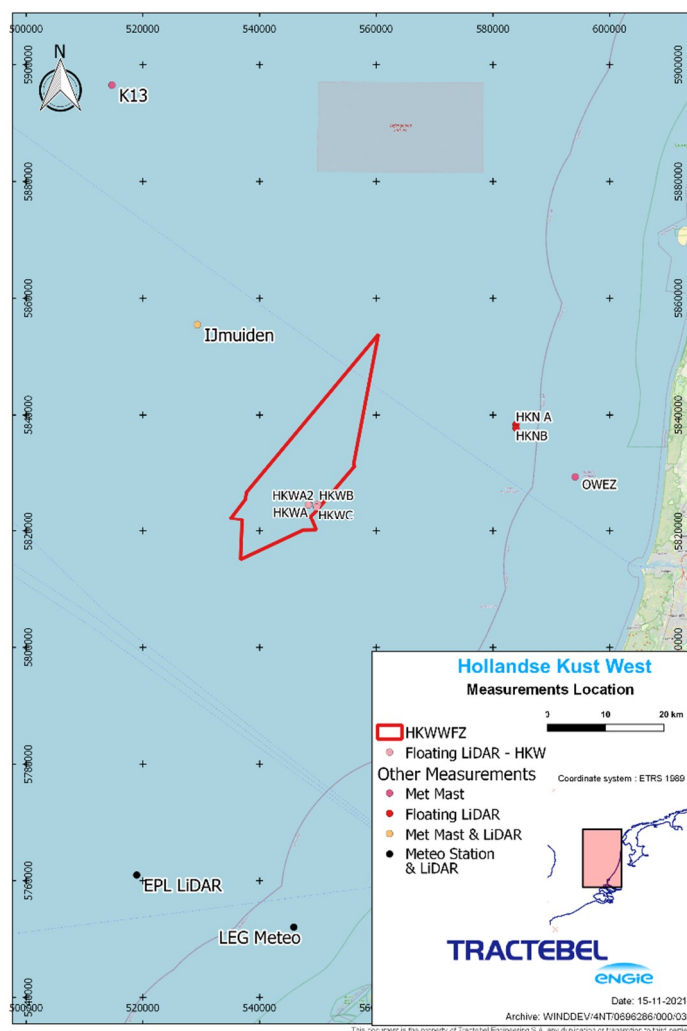


Figure 15: Illustration of the location of the wind measurements considered for the wind resource assessment

5.1.1. HKN Floating LiDARs

As part of the preparation for tendering for the Hollandse Kust (noord) wind project two floating Lidars were deployed by Fugro off the coast of the Netherlands, about 37 km North-East of the HKW site.

The LiDARs were ZephIR 300s devices mounted on floating buoys, as sketched in Figure 4, and as detailed in the Hollandse Kust (noord) wind resource assessment by Oldbaum (25). The buoys were located about 0.6 km from one another, and were periodically replaced during the two years of measurements. Measurements heights were 30 and 40 to 200 m MSL in 20 m intervals.

The data received from ECN (Energy Research Centre of the Netherlands) part of TNO had been pre-processed by Fugro and was quality-checked for erroneous data. Similar as for the floating Lidars of Hollandse Kust (west) campaign, 180° flips were encountered in the process (as detailed in Section 4.3.1). The availability of HKN B (85 % at 100 m MSL) was found to be slightly higher than the availability at HKN A (81 %). Table 19 provides an overview of the floating Lidar campaign.

TABLE 19: OVERVIEW OF THE HKN FLOATING LIDAR MEASUREMENTS

Wind measurements	EPSG 25831		Distance to site [km]	Measurement period considered	Measurement heights considered		Availability [%]
-	Easting [m]	Northing [m]	-	-	Wind speed [m] MSL	Wind direction [m] MSL	-
HKN A	583 949	5 838 365	37	10/04/2017 - 09/04/2019	30, 40, 60, 80, 100, 120, 140, 160, 180, 200		81 at all heights
HKN B	583 958	5 837 731	36	10/04/2017 - 09/04/2019	30, 40, 60, 80, 100, 120, 140, 160, 180, 200		87, 87, 87, 87, 85, 87, 86, 86, 86, 86

5.1.2. HKZ Floating LiDARs

As part of the preparation for tendering for the Hollandse Kust (zuid) wind project two floating Lidars were deployed by Fugro off the coast of the Netherlands, about 35 km South-East of the HKW site.

The Lidars were ZephIR 300s devices mounted on floating buoys, as illustrated by Figure 4, and as detailed in the Hollandse Kust (zuid) wind resource assessment by Ecofys (26). The buoys were located about 2.5 km from one another. Measurements heights were 30 and 40 to 200 m MSL in 20 m intervals.

The data received from ECN part of TNO had been pre-processed by Fugro and was quality-checked for erroneous data. 180° flips were encountered in the process. The availability of HKZ B (93 % at 100 m MSL) was found to be slightly higher than the availability at HKZ A (91 %). Table 20 provides an overview of the floating Lidar campaign.

TABLE 20: OVERVIEW OF THE HKZ FLOATING LIDAR MEASUREMENTS

Wind measurements	EPSG 25831		Distance to site [km]	Measurement period considered	Measurement heights considered		Availability [%]
-	Easting [m]	Northing [m]	-	-	Wind speed [m] MSL	Wind direction [m] MSL	-
HKZ A	569 092	5 796 203	35	05/06/2016 - 04/06/2018	30, 40, 60, 80, 100, 120, 140, 160, 180, 200		91, 91, 91, 91, 91, 91, 91, 91, 90, 91
HKZ B	568 792	5 793 671	35	05/06/2016 - 04/06/2018	30, 40, 60, 80, 100, 120, 140, 160, 180, 200		94, 94, 94, 94, 93, 93, 93, 93, 93, 93

5.1.3. IJmuiden met mast

The IJmuiden offshore met mast (MMIJ), illustrated by Figure 16 was located about 85 km West of the coast of the Netherlands (27), about 37 km to the North-West of the Hollandse Kust (west) wind farm site.

Two cup anemometers were installed above the top of the mast, at 92 m above LAT. Three cup anemometers were installed at two heights of 27 and 58.5 m above LAT. Three wind vanes were installed at three heights of 26, 58 and 87 m above LAT. There were more instruments on the mast, including several sonic anemometers, as well as pressure, temperature and humidity sensors.

A ZephIR 300s Lidar was installed within the mast structure to provide concurrent data with the met mast data from 90 to 315 m above LAT, as illustrated by Figure 16.

The dataset provided by ECN part of TNO covers the range 03/11/2011 to 11/03/2016, with a main gap in the dataset identified from 26/01/2014 to 31/03/2014. ECN part of TNO included calculated pseudo-signals that were provided as a combination of signals designed to limit the influence of the mast on measurements. The description of this pseudo-signals can be found in (27). Among these pseudo-signals were wind speeds and wind directions at 27 and 58.5 m above LAT, and 26, 58 and 87 m above LAT respectively. The provided dataset had been filtered for errors and invalid data by ECN part of TNO, and was quality-checked for inconsistent data.

Given the offshore conditions, the difference between LAT and MSL is considered negligible.

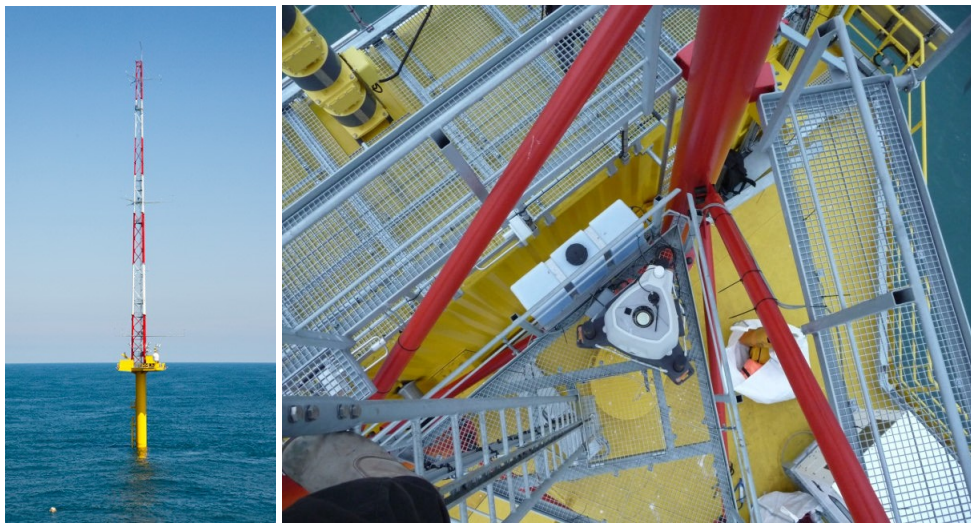


Figure 16: Illustration of the IJmuiden met mast (21) and of the Lidar installation (20)

Lidar data filtering included unbiasing lidar direction and discarding data based on number of packets. Lidar data showed numerous 180° shifts that were corrected for through comparison with wind vane data from the IJmuiden met mast.

TABLE 21: OVERVIEW OF THE IJMUIDEN MET MAST AND LIDAR MEASUREMENTS

Wind measurements	EPSG 25831		Distance to site [km]	Measurement period considered	Measurement heights considered		Availability [%]
-	Easting [m]	Northing [m]	-	-	Wind speed [m] above LAT	Wind direction [m] above LAT	-
IJmuiden met mast	529 340	5 855 469	37	02/11/2011 – 11/03/2016	27, 59, 92	27, 59, 85	93, 93, 83
IJmuiden Lidar	529 340	5 855 469	37	01/11/2011 – 09/03/2016	90, 115, 140, 165, 190		89, 90, 90, 90, 89

5.1.4. Offshore Wind Farm Egmond aan Zee (OWEZ) Met Mast

The OWEZ met mast was erected in 2003 at the Offshore Wind farm Egmond aan Zee, about 15 km off the coast of the Netherlands, and about 44 km to the East of the Hollandse Kust (west) wind farm site, as referenced in Table 22.



Figure 17: illustration of the OWEZ met mast

Three cup anemometers and wind vanes were installed at each of three levels located at heights of 22, 70 and 116 m MSL (28).

A single year of measurement was used, corresponding to measurements prior to the Egmond aan Zee wind farm operation, for measurements not to be affected by the presence of the wind farm.

The data provided by ECN part of TNO was quality-checked for erroneous measurements. A period of missing data was identified at 116 m MSL from November 2005 to January 2006. The influence of the mast structure on measurements was clearly visible, and was corrected for combining instruments following the methodology detailed by ECN part of TNO for the IJmuiden mast and described in (27).

TABLE 22: OVERVIEW OF THE OWEZ MET MAST MEASUREMENTS

Wind measurements	EPSG 25831		Distance to site [km]	Measurement period considered	Measurement heights considered		Availability [%]
-	Easting [m]	Northing [m]	-	-	Wind speed [m] MSL	Wind direction [m] MSL	-
OWEZ met mast	594 102	5 829 389	44	01/07/2005 – 01/07/2006	22, 70, 116	22, 70, 116	95, 97, 85

5.1.5. Lichteiland Goeree (LEG)

Lichteiland Goeree is a platform serving as a beacon to ships located about 18 km off the coast of the Netherlands and about 73 km South of the Hollandse Kust (west) wind farm site, as indicated in Table 23.

A met mast is installed on the platform, as illustrated by Figure 18. The met mast data is managed by the KNMI (Koninklijk Nederlands Meteorologisch Instituut). The dataset was quality-checked for erroneous measurements, leading to an overall availability of 97 %.

A Leosphere Windcube v2 was also installed on the platform, below the helicopter platform, on the 06/10/2014, as illustrated by Figure 18. The device was set to measure atmospheric conditions at heights of 62, and 90 to 290 m MSL in 25 m increments. The Windcube data provided by ECN part of TNO was quality-checked for erroneous data. Timestamps with an availability lower than 80 % were discarded. Several 180° shifts were identified and discarded. This resulted in an availability of 77 % at 90 m MSL. Several gaps were identified in the dataset, the main gap occurring between April and September 2015.



Figure 18: Illustration of the LEG platform and of the Lidar installation, from (21)

TABLE 23: OVERVIEW OF THE LEG LIDAR MEASUREMENTS

Wind measurements	EPSG 25831		Distance to site [km]	Measurement period considered	Measurement heights considered		Availability [%]
-	Easting [m]	Northing [m]	-	-	Wind speed [m] MSL	Wind direction [m] MSL	-
LEG met mast	545 876	5 752 029	73		22		
LEG Lidar	545 876	5 752 029	73	17/11/2014 - 31/12/2019	62, 90, 115, 140, 165, 190, 215, 240, 265, 290		78, 77, 77, 76, 73, 68, 61, 52, 23, 17

5.1.6. Europlatform (EPL)

The Europlatform is a platform used as a beacon to ships, located about 43 km off the coast of Rotterdam, and 71 km South-East of the Hollandse Kust (west) wind farm site, as indicated in Table 24.

A met mast is installed on the edge of the platform, as illustrated by Figure 19. The met mast data is managed by the KNMI. The dataset was quality-checked for erroneous measurements, leading to an overall availability of 99 %.

A Z300s LiDAR was installed below the helicopter deck of the platform on 09/05/2016, as illustrated by Figure 19. The device was set to measure atmospheric conditions at heights of 62, and 90 to 290 m MSL in 25 m increments. The LiDAR data is managed by ECN part of TNO who performed a validation of the device against data from a met mast in their onshore facilities prior to its installation offshore (29). The dataset provided by ECN part of TNO ranged from the 01/07/2016 to the 31/12/2019. The dataset was quality-checked for erroneous measurements: a minimum number of packets was defined based on the distribution of packets, and several 180° flips were identified. Several periods of missing data were identified, in particular from October 2016 to January 2017, April to August 2018 and May to October 2019. This resulted in an overall availability of 66 % at 90 m MSL.



Figure 19: Illustration of the EPL platform and of the Lidar installation, from (21)

TABLE 24: OVERVIEW OF THE EPL LIDAR MEASUREMENTS

Wind measurements	EPSG 25831		Distance to site [km]	Measurement period considered	Measurement heights considered		Availability [%]
-	Easting [m]	Northing [m]	-	-	Wind speed [m] MSL	Wind direction [m] MSL	-
EPL met mast	518 948	5 760 963	71	01/04/2003 – 31/01/2020	19		99
EPL Lidar	518 948	5 760 963	71	01/07/2016 - 31/12/2019	62, 90, 115, 140, 165, 190, 215, 240, 265, 290		66, 66, 66, 66, 66, 66, 66, 66, 65, 65, 65

5.1.7. K13

The K13 platform is an offshore production platform that serves as a link for other platforms in the field of natural gas (30). The platform is located about 100 km off the coast of the Netherlands, and 70 km from the Hollandse Kust (west) wind farm site, as detailed in Table 25.

A ZephIR LiDAR 300M was installed under the helicopter platform in November 2016, and is checked on a regular basis. The LiDAR was set to measure atmospheric conditions at heights of 62, and 90 to 290 m MSL in 25 m increments.

The data was provided by ECN part of TNO, and was quality-checked for erroneous measurements. The dataset was found to be of very high quality, with an availability of 99 % at 90 m MSL.



Figure 20: Overview of the K13 platform and of the K13 LiDAR installation, from (21)

TABLE 25: OVERVIEW OF THE K13 LIDAR MEASUREMENTS

Wind measurements	EPSG 25831		Distance to site [km]	Measurement period considered	Measurement heights considered		Availability [%]
-	Easting [m]	Northing [m]	-	-	Wind speed [m] MSL	Wind direction [m] MSL	-
K13 LiDAR	514 708	5 896 519	70	02/11/2016 - 01/01/2020	62, 90, 115, 140, 165, 190, 215, 240, 265, 290		98, 99, 99, 99, 99, 98, 98, 98, 98, 98

5.2. Wind Flow Models

This section describes wind flow model data that were used in the framework of this study: reanalysis data which consist in datasets of physical variables on a global scale, and mesoscale model data which are generated by mesoscale models over scales of hundreds of kilometres. Reanalysis data were considered for long-term correction, while mesoscale data were considered for horizontal extrapolations.

5.2.1. Reanalysis datasets

Re-analysis combines model data with observations from across the world into a globally complete and consistent dataset using global circulation models (GCMs). These computations require powerful computer clusters and are therefore run by dedicated institutions such as NCEP/NCAR in North America or the ECMWF in Europe. ERA-5 (31) , MERRA-2 (32), ERA-Interim (33) and CFSR (34) are examples of widely used reanalysis datasets.

5.2.1.1. ERA5

The ERA5 (ECMWF Reanalysis 5th generation) dataset is the 5th generation of ECMWF reanalysis datasets. It was designed to replace the ERA-Interim dataset, through the use of higher spatial (31 vs. 79 km) and temporal (hourly vs. six-hourly) resolutions and various improvements such as an updated data assimilation scheme with newly reprocessed datasets. The dataset currently ranges from 1999 to the current period, with a lag of several months with real time. This dataset is being extended to 1979. The dataset provides hourly estimates of global atmospheric data with a resolution of about 31 km in the horizontal, and 137 vertical levels.

In the course of 2019 ERA5 data was made available with a lag of a few days with real time. This specific dataset was named ERA5T. This was made possible by bypassing some of the extensive checks used to generate the standard ERA5. According to the ECMWF ERA5T data is unlikely to differ from ERA5 data. In the context of this analysis, ERA5T has not been considered.

5.2.1.2. CFSR

The CFSR (Climate Forecast System Reanalysis) (35) dataset is a third generation reanalysis dataset made freely available by NCEP/NCAR. It was designed and executed as a global, high-resolution coupled atmosphere–ocean–land surface–sea ice system to provide the best estimate of the state of these coupled domains over the 31-year period ranging from 1979 to 2009. The dataset was then extended (34) up to the present period, with data available with a few days lag with real time. The spatial resolution of the dataset is about 38 km in the horizontal for 64 vertical levels. The dataset is provided as hourly data resulting from a combination of six-hourly reanalysis runs and five hours forecast runs. This extension of the data set is commonly referred to as CFSv2.

5.2.1.3. MERRA-2

The Modern-Era Retrospective analysis for Research and Applications, Version 2 (MERRA-2) is a reanalysis dataset provided by NASA using an upgraded data assimilation process compared to the original MERRA dataset. The dataset consists of hourly time-series ranging from 1980 to the present period, with a lag of 2 to 3 months with real time. The longitudinal and latitudinal resolutions of the dataset are 0.625° and 0.5° , respectively, for 72 vertical layers.

5.2.2. Mesoscale datasets

Mesoscale models, such as the widely used WRF model (36), are numerical models including the laws of physics, that use reanalysis data as inputs, and are used over scales of hundreds of kilometres. They typically use higher spatial resolutions than Global Circulation Models and are therefore expected to be more accurate where the use of GCMs does not allow for an accurate resolution of terrain or land cover variations. These models can be used for long-term correction onshore where terrain complexity discards the use of reanalysis datasets, and for horizontal extrapolation offshore (or simple onshore sites) where required scales and physics typically discard microscale models such as WAsP. Mesoscale models are typically not used with scales lower than several hundred of meters, in which case microscale models such as WAsP or RANS CFD models are used. Microscale models use resolutions of the order of several to tens of meters, and are often preferred to or used in combination with mesoscale models for onshore simulations.

5.2.2.1. KNW

The KNMI North sea Wind atlas (KNW) (37) is based on the downscaling of reanalysis data with the HARMONIE (38) mesoscale weather model. Version 37h1.1 of the model was used, using a horizontal resolution of 2.5 km. 60 levels were used in the vertical dimension with a higher resolution near the ground, where levels follow the surface of the Earth, and a lower resolution further aloft, where levels are pressure-based. Initial and boundary conditions were initially based on 35 years (1979-2013) of 6-hourly ERA-Interim reanalysis data. The dataset was subsequently extended to August 2019. Wind speeds were anchored on measurements from the Cabauw meteorological met mast; a uniform wind shear correction factor was applied throughout the entire domain. The model was validated against data available in the North Sea (39).

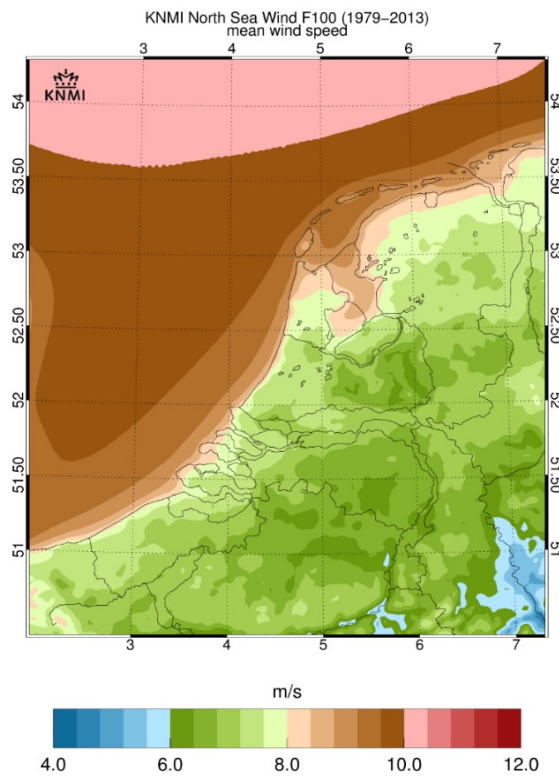


Figure 21: Average wind speed at 100 m height for the whole KNW-domain and the 1979-2013 period

5.2.2.2. DOWA

The Dutch Offshore Wind Atlas (DOWA) (40), (41) is a project aiming at improving on the KNW atlas. The atlas currently makes use of 11 years (2008-2018) of ERA5 reanalysis data. While the use of ERA5 represents an improvement compared to the use of ERA-Interim for the KNW, 11 years of data is less than the 35 years of the KNW to capture the variability of the North sea wind climate. Version 40h1.2.tg2 of the HARMONIE mesoscale model was used, which includes an improved turbulence model compared to version 37h1.1 used for the KNW, resulting in improved comparisons with satellite data (42). The methodology used for computations was also improved with “3D” (less advanced than “4D”) assimilation of various datasets, including ASCAT high-resolution satellite surface wind fields and MODE-S EHS aircraft wind profile measurements, which are expected to reduce forecasting errors. The model also makes use of a larger computational domain than for the KNW atlas, see Figure 22. Additionally, DOWA was generated without the need for “cold starts” (i.e. every 3h forecast cycle was initialized from the previous 3h HARMONIE forecast, while KNW computations were initialized from raw re-analysis data) which is expected to improve the representation of the diurnal cycle. Given these improvements wind shear correction used for the KNW atlas was not deemed required for the DOWA atlas.

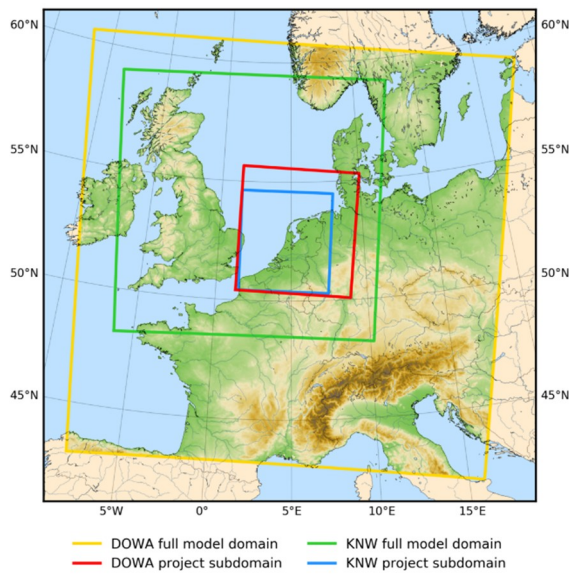


Figure 22: : Illustration of the extents of the HARMONIE domain for the DOWA (yellow) vs. the KNW (green) atlas (34)

5.2.2.3. NEWA

The New European Wind Atlas (NEWA) (43), (44), (45) was generated using 10 years (2009 to 2018) of ERA5 re-analysis data that were downscaled with the WRF (36) mesoscale software. WRF is the most widely used mesoscale model, and makes use of “4D” (more advanced than “3D”) data assimilation techniques. It is currently available over the area shown by Figure 23 with a horizontal resolution of 3 km. Details about the model setup can be found in (46), and are illustrated by the table in Figure 24. In the same publication, the authors mention sensitivity studies that were conducted to find an optimal setup of the WRF model, and the use of offshore data available in the vicinity of Hollandse Kust (west) for this purpose. The model validation covers a wide range of wind conditions, from homogeneous onshore conditions (e.g. Cabauw), to offshore (e.g. FINO1) and coastal conditions. It is to be highlighted that nudging was used in order to generate this dataset, the consequence being that if the dataset is evaluated at the points used for nudging, model error will appear artificially low.

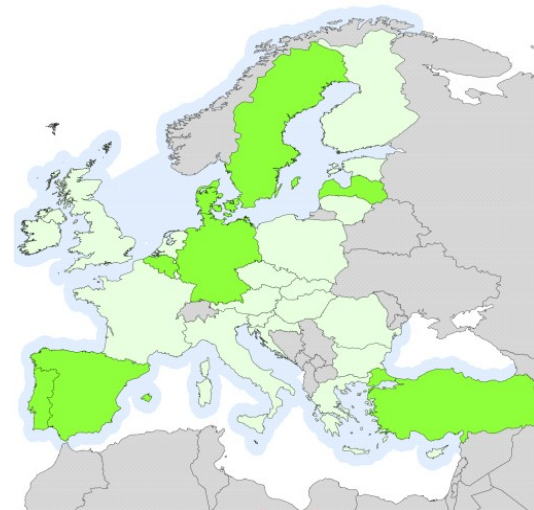


Figure 23: Illustration of the offshore coverage (blue) of the NEWA, from (36)

WRF version	3.8.1 (modified PBL + icing code)
Grid	3 nests: 27 km, 9 km, 3 km; 61 vertical levels, 1-way nesting
Numerical options	480 cores, IO Quilting (1 node used for output)
Land use data	CORINE 100 m, ESA CCI where CORINE not available
Dynamical forcing	ERA5 reanalysis ($0.3^\circ \times 0.3^\circ$ resolution)
SST	OSTIA SST and sea-ice ($1/20^\circ$, approx. 5 km)
Lake temperature	average ground temperature from ERA5, lakes are removed when temperature is present in OSTIA
Land surface model	NOAH-LSM
Simulation length	8 days, including 24 h spin-up
Nudging	Spectral nudging in D1 only, above PBL and level 20
Time step	adaptive (where working)
PBL	MYNN (modified) (5)
Surface layer	MO (Eta similarity) (2)
Microphysics	WRF Single-Moment 5-class scheme (4)
Radiation	RRTMG scheme (4), 12 min calling frequency
Cumulus Parameterisation	Kain-Fritsch scheme (1) on D1 and D2
Icing	WSM5 + icing code + sum of qcld and qcice
Diffusion	Simple diffusion (option 1) 2D deformation (option 4) 6th order positive definite numerical diffusion (option 2) rates of 0.06, 0.08, and 0.1 for D1, D2, and D3 vertical damping.
Advection	Positive definite advection of moisture and scalars.

Figure 24: Main parameters for the simulation of the NEWA, from (46)

5.2.2.4. 3TIER-ERA5

3Tier (acquired by Vaisala) (47) uses numerical weather prediction modelling to downscale global wind datasets from various re-analysis datasets, including ERA5, ERA-Interim and Merra-2. Model output was validated and anchored on a global dataset. The output is a global dataset spanning over 30 years with a horizontal resolution of 5 km. Data is provided from 50 to 200 m above ground level and is typically available with a 3 to 4-months lag with real time. The model captures mesoscale processes that affect the wind climate on site which is expected to improve correlations compared to plain re-analysis data. While this model usually provides excellent long-term trends, mean wind speed at specific locations are typically associated to high uncertainties.

5.2.2.5. EMD-WRF-ERA5

The EMD-WRF-ERA5 (48) dataset was generated by EMD, as a replacement to the ConWx model which was discontinued following the discontinuation of the ERA-Interim dataset. This mesoscale model (48) uses ERA5 re-analysis data that are downscaled with the WRF mesoscale software version 3.4. The spatial resolution of the dataset is of approximately 3 km. The dataset contains wind speed and direction at a temporal resolution of 1 hour. On this dataset, the typical 3-4 months lag with real time is applicable. The dataset has been validated against a set of met mast measuring at 50 meters and above (49).

6. WIND CLIMATE ASSESSMENT

For the purpose of this WRA, and specifically to lower the overall uncertainty of the wind resource assessment, three main data sources were identified and merged into one unique data source. Section 6.1 describes how these three data sources were selected. Wind climate modelling will be described in Sections 6.2, 6.3 and 6.4 with respectively the approach for vertical extrapolation, long term correction and horizontal extrapolation. Finally, uncertainties associated with the wind climate assessment will be discussed in Section 6.5.

6.1. Main Source Selection

6.1.1. Methodology

The rationale behind the selection of the sources is to lower the overall uncertainties of the assessment. Indeed, the combination of several (partially) independent results allows to decrease the overall uncertainties (50). This methodology was also used in previous wind resource assessments in the Dutch North Sea (25), (26). In this assessment, a similar approach was used to select the three main sources of measurements.

The combination of uncertainties can be written as (43):

$$u_{\text{combined}} = \sqrt{\sum_{k=1}^{N_u} \left(\sum_{i=1}^{N_m} w_i^2 u_{i,k}^2 + 2 \sum_{i=1}^{N_m-1} \sum_{j=i+1}^{N_m} c_{i,j,k} w_i w_j u_{i,k} u_{j,k} \right)}$$

where :

- $u_{i,k}$ is uncertainty in wind speed uncertainty component k and for measurement source i ;
- w_i is the weight given to measurement source i , proportional to the inverse of the uncertainty of the measurement;
- $N_m = 3$ is the number of measurements sources that are to be combined;
- $c_{i,j,k}$ is the correlation coefficient for uncertainty component k between measurement sources i and j ; and
- N_u is the number of uncertainty components.

The source selection was based on the characteristics of the measurement sources presented in Sections 4 and 5.1. An evaluation of related uncertainties was performed on:

- 1) Instrument accuracy: uncertainty on measurements of wind speed by individual instruments. Includes calibration uncertainty. Note that the uncertainties for the HKW LiDARs have been re-evaluated during the study. However, for weight-computing the initial values have been kept;
- 2) Instrument mounting: uncertainty due to effects of masts on measurements or other types of interferences. For masts, includes tilted anemometers, separation concerns (due to boom length, boom width, etc.) or any other mounting issues. For remote sensing, includes physical or atmospheric

- interferences (such as fog, rain, aerosols, atmospheric stability) on measurements;
- 3) Data quality and metadata: uncertainty regarding possible biases due to any removed or missing data or lack of quality metadata. Includes uncertainty due to non-encrypted data² or non-traceable data sources, or inconsistencies/contradictory in metadata;
 - 4) Data processing: uncertainty component linked to the quality of the data processing, taking into account potential human errors or flaws in filtering methodologies;
 - 5) Representativeness: uncertainty indicating how well the data will perform in the Measure-Correlate-Predict approach, but only linked to the length of data available (intrinsic characteristic). The evaluation is based on the Klintø model (51), where all other parameters were fixed such that a 1-year long measurement would yield a 1 % of uncertainty. As mentioned in Section 4.3.4 the 2 weeks of missing wind direction data was not found to have any significant impact on outputs. It was therefore assumed not to significantly impact uncertainty;
 - 6) Vertical extrapolation to 100 m: uncertainty of representativeness of shear or other extrapolation model up to hub height. Also could include the extent to which the hub-height wind speed is not representative of the rotor plane average wind speed;
 - 7) Horizontal extrapolation to the HKWWFZ: uncertainty characterised by the distance to site. Accounts for additional biases that could occur due to horizontal extrapolation from each of the measurement locations to the HKW location described in Table 25

The values for $u_{t,k}$ can be found in Table 26.

The correlation coefficients have to be determined. For the purpose of this study, correlation coefficients were set to 1 for uncertainty components which were found to be dependent across measurement sources and 0 for those which were found to be independent. The following uncertainties were considered independent:

- Data Quality;
- Vertical extrapolation; and
- Representativeness.

Another set of uncertainties can be considered independent, given the fact that either the measurement device or the data processor are different between two measurements:

- Instrument accuracy, which is considered independent if the measurement devices are of a different type;
- Instrument mounting, which is also considered independent if the measurement devices are of a different type; and
- Data processing, which is considered independent if the party that processed the data is different for two measurement datasets.

Finally, the uncertainties due to the horizontal extrapolation are considered to be dependent.

TABLE 26: MEASUREMENT RELATED UNCERTAINTIES FOR ALL CONSIDERED WIND MEASUREMENT SOURCES

Uncertainty Category	Independence	HKW	HKN	HKZ	MMIJ	K13	LEG (Lidar)	EPL (Lidar)	OWEZ
Instrument accuracy	Instrument	2.56 %	3.30 %	3.30 %	2.00 %	2.50 %	2.50 %	2.50 %	2.00 %
Instrument mounting	Instrument	0.50 %	0.50 %	0.50 %	1.00 %	0.50 %	0.50 %	0.50 %	2.50 %
Data quality and metadata	Independent	1.00 %	1.00 %	1.00 %	0.50 %	1.00 %	1.00 %	1.00 %	1.50 %
Data Processing	Processor	1.00 %	1.00 %	1.00 %	1.00 %	1.00 %	1.00 %	1.00 %	1.00 %
Representativeness	Independent	0.81 %	0.81 %	0.81 %	0.64 %	0.71 %	0.61 %	0.69 %	1.00 %
Extrapolation to 100 m	Independent	0.00 %	0.00 %	0.00 %	0.80 %	1.00 %	1.00 %	1.00 %	1.50 %
Horizontal extrapolation to HKWWFZ	Dependent	0.00 %	0.50 %	0.50 %	0.50 %	1.00 %	2.50 %	1.00 %	0.50 %
Total uncertainty per location	-	3.08 %	3.75 %	3.75 %	2.75 %	3.32 %	4.02 %	3.31 %	4.12 %

6.1.2. Results

Based on the methodology described above, the different measurement source uncertainties were combined with one another. As HKW represents on-site measurements they were considered as the main source of the assessment. The results of the application of the methodology described above to the pool of available measurements can be found in Table 27.

TABLE 27: COMBINED UNCERTAINTIES FOR HKW AND TWO OTHER MEASUREMENT SOURCES

Combined uncertainties	HKN	HKZ	MMIJ	K13	LEG (Lidar)	EPL (Lidar)	OWEZ
HKN		3.31	2.26	3.04	3.14	3.04	2.58
HKZ			2.26	3.04	3.14	3.04	2.58
MMIJ				2.17	2.23	2.17	2.21
K13					2.98	2.88	2.43
LEG (Lidar)						2.98	2.53
EPL (Lidar)							2.43
OWEZ							

As indicated in Table 27, the ideal combination of main sources, leading to the lowest uncertainty involves combining the measurements of HKW with those of MMIJ. The third source of measurements can be chosen between K13, LEG, EPL or OWEZ which lead to similar values, in comparison to the uncertainty of this calculation. Therefore, for the selection of the third source, an arbitrary decision was made. K13 was discarded because one measurement source (MMIJ) was already available in the same direction from HKW, but closer to it. Additionally, since the main particularity of the site is an expected (onshore to offshore) gradient, it was decided to use OWEZ to balance MMIJ, versus LEG and EPL which were also located further than OWEZ from HKW.

6.2. Vertical Extrapolation

In this section, the vertical extrapolation of the three individual selected main sources to 100 m MSL is presented. For the vertical extrapolation of the merged wind climate to other heights, the reader may refer to Section 7.1.4, where the applicable values of wind shear are detailed.

6.2.1. Wind Shear Calculation

The wind shear was calculated for each individual data source, based on 2 heights as close as possible from 100 m MSL.

Wind shear values were derived by binning measurements into several wind directions, periods of the day and periods of the year bins in order to obtain a 3D shear matrix, which is presented for MMIJ and HKW in **Annex B**. This methodology allows to account for directional variations which could have a strong diurnal and seasonal influence. This is a simplified approach to account for the potential impact of the atmospheric stability condition on the vertical extrapolation.

As for HKW, measurements were available at 100 m MSL, shear values were derived but no vertical extrapolation was required. For IJmuiden, the vertical extrapolation of the met mast measurements were validated by the LiDAR device installed on the platform.

The heights and measurement periods selected to derive shear coefficients are presented in Table 28 for each individual measurement location. The shear coefficients per wind direction are presented in Table 29 and represented graphically in Figure 25. In general, the results are in line with expected values in offshore conditions. For all measurement locations, higher values were derived for the dominant wind directions. For OWEZ, the relatively close distance to the shore seems to influence the shear coefficient for Easterly winds.

TABLE 28: WIND SHEAR CALCULATION ASSUMPTIONS FOR HKW, MMIJ AND OWEZ AT 100 M MSL

Measurement Location	Considered period	Considered heights [m MSL]	α
HKW	07/02/19 – 06/02/21	80, 100 & 120	0.09
IJmuiden Lidar	01/11/2011 - 09/03/2016	90 & 115	0.09
OWEZ	01/07/2005 - 30/06/2006	70 & 116	0.08

TABLE 29: DIRECTIONAL SHEAR COEFFICIENTS FOR THE THREE MAIN DATA SOURCES AT 100 M MSL

Shear	N	NNE	ENE	E	ESE	SSE	S	SSW	WSW	W	NNW	NNW	Average
HKW	0.03	0.03	0.03	0.06	0.06	0.09	0.10	0.13	0.11	0.07	0.05	0.04	0.09
MMIJ	0.07	0.07	0.06	0.04	0.06	0.08	0.10	0.15	0.10	0.09	0.06	0.06	0.09
OWEZ	0.04	-0.01	0.03	0.08	0.12	0.13	0.13	0.15	0.12	0.08	0.04	0.05	0.08



Figure 25: Directional shear at 100 m MSL at HKW, MMIJ and OWEZ, based on measurements

6.2.2. Short Term Wind Climates at 100 m MSL

The short-term wind climates (over the periods given in Table 10, Table 21 and Table 22) were extrapolated to 100 m MSL, which corresponds to the height that was used for the alignment with the metocean desk study (see S 7). The wind climates at each individual position are characterised by the parameters given in Table 30. Note that the corresponding measurement periods are non-concurrent.

TABLE 30: EXTRAPOLATED WIND SPEED AT 100 M MSL, FOR THE THREE MAIN DATA SOURCES

Location	Height [m MSL]	Statistical Mean wind speed [m/s]	Weibull fitted wind speed [m/s]	A parameter [m/s]	k parameter
HKW	100	10.06	10.10	11.41	2.23
MMIJ	100	10.36	10.41	11.75	2.23
OWEZ	100	9.02	9.28	10.46	2.45

6.3. Long-Term Correction

Three short-term wind climates were derived and had to be corrected to a long-term reference period using the so-called MCP (Measure Correlate Predict) method. In this assessment, a comparative analysis of three different approaches has been performed (52):

- Linear Regression with Gaussian Scatter;
- Matrix procedure; and
- Neural Network.

To complete the long-term correction, several reference data sets have been compared. These data sets have been presented in Sections 5.1.5 and 5.2.1 and are again listed hereunder:

- ERA5;
- Merra2;
- CFSv2; and
- LEG.

Apart from three reanalysis data sets, the historical data of the meteorological station of LEG has been used as a benchmark.

6.3.1. Long-term evaluation

To evaluate the performance of the MCP approach, the following KPIs were used:

- Coefficient of determination (R^2);
- Mean Average Error (MAE);
- Root Mean Square Error (RMSE); and
- Mean Bias Error (MBE).

Reference datasets are taken at the closest grid point to each of the individual locations. The exact position considered for each dataset and reference period are presented in Table 31 and illustrated by Figure 26. As indicated in the table, the covered period is different for the different datasets. This has however no implication on the studied KPIs, since only concurrent data is analysed for these. Note that the LEG dataset was not updated when the 24 months dataset at HKW was made available. This choice was made considering that:

- with the 12 months dataset correlations with other re-analysis datasets was superior
- differences in statistics between correlations with the 12 and 24 months statistics showed a marginal difference.

Therefore correlations with LEG was anticipated not to be superior to correlations with re-analysis datasets, which was confirmed by the study updated by Deltares for the 24 months dataset (15).

Table 32, Table 33 and Table 34 provide an overview of the main KPIs for each combination of reference data set and MCP approach. All statistics are given as a function of wind speed based on hourly averages. The same results can be found in **Annex C** as a function of energy.

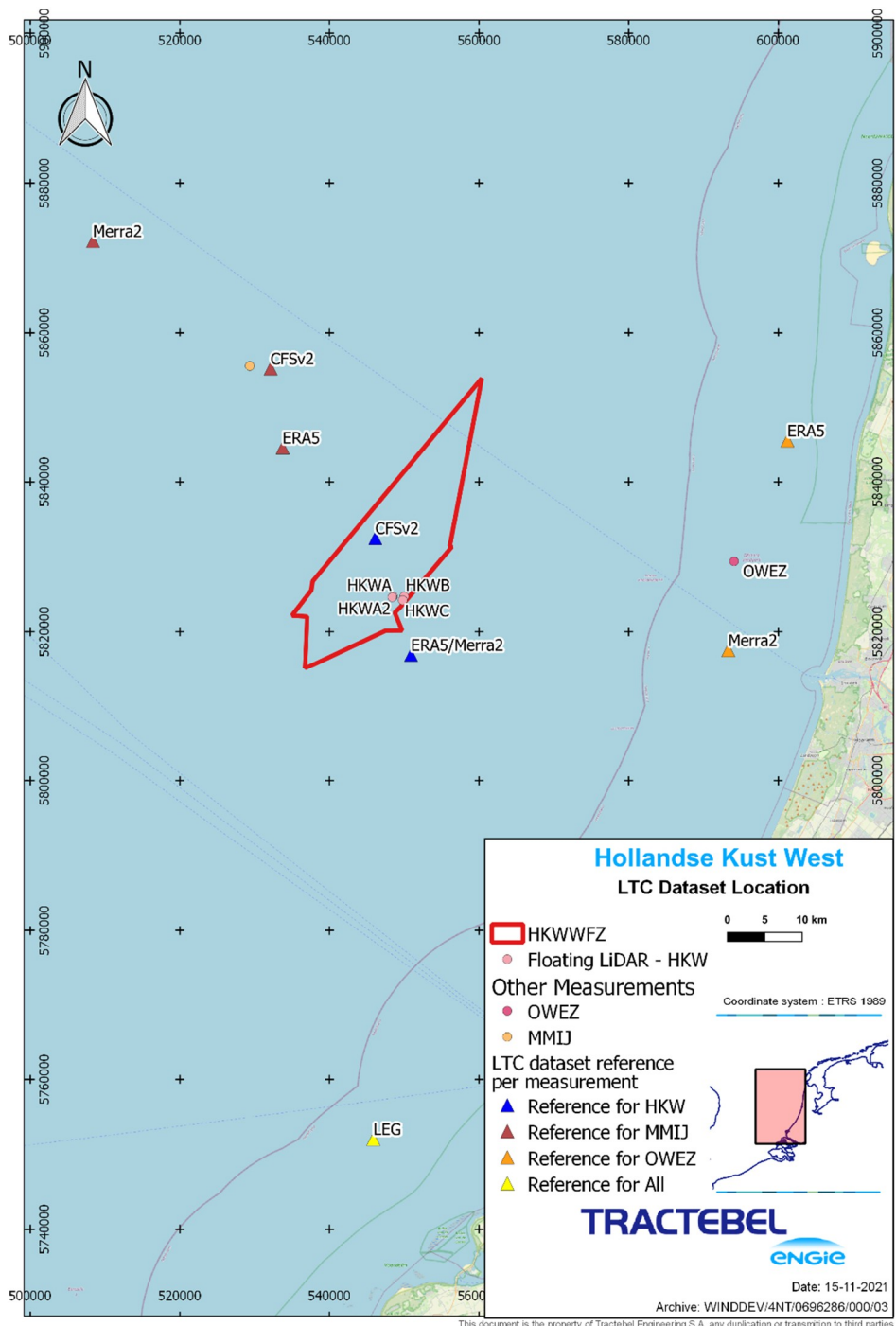


Figure 26: Illustration of the location of the reference dataset considered for the LTC

TABLE 31: GENERAL DESCRIPTION OF REFERENCE DATA SETS

Reference dataset	Location for HKW (EPSG 25831)		Location for MMIJ (EPSG 25831)		Location for OWEZ (EPSG 25831)		Time period covered		Time res.
-	Easting [m]	Northing [m]	Easting [m]	Northing [m]	Easting [m]	Northing [m]	start	end	
ERA5	550 911	5 816 916	533 748	5 844 577	601 243	5 845 515	01/11/1999	29/02/2021	1 h
Merra2	550 911	5 816 916	508 388	5 872 277	593 336	5 817 540	01/11/1999	29/02/2021	1 h
CFSv2	546 135	5 832 502	532 144	5 855 130	N/A ³	N/A	01/11/2011	29/02/2021	1 h
LEG	545 876	5 752 029	545 876	5 752 029	545 876	5 752 029	01/11/1999	29/02/2020	10 min

Reference dataset	Distance from measurements (km)		
-	HKW	MMIJ	OWEZ
ERA5	7.9	11.8	17.6
Merra2	7.9	26.9	11.9
CFSv2	8.4	2.8	N/A
LEG	72.7	104.8	91.2

TABLE 32: KPI'S OF EACH MCP APPROACH AND REFERENCE DATA SET FOR HKW

HKW					
Reference Dataset	MCP Method	MBE [%]	MAE [%]	RMSE [%]	Pearson R
ERA5	Regression	-0.20	9.76	13.20	0.961
	Matrix	0.71	9.84	12.23	0.961
	Neural Network	-0.21	9.90	13.34	0.961
Merra2	Regression	-0.22	11.35	15.24	0.948
	Matrix	0.34	11.48	15.32	0.948
	Neural Network	-0.31	11.48	15.43	0.947
CFSv2	Regression	-0.26	12.55	16.66	0.938
	Matrix	1.24	12.70	16.73	0.938
	Neural Network	-0.21	12.53	16.65	0.938
LEG	Regression	-0.48	16.34	21.33	0.885
	Matrix	1.83	16.48	21.50	0.884
	Neural Network	-0.49	16.63	21.64	0.879

³ No concurrent CFSv2 data available

TABLE 33: KPI'S OF EACH MCP APPROACH AND REFERENCE DATA SET FOR IJMUIDEN

MMIJ					
Reference Dataset	MCP Method	MBE [%]	MAE [%]	RMSE [%]	Pearson R
ERA5	Regression	-0.14	9.53	12.96	0.963
	Matrix	1.17	9.61	13.03	0.963
	Neural Network	-0.13	9.73	13.20	0.962
Merra2	Regression	-0.17	11.20	15.06	0.950
	Matrix	0.17	11.34	15.18	0.949
	Neural Network	-0.26	11.20	15.07	0.949
CFSv2	Regression	-0.20	12.30	16.30	0.941
	Matrix	1.36	12.44	16.38	0.940
	Neural Network	-0.28	12.29	16.32	0.941
LEG	Regression	-1.08	19.80	26.36	0.837
	Matrix	2.42	19.99	26.46	0.836
	Neural Network	-1.15	19.92	26.56	0.835

TABLE 34: KPI'S OF EACH MCP APPROACH AND REFERENCE DATA SET FOR OWEZ

OWEZ					
Reference Dataset	MCP Method	MBE [%]	MAE [%]	RMSE [%]	Pearson R
ERA5	Regression	-0.23	11.83	15.97	0.944
	Matrix	0.29	11.83	15.98	0.944
	Neural Network	-0.35	11.93	16.02	0.944
Merra2	Regression	-0.37	13.32	17.72	0.931
	Matrix	0.31	13.47	17.83	0.930
	Neural Network	-0.27	13.14	17.49	0.933
CFSv2	Regression				
	Matrix				
	Neural Network				
LEG	Regression	-0.50	18.70	24.55	0.862
	Matrix	-0.08	18.84	24.64	0.861
	Neural Network	-0.86	18.80	24.67	0.862

As expected, ERA5 outperforms the other reference datasets for the three measurement locations. CFSv2 was not used at the OWEZ measurement location due to a lack of overlap in the measurement period. In terms of correlation, using a meteorological station (LEG) seems a less suitable alternative as the value is significantly lower than all reanalysis data. The distinction in correlation between different reanalysis data sets is more difficult although ERA5 shows the highest value for each individual measurement location. This trend is also observed when comparing the other KPIs. ERA5 data scores better for MBE, MAE and RMSE. Consequently, ERA5 was selected as the reference long-term data set.

The trend for the different MCP methods is less obvious. The selected KPIs do not allow to clearly identify a most suitable approach as very similar values are found for each set of input data (measurement and reference data).

Another criteria that is evaluated is the fit in diurnal and monthly profiles between the measured and estimated time series. In general, Table 35,

Table 36 and Table 37 (and the graphs in **Annex C**) indicate a good agreement in monthly profile and no clear outliers are present in the results. However, the diurnal profile is significantly better estimated by the Neural Network approach as this data learning technique is specifically developed to attempt to fit the diurnal profile of the measured data.

Additionally, the impact of the LTC method on the wind speed distribution and Weibull fit was analyzed. The plots of the distribution and its Weibull fit for all 3 considered methods are given in **Annex E**, together with the difference between both. It can also be seen on the plots that the statistical mean wind speed is quite different from the Weibull mean wind speed for all 3 methods and at all 3 locations. Table 35 to Table 37 also show the R² between the long-term wind distribution and the Weibull fit. No firm conclusion can be drawn from these R² values. An evaluation of the difference in energy production between the frequency distribution and Weibull fit has been performed. This evaluation showed that the lowest difference could be found for the Neural Network method.

Based on this evaluation, the Neural Network approach combined with ERA5 were selected as the most suitable alternative for the long-term correction.

TABLE 35: CORRELATION COEFFICIENTS FOR THE DIURNAL AND MONTHLY PROFILES FOR HKW MEASURED AND ESTIMATED LTC TIME SERIES, CORRELATION COEFFICIENT BETWEEN WIND SPEED DISTRIBUTION AND WEIBULL FIT

HKW				
Reference Dataset	MCP Method	Diurnal profile R ²	Monthly profile R ²	Frequency distribution - Weibull fit R ²
ERA5	Regression	0.812	0.998	0.981
	Matrix	0.808	0.998	0.999
	Neural Network	0.883	0.998	0.999

TABLE 36: CORRELATION COEFFICIENTS FOR THE DIURNAL AND MONTHLY PROFILES FOR IJMUIDEN MEASURED AND ESTIMATED LTC TIME SERIES, CORRELATION COEFFICIENT BETWEEN WIND SPEED DISTRIBUTION AND WEIBULL FIT

MMIJ				
Reference Dataset	MCP Method	Diurnal profile R ²	Monthly profile R ²	Frequency distribution - Weibull fit R ²
ERA5	Regression	0.693	0.996	0.998
	Matrix	0.692	0.996	0.998
	Neural Network	0.823	0.996	0.994

TABLE 37: CORRELATION COEFFICIENTS FOR THE DIURNAL AND MONTHLY PROFILES FOR OWEZ MEASURED AND ESTIMATED LTC TIME SERIES, CORRELATION COEFFICIENT BETWEEN WIND SPEED DISTRIBUTION AND WEIBULL FIT

OWEZ				
Reference Dataset	MCP Method	Diurnal profile R ²	Monthly profile R ²	Frequency distribution - Weibull fit R ²
ERA5	Regression	0.673	0.995	0.996
	Matrix	0.671	0.995	0.994
	Neural Network	0.827	0.995	0.994

6.3.2. Long-Term Wind Climate

The long-term statistical and Weibull-fitted average wind speeds at each measurement location and at 100 m MSL are presented in the following table. The 20 years period (from the 31/10/1999 to the 31/10/2019) used for the report with 12 months of data was retained for the long-term climate in order to avoid potential changes due to the choice of a different long-term reference period. Note that the Weibull fitted wind speed presented in this table at the HKW site is of 9.74 m/s, which happens to be equal to the long-term wind speed at the HKWWFZ centre. This is a coincidence, as it is the combination of statistical mean wind speeds at HKW, MMIJ and OWEZ extrapolated horizontally with the DOWA mesoscale model which lead to the long-term wind speed at the HKWWFZ centre.

TABLE 38: LONG-TERM WIND SPEEDS AT 100 M MSL AT THE MAIN MEASUREMENT DATASET LOCATIONS

Site Measurement	Height [m MSL]	Considered period	Statistical mean wind speed [m/s]	Weibull fitted wind speed [m/s]
HKW	100	31/10/1999 – 31/10/2019	9.58	9.74
MMIJ	100	31/10/1999 – 31/10/2019	9.91	10.05
OWEZ	100	31/10/1999 – 31/10/2019	9.49	9.60

The long-term Weibull parameters per wind direction sector are presented in the following tables.

TABLE 39: LONG-TERM WEIBULL PARAMETERS AND FREQUENCY BY SECTOR AT 100 M MSL [HKW]

Sector	A parameter [m/s]	k parameter	Frequency [%]	Weibull fitted wind speed [m/s]
N	9.22	2.32	6.61	8.17
NNE	9.17	2.45	6.19	8.13
ENE	9.80	2.70	6.85	8.72
E	9.76	2.50	6.61	8.66
ESE	9.08	2.35	5.06	8.05
SSE	9.10	2.25	4.88	8.06
S	11.63	2.39	7.73	10.31
SSW	13.20	2.59	13.54	11.72
WSW	12.77	2.60	15.55	11.34
W	11.43	2.31	10.46	10.13
WNW	10.62	2.27	8.62	9.41
NNW	10.18	2.24	7.91	9.01
Average	11.00	2.30	100.00	9.74

TABLE 40: LONG-TERM WEIBULL PARAMETERS AND FREQUENCY BY SECTOR AT 100 M MSL [MMIJ]

Sector	A parameter [m/s]	k parameter	Frequency [%]	Weibull fitted wind speed [m/s]
N	9.32	2.26	6.19	8.25
NNE	9.22	2.46	5.64	8.18
ENE	10.09	2.63	6.42	8.97
E	10.32	2.54	6.57	9.16
ESE	9.82	2.40	5.22	8.70
SSE	10.05	2.29	5.24	8.91
S	12.04	2.34	8.46	10.67
SSW	13.51	2.63	15.09	12.00
WSW	12.88	2.60	14.43	11.44
W	11.70	2.27	10.59	10.37
WNW	10.71	2.26	8.60	9.49
NNW	10.36	2.18	7.56	9.17
Average	11.35	2.31	100	10.05

TABLE 41: LONG-TERM WEIBULL PARAMETERS AND FREQUENCY BY SECTOR AT 100 M MSL [OWEZ]

Sector	A parameter [m/s]	k parameter	Frequency [%]	Weibull fitted wind speed [m/s]
N	8.67	2.51	5.70	7.70
NNE	8.67	2.78	5.66	7.72
ENE	9.18	2.75	6.70	8.17
E	9.33	2.66	7.18	8.30
ESE	8.75	2.51	5.08	7.76
SSE	9.21	2.30	4.96	8.16
S	11.55	2.27	8.29	10.23
SSW	13.50	2.58	13.99	11.99
WSW	12.77	2.31	14.81	11.32
W	11.33	2.15	10.67	10.03
WNW	10.18	2.22	9.45	9.02
NNW	9.93	2.17	7.51	8.80
Average	10.84	2.20	100	9.60

The following figure shows the Weibull fit and the measured frequency distribution of the wind speed for the LTC wind climate at the HKW location.

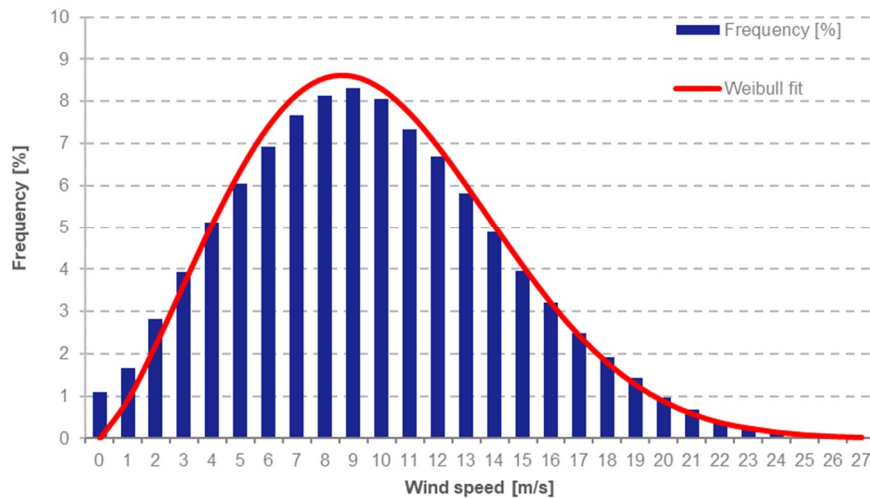


Figure 27: Frequency distribution and Weibull fit for LTC wind climate at HKWWFZ

Table 38 shows that in terms of mean wind speed, the Weibull fit is not fitting well with the measured wind speed. As discussed in 6.3.1 and in **Annex E**, this is not directly linked to the methodology that was used to perform the LTC, but is rather linked to the measured wind climate on site. This is also presented in Section 4.4.2 when comparing the short-term wind climate histogram and Weibull distribution fit, although, by coincidence, the statistical and Weibull average do agree well. By looking at the plots presented in **Annex E**, it seems however that the Neural Network method results in an acceptable agreement between frequency distribution and Weibull fit.

6.4. Horizontal Extrapolation

As basic linear models are not able to capture the horizontal gradient between the coast and (far) offshore, the horizontal extrapolation is accomplished by means of a mesoscale model. As presented in Section 5.2.2, different models are available in the Dutch North Sea and a suitable validation approach must be derived.

Section 6.4.1 below details the methodology that was used for the validation, which was developed with the support of the Environmental and Applied Fluid Dynamics Department of the Von Karman Institute (Professor Jeroen Van Beeck and Sophia Buckingham).

Section 6.4.2 details the methodology that was used for the horizontal extrapolation from measurement locations to the selected nodes.

6.4.1. Mesoscale Model Selection

To select the most suitable mesoscale model to perform the horizontal extrapolation, the different models are validated against the numerous measurement campaigns that have been performed in the Dutch North Sea.

The characteristics of the different available models have been presented in Section 5.2.2 and are listed below:

- KNW
- DOWA
- NEWA
- 3TIER-ERA5
- EMD-WRF-ERA5

In an attempt to reduce uncertainty, an ensemble model of the various datasets is also produced by the combination of the various datasets above.

The performance of each model were evaluated using the measurement campaigns presented in Table 42. All these measurement campaigns are taken at or extrapolated to 100 m MSL, which is the reference height at the 6 nodes and a model height available for each of the mesoscale models. As the mesoscale data sets were not available at the exact position of each measurement station, the timeseries of the 4 closest nodes were interpolated based on an inverse distance weighting approach. To avoid any bias due to long-term correction, and as opposed to previous assessments in the Dutch North Sea (25) (26), measured data were compared to mesoscale data on a short-term basis. The corresponding measurement periods are indicated in Table 42 as well. In order to avoid any seasonal bias full years of concurrent data were used, when available. However, a few combinations (e.g. measured OWEZ versus mesoscale NEWA data) required an extension of the mesoscale data based on an MCP approach.

TABLE 42: MEASUREMENT PERIODS CONSIDERED FOR MESOSCALE SELECTION

Measurement location	Period Considered
HKW	07/02/2019 – 06/02/2021
HKN	01/01/2018 – 31/12/2018
HKZ	04/06/2016 – 03/06/2018
IJmuiden	01/01/2012 – 31/12/2015
OWEZ	01/07/2005 – 30/06/2006
EPL Lidar	01/01/2017 – 31/12/2018
LEG Lidar	01/01/2015 – 31/12/2018
K13	01/01/2017 – 31/12/2018

In this wind resource assessment, the mesoscale data set is used exclusively for the horizontal extrapolation of the selected measurement sources throughout the Wind Farm Zone (WFZ). Consequently, the evaluation of the most suitable model is specifically focused on validation of the horizontal gradient and this must be reflected in the derived evaluation metrics. At each one of the identified locations, the following evaluation was made between modelled and measured data:

- Comparison of the bias at each measurement location with the mean bias over all the locations both in average wind speed and wind direction:
 - Ensuring the horizontal wind speed distribution is sufficiently represented by the mesoscale model;
- Correlation coefficient of the wind speed and direction of each individual measurement station:
 - Ensuring the mesoscale time series capture the variations of the individual measured time series;
- Comparison of the energy rose at each individual measurement station; and
 - Ensuring the mesoscale time series represent the energy rose of the individual measured time series.

To ensure that reliable on-site measurements have a larger influence than low-quality measurements further away from the site, a weight was derived per measurement location. This weight was applied to the above evaluation metrics. Weights were derived based on the inverse of the uncertainty (see Table 26), with the uncertainty derived as presented in Section 6.1.1. Table 43 provides the weight of each individual measurement location.

TABLE 43: WEIGHTS OF MEASUREMENT LOCATIONS

Measurement location	Weight
HKW	0.140
HKN	0.115
HKZ	0.115
IJmuiden	0.157
OWEZ	0.105
EPL Lidar	0.130
LEG Lidar	0.107
K13	0.130

The resulting metrics for each model are presented in Table 44. Detailed results per location can be found in **Annexes F, G and H**. For the defined metrics, NEWA and 3TIER-ERA5 show the lowest performance, as illustrated by values in red in Table 44. The other models show a relatively similar performance. KNW shows a slightly lower performance than DOWA; which was expected as DOWA was designed to improve on KNW using a more advanced mesoscale model (improved version of the Harmonie model) and more advanced reanalysis input data (ERA5 compared to ERA-Interim) (46). Although not specifically developed for the Dutch North Sea, EMD-WRF-ERA5 was found to perform similarly to DOWA for the defined metrics. The ensemble model was found to perform well compared to other datasets albeit with negligible impact on final results. Given these slight differences between the best models, DOWA, which is the most recent model designed for the North Sea, was chosen as the reference model for the horizontal extrapolation.

TABLE 44: WEIGHTED RESULTS; FIGURES IN RED SHOW NUMBERS THAT REFLECT A LOWER PERFORMANCE COMPARED TO OTHER MODELS

Measured parameter	Metric	Mesoscale model					
		KNW	DOWA	NEWA	3TIER-ERA5	EMD-WRF-ERA5	Ensemble
Average wind speed	Bias Wave - Average Bias [m/s]	0.008	0.008	0.007	0.016	0.007	0.008
	Correlation [r]	0.87	0.88	0.81	0.90	0.88	0.90
Average wind direction	Bias dave - Average Bias [°]	1	1	1	1	1	1
	Correlation [r]	0.90	0.91	0.85	0.88	0.91	0.92
Energy rose	Bias f ave [°]	5	6	7	6	7	6

6.4.2. Extrapolation to nodes

An essential part of this assignment is to align the estimated wind resource with the metocean desk study performed by DHI (see Section 7). For the alignment, six (6) nodes have been defined and the selected mesoscale data was used to extrapolate the three reference long-term time series presented in Section 6.3 to these site nodes. The exact position of each node is described in Table 45 and graphically shown in Figure 28.

TABLE 45: LOCATION OF THE NODES

Nodes	Location [EPSG 25831]	
-	Easting [m]	Northing [m]
HKW LiDAR	549 250	5 824 678
S30	540 612	5 830 154
S2	548 886	5 840 067
S22	558 354	5 851 409
S23	559 589	5 849 713
S24	556 675	5 834 446

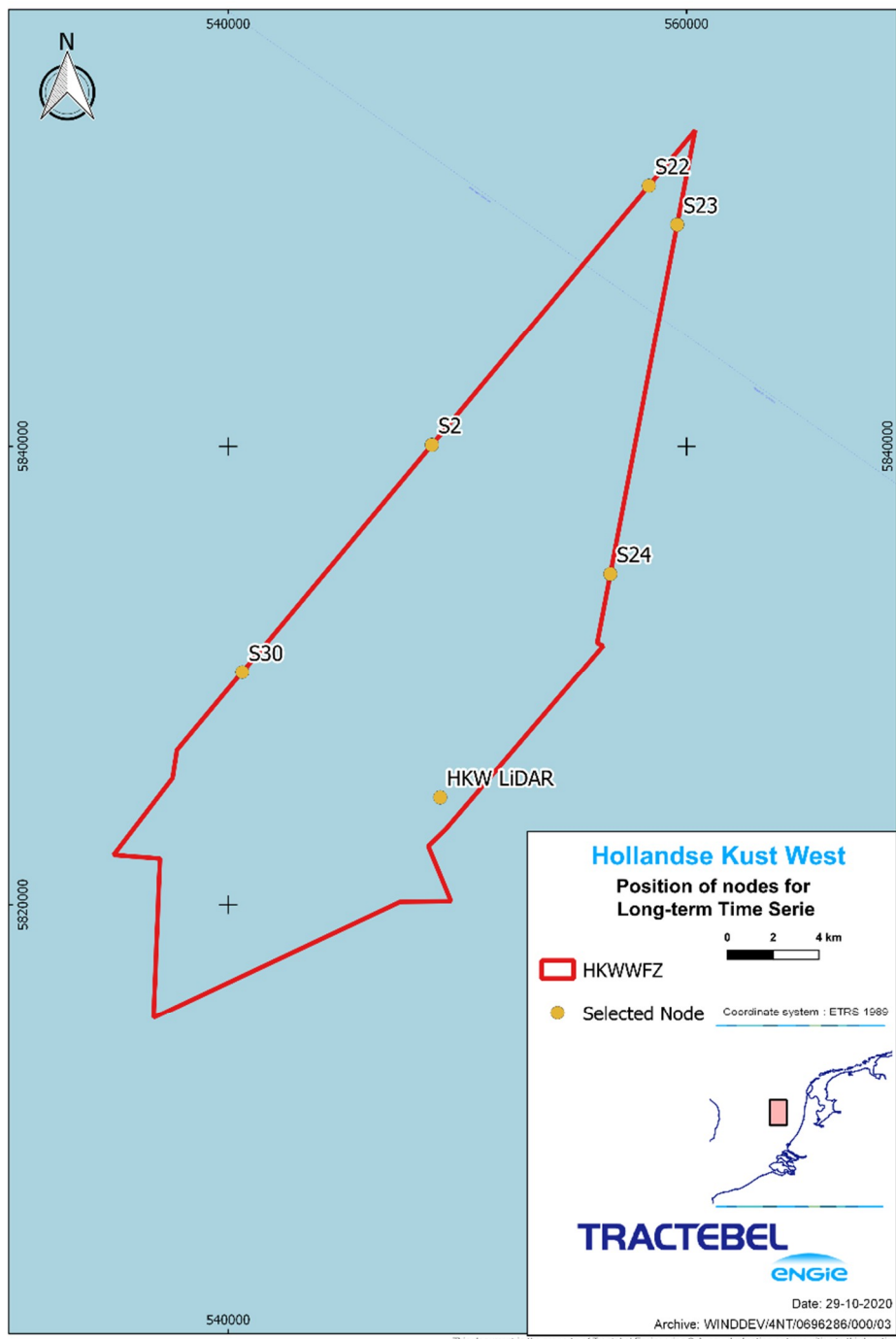


Figure 28: Illustration of the node locations

In order to extrapolate long-term wind climates presented in Section 6.3.2 to node locations, the following steps were undertaken at each node:

- the DOWA mesoscale model was used to derive sector-wise speed-up ratios between the node and measurement locations HKW, MMIJ and OWEZ;
- long-term time series at HKW, MMIJ and OWEZ were extrapolated to the node location based on these sector-wise speed-up ratios;
- Each one of the resulting timeseries was assigned a weight computed as the inverse of the uncertainty on wind speed estimated for this timeseries, as detailed in Section 6.1.1 and in Section 6.5 below;
- The three timeseries were finally sum-weighted to lead to a final time-series at the target node.

Table 46 illustrates this process for the main HKW LiDAR node. Long-term time series of wind speed and direction at HKW, MMIJ and OWEZ with statistical mean wind speeds of 9.58, 9.91, and 9.49 m/s respectively, were used. These time-series were extrapolated horizontally to the HKW LiDAR node using sector-wise speed-up ratios from the DOWA mesoscale model. This led to three time series with average wind speeds of 9.58, 9.80, and 9.85 m/s. These three time series were sum-weighted using weights of 0.35, 0.39 and 0.26 for time series originating from HKW, MMIJ and OWEZ, respectively. This led to a resulting time series with an average wind speed of 9.74 m/s. Table 46 shows that individual wind speed estimates from HKW, MMIJ and OWEZ are within 1.6% of the final wind speed estimate, i.e. within the range of expected uncertainties detailed in Sections 6.1.1 and 6.5 below.

TABLE 46: ILLUSTRATION OF THE EXTRAPOLATION TO THE MAIN HKW NODE

Site Measurement	Statistical mean wind speed at 100 m MSL [m/s]	DOWA mean wind speed at 100 m MSL, at source location [m/s]	Wind speed extrapolated to HKW at 100 m MSL [m/s]	Weights	Difference with sum-weighted wind speed
HKW	9.58	9.73	9.58	0.35	-1.6%
MMIJ	9.91	9.83	9.80	0.39	0.8%
OWEZ	9.49	9.39	9.85	0.26	1.0%

6.5. Uncertainty Assessment

In addition to the uncertainties presented in Section 6.1.1, several new uncertainties have been introduced by converting the measurements to long-term wind climates at the different locations and extrapolating them to 100 m MSL. The uncertainties related to the vertical extrapolation were already introduced in Section 6.1.1.

The long-term correction also introduced a set of uncertainties:

- Interannual variability: uncertainty regarding whether the true long-term mean wind speed will occur over the project life; and
- Reference Site (MCP): correlation uncertainty and uncertainty associated with consistency and quality of long-term references, measured or modelled.

Since the same reference dataset (ERA5) was used for all LTCs, the uncertainties related to the LTC are considered to be dependent.

Additionally, an additional horizontal extrapolation uncertainty is introduced, accounting for the extrapolation within the HKWWFZ itself.

The final uncertainties for each one of the wind datasets are provided in Table 47 which also indicates the independence condition of each uncertainty component.

These uncertainties were then combined following the methodology described in 6.1.1, similarly to what was done for the wind climate.

This approach yields a total uncertainty of 3.22 % on predicted mean wind speeds at 100 m MSL.

TABLE 47: CONSIDERED UNCERTAINTIES

Uncertainty Category	#	Sub category	Effect on	Independance	Value (in σ)		
					HKW	MMIJ	OWEZ
1. Site measurement	1a	Instrument accuracy	wind speed	Instrument	2.56 %	2.0 %	2.0 %
	1b	Instrument mounting	wind speed	Instrument	0.5 %	1.0 %	2.5 %
	1c	Data quality and metadata	wind speed	Independent	1.0 %	0.5 %	1.5 %
	1d	Data Processing	wind speed	Processor	1.0 %	1.0 %	1.0 %
2. Historic wind resource	2a	Representativeness	wind speed	Independent	0.81 %	0.6 %	1.0 %
	2b	Reference Site (MCP)	wind speed	Reference Dataset	2.0 %	1.9 %	2.8 %
3. Vertical extrapolation	3a	Extrapolation to 100 m	wind speed	Independent	0.0 %	0.8 %	1.5 %
4. Future wind variability	4a	Interannual variability (20 year uncertainty)	wind speed	Dependent	0.7 %	0.7 %	0.9 %
5. Spatial variation	5a	Horizontal extrapolation to HKWWFZ	wind speed	Dependent	0.0 %	0.5 %	0.5 %
	5b	Horizontal extrapolation within HKWWFZ	wind speed	Dependent	0.5 %	0.5 %	0.5 %
Combined Uncertainty				wind speed	3.22 %		

7. WIND FARM ZONE WIND CLIMATE

One single time series at 100 m was created at each one of the six pre-defined site nodes. These time series were created by:

- using the three identified main data sources HKW, MMIJ and OWEZ;
- using the DOWA mesoscale model to derive the sector-wise speed-up ratios between the individual site nodes and measurement locations HKW, MMIJ and OWEZ;
- extrapolating each time series based on these ratios to the site nodes; and
- merging the timeseries based on a weight derived from the measurement uncertainty.

Each of these steps has been described in Section 6. The following sections describe the results of this estimated wind climate, the expected stability conditions, the alignment with DHI and finally the uncertainties associated with this wind climate.

Additional time series at 10, 60, 120, 160, 200, 250 and 300 m are extrapolated from the 100 m time series applying the shear coefficient described in 7.1.4. These time series are published on the client RVO's website.

7.1. Wind Climate

7.1.1. Wind Speed

The long-term wind climates for each one of the six selected nodes at 100 m MSL are characterised by the parameters presented in Table 48. Monthly averaged wind speeds for the complete considered period are provided in **Annex I**.

As expected, the wind speeds at the nodes closer to shore (S24 & HKW) are lower than the ones further away, which follows the trend of the various wind atlas and mesoscale models available in the Dutch North Sea.

TABLE 48: MEASURED WIND SPEED

Anemometer	Height [m MSL]	Considered period	Statistical mean wind speed [m/s]
HKW	100	01/11/1999 – 01/11/2019	9.74
S2	100	01/11/1999 – 01/11/2019	9.77
S22	100	01/11/1999 – 01/11/2019	9.77
S23	100	01/11/1999 – 01/11/2019	9.76
S24	100	01/11/1999 – 01/11/2019	9.73
S30	100	01/11/1999 – 01/11/2019	9.78

7.1.2. Weibull Distribution

The long-term wind climates at the location of the six selected nodes at 100 m MSL are characterised by the Weibull parameters presented in Table 49. Detailed Weibull parameters and frequency by sector for site node HKW location are presented in Table 50. The detailed results of the five other nodes presented in Annex I.

TABLE 49: WEIBULL PARAMETERS AT THE 6 NODE LOCATIONS

Anemometer	Height [m MSL]	Weibull fitted wind speed [m/s]	A parameter [m/s]	k parameter
HKW	100	9.84	11.10	2.316
S2	100	9.87	11.14	2.320
S22	100	9.87	11.14	2.321
S23	100	9.86	11.13	2.321
S24	100	9.83	11.10	2.319
S30	100	9.87	11.15	2.316

TABLE 50: LONG-TERM WEIBULL PARAMETERS AND FREQUENCY BY SECTOR AT 100 M MSL – NODE HKW LIDAR

Sector	A parameter [m/s]	k parameter	Frequency [%]	Mean wind speed [m/s]
N	9.12	2.38	5.98	8.09
NNE	9.29	2.63	5.94	8.25
ENE	9.96	2.75	7.00	8.86
E	9.89	2.61	6.67	8.79
ESE	9.24	2.46	4.92	8.20
SSE	9.38	2.33	4.78	8.31
S	11.70	2.38	7.64	10.37
SSW	13.29	2.63	14.26	11.81
WSW	12.89	2.54	15.88	11.44
W	11.46	2.26	10.67	10.15
WNW	10.42	2.30	8.72	9.23
NNW	10.08	2.23	7.55	8.93

The following figure shows the Weibull fit overlaid on the frequency distribution of the wind speed at 100 m MSL.

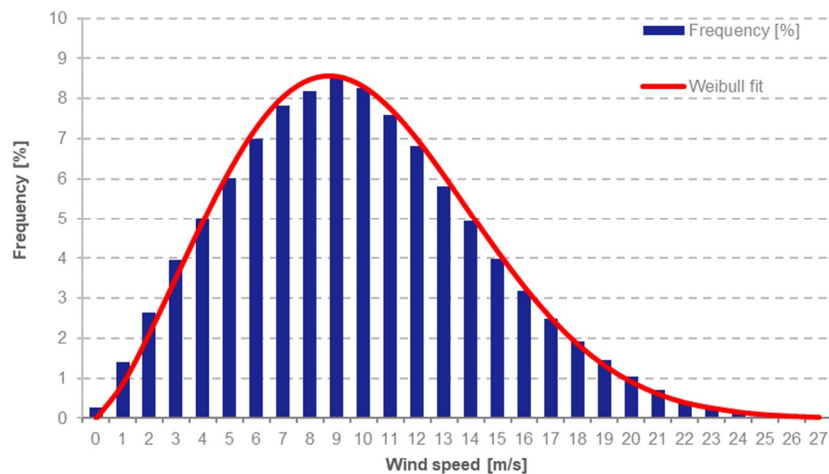


Figure 29: Frequency distribution and Weibull fit – Node HKW LiDAR

Table 48 and Table 49 show that in terms of mean wind speed the Weibull fit is not fitting well with the measured wind speed. As developed in 6.3, all LTC methods seem to result in the same mismatch.

7.1.3. Wind Direction

The following figures show the frequency and energy roses for the HKW LiDAR node location. As the wind rose and energy rose of the five other nodes are similar, the wind roses for all the selected nodes are presented in **Annex I**. The SSW and WSW wind directions provide the largest amount of wind energy (17.4 % and 19.4 % respectively).

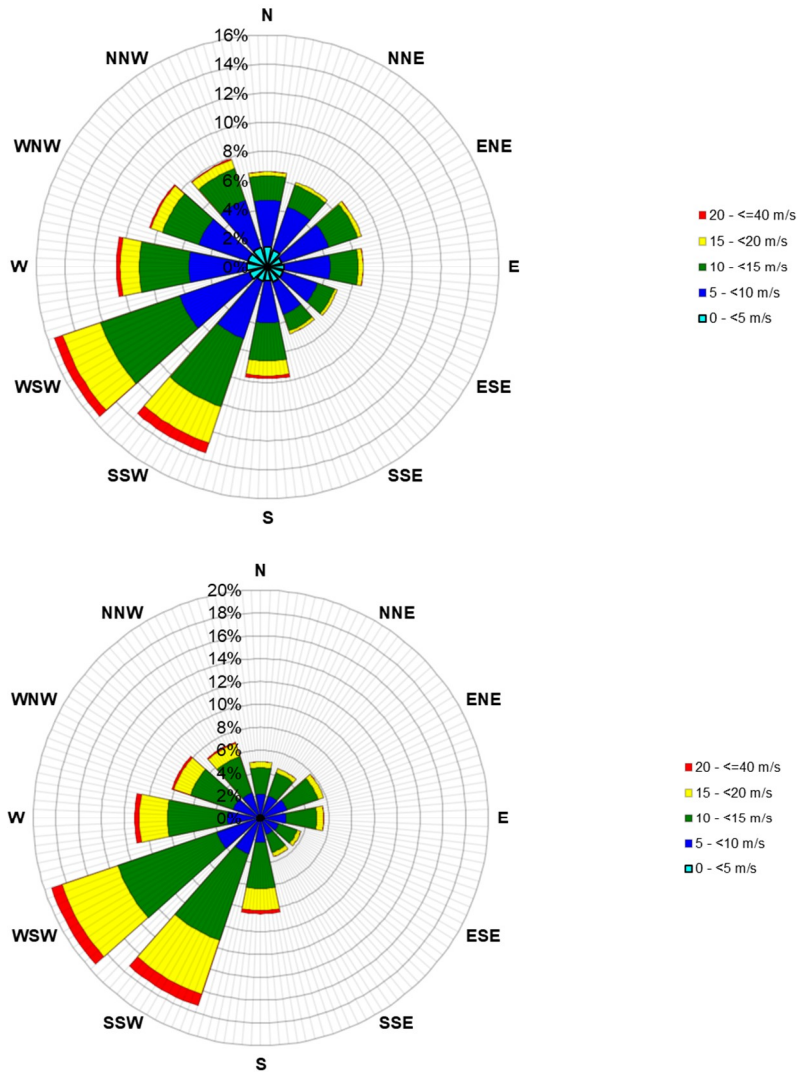


Figure 30: Frequency (top) and energy (bottom) roses at 100 m MSL – Node HKW LiDAR

7.1.4. Wind Shear

Wind shear at the six selected nodes is based on measured wind shear at HKW. The shear considered for the six nodes is described by sector in Table 51 and presented graphically in Figure 31. Wind shear is relatively high in the main wind directions; this is confirmed by measurements from other sources such as the IJmuiden met mast, see Section 6.2.1.

TABLE 51: WIND SHEAR POWER LAW EXPONENT BY SECTOR

Mast ID	α
N	0.03
NNE	0.03
ENE	0.03
E	0.06
ESE	0.06
SSE	0.09
S	0.1
SSW	0.13
WSW	0.11
W	0.07
WNW	0.05
NNW	0.04

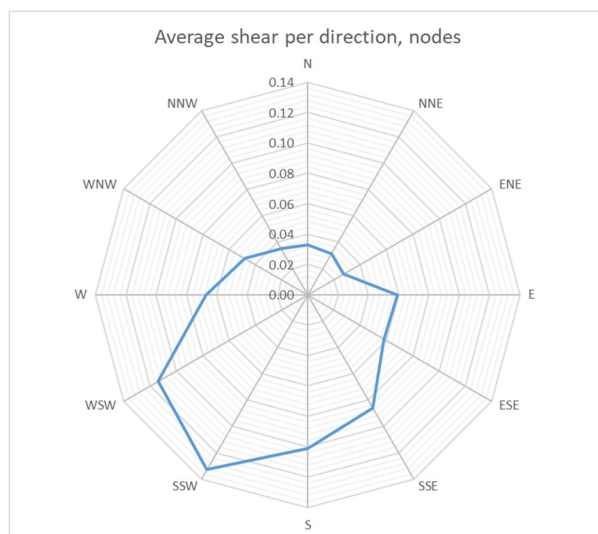


Figure 31: Directional shear at 100 m MSL at the 6 node locations

7.1.5. Diurnal and Monthly Profiles

The following figures show the typical daily and seasonal patterns of wind speed versus wind direction at 100 m MSL at the HKW LiDAR node.

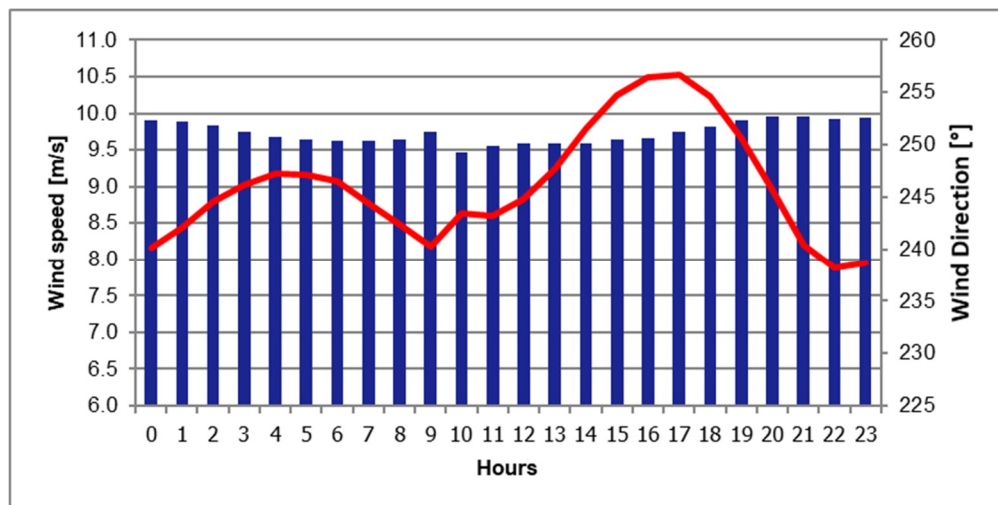


Figure 32: Diurnal profile of wind speed (blue) vs. wind direction (red) at 100 m MSL – HKW LiDAR Node

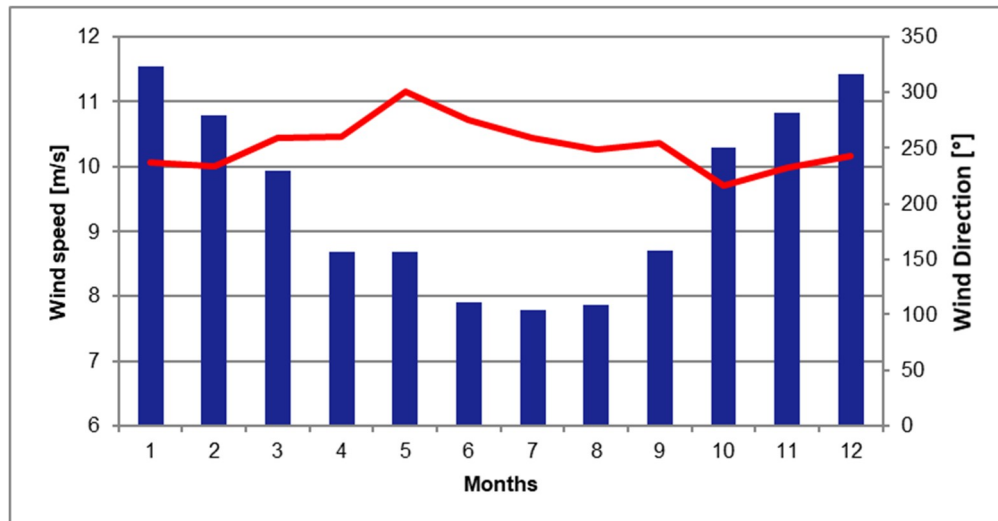


Figure 33: Monthly profile of wind speed (blue) vs. wind direction (red) at 100 m MSL – HKW LiDAR Node

The following figures present the variation of the daily and monthly mean wind speed of the 6 nodes. The variation of the pattern from node to node are very limited and the detailed results for the 5 other nodes are presented in **Annex I**.

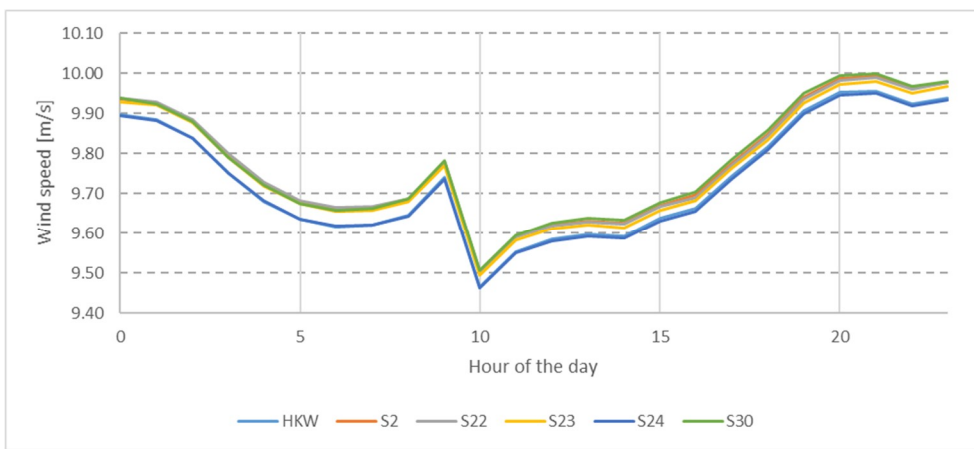


Figure 34: Diurnal profiles of wind speed at 100 m AMSL – All nodes

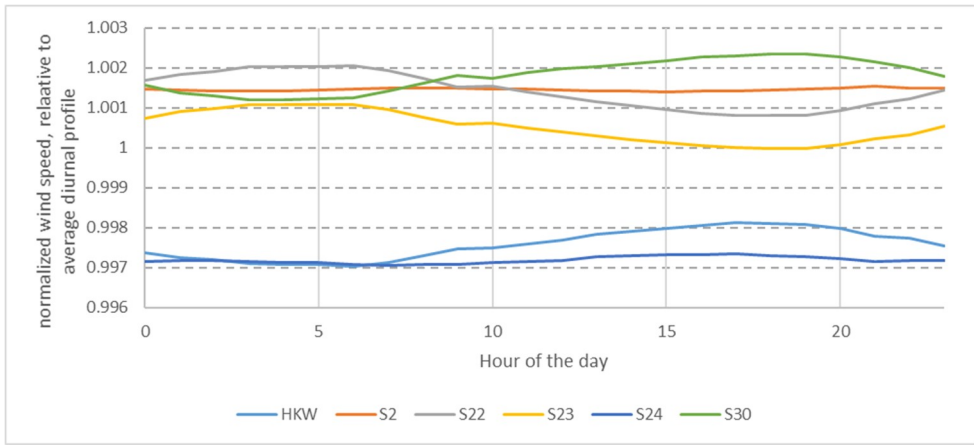


Figure 35: Diurnal profiles of wind speed normalised at 100 m MSL – All nodes

Wind speed is higher during the night from 10pm until 3pm before decreasing during the day to reach a minimum value of 9.26 m/s.

The highest wind speeds are predicted to occur during the autumn and winter season (from October to March).

The jump in wind speed that can be seen in Figure 34 between 10 and 11am is due to a mismatch between ERA5 data assimilation cycles (that run from 10am to 9pm UTC and 10pm to 9am UTC): for each new cycle the model uses an initial state that does not necessarily correspond to the end state of the previous cycle. This had already been observed for previous WRAs (25). As DOWA is derived from ERA5 data (cf. 5.2.2.2), this mismatch between assimilation cycles impacts the daily profile of the long-term wind climate calculated.

7.2. Stability Conditions

7.2.1. Stability classification

The stability conditions of the offshore site were assessed based on online ERA5 environmental data. These conditions were assessed for a period concurrent with the available measurement data at met mast IJmuiden, from the 01/01/2012 to the 21/12/2015. The stability was calculated based on the inverse of Obukhov length ($1/L$) and classified in three main categories : Stable, Neutral and Unstable.

TABLE 52: CLASSIFICATION OF STABILITY BASED ON THE $1/L$ VALUE

MOL	$1/L < -0.005$	$-0.005 < 1/L < 0.005$	$1/L > 0.005$
Stability Class	Unstable	Neutral	Stable
Weight (%)	17.7 %	45.0 %	37.3 %

Figure 36, Figure 37 and Figure 40: Monthly variation of the shear at 100 m at the IJmuiden met mast location

Table 50 represents the percentage of time associated with each one of the conditions.

Figure 34 represent the diurnal, monthly and directional variation of the stability conditions in the vicinity of the zone of interest.

The figures show a predominance of neutral and unstable conditions versus stable conditions, which is expected offshore (stable conditions would typically be expected to be more frequent onshore).

As expected, while the frequency of neutral conditions remains mostly unchanged, the climate shows slightly more stable conditions during the night (from 17 until 4 UTC) than during the day. The amplitude of the diurnal variation is representative of offshore conditions; by contrast onshore conditions could typically show 80 % of unstable conditions around mid-day, and 80 % of stable conditions during the night. Similarly the monthly pattern shows a limited amount of stable conditions, with limited amplitude, which is expected onshore and contrasts with what would be expected onshore, where stable conditions could typically be over 50 % during Winter and unstable conditions around 50 % during Summer.

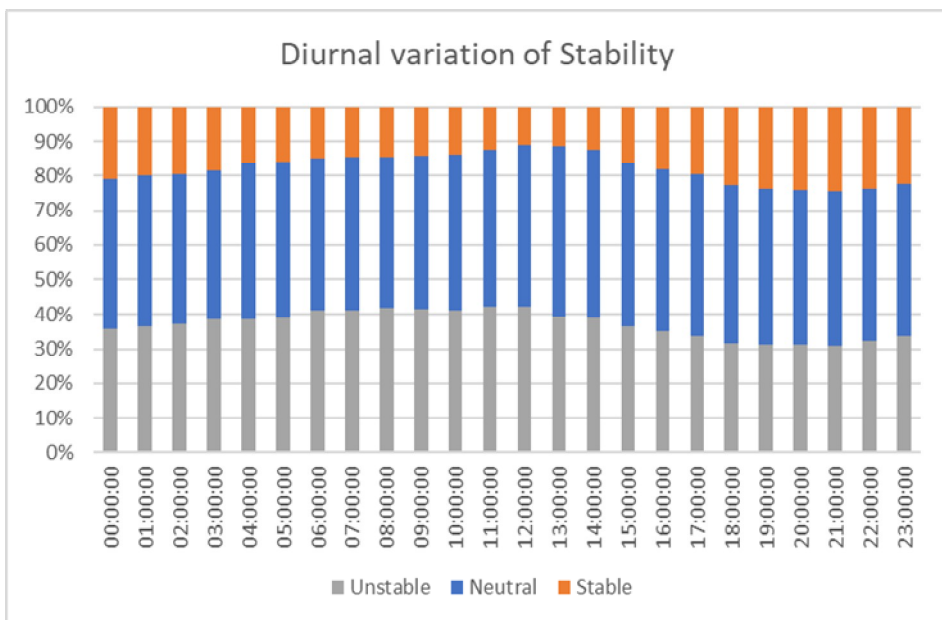


Figure 36: Diurnal variation of stability at the IJmuiden met mast location

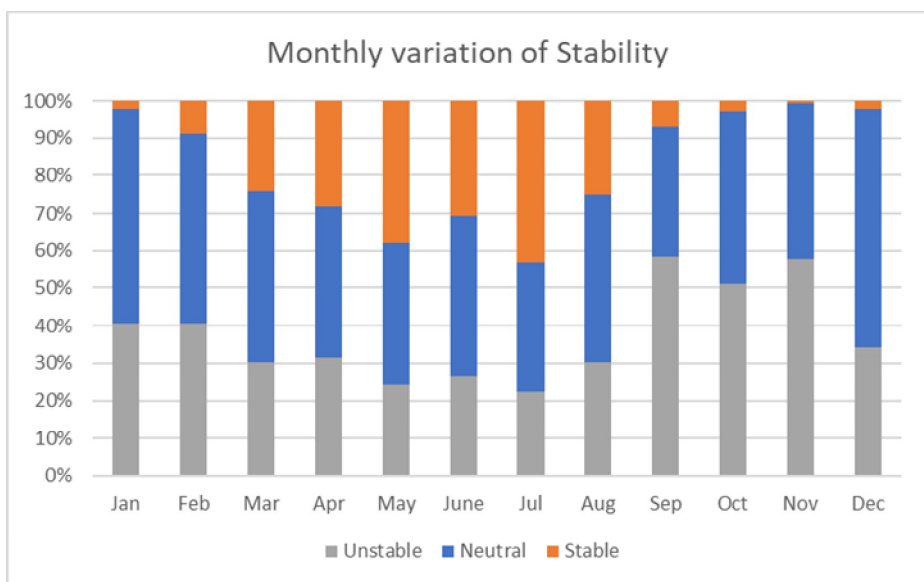


Figure 37: Monthly variation of stability at the IJmuiden met mast location

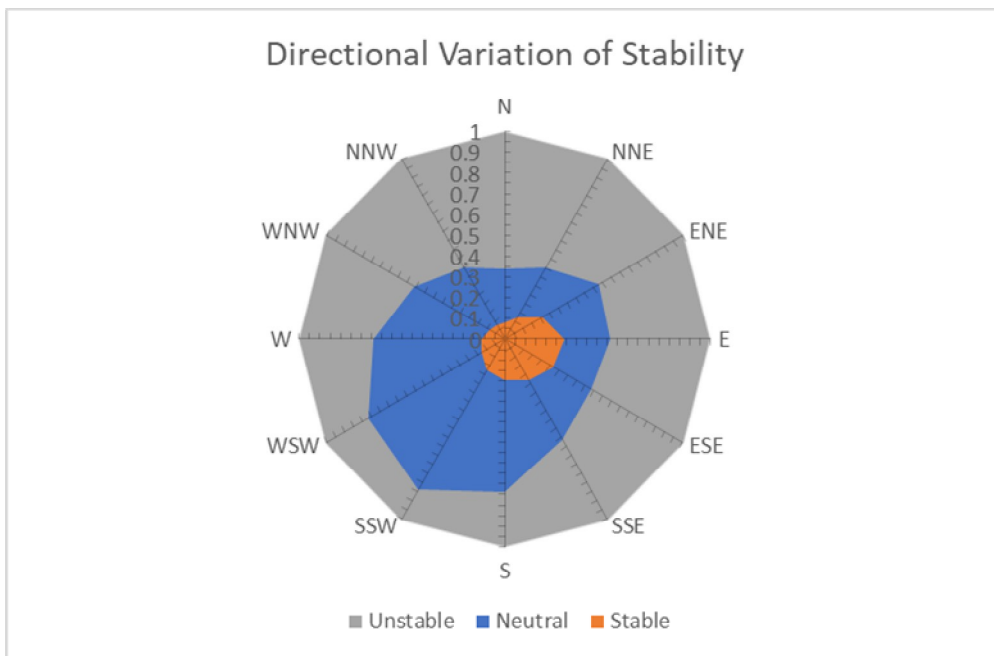


Figure 38: Directional variation of stability at the IJmuiden met mast location

7.2.2. Link with shear values

The shear matrices have been used to investigate a possible link with the stability conditions at the wind farm site.

By comparing with the directional shear variation presented in 7.1.4 with the one shown in Figure 38, it can be seen that the highest shear values are reached in the direction with the least instability and the most neutral conditions. According to this figure, the directions with the lower shear values (ENE, E and ESE) correspond to the least unstable conditions.

Similarly, the diurnal and monthly profiles of the wind shear described in **Annex B** and presented graphically in Figure 39 and Figure 40 can be compared with the stability shown in Figure 36 and Figure 37.

The general trend indicates that the shear is higher between 5pm (17) and 4am (especially between August and March). Similarly, Figure 36 shows that the climate tends to be slightly more stable during this period.

When looking at the monthly (or seasonal) evolution of wind shear, the highest values can be seen during spring and summer (March to August) when the atmosphere tends to be more stable, see Figure 37.

Diurnal, seasonal and directional variations of wind shear are therefore in line with stability variations, although the comparison does not use concurrent periods as wind shear was calculated based on the short-term measured wind climate while stability conditions were derived from 20 years of ERA-5 data.

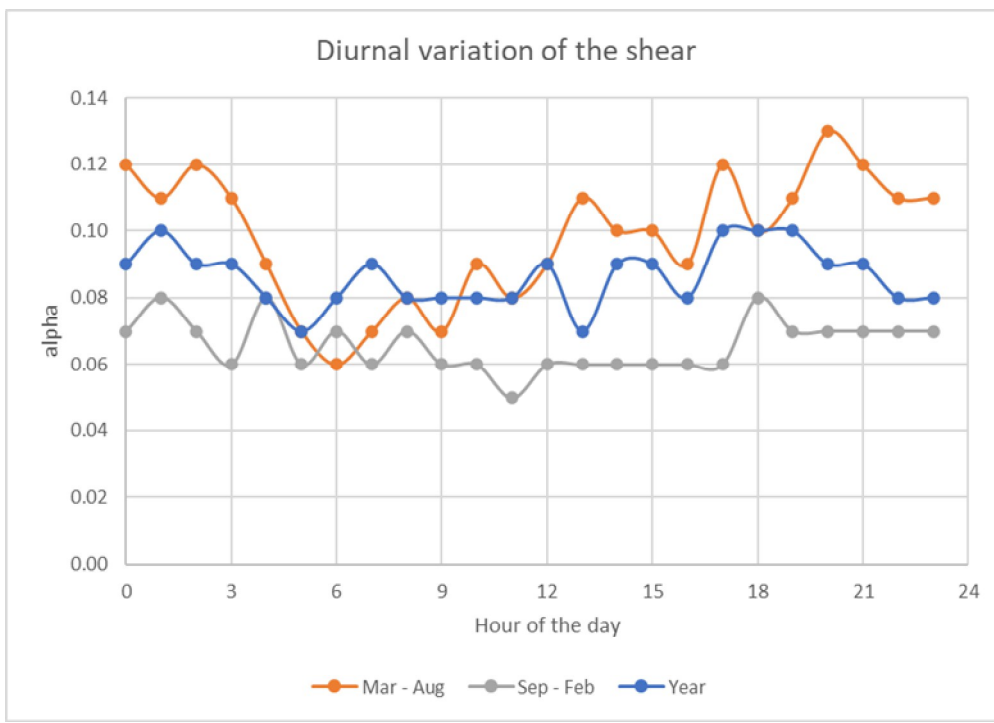


Figure 39: Diurnal variation of wind shear at 100 m at the IJmuiden met mast location

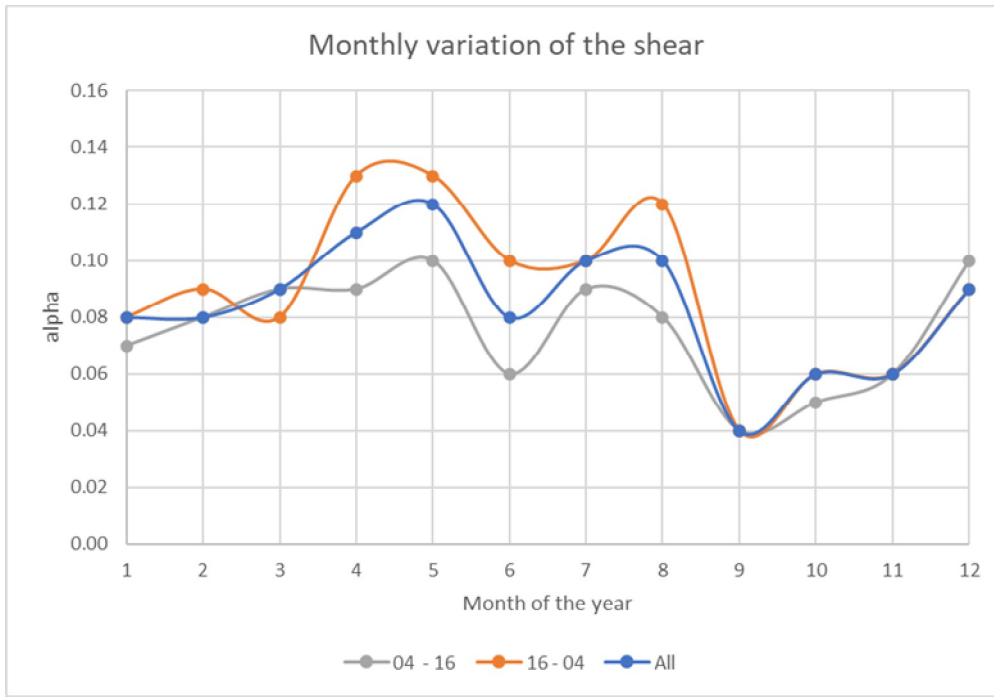


Figure 40: Monthly variation of the shear at 100 m at the IJmuiden met mast location

7.3. Comparison with other Sources

In the following, the wind climate presented in Section 7.1 will be compared with wind climates from several other sources, in the same region (Dutch North Sea).

7.3.1. Alignment with MetOcean Desk Study

In order to provide comfort to the user, part of the assignment consisted in aligning the estimated wind resource, by means of the average wind speed, at the 6 nodes with the metocean desk study performed by DHI. This alignment was performed at a time when only the first 12 months of the measurement campaign were available. To ensure a proper alignment a fixed alignment height, 100 above MSL was selected and a concurrent reference period were defined. This comparison showed a good agreement with deviations between -0.01 m/s and 0.11 m/s which is within the predefined boundaries. Apart from the wind speed, a comparison of the wind direction showed a good fit as well. A detailed comparison is provided in **Annex J**, which is based on the first 12 months of the measurement campaign.

In order to ensure that the alignment was still valid using 24 months of measured data at HKW, comparisons were performed between datasets obtained using 12 months of measurements at HKW and datasets obtained with 24 months of data. These comparisons showed that differences in wind speed between the datasets ranged between 0.01 and 0.02 m/s at the 6 nodes, with correlations on wind speed and directions of 0.98 and 0.99, respectively, for all 6 nodes. These low differences on wind speed associated with high correlations on wind speed and wind direction confirm that the alignment still holds with the updated dataset.

7.3.2. Previous Studies

As in the Dutch North Sea several offshore project have been developed in recent years, numerous studies have been performed in the area, and in particular:

- The wind resource assessment for the HKZWFZ by Ecofys (26);
- The wind resource assessment for the HKNWFZ by Oldbaum (25)

The assessment of the HKZWFZ focused on an area further South and closer to the coast compared to the HKWWFZ, as illustrated by Figure 41. The study used measurement data from an in-situ floating LiDAR combined with data from the OWEZ met mast. Data from the LEGO platform was used for the long-term correction, and the ConWx mesoscale model was used for the horizontal extrapolation. It is worth noting that at the time the study was released the ERA5, KNW and DOWA datasets were not yet available. Wind speed at the centre of the HKZWFZ was estimated to be $9.44 \text{ m/s} \pm 0.38 \text{ m/s}$ at 100 m above sea level. This is to be compared with $9.74 \text{ m/s} \pm 0.31 \text{ m/s}$ for the current analysis. Higher wind speeds were expected at the HKWWFZ given its location further offshore. A slightly lower uncertainty could also be expected given the use of 3 data sources instead of two and the use of new generation models. The highest wind speed gradient per km between 2 nodes was found to be 0.21 %/km for the HKZWFZ, compared to 0.05 %/km for the present study. This was expected, given the location further offshore.

The assessment of the HKNWFZ focused on an area further West and closer to the coast compared to the HKWWFZ, as illustrated by Figure 41. The study used measurement data from an in-situ floating LiDARs combined with data from the OWEZ met mast. ERA5 data was used for the long-term correction, and the KNW mesoscale model was used for the horizontal extrapolation. The DOWA model was not yet available at the time the study was released. Wind speed at the center of the HKNWFZ was estimated to be 9.56 m/s \pm 0.39 m/s at 100 m above sea level, compared with 9.74 m/s \pm 0.31 m/s for the current analysis. Higher wind speeds were expected at the HKWWFZ given its location further offshore. A slightly lower uncertainty could also be expected given the use of 3 data sources instead of two and the use of the new generation DOWA mesoscale model. A wind speed gradient of 0.14 %/km was computed for the HKZWFZ, compared to 0.05 %/km for the present study, which was expected, given the location further offshore.

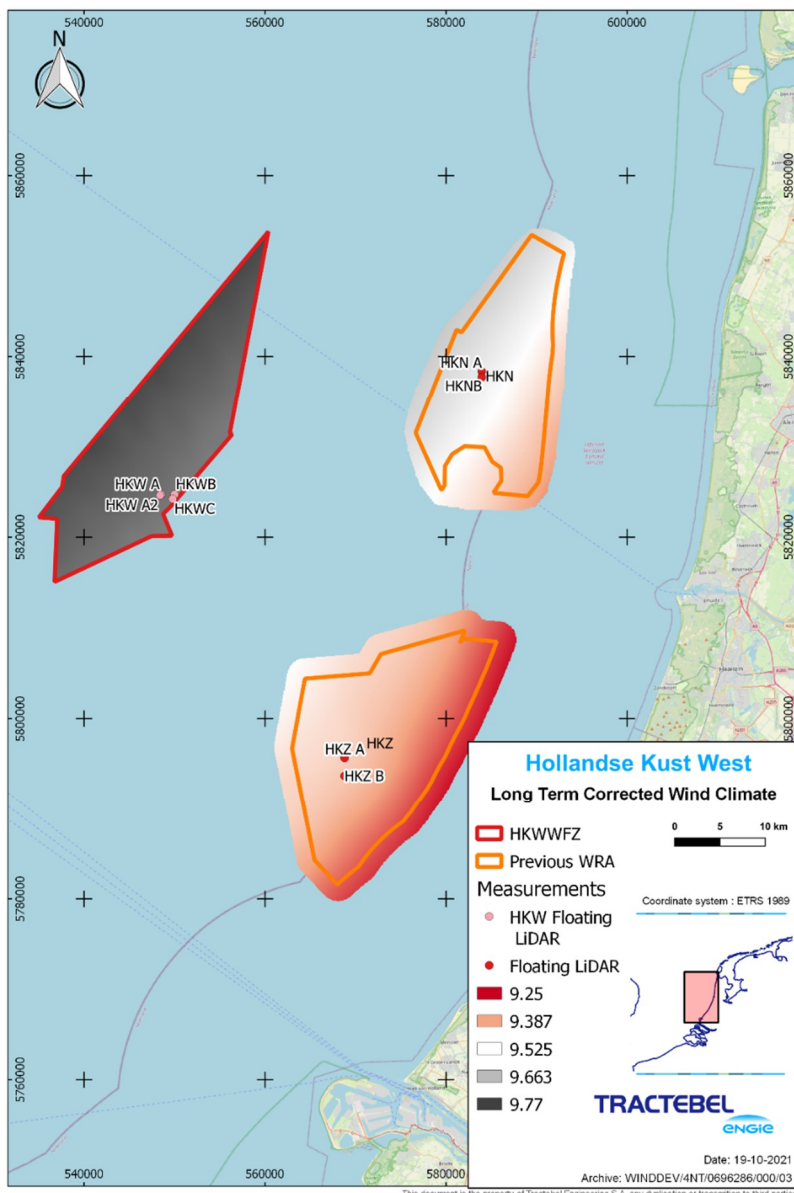


Figure 41: Comparison of Long-term wind climate between HKWWFZ, HKN and HKZ at 100 m. Coordinates are in UTM31N, ETRS89

7.3.3. Wind Atlases

Additionally, the wind climate is compared to datasets that have been analysed in Section 5.2.2. For each of the wind atlases, the mean wind speed at the HKW measurement location is compared to the one found in 7.1.

7.3.3.1. KNW

The KNW dataset is described in Section 5.2.2.1 of this report. Figure 42 represents the wind speed gradient at 100 m over the Dutch shelf of the North Sea obtained with the KNW dataset with a resolution of 200 m.

The average wind speed at 100 m over the last 20 years at the HKW measurement location is 9.64 m/s. The difference with the wind climate assessed in the report is about 0.1 m/s or 1.0 % on the mean wind speed.

The gradient for the KNW, computed based on the same nodes points as above for the HKW WRA, is 0.04 %/km, versus 0.05 %/km for the present study.

The mean wind speed and gradient being very similar between the studied wind climate and the one extracted from KNW, this indicates a good agreement between both sources. This does not come as a surprise, as the KNW was specifically developed for the Dutch North Sea.

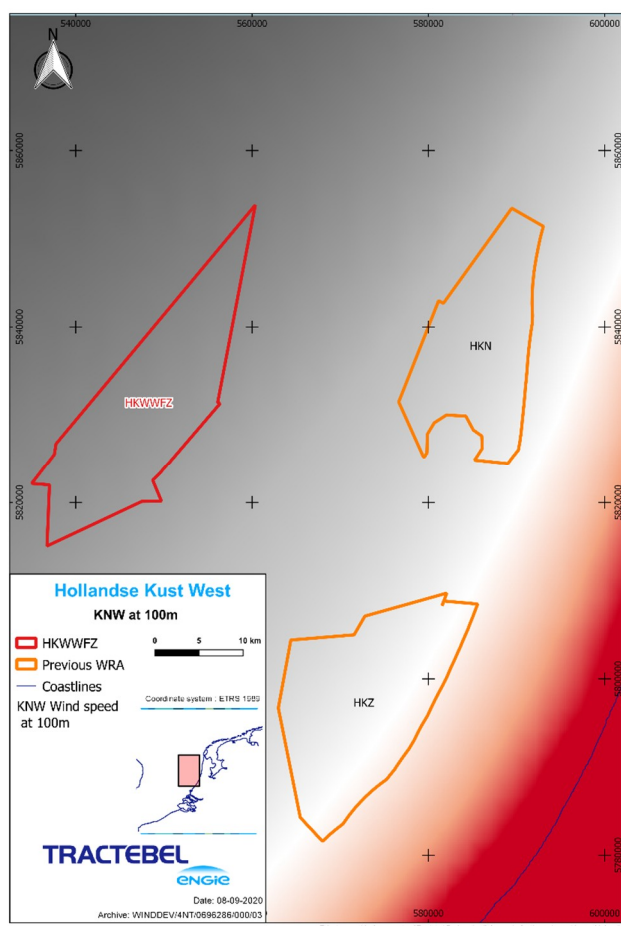


Figure 42: Wind Speed at 100 m from KNW dataset with 200 m resolution. Coordinates are in UTM31N, ETRS89

7.3.3.2. NEWA

The NEWA dataset is described in Section 5.2.2.3 of this report. Figure 43 represents the wind speed gradient at 100 m over the Dutch shelf of the North Sea obtained with NEWA dataset with a resolution of 200 m.

The average wind speed at 100 m over the 10 years of the available dataset at HKW measurement location is 9.29 m/s. The difference with the wind climate assessed in the report is about 0.45 m/s or 4.6 % on the mean wind speed.

The gradient that has been computed as defined in 7.3.1 and 7.3.3.1 is 0.04 %/km, versus 0.05 %/km for the present study.

The gradient that was found in this study agrees well with the one from NEWA, whereas the mean wind speed shows a difference between both. This difference could be explained by the fact that NEWA is not primarily focused on the offshore wind climate.

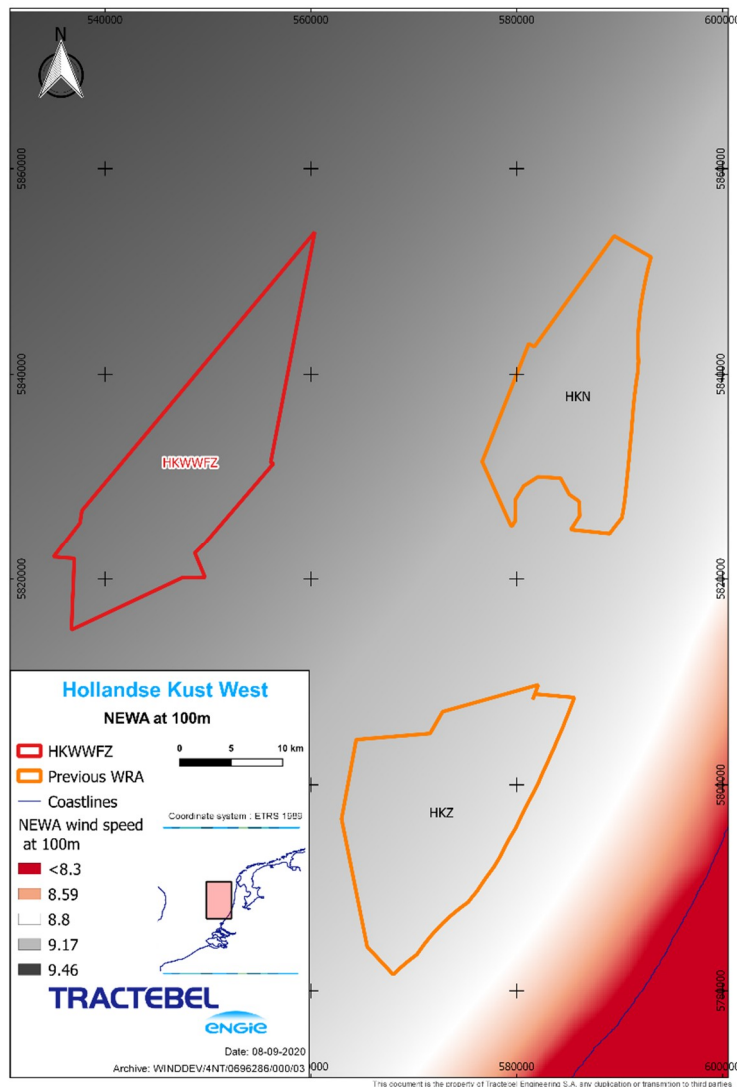


Figure 43: Wind Speed at 100 m from NEWA dataset with 200 m resolution. Coordinates are in UTM31N, ETRS89

7.3.3.3. DOWA

The DOWA dataset is described in Section 5.2.2.2 of this report. Figure 44 represents the wind speed gradient at 100 m over the Dutch shelf of the North Sea obtained with DOWA dataset with a resolution of 200 m.

The average wind speed at 100 m over the 10 years of the available dataset at HKW measurement location is 9.73 m/s. The difference with the wind climate assessed in the report is about 0.01 m/s or 0.1 % on the mean wind speed.

The gradient that has been computed as defined in 7.3.1 and 7.3.3.1 is 0.04 %/km, versus 0.05 %/km for the present study.

The study and DOWA agree very well in terms of mean wind speed and gradient.

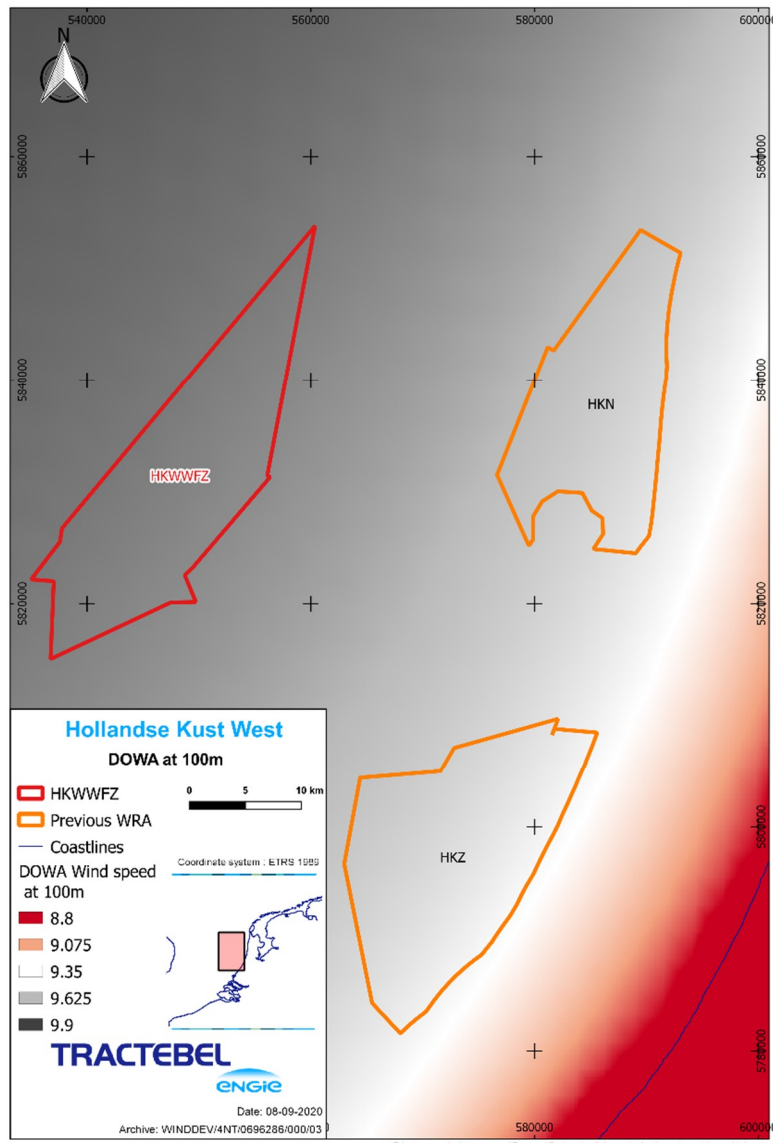


Figure 44: Wind Speed at 100 m from DOWA dataset with 200 m resolution. Coordinates are in UTM31N, ETRS89

7.3.4. Conclusion

In light of the comparisons against other sources that have been performed hereabove, it can be said that the results of this study agree well with the other sources and fit the general observations concerning wind climates in the Dutch North Sea:

- The further west, hence the further away from the Dutch shore, the higher the mean wind speed; and
- The further west, the lower the wind speed gradient.

Indeed the influence of the coast becomes less and less visible as you move away from the shore.

8. WAKE ASSESSMENT

The main objective of the assignment is to provide an assessment of the wind resources over the Hollandse Kust (west) Wind Farm Zone (HKWWFZ). In addition, a preliminary analysis of the impact of internal and external wake effects on the Hollandse Kust (west) wind farm was also carried out. In this assessment, wake effects of neighbouring operational and planned offshore wind farms were modelled for two preliminary layouts for the HKWWFZ considering the most recent offshore wind turbine models above 10 MW.

An ensemble approach was applied for internal wake modelling considering various engineering models. A state-of-the art wake model was used to model interactions of the planned wind farm with the atmosphere and the effect of other offshore wind farms on the Hollandse Kust (west) wind farm. Computations using this state-of-the-art model were performed by Professor Johan Meyers from the KUL and his team, who developed this specific model. This approach has been benchmarked against an “industry best practice” approach performed by Tractebel. Models and their respective outputs are described in details in the paragraphs below.

Due to the timeline and different phases of this assignment, the wake assessment presented here is based on a combination of 3 data sets as described in Section 6, but based on 9 months of measurements data at HKW. As the extension of the measurement campaign from 9 to 24 months showed a negligible impact on the resulting wind climate, and as the objective of the wake assessment is to provide a high level range of wake effects rather than a detailed analysis, an update of the wake assessment based on the 24 months dataset was not deemed necessary.

8.1. Preliminary Turbine Layouts

In order to assess the wake effects, two different layouts were compared corresponding to two theoretical wind turbine types with the following characteristics:

- WT-type 1: 13 MW, rotor diameter 220 m and hub height of 138 m
- WT-type 2: 10 MW, rotor diameter 200 m and hub height of 125 m

The presented wind turbine types and their respective hub heights have been chosen to fit the expected wind turbine type when the HKWWFZ will be constructed and a type that is considered today as state-of-the-art.

Two WRGs (Wind Resource Grids) were generated at 138 m and 125 m MSL from the selected mesoscale model (DOWA) anchored on the long-term time series at the six nodes: long-term time series were first extrapolated to target hub heights using wind shear inferred from the IJmuiden met mast before being converted to six sets of Weibull parameters; these Weibull parameters were then extrapolated to each point of the WRG grid using directional wind speed ratios generated from all DOWA time-series available within the domain, and combined using an inverse distance weighting. The long-term time series are based on 9 month measurement data and have not been updated with the latest measurement at HKW location.

These WRGs were combined with the Hollandse Kust (west) wind farm site boundaries to design a wind farm layout. Each of these layouts was optimized on a yield basis (taking into account a buffer of 110 m from the site boundaries). Layout and restriction areas are illustrated in Figure 66 and Figure 67 (in **Annex K**). The exact coordinates of the two layouts are provided in Table 80 and Table 82 (in **Annex K**). Indicative power and Ct curves considered for the two WT-types are provided in Table 84.

8.2. Wake Modelling

An ensemble approach was chosen to assess wake effects affecting the Hollandse Kust (west) wind farm:

- wake effects were computed based on industry-standard practices using Park 1, Park 2, and eddy-viscosity wake models.
- a state-of-the-art “three-layer” model (TLM) developed at the KUL was then used to provide an assessment of wind farm blockage and of wake losses due to neighbouring offshore wind farms. Wind farm blockage is defined here as a loss due to the interaction of the wind farm with the atmospheric boundary layer, i.e. potentially differing from the industry-standard definition suggested by DNV-GL (53).

This section first describes internal wake effects from industry-standard models, then presents outputs of the three-layer model, and concludes by their combination into an estimation of overall wake losses.

8.2.1. Industry-standard wake modelling

In the ensemble model, it was initially decided to include the Eddy viscosity model and two variations of the Jensen wake model (54) which are commonly used in the wind industry (Park 1 and Park 2). As wake losses are significantly influenced by atmospheric stability, in a third variation, the Jensen model was run for a range of stability conditions (unstable, neutral and stable conditions) and its outputs were weighted according to the occurrence of each stability condition. This approach ensures that less frequent wakes occurring from most stable conditions and resulting in higher wake losses are considered, while they could be filtered out by the use of a single decay constant.

Standard Park 1 and Park 2 wake computations were used with standard parameters, using wake decay constants of 0.038 and 0.06, based on the consultant’s experience of offshore wind farm wakes and from recommendations from the Technical University of Denmark’s (DTU) (55). Those approaches have been derived from literature, best practices and an extensive validation campaign with the results collected during of WindEurope’s Comparison of Resource and Energy Yield Assessment Procedures (CREYAP) program (56).

The eddy viscosity model used as main parameter turbulence intensity measured at the IJmuiden met mast, extrapolated to target hub heights. The IJmuiden mast was preferred to turbulence intensity from Lidar measurements because wind industry techniques have been designed around cup anemometers which output values of turbulence that typically differ from values measured by Lidars which are representative of a volume rather than a point. The IJmuiden met mast was preferred to the Offshore Wind Farm Egmond aan Zee (OWEZ) met mast due to its location further offshore, more representative of the offshore wind farm as literature indicates measured TI are considered to be in-line when the region tends to be similar (57); however both masts showed similar levels of turbulence intensity, close to 6 %.

The third variation of the Jensen model (Park 2 – stability weighted) used one wake decay constant per stability class. Stability classes were derived from ERA5 data (see 7.2), and associated to turbulence measurements measured at the IJmuiden mast. This led to an average turbulence intensity per stability class, that was used to compute a wake decay constant per stability class, following the Windpro recommendations for offshore wind farms (55): wake decay constants were computed multiplying turbulence intensity by 0.8 for the Park 2 model. The three individual computations corresponding to stable, neutral, and unstable cases were finally weighted based on their corresponding occurrences. Using this method with an average turbulence intensity of 6 % leads to a wake decay coefficient of 0.048, which is lower than the default coefficient of 0.06 used in the Standard Park 2 calculation above. Therefore, this third computation is expected to be more conservative and lead to higher wake losses than the Standard Park 2 calculation.

Table 53 presents the outcome of these computations for the two reference layouts. These figures do not take into account any large wind farm correction, as large scale effects were accounted for by the three-layer model. The difference in the approach taken to compute the wake decay coefficient for the Standard Park 2 and Stability-weighted Park 2 computations leads to a difference of 13/15 % on wake losses, which is lower than the uncertainty of 25/30 % on wake losses typically assumed in the industry.

TABLE 53: PREDICTED INTERNAL WAKE LOSSES FOR THE TWO REFERENCE LAYOUTS USING INDUSTRY-STANDARD MODELS

Wake model	Park 1	Park 2	Eddy-viscosity	Park 2 - Stability weighted
13MW Layout	10.9 %	10.3 %	6.0 %	11.8 %
10 MW Layout	11.0 %	10.8 %	5.7 %	12.2 %

8.2.2. Three-layer model

Considering the size of the Hollandse Kust (west) wind farm, it is expected it will interact with the atmospheric boundary layer and the local meso-scale weather system. Therefore, on top of an industry best practice evaluation it is crucial to also evaluate losses due to “blockage” (interaction of the wind farm with the atmospheric boundary layer) and losses due to the presence of operating neighbouring wind farms (long distance wind farm cluster wake effects).

The importance of blockage and gravity waves effects have been demonstrated by DNV-GL (53) and by the KUL team (58). However, the combined importance of local (i.e. at HKW level) and long-distance (i.e. from other wind farms than HKW) effects yields to an area of interest too large for high-accuracy LES computations to be considered. This is the reason why a three-layer model (TLM) was developed by KUL, and used within the framework of the present assessment. Details of the work performed by KUL is provided in **Annex L** : Three-layer wake modelling, by KUL, and summarised below.

The TLM is a fast engineering model developed using insights from LES simulations which incorporates gravity-wave feedback aside from classical windfarm wake effects to yield more accurate yield estimations (59). This model represents the atmosphere in three layers, using the Taylor-Goldstein equations to parametrise gravity-wave radiation, with coupling to a classical Gaussian wake-merging (GWM) model (60) to represent effects in the wind farm.

KUL performed four simulations of one year each considering two different layouts for the Hollandse Kust (west) wind farm with and without the existing of future wind farms. The simulations were fed using one year of ERA-5 data at the central node location. The one-year dataset was selected to be representative of long-term conditions expected at the central node in terms of wind speed and direction. Specifically, the date range 23/06/2001 to 23/06/2002 was used. Figure 45 illustrates the wind farms that were considered for the assessment, the coordinates of which are provided in **Annex A**.

Figure 46 illustrates the model’s outputs, and specifically its ability to simulate the atmospheric response to the presence of operating wind farms depending on stability conditions.

As shown in Table 54 this leads to an overall wake loss of 16.0 % and 16.7 % for the 13 MW and 10 MW layouts respectively, including a large contribution of neighbouring offshore wind farms of about 7 %.

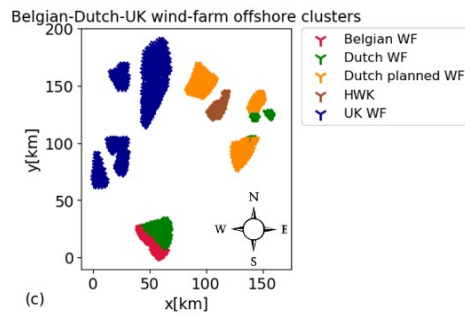


Figure 45: Illustration of the neighbouring wind farms considered for the three-layer model assessment

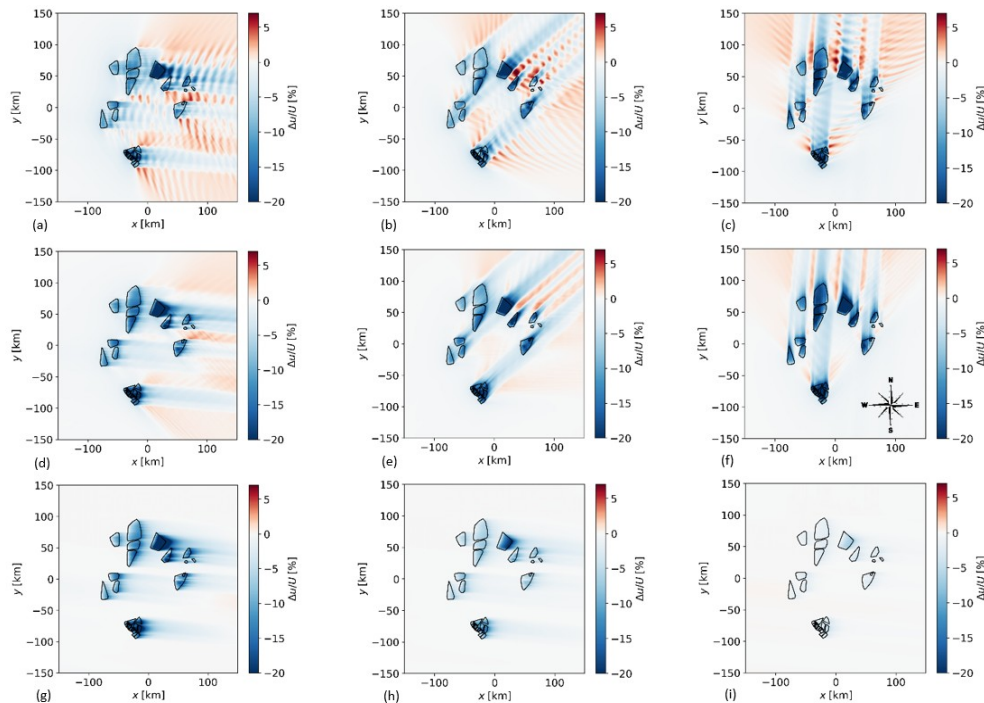


Figure 46: Illustration of the reduction in wind speed due to operating wind farms, for very stable, stable and neutral conditions (top to bottom, respectively) for Westerly, South-Westerly and Southerly winds (left to right, respectively)

TABLE 54: ESTIMATION OF WAKE LOSSES USING THE THREE-LAYER MODEL

	HKW wakes	HKW blockage	Neighbouring offshore wind farms
13 MW layout	6.8 %	2.3 %	7.0 %
10 MW layout	7.5 %	2.3 %	6.9 %

8.2.3. Combined wake losses

Internal wake effects were accounted for using an ensemble approach through the averaging of all available engineering models, see Table 55.

TABLE 55: INTERNAL WAKE LOSSES FROM THE ENSEMBLE MODEL

	Average ("Ensemble")	Min (of all wake models)	Max (of all wake models)
13 MW layout	9.2 %	6.0 %	11.8 %
10 MW layout	9.4 %	5.7 %	12.2 %

Outputs from the TLM were used in order to account for blockage and effects from other offshore wind farms. This led to combined wake losses of about 18.5 %, as shown by Table 56, including a loss of approximately 7 % from neighbouring offshore wind farms, which could not be reproduced using standard wind-industry models (which anticipate a much smaller value). While these figures suggest that the combined impact of neighbouring wind farms and wind farm blockage should be a subject of attention to the reader of this document, they are associated with a large uncertainty, as shows the spread between the various computations. Therefore, it is recommended for users of this document to satisfy themselves of the influence of neighbouring farms.

TABLE 56: COMBINED WAKE LOSSES

	Average	Min	Max
13 MW layout	18.5 %	15.3 %	21.1 %
10 MW layout	18.6 %	14.9 %	21.4 %

9. CONCLUSIONS

This report describes the wind resource assessment performed at the Hollandse Kust (west) Wind Farm Zone (HKWWFZ).

To estimate the wind resource, three independent measurement campaigns have been used. An extensive selection process has pointed out that the on-site measurement campaign, derived from three LIDAR Buoys and two met mast campaigns (OWEZ and IJmuiden) in the vicinity of the site resulted in the lowest uncertainty. Those measurements have been merged into one unique data set based on the inverse of the uncertainties.

To correct the short-term measurements to a long-term period, a benchmark analysis of different MCP approaches and reanalysis datasets was performed. From this analysis, ERA5 as a reference data set and the Neural Network MCP approach were selected for their likeliness to minimize long-term correlation uncertainties.

In the (Dutch) part of the North Sea several mesoscale data sets are available. From those data sets, a suitable model must be derived. Therefore, an extensive validation has been performed and all models showed a good fit with the measured data in the (direct) vicinity of the HKWWFZ, with DOWA, EMD-ERA5 and an ensemble model showing best results. The DOWA mesoscale model was selected to extrapolate the wind climate throughout the Wind Farm Zone (WFZ). Part of the assessment consisted in aligning the wind climate with the metocean study. This alignment showed an agreement within the pre-defined boundaries of 0.1 m/s at 6 site nodes within the Wind Farm Zone (WFZ).

Mean wind speed at the Wind Farm Site centre at 100 m MSL was predicted to be 9.74 +/- 0.31 m/s.

Due to the non-optimal orientation of Hollandse Kust (west) Wind Farm Zone (HKWWFZ) and the vicinity of many future wind farms, wake effects will play an important role when assessing the energy yield of the (offshore) wind farm. Therefore, an ensemble wake model, based on the combination of an industrial and state-of-the-art research model, was used to evaluate the expected wake effects for two typical wind farm scenarios. This highlighted that apart from the internal wake effects, external wake effects from the neighbouring wind farms as well as wind farm blockage are expected to have an important contribution to the wake effects. Two scenarios have been evaluated and the overall wake loss is estimated at 18.6 and 18.4 % for the wind farm layouts consisting to respectively 10 and 13 MW wind turbine capacity. While these figures suggest that wake effects should be a subject of attention, they are associated with a large uncertainty. Therefore, it is recommended for users of this document to satisfy themselves with the influence of neighbouring farms.

10. REFERENCES

1. Government of the Netherlands. *Energy Agreement for Sustainable Development*. 2013.
2. Government of the Netherlands. *Offshore Wind Energy Roadmap 2030*. 2018.
3. Government of the Netherlands. *Ministerial Order for Offshore Wind Energy 2015 SDE+*. 2015.
4. RVO . RVO Offshore Wind Web Site - General Information Hollandse Kust (west).<https://offshorewind.rvo.nl/>. https://offshorewind.rvo.nl/generalw
5. Tractebel. *Wind resource assessment - Hollandse Kust (West) Wind Farm Zone*. s.l. : Tractebel, 2020.
6. Fugro. *Supply of Meteorological and Oceanographic data at Hollandse Kust (west) - Year 1 Summary: 5 February 2019 - 15 February 2020 - C75432_12M_R2_IP_D*. 12/10/2020.
7. The Carbon Trust. *Carbon Trust Offshore Wind Accelerator roadmap for the commercial acceptance of floating LIDAR technology*. . 21 November 2013. CTC 819 Version 1.0.
8. DNV GL. *Assessment of the Fugro/Oceanor Seawatch Floating Lidar Verification at RWE IJmuiden Met Mast*. Tech. Rep. GLGH-4257 13 10378-R-0003, Rev. B, issue date 2015-01-30. s.l. : DNV GL, 2015.
9. DNV GL. *Assessment of the Fugro Seawatch Wind LiDAR Buoy WS 187 Pre-Deployment Validation at Frøya, Norway*. 2019. 10129033-R-6, Rev. E.
10. DNV GL. *Assessment of the Fugro Seawatch Wind LiDAR Buoy WS 188 Pre-Deployment Validation at Frøya, Norway*. 2019. 10129033-R-7, Rev. D.
11. DNV GL. *Quality assessment of the Fugro Seawatch Wind Lidar Buoy WS170*. 2019. 10166838-R-1, Rev. A.
12. DNV GL. *WS170 Independent performance verification of Seawatch Wind Lidar Buoy at the LEG offshore*. 2021. 10298247-R-1, Rev. A.
13. Slinger, C et Harris, M. *Introduction to continuous-wave Doppler lidar*. Boulder, USA : Summer School in Remote Sensing for Wind Energy, 2012.
14. Jaynes, D W, et al. *MTC final progress report: LIDAR*. Boston, USA : Renewable Energy Research Laboratory, Department of Mechanical and Industrial Engineering, University of Massachusetts, 2007.
15. Deltares. *Hollandse Kust (west) Field Measurement Campaign Validation Report - Feb 2019 to Feb 2021*. 2021.
16. MEASNET. *Evaluation of site-specific wind conditions*. 2016, April. Version 2.
17. DNV GL. *ZX818 - Independent analysis and reporting of ZX Lidars performance verification executed by Zephir Ltd. at Pershore test site, including IEC compliant validation analysis*. 2018. 10108274-R-0016, Rev. A.

18. DNV GL. *ZX802 - Independent analysis and reporting of ZX Lidars performance verification executed by Zephir Ltd. at Pershore test site, including IEC compliant validation analysis.* 2018. 10108274-R-0015, Rev. A.
19. Fugro. *Supply of Meteorological and Oceanographic data at Hollandse Kust (west) - 24-month summary campaign report: 5 February 2019 - 11 February 2021.* 30/08/2021. C75432_24M_R3_D.
20. The Carbon Trust. *Carbon Trust Offshore Wind Accelerator Roadmap for the Commercial Acceptance of Floating LiDAR Technology.* October 2018.
21. DNV GL. *Assessment of the Fugro OCEANOR Seawatch Wind LiDAR Buoy WS 170 Pre-Deployment Validation at Frøya, Norway.* 2017. GLGH-4270 17 14462-R-0002, Rev. C.
22. DNV GL. *ZP585 - Independent analysis and reporting of ZX Lidars performance verification executed by Zephir Ltd. at Pershore test site, including IEC compliant validation analysis.* 2018. GLGH-4270 17 14677 258-R-0025, Rev. A.
23. EMD. *WindPRO 2.7 User Guide.* 2010.
24. Troen, I et Petersen, E.L. *European Wind Atlas.* s.l. : Risø National Laboratory, 1989. ISBN 87-550-1482-8.
25. Oldbaum. *Wind Resource Assessment for Hollandse Kust (noord) Wind Farm Zone.* Netherlands : s.n., 2019. HKN_20190312_OBL_WRA-HKN_V5_OF.
26. Ecofys WTTS. *Hollandse Kust (zuid) Offshore Wind Farm Zone: Combined Wind Resource Assessment.* Netherlands : s.n., 2017. ESMWT17659.
27. Werkhoven, E et Verhoef, J. *Offshore Meteorological Mast IJmuiden – Abstract of Instrumentation Report.* s.l. : ECN-Wind Memo-12-010, 2012.
28. Kouwenhoven, HJ. *User manual data files meteorological mast NoordzeeWind.* s.l. : NoordzeWind, 2007.
29. Wouters, D A et Wagenaar, J W. Verification of the ZephIR 300 LiDAR at the ECN LiDAR Calibration Facility for the offshore Europlatform measurement campaign. 2018, Vol. 2017, p. 2016.
30. ECN. Wind @ Sea. *windopzee.* [Online] ECN, 2020. <https://www.windopzee.net/meet-locaties/meteomast-ijmuiden-mmij/>.
31. Copernicus. Copernicus Climate Change Service (C3S): ERA5: Fifth generation of ECMWF atmospheric reanalyses of the global climate. ECMWF. [Online] Copernicus Climate Change Service Climate Data Store (CDS), 2017. <https://cds.climate.copernicus.eu/cdsapp#!/home>.
32. *The Modern-Era Retrospective Analysis for Research and Applications, Version 2 (MERRA-2).* Ronald Gelaro, et al. s.l. : J. Clim., doi: 10.1175/JCLI-D-16-0758.1, 2017.
33. *The ERA-Interim reanalysis: configuration and performance of the data assimilation system.* D. P. Dee, et al. 656, s.l. : Quarterly Journal of the Royal Meteorological Society, 2011, Vol. 137.

34. *The NCEP Climate Forecast System Version 2*. Saha, Suranjana, et. al. s.l. : Bull. Amer. Meteor. Soc, 2014, Vol. 91, 1015–1058, (DOI: 10.1175/JCLI-D-12-00823.1).
35. *The NCEP Climate Forecast System Reanalysis*. Saha, Suranjana, et. al., s.l. : Bull. Amer. Meteor. Soc., 2010, Vol. 91(8), 1015-1057 (DOI: 10.1175/2010BAMS3001.1).
36. Skamarock, W. C., J. B. Klemp, J. Dudhia, D. O. Gill, Z. Liu, J. Berner, W. Wang, J. G. Powers, M. G. Duda, D. M. Barker, and X.-Y. Huang. *A Description of the Advanced Research WRF Version 4*. s.l. : NCAR Tech. Note, 2019. NCAR/TN-556+STR, 145 pp..
37. Royal Netherlands Meteorological Institute. KNW (KNMI North sea Wind) Atlas. [Online] <http://projects.knmi.nl/knw/>.
38. Seity, Y, et al. The AROME-France convective-scale operational model. 2011, Vol. 139, 3, pp. 976-991.
39. Stepek, A, et al. *Validation of KNW atlas with publicly available mast observations (Phase 3 of KNW project)*. s.l. : Tech. rep., KNMI Technical Report TR352, 2015.
40. Royal Netherlands Meteorological Institute. Dutch Offshore Wind Atlas. [Online] <https://www.dutchoffshorewindatlas.nl/>.
41. Wijnant, I L, et al. The Dutch Offshore Wind Atlas (DOWA): description of the dataset.
42. Bengtsson, Lisa, et al. The HARMONIE-AROME model configuration in the ALADIN-HIRLAM NWP system. 2017, Vol. 145, 5, pp. 1919-1935.
43. Mann, Jakob. *Overview of the New European Wind Atlas Project*. s.l. : Zenodo, 2019.
44. *The Making of the New European Wind Atlas, Part 1: Model Sensitivity*. Hahmann, Andrea, et al. 2020. 10.5194/gmd-2019-349.
45. *The Making of the New European Wind Atlas – Part 2: Production and Evaluation*. Hahmann, Andrea, et al. 2020. 10.5194/gmd-2020-23.
46. Witha, B, et al. WRF model sensitivity studies and specifications for the NEWA mesoscale wind atlas production runs. 2019, Vol. 2682604.
47. Vaisala. How was the 5 km global wind dataset created? *3TIER by Vaisala*. [Online] <https://www.3tier.com/en/support/wind-online-tools/how-was-data-behind-your-prospecting-map-created/>.
48. EMD International A/S. *EMD-WRF Global On-demand Mesoscale Services ERA5, ERA-Interim, MERRA2 and CFSR*. s.l. : EMD, 2018.
49. EMD International A/S. *Technical Note: Validation of EMD-WRF EUROPE+ (ERA5) mesoscale data*. s.l. : EMD, 2020.
50. IEC. *IEC 61400-12-2 Wind turbines - Part 12-2: Power performance of electricity-producing wind turbines based on nacelle anemometry*. Geneva, Switzerland : IEC, 2013. 978-2-83220-658-4.

51. *Long-term correction: Uncertainty model using different Long-term data.* Klintø, Frank. London : Wind Power Conference 2015 -Wind Resource Assessment, 2015.
52. EMD International A/S. *windPRO 3.3 User manual : 3. Energy calculation.* 2019.
53. Bleeg, James, et al. Wind farm blockage and the consequences of neglecting its impact on energy production. 2018, Vol. 11, 6, p. 1609.
54. Katic I., Hojstrup J. and Jensen N.O. *A Simple Model for Cluster Efficiency.* Rome : European Wind Energy Association Conference and Exhibition, 1986.
55. Per, Nielsen. *Recommendations for wake loss calculation for offshore wind farms.* s.l. : EMD international, 2019.
56. *Offshore CREYAP Part 2 – final results.* Mortensen Niels G, Nielsen Morten and Hans E Jørgensen. Helsinki : EWEA Resource Assessment, 2015.
57. Peter, Argyle, et al. *A Comparison of the UK Offshore Wind Resource from the Marine Data Exchange.* Hamburg: Windeurope Summit : s.n., 2016.
58. *Gravity Waves and Wind-Farm Efficiency in Neutral and Stable Conditions.* Allaerts, D et Meyers, J. s.l. : Boundary Layer Meteorology, 2018, Vol. 166, 269-299.
59. *Sensitivity and feedback of wind-farm-induced gravity waves.* Allaerts, D et Meyers, J. s.l. : Journal of Fluid Mechanics, 2019, Vol. 862, 990-1028.
60. *Analytical modeling of wind farms: A new approach for power prediction.* Niayifar, A et Porté-Agel, F. 741, s.l. : Energies, 2016, Vol. 9.
61. *Meteorological Measurements OWEZ.* Eecen, PJ et Machielse, LA, Curvers, AP. Amsterdam : Noordzee Wind, 2007.
62. DTU Wind Energy. *WAsP 11.4.* Roskilde : DTU Wind Energy.

11. APPENDICES

- ANNEX A: EXISITING AND PLANNED WIND FARMS
- ANNEX B: Wind shear matrices at MMIJ and HKW
- ANNEX C: LTC – KPI results for the long-term correction based on Energy
- ANNEX D: LTC – Diurnal and Monthly Profiles of LTC Wind Climate
- ANNEX E: LTC – Weibull fits and frequency distributions
- ANNEX F: Mesoscale data Validation - Mean wind speed results
- ANNEX G: Mesoscale data Validation - Wind direction
- ANNEX H: Mesoscale data Validation - Energy Rose
- ANNEX I : Long-term wind climate at the 6 nodes
- ANNEX J : Comparison between Tractebel and DHI Metocean Desk Study Results
- ANNEX K : WTG Coordinates HKWWFZ
- ANNEX L : Three-layer wake modelling, by KUL

ANNEX A: EXISITING AND PLANNED WIND FARMS

Existing Dutch wind farms

Luchterduinenen		Egmond Aan Zee (OWEZ)		Prinses Amalia park				
V112-3.0 MW HH: 79 m		V90-3.0 MW HH: 70 m		V80-2.0 MW HH: 57 m				
WTG	(UTM WGS84)		WTG	(UTM WGS84)		WTG	(UTM WGS84)	
	x	y		x	y		x	y
1	579 282	5 803 658	1	597 181	5 826 380	1	584 022	5 829 007
2	578 737	5 803 948	2	596 756	5 826 863	2	583 071	5 829 056
3	578 191	5 804 238	3	596 339	5 827 338	3	583 532	5 828 757
4	577 645	5 804 529	4	595 914	5 827 822	4	583 994	5 828 458
5	577 100	5 804 819	5	595 490	5 828 305	5	584 455	5 828 159
6	576 554	5 805 110	6	595 065	5 828 789	6	582 103	5 829 063
7	579 584	5 804 435	7	594 633	5 829 281	7	582 570	5 828 772
8	579 053	5 804 718	8	594 208	5 829 764	8	583 037	5 828 481
9	578 521	5 805 000	9	593 783	5 830 248	9	583 503	5 828 191
10	577 990	5 805 283	10	593 366	5 830 739	10	583 970	5 827 900
11	577 458	5 805 566	11	592 933	5 831 216	11	584 437	5 827 608
12	576 927	5 805 849	12	592 508	5 831 700	12	584 904	5 827 318
13	579 889	5 805 212	13	598 189	5 826 748	13	585 371	5 827 027
14	579 372	5 805 487	14	597 764	5 827 232	14	581 585	5 828 734
15	578 855	5 805 762	15	597 339	5 827 715	15	582 057	5 828 452
16	578 337	5 806 037	16	596 914	5 828 199	16	582 529	5 828 170
17	577 820	5 806 312	17	596 234	5 828 973	17	583 002	5 827 888
18	577 303	5 806 588	18	595 809	5 829 457	18	583 474	5 827 606
19	580 182	5 805 968	19	595 384	5 829 940	19	583 946	5 827 323
20	579 678	5 806 236	20	594 959	5 830 424	20	584 418	5 827 041
21	579 175	5 806 503	21	594 534	5 830 908	21	584 890	5 826 759
22	578 672	5 806 771	22	598 548	5 827 853	22	585 362	5 826 477
23	578 169	5 807 039	23	598 119	5 828 338	23	581 068	5 828 385
24	577 666	5 807 306	24	597 695	5 828 826	24	581 545	5 828 111
25	580 524	5 806 709	25	597 038	5 829 572	25	582 024	5 827 839
26	580 037	5 806 968	26	596 560	5 830 116	26	582 500	5 827 566
27	579 550	5 807 227	27	596 135	5 830 600	27	582 978	5 827 293
28	579 063	5 807 486	28	595 710	5 831 084	28	583 455	5 827 020
29	578 575	5 807 745	29	595 285	5 831 568	29	583 932	5 826 747
30	578 088	5 808 005	30	598 868	5 828 998	30	584 410	5 826 473
31	580 867	5 807 450	31	598 446	5 829 486	31	584 887	5 826 200
32	580 392	5 807 703	32	597 796	5 830 224	32	581 041	5 827 763
33	579 917	5 807 955	33	597 312	5 830 776	33	581 523	5 827 499
34	579 442	5 808 207	34	596 887	5 831 260	34	582 005	5 827 235
35	578 968	5 808 460	35	596 462	5 831 744	35	582 488	5 826 971

Luchterduinenen		Egmond Aan Zee (OWEZ)		Prinses Amalia park	
V112-3.0 MW HH: 79 m		V90-3.0 MW HH: 70 m		V80-2.0 MW HH: 57 m	
WTG	(UTM WGS84)	WTG	(UTM WGS84)	WTG	(UTM WGS84)
	x y		x y		x y
1	579 282 5 803 658	1	597 181 5 826 380	1	584 022 5 829 007
36	578 493 5 808 712	36	596 037 5 832 228	36	582 970 5 826 707
37	581 237 5 808 169			37	583 452 5 826 443
38	580 640 5 808 486			38	583 935 5 826 179
39	580 144 5 808 749			39	584 417 5 825 915
40	579 648 5 809 013			40	584 900 5 825 651
41	581 602 5 808 841			41	580 531 5 827 405
42	580 591 5 809 287			42	581 019 5 827 150
43	581 920 5 809 650			43	581 506 5 826 895
				44	581 993 5 826 640
				45	582 481 5 826 385
				46	582 968 5 826 130
				47	583 455 5 825 875
				48	583 942 5 825 620
				49	584 430 5 825 365
				50	580 527 5 826 802
				51	581 019 5 826 556
				52	581 511 5 826 310
				53	582 002 5 826 064
				54	582 494 5 825 818
				55	582 986 5 825 571
				56	583 478 5 825 325
				57	580 547 5 826 228
				58	581 043 5 825 990
				59	581 539 5 825 752
				60	582 035 5 825 515

Planned Dutch wind farms

The layout of the planned wind farms of Hollandse Kust (noord) and (zuid) are fully indicative layouts and have been assessed by Tractebel, and solely for the use of this report.

Hollandse Kust (noord)		Hollandse Kust (zuid)	
Wind turbine -220 m rotor diameter – 13 MW HH: 138 m		Wind turbine -200 m rotor diameter – 10 MW HH: 125 m	
WTG	(UTM WGS84)	WTG	(UTM WGS84)
	x y		x y
1	586132 5848601	1	564 552 5 804 263
2	581012 5841521	2	564 852 5 803 163
3	582372 5843401	3	565 752 5 804 363
4	586412 5847561	4	566 252 5 802 563
5	588492 5849321	5	567 352 5 804 463
6	578612 5836161	6	566 552 5 801 463
7	581492 5840081	7	568 152 5 803 663
8	587532 5845721	8	573 152 5 807 063
9	577852 5833201	9	567 252 5 799 863
10	589172 5848561	10	568 952 5 802 763
11	580292 5835601	11	574 052 5 806 563
12	581812 5838921	12	575 452 5 807 663
13	589572 5847601	13	569 352 5 801 463
14	580612 5834441	14	569 752 5 800 263
15	589852 5846561	15	576 752 5 808 063
16	582612 5838281	16	571 852 5 801 963
17	590292 5844921	17	574 652 5 804 663
18	582732 5842081	18	575 252 5 802 463
19	583292 5835881	19	569 252 5 804 563
20	590572 5843881	20	575 752 5 804 263
21	583532 5845001	21	576 652 5 803 763
22	583812 5833961	22	575 852 5 806 263
23	590852 5842841	23	577 352 5 802 963
24	583052 5840921	24	563 752 5 799 963
25	584252 5837841	25	578 352 5 802 563
26	585332 5834201	26	569 952 5 803 763
27	591132 5841801	27	570 452 5 802 863
28	585052 5842441	28	571 452 5 803 863
29	586932 5835441	29	571 552 5 800 663
30	584412 5846241	30	571 852 5 805 263
31	586132 5840481	31	563 952 5 801 263
32	590852 5840521	32	573 052 5 801 963
33	587972 5847321	33	572 852 5 804 863

Hollandse Kust (noord)			Hollandse Kust (zuid)		
Wind turbine -220 m rotor diameter – 13 MW HH: 138 m			Wind turbine -200 m rotor diameter – 10 MW HH: 125 m		
WTG	(UTM WGS84)		WTG	(UTM WGS84)	
	x	y		x	y
34	586652	5834161	34	576 252	5 801 763
35	586492	5839401	35	565 052	5 799 863
36	588132	5844561	36	563 252	5 797 063
37	583972	5844041	37	563 552	5 796 163
38	589052	5843481	38	563 852	5 795 063
39	585732	5835601	39	565 652	5 796 963
40	585292	5845401	40	564 852	5 793 963
41	588292	5840241	41	567 152	5 796 963
42	578212	5834521	42	567 452	5 795 863
43	589332	5842441	43	569 152	5 796 963
44	585652	5844401	44	569 652	5 796 163
45	589132	5839601	45	564 352	5 790 563
46	589612	5841401	46	564 452	5 796 963
47	579052	5833281	47	569 952	5 795 163
48	579492	5838361	48	570 252	5 794 063
49	585412	5841401	49	570 552	5 793 163
50	581852	5834601	50	570 852	5 792 263
51	586652	5842241	51	564 252	5 791 563
52	585492	5837841	52	565 352	5 790 163
53	586172	5843521	53	565 152	5 792 863
54	580012	5839721	54	565 852	5 791 963
55	587412	5840841	55	565 252	5 795 463
56	581972	5835841	56	566 252	5 791 063
57	583372	5839761	57	566 752	5 793 163
58	584252	5839161	58	567 052	5 790 563
			59	568 652	5 795 063
			60	569 052	5 793 763
			61	569 752	5 792 063
			62	566 352	5 795 763
			63	567 152	5 794 663
			64	568 552	5 791 763
			65	563 752	5 793 763
			66	568 052	5 792 563
			67	567 952	5 794 063
			68	566 052	5 794 463
			69	563 952	5 792 563
			70	566 952	5 792 063
			71	572 552	5 798 763
			72	572 152	5 797 163

Hollandse Kust (noord)		Hollandse Kust (zuid)			
Wind turbine -220 m rotor diameter – 13 MW HH: 138 m		Wind turbine -200 m rotor diameter – 10 MW HH: 125 m			
WTG	(UTM WGS84)		WTG	(UTM WGS84)	
	x	y		x	y
	73	573 852		5 799 063	
	74	573 252		5 796 763	
	75	582 352		5 807 863	
	76	575 152		5 799 363	
	77	576 452		5 799 663	
	78	582 052		5 806 663	
	79	572 552		5 793 763	
	80	583 952		5 808 463	
	81	575 852		5 797 263	
	82	577 752		5 799 963	
	83	581 452		5 804 363	
	84	572 852		5 792 663	
	85	584 352		5 807 263	
	86	576 652		5 795 763	
	87	585 152		5 808 363	
	88	573 352		5 791 763	
	89	578 252		5 799 063	
	90	577 052		5 794 563	
	91	580 152		5 799 263	
	92	583 652		5 804 563	
	93	576 252		5 791 563	
	94	580 452		5 798 163	
	95	584 052		5 806 063	
	96	577 352		5 793 463	
	97	578 952		5 800 263	
	98	580 052		5 796 463	
	99	572 852		5 794 963	
	100	581 552		5 799 463	
	101	577 652		5 792 363	
	102	581 252		5 805 463	
	103	574 052		5 795 163	
	104	578 652		5 793 863	
	105	575 552		5 796 063	
	106	564 852		5 788 263	
	107	566 152		5 789 063	
	108	567 352		5 789 363	
	109	567 752		5 788 363	
	110	568 852		5 789 763	
	111	570 352		5 790 163	

Hollandse Kust (noord)		Hollandse Kust (zuid)			
Wind turbine -220 m rotor diameter – 13 MW HH: 138 m		Wind turbine -200 m rotor diameter – 10 MW HH: 125 m			
WTG	(UTM WGS84)		WTG	(UTM WGS84)	
	x	y		x	y
112	571 552	5 790 463			
113	566 052	5 784 463			
114	572 052	5 789 563			
115	566 452	5 783 463			
116	572 352	5 788 463			
117	567 152	5 782 663			
118	573 252	5 789 963			
119	572 652	5 787 363			
120	567 152	5 785 963			
121	573 752	5 789 063			
122	568 252	5 782 063			
123	574 052	5 787 963			
124	565 352	5 785 663			
125	575 052	5 789 063			
126	569 252	5 783 063			
127	567 552	5 784 863			
128	568 652	5 787 863			
129	567 852	5 783 763			
130	570 652	5 784 263			
131	565 052	5 786 963			
132	568 352	5 786 563			
133	569 852	5 788 163			
134	568 952	5 784 763			
135	570 852	5 789 263			
136	570 152	5 785 163			
137	572 252	5 786 163			
138	566 152	5 787 663			
139	570 652	5 787 063			
140	571 852	5 786 263			

ANNEX B: WIND SHEAR MATRICES AT MMIJ AND HKW

Section analyses the link between stability conditions and wind shear values. This analysis implied looking at wind shear values for specific times of the day and periods of the year. In the following tables only bins with more than 5 samples are considered. In case insufficient samples are provided for a particular bin, the shear for that bin will be taken based on following priority:

- 1) Annual value for the direction and diurnal period.
- 2) Mean value for the nearest two directions
- 3) Overall mean

MMIJ

Table 57 shows the monthly shear values split into 2 diurnal periods, regardless of the direction. Table 58 shows diurnal shear values, split into 2 seasons, regardless of the direction.

The diurnal periods in Table 57 have been selected based on observations made in Table 58: indeed, it can be seen that the shear tends to be lower between 4am and 4pm.

Inversely, the seasonal periods in Table 58 were chosen based on observations from Table 57: from March until August, the average shear values are lower than during the rest of the year.

Table 59 shows the shear matrix, where 12 directional, 6 seasonal and 12 diurnal bins were considered.

HKW

The same analysis was carried out for HKW and can be found in tables Table 60, Table 61 and Table 62 (shear matrix).

TABLE 57: SHEAR MATRIX AT MMIJ AT 100 M FOR 2 DIURNAL BINS, 12 SEASONAL BINS AND 1 DIRECTIONAL BIN

ALL DIRECTIONS	Jan	Feb	Mar	Apr	May	Jun	Jul	Aug	Sep	Oct	Nov	Dec	Year
04 - 16	0.07	0.08	0.09	0.09	0.10	0.06	0.09	0.08	0.04	0.05	0.06	0.10	0.08
16 - 04	0.08	0.09	0.08	0.13	0.13	0.10	0.01	0.12	0.04	0.06	0.06	0.09	0.09
All	0.08	0.08	0.09	0.11	0.12	0.08	0.01	0.10	0.04	0.06	0.06	0.09	0.09

TABLE 58: SHEAR MATRIX AT MMIJ AT 100 M FOR 24 DIURNAL BINS, 2 SEASONAL BINS AND 1 DIRECTIONAL BIN

ALL DIRECTIONS	Mar - Aug	Sep - Feb	Year
0	0.12	0.07	0.09
1	0.11	0.08	0.10
2	0.12	0.07	0.09
3	0.11	0.06	0.09
4	0.09	0.08	0.08
5	0.07	0.06	0.07
6	0.06	0.07	0.08
7	0.07	0.06	0.09
8	0.08	0.07	0.08
9	0.07	0.06	0.08
10	0.09	0.06	0.08
11	0.08	0.05	0.08
12	0.09	0.06	0.09
13	0.11	0.06	0.07
14	0.10	0.06	0.09
15	0.10	0.06	0.09
16	0.09	0.06	0.08
17	0.12	0.06	0.10
18	0.10	0.08	0.10
19	0.11	0.07	0.10
20	0.13	0.07	0.09
21	0.12	0.07	0.09
22	0.11	0.07	0.08
23	0.11	0.07	0.08
All	0.10	0.07	0.09

TABLE 59: SHEAR MATRIX AT MMIJ AT 100 M FOR 12 DIURNAL BINS, 6 SEASONAL BINS AND 12 DIRECTIONAL BIN

ALL DIRECTIONS	Jan - Feb	Mar - Apr	May - Jun	Jul - Aug	Sep - Oct	Nov - Dec	Year
00-02	0.09	0.11	0.12	0.12	0.04	0.09	0.09
02-04	0.09	0.10	0.13	0.10	0.04	0.08	0.09
04-06	0.08	0.07	0.08	0.08	0.03	0.07	0.08
06-08	0.09	0.07	0.05	0.08	0.05	0.07	0.08
08-10	0.07	0.08	0.07	0.09	0.04	0.07	0.08
10-12	0.07	0.09	0.07	0.09	0.05	0.07	0.08
12-14	0.07	0.10	0.10	0.09	0.05	0.07	0.08
14-16	0.07	0.12	0.10	0.09	0.05	0.08	0.09
16-18	0.07	0.11	0.11	0.10	0.08	0.08	0.09
18-20	0.08	0.12	0.12	0.11	0.05	0.07	0.10
20-22	0.08	0.10	0.12	0.13	0.06	0.08	0.09
22-24	0.08	0.10	0.11	0.10	0.05	0.08	0.08
All	0.08	0.10	0.10	0.10	0.05	0.08	0.09

N	Jan - Feb	Mar - Apr	May - Jun	Jul - Aug	Sep - Oct	Nov - Dec	Year
00-02	0.04	0.08	0.07	0.07	0.05	0.06	0.07
02-04	0.04	0.07	0.06	0.07	0.04	0.02	0.06
04-06	0.07	0.12	0.09	0.05	0.01	0.02	0.03
06-08	0.10	0.09	0.08	0.10	0.05	0.04	0.08
08-10	0.06	0.07	0.04	0.22	0.06	0.04	0.08
10-12	0.03	0.03	0.06	-0.14	0.13	0.08	0.06
12-14	0.03	0.12	0.10	0.06	0.12	0.01	0.08
14-16	0.05	0.10	0.09	0.13	0.03	0.06	0.08
16-18	0.07	0.06	0.11	0.03	-0.04	0.05	0.07
18-20	0.14	0.05	0.05	0.05	0.03	0.03	0.05
20-22	0.04	0.10	0.11	0.12	0.07	0.08	0.09
22-24	0.06	0.08	0.05	0.07	0.03	0.03	0.04
All	0.05	0.08	0.08	0.08	0.05	0.04	0.07

NNE	Jan - Feb	Mar - Apr	May - Jun	Jul - Aug	Sep - Oct	Nov - Dec	Year
00-02	0.01	0.01	0.06	0.10	0.09	0.05	0.07
02-04	0.06	0.08	0.09	0.01	-0.03	0.02	0.05
04-06	0.01	0.09	0.04	0.02	0.08	0.10	0.07
06-08	0.06	0.11	0.06	0.03	0.02	0.03	0.06
08-10	0.02	0.07	0.08	0.08	0.09	0.03	0.07
10-12	0.04	0.02	0.07	0.07	0.03	0.01	0.04
12-14	0.04	0.12	0.08	0.03	0.04	0.02	0.06
14-16	0.09	0.08	0.04	0.04	0.03	0.02	0.08
16-18	0.01	0.13	0.08	0.02	0.08	0.08	0.09
18-20	0.09	0.01	0.11	0.05	0.02	0.02	0.06
20-22	0.03	0.07	0.10	0.05	0.04	0.00	0.06
22-24	0.03	-0.02	0.04	0.15	0.02	0.02	0.07
All	0.04	0.07	0.07	0.05	0.04	0.03	0.06

ENE	Jan - Feb	Mar - Apr	May - Jun	Jul - Aug	Sep - Oct	Nov - Dec	Year
00-02	0.05	0.02	0.18	0.12	0.27	0.01	0.08
02-04	0.05	0.07	-0.02	0.05	0.01	0.01	0.07
04-06	0.03	0.17	0.06	0.03	0.00	0.04	0.05
06-08	0.04	0.07	0.02	0.05	0.03	0.04	0.03
08-10	0.03	0.09	-0.04	-0.01	0.01	0.02	0.02
10-12	0.01	0.07	-0.09	0.09	0.06	0.05	0.02
12-14	0.03	0.09	-0.05	0.09	0.02	0.18	0.04
14-16	0.05	0.04	0.01	0.01	0.03	0.07	0.04
16-18	0.05	0.11	-0.01	0.14	0.04	-0.01	0.04
18-20	0.05	0.11	0.15	0.17	0.05	0.11	0.10
20-22	0.09	0.11	0.23	0.17	-0.01	0.04	0.15
22-24	0.02	0.06	0.12	0.12	0.10	0.06	0.09
All	0.04	0.09	0.06	0.08	0.05	0.05	0.06

E	Jan - Feb	Mar - Apr	May - Jun	Jul - Aug	Sep - Oct	Nov - Dec	Year
00-02	0.02	0.09	0.12	0.09	0.03	0.06	0.09
02-04	0.06	0.16	0.11	0.15	0.02	0.10	0.07
04-06	0.03	0.12	0.09	-0.07	0.00	0.03	0.04
06-08	0.03	-0.02	0.06	0.13	0.05	0.06	0.03
08-10	0.01	0.22	-0.01	0.00	-0.02	-0.01	0.03
10-12	0.05	0.18	-0.04	0.15	0.03	0.03	0.04
12-14	0.00	0.08	-0.07	0.07	0.00	0.04	0.02
14-16	0.04	0.14	-0.06	-0.09	0.00	0.07	0.00
16-18	0.03	0.26	0.02	-0.22	-0.01	0.02	-0.01
18-20	0.06	0.07	0.12	-0.05	-0.06	0.02	0.01
20-22	0.05	0.04	-0.01	0.05	0.02	0.00	0.03
22-24	0.05	0.08	0.18	0.04	0.04	0.10	0.07
All	0.03	0.10	0.03	0.03	0.03	0.04	0.04

ESE	Jan - Feb	Mar - Apr	May - Jun	Jul - Aug	Sep - Oct	Nov - Dec	Year
00-02	0.04	-0.13	0.11	0.12	0.04	0.02	0.04
02-04	0.03	0.00	0.08	0.20	0.09	0.06	0.08
04-06	0.03	0.09	0.13	0.24	0.02	0.05	0.05
06-08	0.04	0.01	0.20	0.18	0.07	0.01	0.08
08-10	0.05	0.11	0.12	0.05	0.01	0.03	0.04
10-12	0.02	0.06	0.09	0.16	0.08	0.06	0.07
12-14	0.01	0.05	0.07	0.05	0.08	0.14	0.06
14-16	0.01	0.21	0.17	0.15	0.18	0.04	0.09
16-18	0.04	0.05	0.03	0.09	0.28	0.07	0.07
18-20	0.04	0.14	0.02	0.01	0.12	0.01	0.06
20-22	0.08	0.03	0.08	0.01	0.15	0.01	0.05
22-24	0.05	0.12	0.08	0.21	0.11	0.01	0.09
All	0.04	0.06	0.10	0.12	0.06	0.05	0.06

SSE	Jan - Feb	Mar - Apr	May - Jun	Jul - Aug	Sep - Oct	Nov - Dec	Year
00-02	0.06	0.06	0.12	0.14	-0.06	0.08	0.11
02-04	0.00	0.07	0.20	0.11	0.06	0.08	0.12
04-06	0.02	0.04	0.01	0.12	0.05	0.02	0.05
06-08	0.05	0.06	-0.12	0.04	0.06	0.06	0.03
08-10	0.08	0.03	0.00	-0.05	0.07	0.13	0.06
10-12	0.06	0.11	0.24	0.07	0.10	0.05	0.05
12-14	0.07	0.14	0.22	0.04	0.08	0.03	0.10
14-16	0.05	0.19	0.07	0.08	0.16	0.08	0.10
16-18	0.07	0.16	0.11	0.11	0.15	0.12	0.09
18-20	0.07	0.16	0.24	0.13	0.09	0.06	0.09
20-22	0.08	0.09	-0.02	0.10	0.14	0.02	0.11
22-24	0.04	0.04	0.18	0.11	0.04	0.08	0.09
All	0.05	0.10	0.10	0.08	0.08	0.07	0.08

S	Jan - Feb	Mar - Apr	May - Jun	Jul - Aug	Sep - Oct	Nov - Dec	Year
00-02	0.06	0.21	-0.03	0.18	0.08	0.08	0.12
02-04	0.09	0.10	0.16	-0.06	0.06	0.09	0.09
04-06	0.07	0.11	-0.05	0.03	0.06	0.15	0.08
06-08	0.08	0.11	-0.01	0.08	0.11	0.11	0.08
08-10	0.10	0.09	0.09	0.14	0.03	0.06	0.10
10-12	0.09	0.23	0.16	0.14	0.05	0.06	0.09
12-14	0.07	0.28	0.14	0.17	0.06	0.10	0.12
14-16	0.09	0.19	0.05	0.12	0.07	0.10	0.11
16-18	0.05	0.09	0.13	0.16	0.15	0.11	0.09
18-20	0.10	0.11	0.01	0.16	0.17	0.10	0.14
20-22	0.11	0.13	0.13	0.16	0.09	0.11	0.13
22-24	0.11	0.16	0.10	0.07	0.14	0.07	0.09
All	0.09	0.15	0.05	0.12	0.09	0.09	0.10

SSW	Jan - Feb	Mar - Apr	May - Jun	Jul - Aug	Sep - Oct	Nov - Dec	Year
00-02	0.12	0.10	0.15	0.13	0.10	0.12	0.15
02-04	0.11	0.16	0.20	0.15	0.13	0.12	0.15
04-06	0.11	0.19	0.20	0.14	0.11	0.13	0.14
06-08	0.10	0.11	0.15	0.14	0.10	0.12	0.14
08-10	0.17	0.19	0.17	0.17	0.06	0.13	0.12
10-12	0.13	0.17	0.18	0.17	0.04	0.12	0.14
12-14	0.12	0.17	0.16	0.17	0.05	0.12	0.11
14-16	0.13	0.23	0.21	0.12	0.06	0.10	0.15
16-18	0.09	0.20	0.20	0.14	0.06	0.10	0.15
18-20	0.15	0.20	0.22	0.21	0.07	0.12	0.16
20-22	0.10	0.21	0.25	0.17	0.09	0.12	0.18
22-24	0.16	0.21	0.17	0.14	0.09	0.08	0.16
All	0.12	0.18	0.19	0.15	0.07	0.12	0.15

WSW	Jan - Feb	Mar - Apr	May - Jun	Jul - Aug	Sep - Oct	Nov - Dec	Year
00-02	0.09	0.13	0.23	0.13	0.04	0.11	0.11
02-04	0.13	0.08	0.22	0.10	0.04	0.09	0.11
04-06	0.11	0.04	0.19	0.04	0.06	0.06	0.10
06-08	0.11	0.12	0.21	0.06	0.05	0.10	0.09
08-10	0.11	0.11	0.08	0.12	0.04	0.06	0.08
10-12	0.05	0.09	0.05	0.12	0.02	0.08	0.09
12-14	0.07	0.11	0.19	0.08	0.03	0.07	0.11
14-16	0.10	0.15	0.23	0.09	0.03	0.09	0.07
16-18	0.07	0.05	0.08	0.09	0.04	0.10	0.09
18-20	0.08	0.09	0.10	0.10	0.05	0.12	0.10
20-22	0.13	0.14	0.20	0.15	0.08	0.12	0.12
22-24	0.14	0.15	0.18	0.13	0.07	0.12	0.11
All	0.11	0.11	0.14	0.10	0.05	0.10	0.10

W	Jan - Feb	Mar - Apr	May - Jun	Jul - Aug	Sep - Oct	Nov - Dec	Year
00-02	0.19	0.13	0.13	0.12	0.00	0.07	0.13
02-04	0.14	0.12	0.12	0.12	0.06	0.07	0.11
04-06	0.11	0.11	0.08	0.09	0.03	0.04	0.08
06-08	0.15	0.12	0.00	0.07	0.03	0.06	0.09
08-10	0.12	0.08	0.08	0.06	0.05	0.06	0.08
10-12	0.07	0.10	0.06	0.05	0.05	0.06	0.06
12-14	0.09	0.05	0.10	0.01	0.03	0.04	0.08
14-16	0.07	0.10	0.10	0.12	0.05	0.08	0.09
16-18	0.05	0.18	0.16	0.06	0.09	0.06	0.09
18-20	0.11	0.22	0.22	0.04	0.03	0.04	0.11
20-22	0.08	0.13	0.20	0.05	0.03	0.04	0.10
22-24	0.12	0.13	0.15	0.05	0.02	0.03	0.06
All	0.10	0.14	0.11	0.07	0.04	0.06	0.09

WNW	Jan - Feb	Mar - Apr	May - Jun	Jul - Aug	Sep - Oct	Nov - Dec	Year
00-02	0.03	0.16	0.16	0.03	0.06	0.04	0.07
02-04	0.02	0.15	0.06	0.06	0.06	0.04	0.08
04-06	0.09	0.03	0.13	0.04	0.02	0.04	0.07
06-08	0.06	0.06	0.06	0.00	0.01	0.05	0.04
08-10	0.08	0.08	0.02	0.01	-0.01	0.05	0.03
10-12	0.06	0.13	0.07	0.03	0.01	0.08	0.04
12-14	0.06	0.05	0.12	0.05	0.04	0.17	0.06
14-16	0.05	0.04	0.07	0.03	0.02	0.03	0.06
16-18	0.07	0.19	0.11	0.02	0.03	0.03	0.06
18-20	0.06	0.08	0.08	0.01	0.07	0.02	0.06
20-22	0.05	0.09	0.09	0.01	0.06	0.04	0.08
22-24	0.04	0.08	0.13	0.03	0.06	0.02	0.06
All	0.05	0.09	0.10	0.04	0.04	0.03	0.06

NNW	Jan - Feb	Mar - Apr	May - Jun	Jul - Aug	Sep - Oct	Nov - Dec	Year
00-02	0.09	0.18	0.07	0.16	0.02	0.04	0.06
02-04	0.10	0.07	0.10	0.03	0.06	0.03	0.07
04-06	0.10	0.14	0.17	0.04	0.03	0.02	0.05
06-08	0.07	-0.08	0.02	0.04	0.07	0.00	0.03
08-10	0.10	0.11	0.04	0.12	0.01	0.04	0.08
10-12	0.07	0.09	0.09	0.16	0.03	0.07	0.07
12-14	0.08	0.06	0.10	0.08	0.01	0.01	0.05
14-16	0.10	0.06	0.11	0.00	0.00	0.04	0.04
16-18	0.05	0.11	0.07	0.09	0.06	0.01	0.07
18-20	0.05	0.06	0.08	0.01	0.03	0.03	0.07
20-22	0.04	0.05	0.06	0.05	0.02	0.09	0.06
22-24	0.04	0.04	0.09	0.03	0.02	0.05	0.06
All	0.07	0.05	0.08	0.04	0.03	0.03	0.06

TABLE 60: SHEAR MATRIX AT HKW AT 100 M FOR 2 DIURNAL BINS, 12 SEASONAL BINS AND 1 DIRECTIONAL BIN

ALL DIRECTIONS	Jan	Feb	Mar	Apr	May	Jun	Jul	Aug	Sep	Oct	Nov	Dec	Year
04 - 16	0.08	0.13	0.10	0.06	0.07	0.11	0.08	0.05	0.05	0.05	0.04	0.07	0.08
16 - 04	0.07	0.14	0.13	0.11	0.07	0.10	0.09	0.05	0.06	0.06	0.06	0.06	0.09
All	0.08	0.14	0.12	0.09	0.07	0.11	0.09	0.05	0.06	0.05	0.05	0.07	0.09

TABLE 61: SHEAR MATRIX AT HKW AT 100 M FOR 24 DIURNAL BINS, 2 SEASONAL BINS AND 1 DIRECTIONAL BIN

ALL DIRECTIONS	Mar - Aug	Sep - Feb	Year
0	0.11	0.07	0.09
1	0.14	0.09	0.10
2	0.12	0.07	0.09
3	0.10	0.08	0.09
4	0.08	0.09	0.09
5	0.08	0.08	0.07
6	0.08	0.06	0.08
7	0.08	0.06	0.08
8	0.10	0.07	0.08
9	0.09	0.08	0.08
10	0.10	0.08	0.08
11	0.09	0.09	0.08
12	0.08	0.08	0.07
13	0.04	0.07	0.07
14	0.06	0.07	0.07
15	0.05	0.07	0.08
16	0.05	0.08	0.08
17	0.08	0.07	0.09
18	0.10	0.08	0.09
19	0.08	0.08	0.08
20	0.09	0.09	0.09
21	0.11	0.08	0.10
22	0.10	0.07	0.09
23	0.10	0.07	0.10
All	0.09	0.07	0.09

TABLE 62: SHEAR MATRIX AT HKW AT 100 M FOR 12 DIURNAL BINS, 6 SEASONAL BINS AND 12 DIRECTIONAL BIN

ALL DIRECTIONS	Jan - Feb	Mar - Apr	May - Jun	Jul - Aug	Sep - Oct	Nov - Dec	Year
00-02	0.11	0.11	0.12	0.10	0.08	0.06	0.10
02-04	0.13	0.10	0.12	0.10	0.05	0.05	0.09
04-06	0.12	0.10	0.10	0.07	0.06	0.06	0.08
06-08	0.09	0.12	0.09	0.07	0.06	0.05	0.08
08-10	0.11	0.08	0.07	0.06	0.04	0.04	0.08
10-12	0.14	0.07	0.10	0.05	0.06	0.07	0.08
12-14	0.11	0.07	0.09	0.06	0.06	0.07	0.07
14-16	0.09	0.05	0.09	0.05	0.08	0.05	0.08
16-18	0.09	0.13	0.07	0.05	0.05	0.06	0.08
18-20	0.10	0.11	0.11	0.06	0.06	0.06	0.08
20-22	0.10	0.13	0.10	0.06	0.05	0.07	0.10
22-24	0.11	0.10	0.08	0.10	0.05	0.05	0.10
All	0.11	0.10	0.09	0.07	0.06	0.06	0.09

N	Jan-Feb	Mar-Apr	May-Jun	Jul-Aug	Sep-Oct	Nov-Dec	Year
00-02	0.02	0.01	0.08	0.01	0.03	0.11	0.03
02-04	-0.01	0.10	0.01	0.04	0.07	0.01	0.02
04-06	0.03	0.04	0.06	0.02	0.07	0.02	0.03
06-08	-0.01	0.21	0.05	0.02	0.09	0.06	0.02
08-10	0.05	0.11	0.06	0.09	0.03	0.01	0.09
10-12	0.02	-0.01	0.15	0.04	0.02	0.08	0.06
12-14	0.03	0.12	0.03	-0.02	0.08	0.07	0.06
14-16	0.02	-0.02	0.08	-0.01	0.00	0.02	0.03
16-18	0.06	0.09	0.02	-0.11	0.05	0.00	0.03
18-20	-0.03	0.06	0.06	0.02	-0.02	0.04	-0.01
20-22	0.01	0.06	0.06	0.02	0.02	0.01	0.01
22-24	-0.02	-0.02	0.04	0.02	0.05	0.07	0.03
All	0.01	0.06	0.07	0.00	0.04	0.05	0.03

NNE	Jan-Feb	Mar-Apr	May-Jun	Jul-Aug	Sep-Oct	Nov-Dec	Year
00-02	0.07	0.04	-0.06	0.05	0.17	-0.01	0.04
02-04	0.08	0.01	0.14	-0.01	0.09	0.04	0.07
04-06	0.05	0.11	-0.05	-0.18	0.15	0.04	0.05
06-08	-0.04	0.02	0.04	-0.04	0.09	-0.01	0.04
08-10	0.01	0.01	-0.02	-0.10	0.12	0.04	0.03
10-12	0.00	0.05	0.13	-0.09	0.09	-0.02	0.10
12-14	0.03	0.06	0.05	0.15	0.01	0.02	0.05
14-16	-0.02	0.01	0.01	-0.29	0.01	0.06	0.03
16-18	0.07	0.04	0.04	-0.19	0.00	-0.03	0.00
18-20	0.05	0.06	0.04	-0.30	0.00	0.13	0.03
20-22	-0.07	0.06	0.00	0.09	0.01	0.00	0.03
22-24	-0.06	0.05	-0.02	0.06	-0.03	0.01	0.00
All	0.01	0.05	0.02	-0.08	0.06	0.04	0.03

ENE	Jan-Feb	Mar-Apr	May-Jun	Jul-Aug	Sep-Oct	Nov-Dec	Year
00-02	0.01	0.06	0.13	-0.13	0.02	0.06	0.08
02-04	-0.02	0.04	0.09	-0.55	0.03	0.02	0.02
04-06	0.00	-0.01	0.10	-0.43	0.04	0.10	0.00
06-08	-0.03	0.04	0.04	0.00	0.04	0.02	0.04
08-10	0.01	0.03	0.01	0.04	0.02	0.06	0.03
10-12	-0.10	0.08	-0.01	-0.12	0.04	0.01	0.02
12-14	0.07	-0.06	-0.06	-0.23	0.04	0.03	-0.05
14-16	-0.01	-0.05	0.07	-0.37	0.04	0.00	0.01
16-18	0.00	0.05	-0.07	-0.34	-0.02	0.32	-0.04
18-20	0.03	0.05	0.08	-0.25	-0.09	0.12	0.03
20-22	0.03	0.08	0.15	0.02	0.04	0.01	0.10
22-24	0.00	0.10	0.12	-0.12	0.01	0.10	0.08
All	0.02	0.05	0.07	-0.14	0.02	0.04	0.03

E	Jan-Feb	Mar-Apr	May-Jun	Jul-Aug	Sep-Oct	Nov-Dec	Year
00-02	0.00	0.11	0.16	0.13	0.02	0.18	0.12
02-04	-0.03	0.12	0.14	0.24	0.00	0.17	0.1
04-06	0.03	0.09	0.07	0.08	0.01	0.11	0.06
06-08	0.05	0.14	0.06	0.10	0.02	0.05	0.06
08-10	0.03	0.17	0.05	0.13	0.01	-0.04	0.03
10-12	0.00	0.04	0.09	0.00	0.01	0.01	0.05
12-14	0.00	0.07	0.05	0.26	0.06	0.04	0.05
14-16	0.02	0.12	0.01	-0.11	0.06	-0.04	0.03
16-18	0.02	0.17	0.21	-0.29	-0.01	0.03	0.06
18-20	0.04	0.10	0.13	-0.04	-0.05	0.05	0.04
20-22	-0.01	0.12	-0.08	-0.01	-0.01	-0.05	-0.02
22-24	0.05	0.13	0.06	0.14	0.02	-0.03	0.07
All	0.02	0.10	0.08	0.06	0.01	0.01	0.06

ESE	Jan-Feb	Mar-Apr	May-Jun	Jul-Aug	Sep-Oct	Nov-Dec	Year
00-02	-0.03	0.06	0.12	0.08	0.06	0.05	0.11
02-04	0.16	-0.01	0.22	0.19	0.03	0.06	0.12
04-06	0.17	-0.13	0.21	0.19	0.07	0.01	0.09
06-08	0.05	-0.82	0.21	0.01	0.04	0.11	0.01
08-10	0.05	0.07	0.16	0.08	0.04	0.17	0.09
10-12	-0.02	0.01	0.07	0.17	-0.11	0.00	0.06
12-14	0.01	-0.03	0.07	0.19	0.13	0.00	0.05
14-16	0.03	-0.02	0.19	0.04	0.00	-0.01	0.01
16-18	0.23	0.19	-0.20	0.04	-0.01	0.01	0.05
18-20	0.04	0.11	-0.47	-0.05	0.05	0.01	0.06
20-22	0.00	0.11	0.00	0.15	-0.04	0.04	0.04
22-24	-0.03	0.11	0.05	0.03	-0.01	0.05	0.02
All	0.01	0.03	0.14	0.08	0.06	0.02	0.06

SSE	Jan-Feb	Mar-Apr	May-Jun	Jul-Aug	Sep-Oct	Nov-Dec	Year
00-02	0.04	0.21	0.06	0.05	0.15	0.04	0.11
02-04	0.04	0.10	0.16	0.17	0.07	0.04	0.09
04-06	0.13	0.11	0.21	0.20	0.05	0.04	0.12
06-08	0.06	0.09	0.15	0.20	0.09	0.03	0.08
08-10	0.13	0.03	0.09	0.11	0.05	0.02	0.06
10-12	0.38	0.11	0.05	0.15	0.11	0.07	0.12
12-14	0.06	0.01	0.16	0.20	0.07	0.03	0.06
14-16	-0.08	0.21	0.08	0.34	0.05	0.06	0.11
16-18	-0.29	0.33	-0.01	0.29		0.08	0.20
18-20	0.10	0.23	0.43	0.19	0.05	0.07	0.11
20-22	0.13	0.20	0.03	-0.09	0.03	-0.01	0.05
22-24	0.05	0.19	-0.03	-0.21	0.10	0.10	0.07
All	0.06	0.13	0.10	0.11	0.07	0.05	0.09

S	Jan-Feb	Mar-Apr	May-Jun	Jul-Aug	Sep-Oct	Nov-Dec	Year
00-02	0.15	0.19	0.23	0.08	0.12	0.06	0.11
02-04	0.13	0.21	0.18	0.08	0.02	0.06	0.13
04-06	0.13	0.11	0.10	0.10	0.08	0.05	0.07
06-08	0.27	0.13	0.10	0.13	0.04	0.07	0.09
08-10	0.17	0.17	0.06	0.21	0.10	0.09	0.11
10-12	0.34	0.16	0.03	0.11	0.10	0.11	0.15
12-14	0.19	0.19	0.19	0.15	0.14	0.09	0.10
14-16	0.11	0.17	0.16	0.20	0.07	0.05	0.13
16-18	0.10	0.21	0.09	0.14	0.03	0.08	0.09
18-20	0.16	0.19	0.03	0.18	0.06	0.10	0.10
20-22	0.14	0.22	0.05	0.09	0.04	0.09	0.10
22-24	0.12	0.17	0.11	0.13	0.11	0.03	0.09
All	0.16	0.16	0.09	0.11	0.08	0.07	0.10

SSW	Jan-Feb	Mar-Apr	May-Jun	Jul-Aug	Sep-Oct	Nov-Dec	Year
00-02	0.16	0.18	0.13	0.09	0.08	0.08	0.13
02-04	0.16	0.17	0.13	0.14	0.06	0.10	0.13
04-06	0.17	0.13	0.15	0.14	0.06	0.07	0.12
06-08	0.16	0.15	0.15	0.12	0.08	0.08	0.11
08-10	0.10	0.15	0.06	0.06	0.06	0.07	0.11
10-12	0.13	0.19	0.17	0.11	0.08	0.13	0.14
12-14	0.12	0.2	0.16	0.13	0.06	0.13	0.12
14-16	0.10	0.16	0.17	0.11	0.10	0.08	0.12
16-18	0.12	0.17	0.17	0.15	0.08	0.10	0.14
18-20	0.15	0.22	0.15	0.13	0.06	0.09	0.14
20-22	0.15	0.23	0.16	0.16	0.12	0.11	0.14
22-24	0.19	0.18	0.19	0.13	0.10	0.09	0.14
All	0.15	0.19	0.17	0.13	0.08	0.10	0.13

WSW	Jan-Feb	Mar-Apr	May-Jun	Jul-Aug	Sep-Oct	Nov-Dec	Year
00-02	0.12	0.11	0.21	0.11	0.05	0.05	0.14
02-04	0.12	0.15	0.19	0.08	0.09	0.07	0.14
04-06	0.14	0.13	0.19	0.06	0.06	0.11	0.12
06-08	0.20	0.14	0.06	0.10	0.04	0.08	0.09
08-10	0.18	0.17	0.10	0.07	0.02	0.05	0.07
10-12	0.11	0.13	0.16	0.06	0.05	0.09	0.09
12-14	0.15	0.18	0.16	0.07	0.07	0.13	0.10
14-16	0.15	0.11	0.14	0.04	0.07	0.07	0.11
16-18	0.13	0.14	0.25	0.07	0.08	0.08	0.13
18-20	0.13	0.17	0.23	0.12	0.09	0.06	0.13
20-22	0.19	0.17	0.22	0.15	0.09	0.07	0.13
22-24	0.17	0.12	0.22	0.17	0.08	0.06	0.14
All	0.15	0.15	0.19	0.10	0.06	0.07	0.11

W	Jan-Feb	Mar-Apr	May-Jun	Jul-Aug	Sep-Oct	Nov-Dec	Year
00-02	0.10	0.14	0.12	0.11	0.07	0.03	0.11
02-04	0.13	0.16	0.14	0.04	0.05	0.03	0.08
04-06	0.07	0.08	0.12	0.06	0.03	0.03	0.08
06-08	0.06	0.10	0.06	0.07	0.01	0.01	0.05
08-10	0.08	0.03	0.01	0.04	0.04	0.02	0.05
10-12	0.07	0.06	0.01	0.04	0.06	0.05	0.05
12-14	0.09	0.07	0.07	0.01	0.01	0.03	0.05
14-16	0.04	0.05	0.11	0.05	0.01	0.03	0.08
16-18	0.04	0.04	-0.04	0.03	0.05	0.05	0.06
18-20	0.09	0.05	-0.02	0.06	0.04	0.07	0.07
20-22	0.06	0.10	-0.09	0.09	0.05	0.07	0.08
22-24	0.08	0.09	0.04	0.14	0.04	0.05	0.07
All	0.07	0.09	0.09	0.06	0.04	0.04	0.07

WNW	Jan-Feb	Mar-Apr	May-Jun	Jul-Aug	Sep-Oct	Nov-Dec	Year
00-02	0.05	0.04	0.12	0.09	-0.02	0.02	0.07
02-04	0.02	0.17	0.06	0.10	0.00	0.04	0.06
04-06	0.03	0.06	0.16	0.10	0.08	0.01	0.03
06-08	0.05	-0.02	0.07	0.11	0.00	0.00	0.03
08-10	0.05	0.03	0.00	0.02	0.00	-0.03	0.04
10-12	0.05	0.06	0.12	0.10	0.04	0.03	0.04
12-14	0.07	-0.02	0.07	-0.02	0.05	0.09	0.05
14-16	0.03	0.12	0.05	0.02	0.04	0.02	0.02
16-18	0.03	0.13	0.09	-0.02	-0.01	0.05	0.06
18-20	0.10	0.11	0.15	-0.03	0.02	-0.02	0.04
20-22	0.06	0.17	0.10	-0.05	-0.02	0.01	0.05
22-24	0.06	0.16	0.11	0.06	0.03	0.06	0.07
All	0.05	0.07	0.08	0.04	0.02	0.03	0.05

NNW	Jan-Feb	Mar-Apr	May-Jun	Jul-Aug	Sep-Oct	Nov-Dec	Year
00-02	0.06	0.04	0.05	0.06	0.03	0.15	0.07
02-04	0.08	0.05	0.01	-0.06	-0.01	0.07	0.02
04-06	0.04	0.00	0.04	0.01	0.00	0.01	0.04
06-08	0.05	0.17	0.17	0.04	0.00	0.03	0.06
08-10	0.04	0.08	0.49	0.02	0.04	0.04	0.04
10-12	0.06	0.09	0.02	0.03	0.01	0.07	0.02
12-14	0.01	0.00	0.10	0.04	0.06	0.02	0.05
14-16	0.00	0.04	0.05	0.02	0.04	0.03	0.03
16-18	0.02	0.11	0.00	0.04	0.03	0.07	0.03
18-20	0.02	-0.01	-0.05	-0.03	0.01	0.01	0.03
20-22	0.04	0.01	0.00	0.00	0.00	0.03	0.01
22-24	0.05	0.03	-0.12	-0.01	0.01	0.03	0.01
All	0.04	0.04	0.07	0.01	0.01	0.04	0.04

ANNEX C: LTC – KPI RESULTS FOR THE LONG-TERM CORRECTION BASED ON ENERGY

TABLE 63: LTC KPI'S OF THE MCP METHODS PERFORMED FOR HKW. ALL STATISTICS ARE GIVEN FOR 1 HOUR AVERAGES OF THE ESTIMATED ENERGY PRODUCTION.

Hkw					
Reference Dataset	MCP Method	MBE [%]	MAE [%]	RMSE [%]	Pearson R
ERA5	Regression	0.16	11.86	18.98	0.952
	Matrix	0.17	12.02	19.06	0.951
	Neural Network	0.84	11.89	18.95	0.952
Merra2	Regression	-0.55	13.98	22.00	0.934
	Matrix	0.27	14.16	22.02	0.934
	Neural Network	-0.89	13.95	22.07	0.934
CFSv2	Regression	-0.22	15.77	24.51	0.918
	Matrix	0.18	16.03	24.62	0.917
	Neural Network	-1.02	15.62	24.31	0.919
LEG	Regression	0.48	20.46	30.83	0.864
	Matrix	0.56	20.83	31.16	0.861
	Neural Network	-0.85	20.72	30.63	0.864

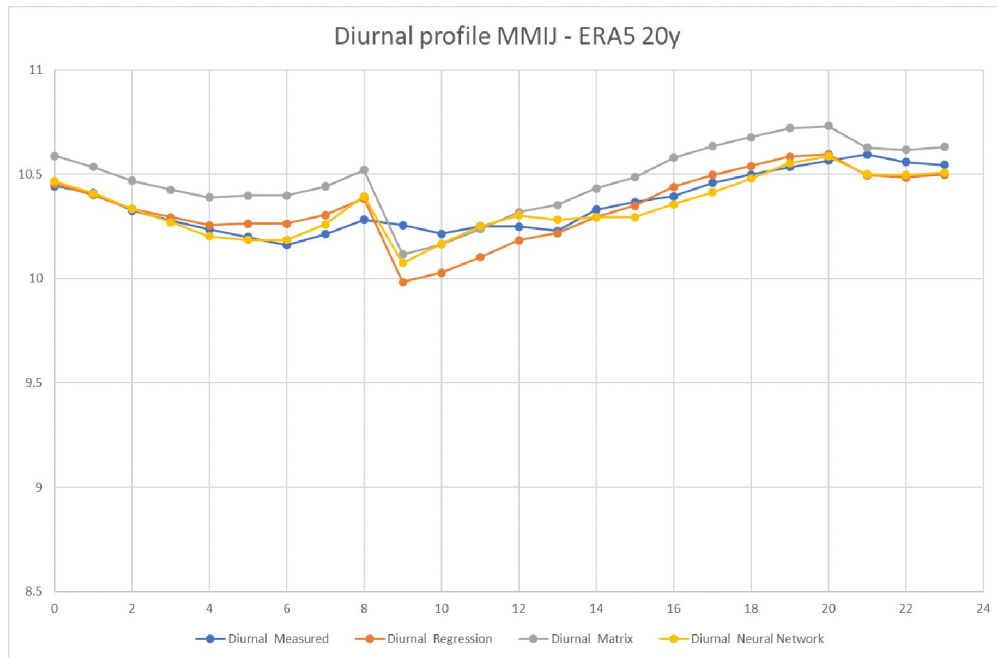
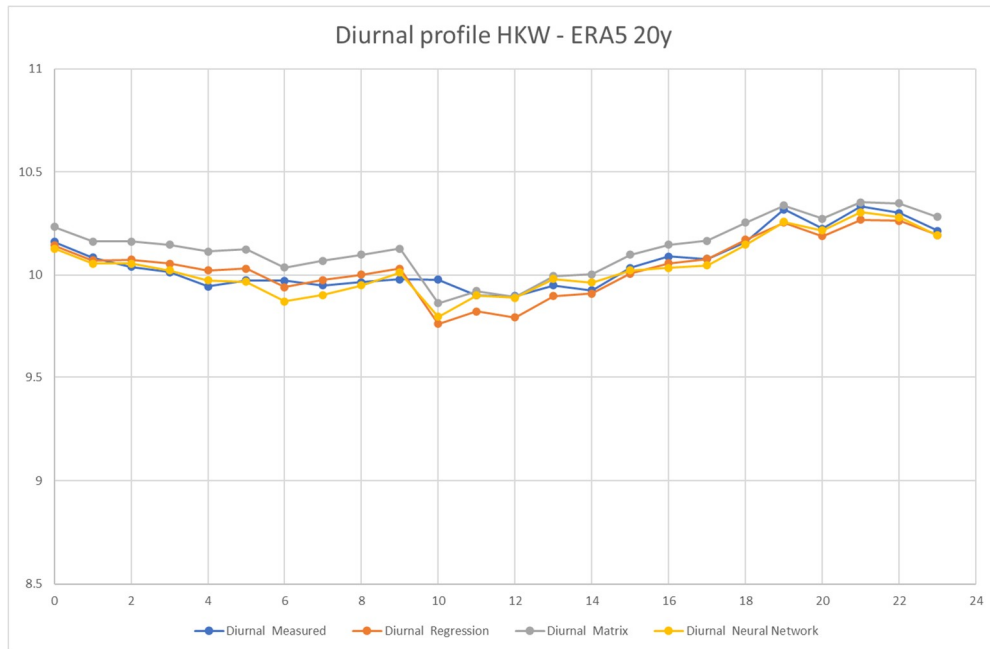
TABLE 64: LTC KPI'S OF THE MCP METHODS PERFORMED FOR MMIJ. ALL STATISTICS ARE GIVEN FOR 1 HOUR AVERAGES OF THE ESTIMATED ENERGY PRODUCTION.

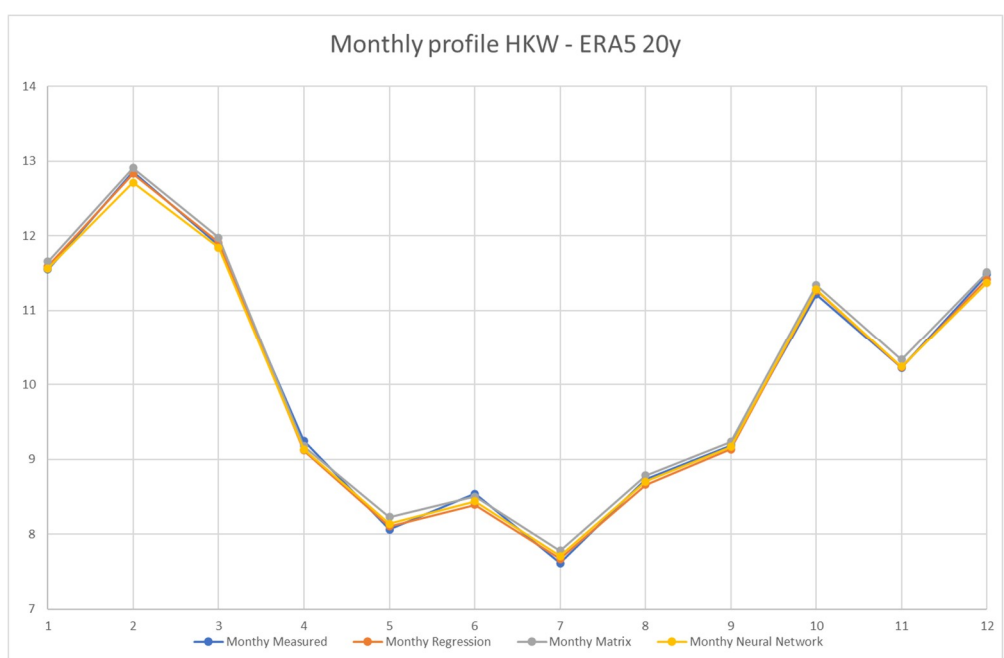
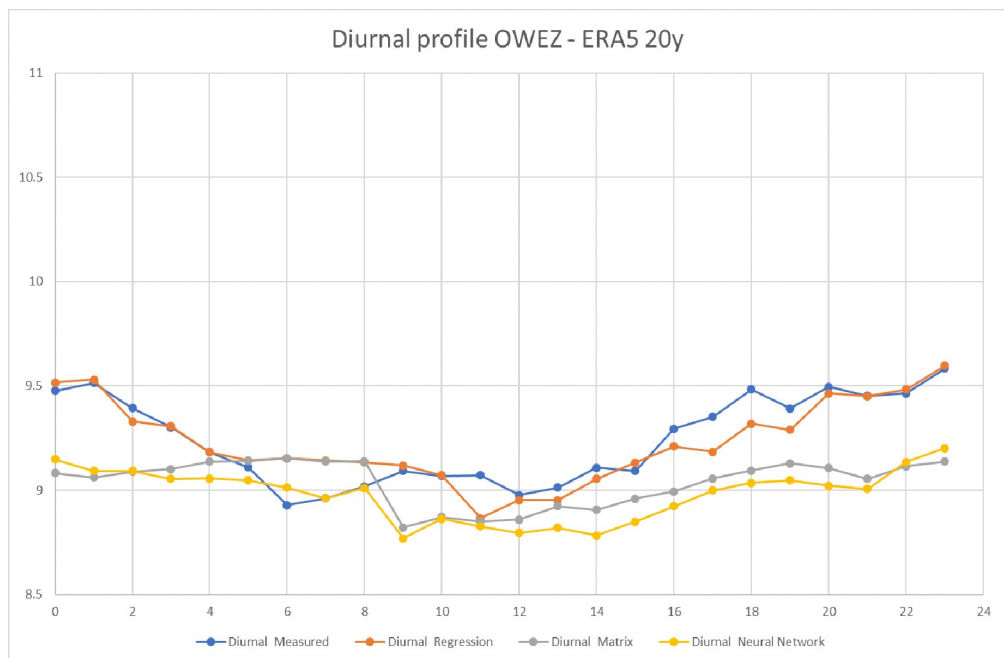
MMIJ					
Reference Dataset	MCP Method	MAE [%]	MAE [%]	RMSE [%]	Pearson R
ERA5	Regression	0.49	11.32	18.59	0.951
	Matrix	2.18	11.51	18.80	0.950
	Neural Network	1.38	11.40	18.66	0.950
Merra2	Regression	0.21	13.46	21.32	0.934
	Matrix	1.34	13.64	21.33	0.934
	Neural Network	0.49	13.42	21.30	0.935
CFSv2	Regression	0.37	15.14	23.76	0.918
	Matrix	2.56	15.41	23.88	0.918
	Neural Network	-0.29	15.03	23.57	0.919
LEG	Regression	0.80	24.26	36.67	0.801
	Matrix	5.93	24.75	37.03	0.797
	Neural Network	-0.01	24.23	36.58	0.801

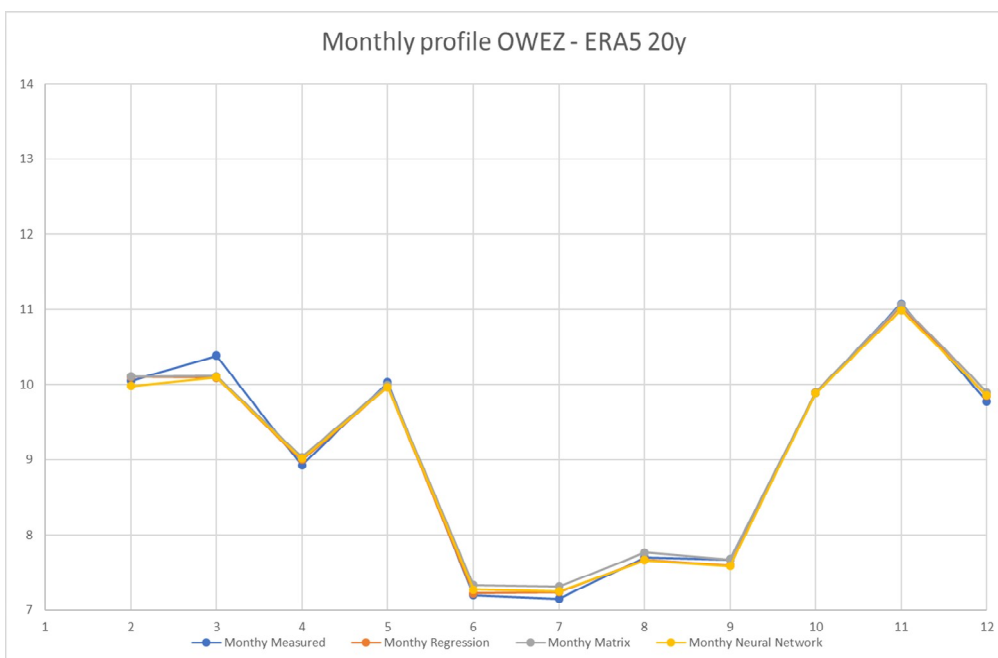
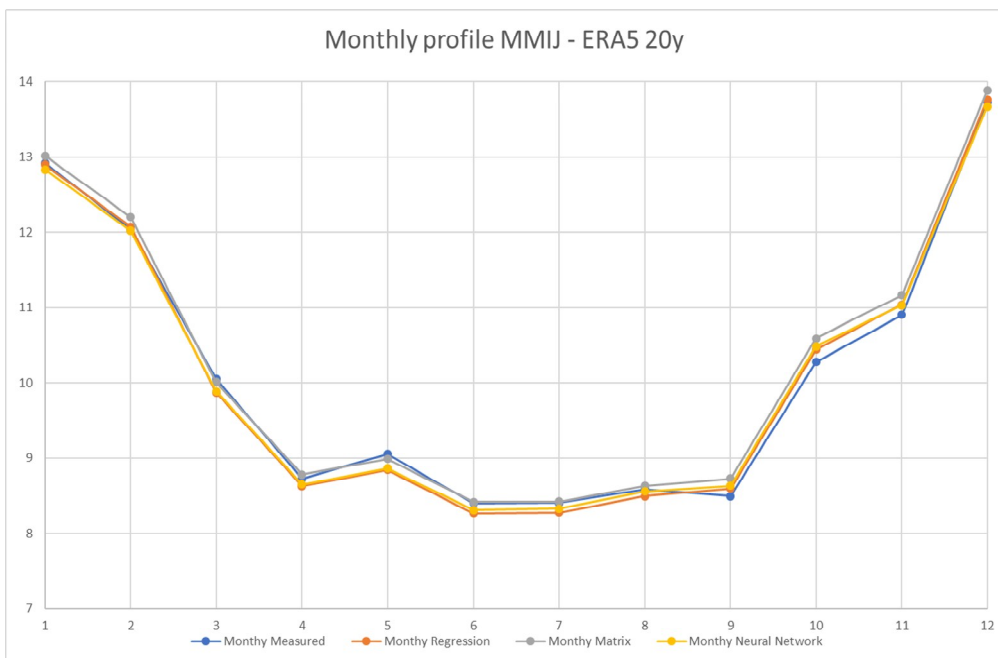
TABLE 65: LTC KPI'S OF THE MCP METHODS PERFORMED FOR OWEZ. ALL STATISTICS ARE GIVEN FOR 1 HOUR AVERAGES OF THE ESTIMATED ENERGY PRODUCTION.

OWEZ					
Reference Dataset	MCP Method	MAE [%]	MAE [%]	RMSE [%]	Pearson R
ERA5	Regression	-0.71	15.11	22.58	0.943
	Matrix	-0.06	15.20	22.58	0.943
	Neural Network	-0.49	15.17	22.56	0.943
Merra2	Regression	-0.76	17.26	25.69	0.926
	Matrix	0.13	17.62	25.81	0.925
	Neural Network	-0.74	16.94	25.42	0.928
CFSv2	Regression				
	Matrix				
	Neural Network				
LEG	Regression	-0.73	24.84	35.91	0.852
	Matrix	-0.18	25.14	35.99	0.849
	Neural Network	-1.94	24.77	35.68	0.854

ANNEX D: LTC – DIURNAL AND MONTHLY PROFILES OF LTC WIND CLIMATE







ANNEX E: LTC – WEIBULL FITS AND FREQUENCY DISTRIBUTIONS

HKW

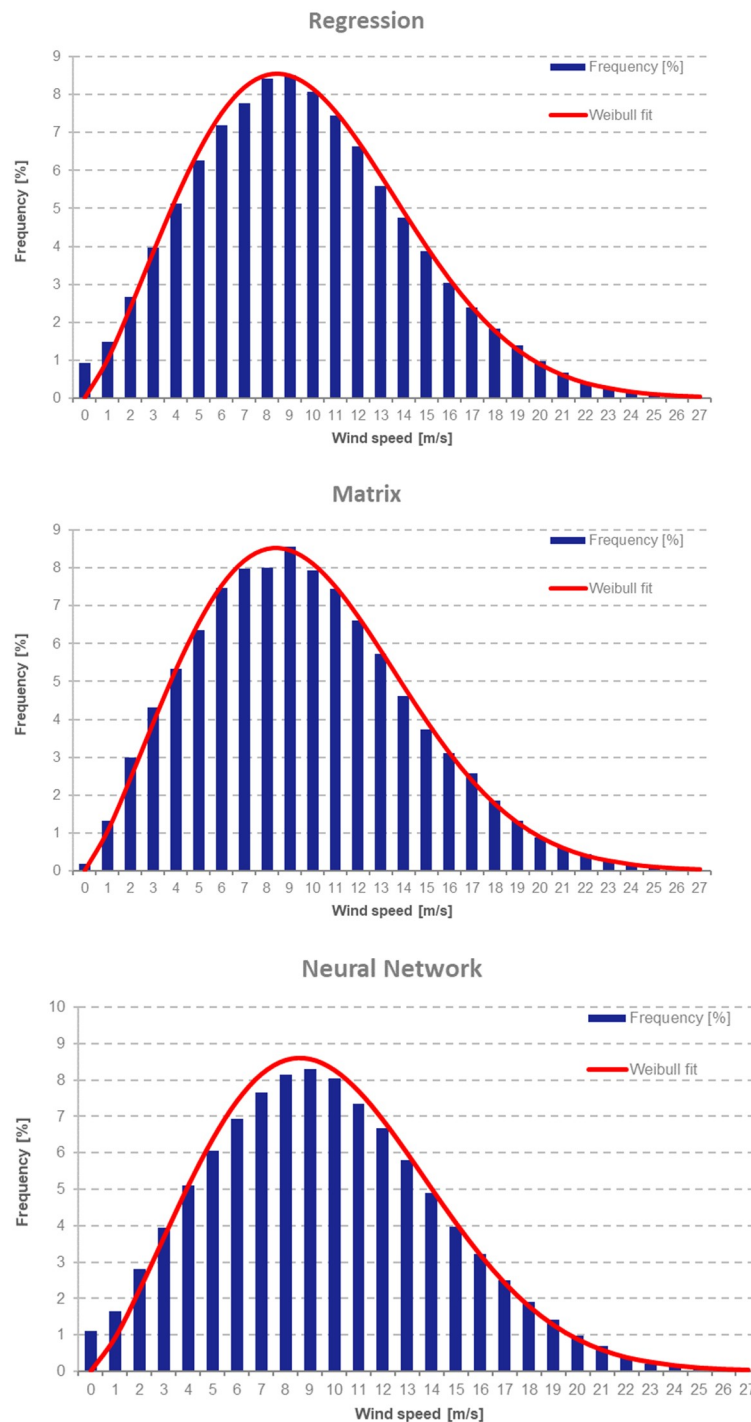


Figure 47: Frequency distribution and Weibull fit at HKW for the long-term corrected wind climate by means of Regression (Top), Matrix method (middle) and Neural Network (bottom)

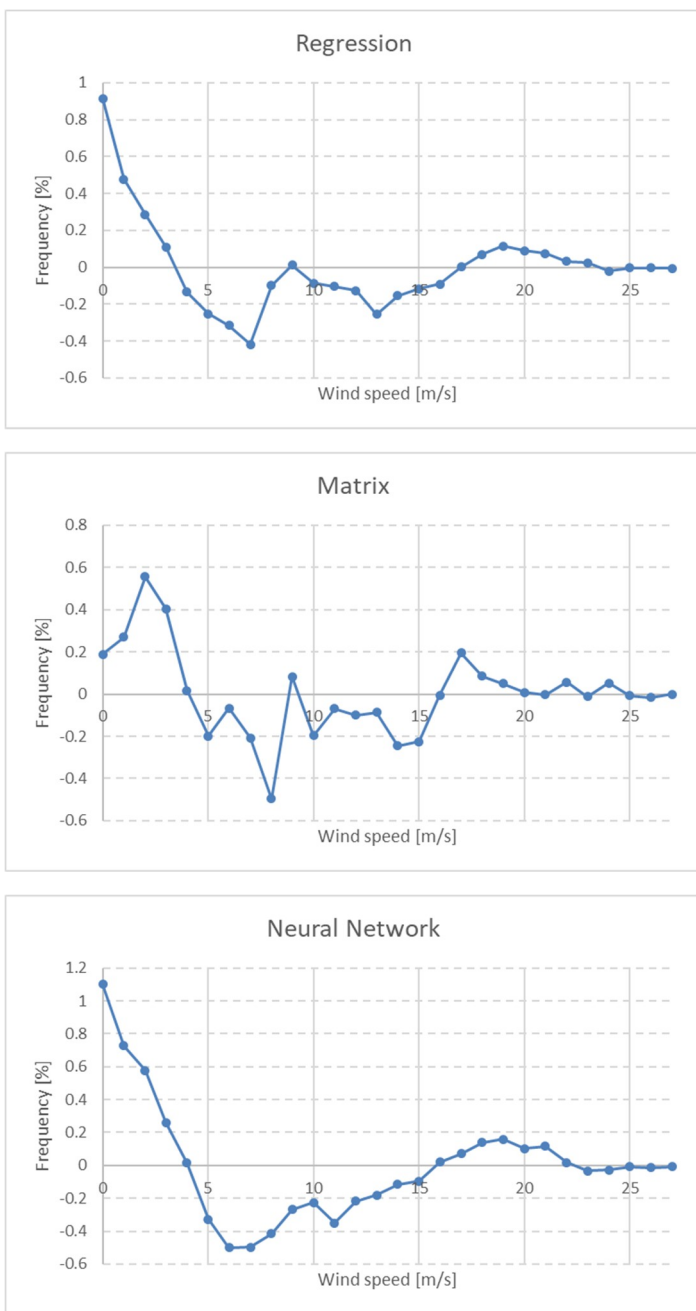


Figure 48: Difference in occurrence frequency between distribution and Weibull fit at HKW for the Regression method (top), Matrix method (middle) and Neural Network method (bottom)

MMIJ

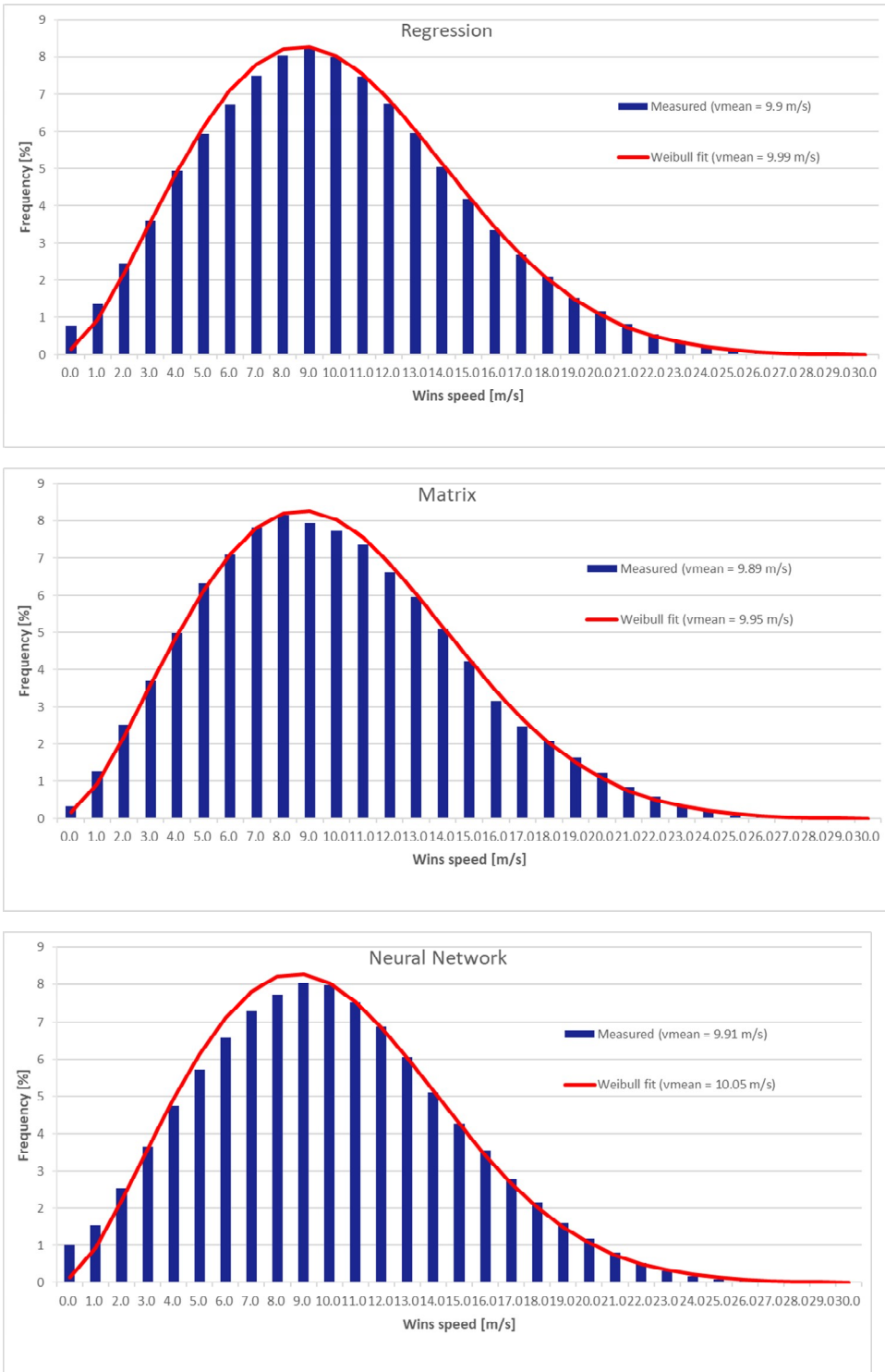


Figure 49: Frequency distribution and Weibull fit at MMIJ for the long-term corrected wind climate by means of Regression (Top), Matrix method (middle) and Neural Network (bottom)

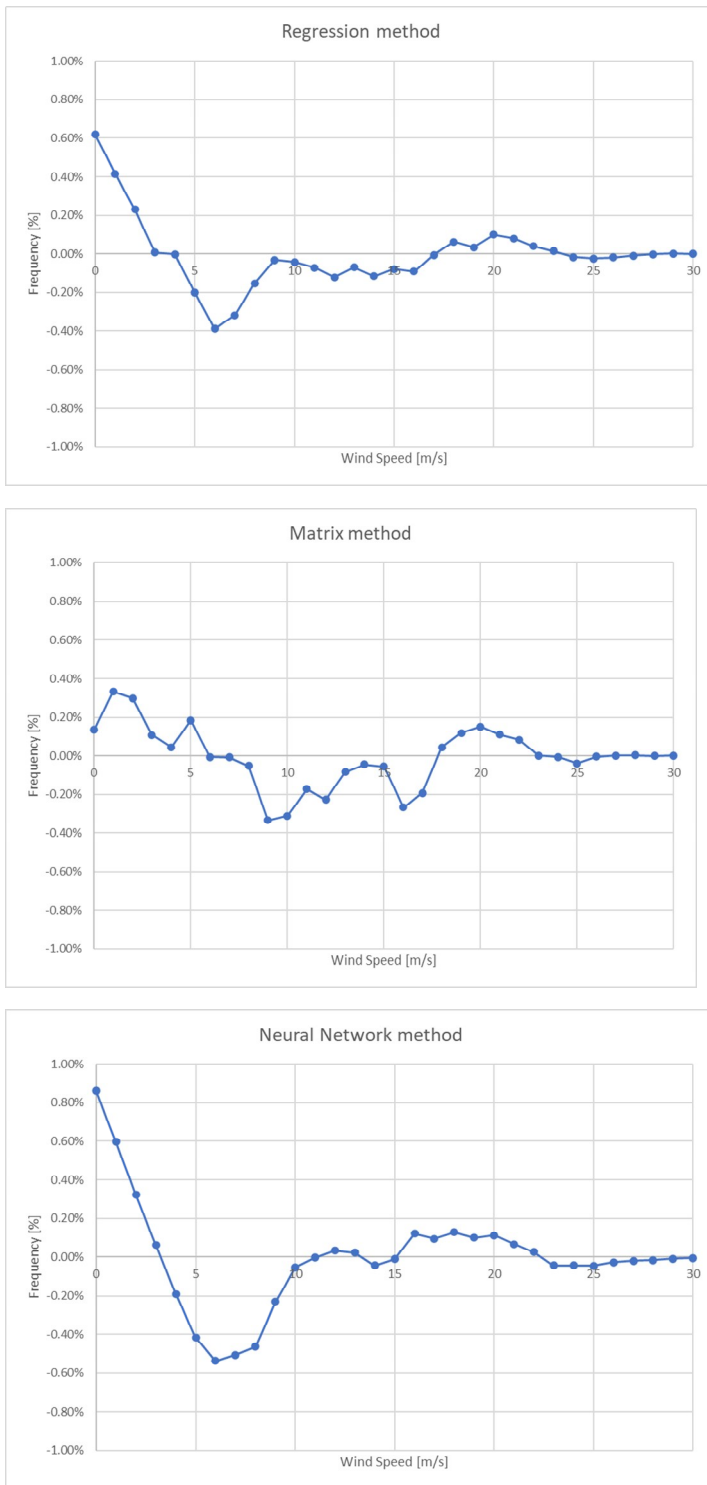


Figure 50: Difference in occurrence frequency between distribution and Weibull fit at MMJ for the Regression method (top), Matrix method (middle) and Neural Network method (bottom)

OWEZ

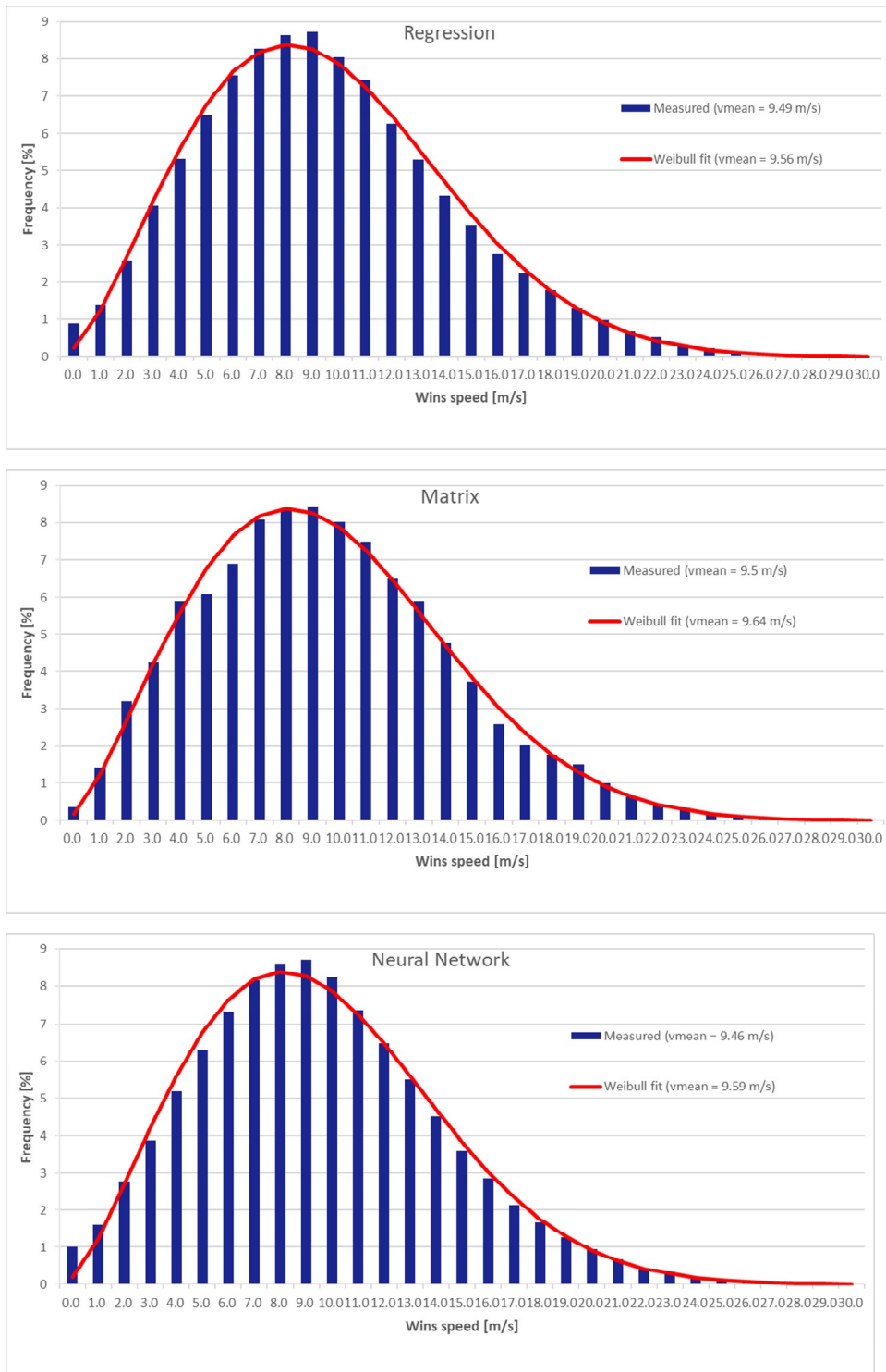


Figure 51: Frequency distribution and Weibull fit at OWEZ for the long-term corrected wind climate by means of Regression (Top), Matrix method (middle) and Neural Network (bottom)

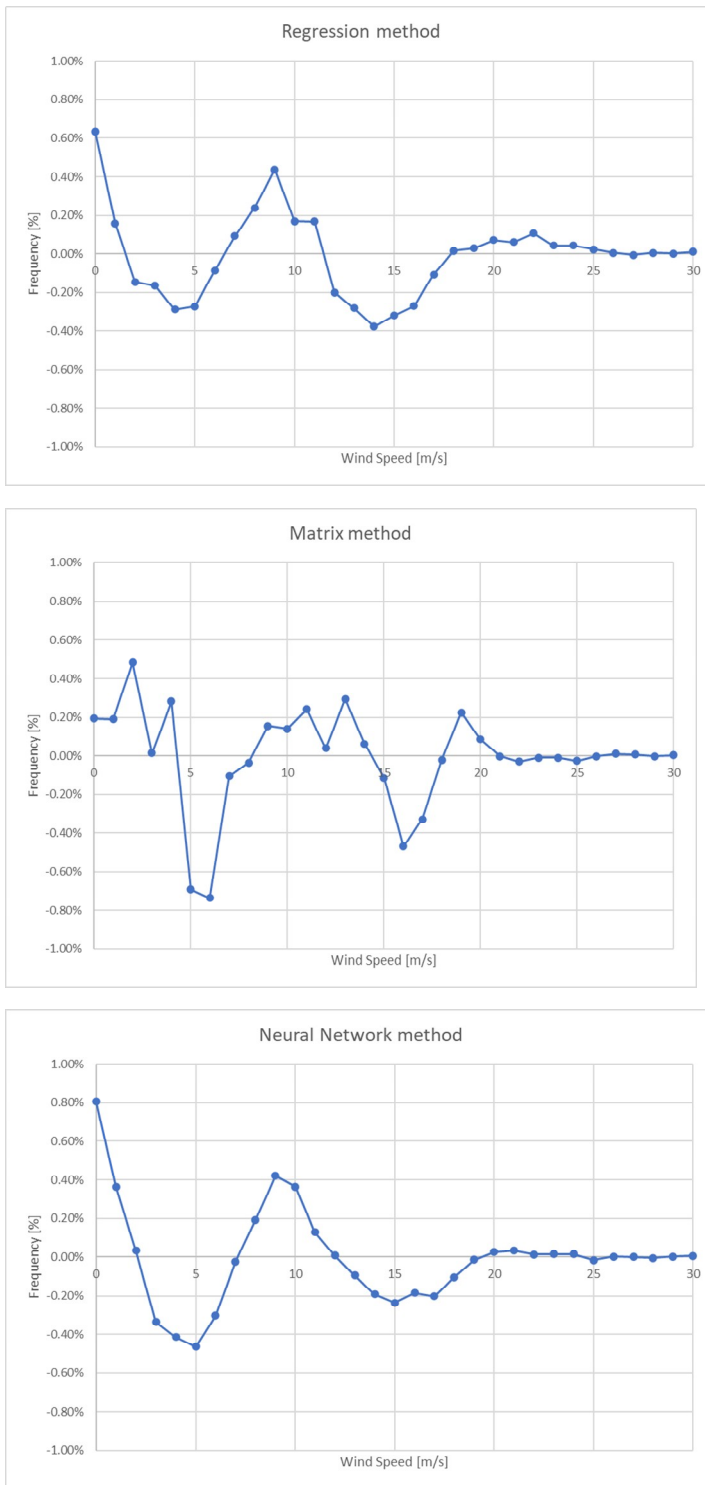


Figure 52: Difference in occurrence frequency between distribution and Weibull fit for the Regression method (top), Matrix method (middle) and Neural Network method (bottom)

ANNEX F: MESOSCALE DATA VALIDATION - MEAN WIND SPEED RESULTS

TABLE 66: CONSISTENCY ON BIAS IN AVERAGE WIND SPEED

Station	Weight measurement station	Mesoscale Model											
		KNW		DOWA		NEWA		3TIER-ERA5		EMD-WRF-ERA5		Ensemble	
Bias Vave[m/s]	Bias Vave - Average Bias	Bias Vave[m/s]	Bias Vave - Average Bias	Bias Vave[m/s]	Bias Vave - Average Bias	Bias Vave[m/s]	Bias Vave - Average Bias	Bias Vave[m/s]	Bias Vave - Average Bias	Bias Vave[m/s]	Bias Vave - Average Bias	Bias Vave[m/s]	Bias Vave - Average Bias
HKW	0.140	0.135	0.025	0.258	0.031	-0.206	0.019	-0.910	0.014	-0.157	0.006	0.114	0.025
HKN	0.115	-0.035	0.001	-0.040	-0.009	-0.338	0.000	-1.010	0.000	-0.125	0.008	-0.067	0.000
HKZ	0.115	-0.057	-0.002	0.033	0.000	-0.312	0.003	-1.128	-0.014	-0.196	0.000	-0.073	-0.001
IJmuiden	0.157	-0.064	-0.003	-0.010	-0.007	-0.390	-0.008	-1.134	-0.020	-0.293	-0.015	-0.123	-0.009
OWEZ	0.105	-0.232	-0.020	-0.040	-0.008	-0.346	-0.001	-1.224	-0.023	-0.260	-0.007	-0.168	-0.011
EPL Lidar	0.130	-0.025	0.002	0.070	0.004	-0.400	-0.008	-0.609	0.052	-0.183	0.002	-0.046	0.002
LEG Lidar	0.107	-0.092	-0.005	-0.005	-0.004	-0.436	-0.010	-1.040	-0.003	-0.260	-0.007	-0.119	-0.006
K13	0.130	0.025	0.009	0.022	-0.002	-0.285	0.007	-1.010	0.000	-0.104	0.012	-0.019	0.006
Average	0.125	-0.04	0.008	0.04	0.008	-0.34	0.007	-1.01	0.016	-0.20	0.007	-0.06	0.008

TABLE 67: CORRELATION COEFFICIENT WIND SPEED (Y=AX+B)

Station	Weight measurement station	Mesoscale Model						
		KNW	DOWA	NEWA	3TIER-ERA5	EMD-WRF-ERA5	Ensemble	
		r	r	r	r	r	r	
HKW		0.140	0.867	0.862	0.802	0.926	0.910	0.897
HKN		0.115	0.877	0.903	0.800	0.915	0.894	0.925
HKZ		0.115	0.873	0.911	0.806	0.909	0.887	0.925
IJmuiden		0.157	0.876	0.890	0.808	0.896	0.876	0.906
OWEZ		0.105	0.852	0.798	0.812	0.883	0.856	0.831
EPL Lidar		0.130	0.851	0.872	0.809	0.877	0.857	0.890
LEG Lidar		0.107	0.856	0.878	0.797	0.880	0.862	0.896
K13		0.130	0.879	0.907	0.812	0.910	0.899	0.923
Result			0.867	0.879	0.806	0.900	0.881	0.900

ANNEX G: MESOSCALE DATA VALIDATION - WIND DIRECTION

TABLE 68: CONSISTENCY ON BIAS IN AVERAGE WIND DIRECTION

Station	Weight measurement station	Mesoscale Model											
		KNW		DOWA		NEWA		3TIER-ERA5		EMD-WRF-ERA5		Ensemble	
Bias dave[m/s]	Bias dave - Average Bias	Bias dave[m/s]	Bias dave - Average Bias	Bias dave[m/s]	Bias dave - Average Bias	Bias dave[m/s]	Bias dave - Average Bias	Bias dave[m/s]	Bias dave - Average Bias	Bias dave[m/s]	Bias dave - Average Bias	Bias dave[m/s]	Bias dave - Average Bias
HKW	0.140	3.898	0.923	-2.119	0.937	-5.003	0.965	4.404	0.288	2.374	0.320	6.375	1.345
HKN	0.115	-3.118	-0.051	-15.972	-0.826	-14.238	-0.271	4.500	0.248	4.206	0.473	-5.392	-0.251
HKZ	0.115	3.735	0.739	-2.638	0.709	-4.098	0.897	12.011	1.112	8.953	1.020	2.980	0.713
IJmuiden	0.157	0.748	0.538	-5.967	0.444	-8.285	0.565	-0.158	-0.394	-3.085	-0.499	-2.778	0.068
OWEZ	0.105	-8.727	-0.632	-8.256	0.056	-9.263	0.274	5.724	0.353	-1.588	-0.176	-5.625	-0.252
EPL Lidar	0.130	-11.619	-1.165	-17.734	-1.165	-21.430	-1.244	-7.478	-1.281	-9.769	-1.285	-12.968	-1.271
LEG Lidar	0.107	-8.564	-0.632	-14.167	-0.577	-18.326	-0.692	-4.629	-0.750	-3.759	-0.414	-8.988	-0.621
K13	0.130	2.210	0.636	-3.514	0.687	-14.431	-0.331	4.429	0.270	3.424	0.433	0.702	0.509
Average		-2.680	0.664	-8.796	0.675	-11.884	0.655	2.350	0.587	0.094	0.578	-3.212	0.629

TABLE 69: CORRELATION COEFFICIENT WIND DIRECTION (Y=AX+B)

Station	Weight measurement station	Mesoscale Model					
		KNW	DOWA	NEWA	3TIER-ERA5	EMD-WRF-ERA5	Ensemble
		r	r	r	r	r	r
HKW		0.140	0.954	0.946	0.953	0.901	0.935
HKN		0.115	0.899	0.910	0.845	0.921	0.912
HKZ		0.115	0.872	0.905	0.823	0.862	0.889
IJmuiden		0.157	0.907	0.920	0.855	0.888	0.913
OWEZ		0.105	0.895	0.891	0.815	0.849	0.897
EPL Lidar		0.130	0.886	0.905	0.852	0.868	0.899
LEG Lidar		0.107	0.877	0.890	0.825	0.847	0.886
K13		0.130	0.904	0.925	0.844	0.905	0.923
Result		0.901	0.913	0.855	0.882	0.908	0.922

ANNEX H: MESOSCALE DATA VALIDATION - ENERGY ROSE

TABLE 70: CONSISTENCY IN ENERGY ROSE

Station	Weight measurement station	Mesoscale Model					
		KNW	DOWA	NEWA	3TIER-ERA5	EMD-WRF-ERA5	Ensemble
		Bias fave[m/s]	Bias fave[m/s]	Bias fave[m/s]	Bias fave[m/s]	Bias fave[m/s]	Bias fave[m/s]
HKW	0.140	-2.937	-4.885	-1.573	-6.468	-8.054	-13.395
HKN	0.115	-0.156	6.280	3.987	2.107	-5.108	0.529
HKZ	0.115	-3.497	-1.904	1.603	-3.730	-7.320	-4.820
IJmuiden	0.157	-1.620	1.492	4.760	1.653	-1.389	-0.978
OWEZ	0.105	-10.807	-4.659	11.164	-7.161	-12.598	-2.096
EPL Lidar	0.130	15.003	16.477	21.283	14.398	11.415	12.142
LEG Lidar	0.107	-3.486	-3.638	-6.006	-12.173	-4.325	-12.177
K13	0.130	-2.583	-6.048	-7.025	-0.550	-4.060	-4.399
Result		4.882	5.674	7.111	5.843	6.576	6.331

ANNEX I : LONG-TERM WIND CLIMATE AT THE 6 NODES

Monthly Mean wind speed

TABLE 71: LONG-TERM MONTHLY MEAN WIND SPEED AT 100 M MSL FOR THE 6 NODES

Anemometer		HKW	S2	S22	S23	S24	S30	HKW	S2	S22	S23	S24	S30
Height (m)		100	100	100	100	100	100	100	100	100	100	100	100
November	1999	11.59	11.63	11.62	11.61	11.58	11.64						
December		14.07	14.11	14.14	14.13	14.08	14.1						
January		11.82	11.85	11.87	11.87	11.83	11.85	9.33	9.4	9.41	9.4	9.34	9.39
February		13.21	13.25	13.27	13.26	13.22	13.24	10.08	10.11	10.09	10.08	10.06	10.13
March		10.56	10.59	10.62	10.62	10.58	10.57	9.95	9.99	9.98	9.98	9.95	10
April		8.39	8.42	8.39	8.38	8.36	8.45	8.02	8.04	8.02	8.02	8.01	8.05
May		8.95	8.97	8.95	8.95	8.94	8.99	7.63	7.61	7.6	7.6	7.62	7.63
June		8.46	8.5	8.51	8.5	8.47	8.49	6.78	6.78	6.77	6.76	6.77	6.79
July		7.18	7.21	7.22	7.22	7.19	7.19	7.08	7.12	7.12	7.11	7.08	7.12
August		6.03	6.04	6.04	6.04	6.02	6.05	9.17	9.2	9.21	9.21	9.18	9.19
September		8.81	8.86	8.85	8.84	8.8	8.87	8.95	8.99	9.01	9	8.96	8.98
October		12.19	12.24	12.23	12.21	12.16	12.27	11.07	11.11	11.1	11.09	11.06	11.12
November	2000	13.03	13.09	13.05	13.04	13	13.12	9.98	10.02	10.01	10	9.97	10.02
December		12.58	12.66	12.65	12.63	12.57	12.67	9.41	9.44	9.44	9.44	9.41	9.44
January		10.27	10.33	10.32	10.3	10.25	10.35	10.63	10.66	10.65	10.64	10.62	10.67
February		9.72	9.77	9.77	9.76	9.73	9.77	11.73	11.78	11.77	11.75	11.71	11.79
March	2001	9.74	9.79	9.77	9.76	9.73	9.81	8.12	8.14	8.12	8.11	8.11	8.16
April		9.9	9.92	9.92	9.91	9.89	9.93	8.7	8.73	8.72	8.71	8.69	8.74

Anemometer		HKW	S2	S22	S23	S24	S30	HKW	S2	S22	S23	S24	S30
Height (m)		100	100	100	100	100	100	100	100	100	100	100	100
May	2002	9.41	9.4	9.37	9.37	9.38	9.42	8.8	8.84	8.84	8.83	8.8	8.84
June		8.05	8.09	8.1	8.1	8.06	8.07	8.51	8.52	8.51	8.51	8.5	8.53
July		7.68	7.71	7.71	7.71	7.68	7.71	8.78	8.81	8.82	8.82	8.79	8.8
August		7.66	7.67	7.67	7.66	7.65	7.68	8.08	8.11	8.12	8.11	8.09	8.1
September		10.31	10.36	10.41	10.4	10.34	10.33	9.9	9.93	9.93	9.92	9.89	9.94
October		12.3	12.34	12.32	12.3	12.27	12.37	10.8	10.87	10.88	10.87	10.8	10.86
November		10.27	10.3	10.34	10.33	10.29	10.27	9.81	9.87	9.86	9.85	9.79	9.88
December		10.52	10.57	10.6	10.59	10.54	10.55	14.58	14.63	14.68	14.67	14.61	14.6
January		12.23	12.26	12.25	12.24	12.21	12.29	12.14	12.21	12.26	12.25	12.18	12.17
February		14.96	14.98	14.97	14.97	14.95	14.99	10.49	10.54	10.56	10.56	10.51	10.53
March		9.75	9.79	9.79	9.78	9.75	9.79	7.74	7.77	7.77	7.77	7.74	7.76
April	2012	9.47	9.51	9.5	9.49	9.46	9.52	9.25	9.29	9.26	9.25	9.23	9.31
May		9.74	9.77	9.74	9.73	9.72	9.8	8.69	8.71	8.7	8.69	8.68	8.73
June		8.3	8.33	8.33	8.33	8.3	8.33	9.66	9.69	9.67	9.66	9.64	9.71
July		8.52	8.53	8.52	8.52	8.51	8.54	7.69	7.71	7.71	7.71	7.69	7.72
August		6.05	6.08	6.09	6.09	6.06	6.08	7.65	7.69	7.69	7.68	7.64	7.7
September		7.92	7.93	7.92	7.91	7.9	7.95	9.56	9.58	9.59	9.59	9.56	9.58
October		10.99	11.07	11.11	11.09	11.01	11.04	9.65	9.68	9.66	9.66	9.64	9.69
November		9.53	9.61	9.6	9.58	9.52	9.62	10.71	10.76	10.74	10.73	10.69	10.78
December		10.34	10.43	10.41	10.39	10.33	10.43	12.22	12.26	12.26	12.25	12.21	12.27
January	2013	11.75	11.79	11.79	11.79	11.75	11.79	10.3	10.35	10.36	10.35	10.3	10.34
February		9.52	9.6	9.6	9.59	9.52	9.59	9.83	9.87	9.87	9.86	9.83	9.87
March		8.66	8.69	8.67	8.66	8.64	8.7	10.41	10.48	10.45	10.43	10.4	10.49
April		10.01	10.05	10.03	10.02	9.99	10.05	9.88	9.9	9.87	9.86	9.86	9.93

Anemometer		HKW	S2	S22	S23	S24	S30	HKW	S2	S22	S23	S24	S30
Height (m)		100	100	100	100	100	100	100	100	100	100	100	100
May	2004	9.02	9.05	9.03	9.03	9	9.06	9.39	9.41	9.41	9.4	9.38	9.42
June		7.26	7.3	7.3	7.29	7.26	7.3	9.52	9.52	9.5	9.5	9.51	9.54
July		7.92	7.96	7.96	7.95	7.92	7.96	6.9	6.89	6.87	6.87	6.88	6.91
August		6.88	6.9	6.91	6.91	6.89	6.89	7.37	7.41	7.4	7.39	7.37	7.41
September		6.45	6.49	6.49	6.49	6.45	6.48	8.52	8.57	8.6	8.59	8.54	8.54
October		10.4	10.47	10.49	10.48	10.42	10.44	12.06	12.12	12.1	12.09	12.04	12.13
November		10.75	10.81	10.79	10.77	10.73	10.82	10.29	10.31	10.32	10.32	10.29	10.31
December		10.82	10.86	10.86	10.86	10.82	10.86	13.38	13.44	13.42	13.41	13.36	13.46
January	2014	12.18	12.25	12.26	12.25	12.19	12.24	12.89	12.98	12.96	12.93	12.86	13.01
February		11.28	11.3	11.31	11.31	11.28	11.29	14.46	14.52	14.47	14.45	14.41	14.58
March		10.22	10.24	10.23	10.23	10.21	10.26	9.78	9.83	9.83	9.82	9.78	9.83
April		8.22	8.28	8.27	8.26	8.22	8.28	8.27	8.31	8.31	8.3	8.27	8.31
May		6.66	6.68	6.69	6.69	6.67	6.68	7.89	7.92	7.91	7.9	7.88	7.93
June		8.55	8.58	8.6	8.6	8.56	8.57	6.15	6.16	6.17	6.16	6.15	6.16
July		6.96	6.99	7.01	7	6.97	6.98	7.72	7.73	7.72	7.72	7.71	7.75
August		8.96	9	9.01	9	8.96	9	9.23	9.26	9.27	9.26	9.23	9.26
September		10.98	11.02	11.04	11.03	10.99	11.01	6.68	6.69	6.7	6.69	6.68	6.69
October		11.38	11.44	11.41	11.4	11.36	11.46	10.84	10.88	10.86	10.85	10.82	10.91
November		9.73	9.78	9.81	9.8	9.75	9.75	9.62	9.71	9.7	9.67	9.6	9.72
December		9.76	9.78	9.79	9.79	9.76	9.77	13.15	13.18	13.21	13.2	13.16	13.17
January	2015	14.11	14.14	14.16	14.15	14.12	14.13	12.73	12.76	12.78	12.77	12.74	12.75
February		10.7	10.72	10.71	10.71	10.69	10.73	10.05	10.1	10.1	10.09	10.05	10.11
March		10.26	10.31	10.32	10.31	10.27	10.3	11.13	11.17	11.18	11.17	11.14	11.16
April		8.44	8.48	8.47	8.46	8.43	8.48	8.03	8.03	8.02	8.02	8.02	8.04

Anemometer		HKW	S2	S22	S23	S24	S30	HKW	S2	S22	S23	S24	S30	
Height (m)		100	100	100	100	100	100	100	100	100	100	100	100	
May	2006	9.32	9.35	9.35	9.34	9.31	9.35	9.58	9.6	9.6	9.6	9.58	9.61	
June		7.75	7.77	7.76	7.75	7.74	7.78	8.69	8.72	8.72	8.71	8.69	8.72	
July		7.42	7.44	7.45	7.45	7.43	7.43	9.08	9.12	9.14	9.13	9.09	9.11	
August		7.72	7.76	7.79	7.78	7.74	7.74	8.51	8.54	8.53	8.52	8.49	8.56	
September		7.7	7.72	7.71	7.71	7.69	7.73	9.32	9.37	9.39	9.38	9.33	9.36	
October		10.22	10.28	10.26	10.24	10.19	10.3	8.32	8.37	8.35	8.34	8.31	8.38	
November		10.62	10.65	10.65	10.64	10.62	10.66	13.9	13.9	13.91	13.9	13.88	13.91	
December		10.56	10.61	10.63	10.62	10.57	10.6	14.84	14.88	14.83	14.82	14.79	14.93	
January		9.87	9.93	9.91	9.89	9.85	9.95	2016	12.94	13.02	13.02	13	12.93	13.02
February		10.49	10.54	10.53	10.52	10.49	10.54		12.06	12.09	12.09	12.09	12.06	12.1
March		10.55	10.6	10.58	10.57	10.54	10.6		9.72	9.76	9.75	9.74	9.71	9.77
April		9.08	9.1	9.11	9.11	9.08	9.09		8.8	8.84	8.85	8.84	8.81	8.83
May		10.04	10.09	10.09	10.08	10.04	10.09		9.26	9.29	9.28	9.27	9.25	9.3
June		7.02	7.03	7.02	7.01	7.01	7.04		7.27	7.27	7.26	7.25	7.25	7.29
July		7.14	7.16	7.14	7.14	7.12	7.18		7.78	7.79	7.79	7.79	7.78	7.8
August		8.39	8.44	8.48	8.47	8.42	8.41		8.57	8.6	8.6	8.59	8.56	8.6
September		8.77	8.82	8.81	8.8	8.76	8.83		8.18	8.22	8.21	8.2	8.17	8.23
October		11.02	11.07	11.07	11.06	11.01	11.07		8.18	8.22	8.22	8.21	8.18	8.22
November		13.33	13.39	13.4	13.39	13.33	13.4		10.23	10.27	10.26	10.25	10.22	10.28
December		12.22	12.25	12.23	12.22	12.2	12.27		10.2	10.24	10.24	10.23	10.19	10.24
January	2007	14.97	14.99	15.03	15.02	14.98	14.98	2017	9.25	9.31	9.32	9.31	9.26	9.29
February		10.17	10.23	10.24	10.22	10.17	10.23		11.73	11.8	11.79	11.78	11.73	11.8
March		11.39	11.43	11.43	11.42	11.39	11.43		10.22	10.26	10.25	10.24	10.21	10.27
April		8.63	8.64	8.62	8.61	8.62	8.65		8.23	8.29	8.32	8.31	8.26	8.26

Anemometer		HKW	S2	S22	S23	S24	S30	HKW	S2	S22	S23	S24	S30
Height (m)		100	100	100	100	100	100	100	100	100	100	100	100
May	2008	8.96	8.95	8.93	8.93	8.94	8.98	8.45	8.48	8.46	8.45	8.43	8.5
June		8.04	8.04	8.03	8.02	8.02	8.06	8.98	9.01	9	8.99	8.97	9.01
July		9.88	9.91	9.91	9.9	9.87	9.91	7.72	7.75	7.75	7.74	7.72	7.75
August		8.06	8.08	8.07	8.07	8.05	8.09	7.29	7.31	7.31	7.31	7.29	7.32
September		9.97	9.99	10	10	9.97	9.98	8.36	8.4	8.41	8.4	8.36	8.39
October		7.69	7.73	7.73	7.72	7.69	7.73	12.49	12.54	12.57	12.56	12.5	12.52
November		11.54	11.61	11.65	11.64	11.57	11.57	10.67	10.72	10.76	10.76	10.7	10.69
December		11.57	11.62	11.62	11.61	11.57	11.62	11.82	11.87	11.9	11.89	11.84	11.85
January		14.45	14.49	14.47	14.46	14.42	14.51	12.83	12.89	12.91	12.89	12.84	12.88
February		10.45	10.49	10.49	10.48	10.44	10.5	10.41	10.48	10.47	10.46	10.4	10.48
March		12.58	12.62	12.65	12.64	12.59	12.61	10.35	10.43	10.43	10.41	10.35	10.42
April	2018	8.91	8.96	8.95	8.94	8.91	8.97	9.48	9.52	9.49	9.48	9.46	9.53
May		9.76	9.79	9.76	9.75	9.74	9.81	8.42	8.46	8.45	8.44	8.42	8.47
June		7.45	7.47	7.47	7.47	7.45	7.47	8.08	8.08	8.06	8.06	8.07	8.09
July		8.52	8.56	8.58	8.57	8.53	8.55	6.74	6.76	6.75	6.75	6.73	6.77
August		9.84	9.87	9.86	9.85	9.83	9.88	7.32	7.35	7.36	7.35	7.32	7.35
September		8.79	8.82	8.81	8.8	8.78	8.83	9.64	9.64	9.64	9.64	9.63	9.66
October		10.75	10.79	10.81	10.8	10.75	10.79	9.91	9.96	9.97	9.96	9.91	9.96
November		11.61	11.66	11.67	11.65	11.61	11.66	11.73	11.83	11.8	11.78	11.7	11.85
December		9.5	9.55	9.56	9.55	9.51	9.54	11.58	11.63	11.65	11.64	11.58	11.62
January	2009	10.6	10.68	10.66	10.65	10.59	10.69	11.19	11.25	11.3	11.29	11.22	11.22
February		9.02	9.07	9.11	9.1	9.05	9.04	10.29	10.32	10.3	10.29	10.27	10.34
March		9.97	10.01	10.05	10.04	9.99	10	11.82	11.87	11.89	11.88	11.83	11.86
April		7.74	7.78	7.75	7.75	7.73	7.79	9.41	9.47	9.45	9.43	9.4	9.49

Anemometer		HKW	S2	S22	S23	S24	S30
Height (m)		100	100	100	100	100	100
May	9.74	9.77	9.76	9.75	9.73	9.79	
	7.31	7.33	7.33	7.32	7.31	7.33	
	9.13	9.16	9.17	9.16	9.13	9.17	
	8.1	8.14	8.14	8.13	8.1	8.14	
	9.59	9.59	9.59	9.59	9.58	9.6	
	9.93	9.98	9.99	9.98	9.93	9.97	
	13.26	13.28	13.25	13.24	13.23	13.32	
	10.85	10.9	10.88	10.87	10.83	10.92	
		HKW	S2	S22	S23	S24	S30
		100	100	100	100	100	100
		7.93	7.95	7.95	7.95	7.93	7.95
		8.31	8.34	8.32	8.31	8.29	8.36
		7.43	7.46	7.47	7.47	7.43	7.46
		9.1	9.12	9.11	9.11	9.09	9.14
		9.73	9.76	9.77	9.76	9.73	9.76
		10.88	10.93	10.93	10.92	10.88	10.94

Weibull Distribution

TABLE 72: LONG-TERM WEIBULL PARAMETERS AT 100 M MSL – NODE S2

Sector	A parameter [m/s]	k parameter	Frequency [%]	Mean wind speed [m/s]
N	9.08	2.38	5.84	8.05
NNE	9.17	2.64	5.79	8.15
ENE	9.99	2.75	6.89	8.89
E	10.00	2.62	6.75	8.89
ESE	9.39	2.47	4.98	8.33
SSE	9.51	2.33	4.83	8.42
S	11.82	2.38	7.66	10.48
SSW	13.34	2.63	14.21	11.85
WSW	12.82	2.54	15.75	11.38
W	11.53	2.27	10.80	10.22
WNW	10.56	2.30	8.90	9.35
NNW	10.13	2.23	7.60	8.97
Average	11.14	2.32	100.00	9.87

TABLE 73: LONG-TERM WEIBULL PARAMETERS AT 100 M MSL – NODE S22

Sector	A parameter [m/s]	k parameter	Frequency [%]	Mean wind speed [m/s]
N	9.04	2.39	5.82	8.01
NNE	9.13	2.64	5.71	8.11
ENE	9.92	2.75	6.85	8.83
E	10.01	2.62	6.84	8.90
ESE	9.40	2.47	5.03	8.33
SSE	9.53	2.32	4.85	8.44
S	11.80	2.38	7.65	10.46
SSW	13.29	2.64	14.13	11.81
WSW	12.79	2.53	15.64	11.35
W	11.64	2.27	10.87	10.31
WNW	10.66	2.30	9.01	9.44
NNW	10.19	2.23	7.61	9.03
Average	11.14	2.32	100.00	9.87

TABLE 74: LONG-TERM WEIBULL PARAMETERS AT 100 M MSL – NODE S23

Sector	A parameter [m/s]	k parameter	Frequency [%]	Mean wind speed [m/s]
N	9.04	2.39	5.83	8.01
NNE	9.14	2.64	5.73	8.12
ENE	9.92	2.75	6.87	8.82
E	9.99	2.62	6.84	8.87
ESE	9.37	2.47	5.02	8.31
SSE	9.50	2.32	4.84	8.42
S	11.78	2.39	7.64	10.44
SSW	13.27	2.63	14.12	11.79
WSW	12.79	2.53	15.66	11.36
W	11.63	2.27	10.87	10.30
WNW	10.64	2.29	8.98	9.43
NNW	10.19	2.23	7.60	9.02
Average	11.13	2.32	100.00	9.86

TABLE 75: LONG-TERM WEIBULL PARAMETERS AT 100 M MSL – NODE S24

Sector	A parameter [m/s]	k parameter	Frequency [%]	Mean wind speed [m/s]
N	9.10	2.39	5.93	8.06
NNE	9.24	2.64	5.87	8.21
ENE	9.92	2.75	6.98	8.83
E	9.91	2.61	6.75	8.80
ESE	9.25	2.47	4.96	8.21
SSE	9.40	2.32	4.81	8.33
S	11.68	2.38	7.61	10.35
SSW	13.26	2.64	14.17	11.78
WSW	12.84	2.53	15.78	11.40
W	11.52	2.26	10.76	10.20
WNW	10.52	2.30	8.83	9.32
NNW	10.13	2.23	7.56	8.97
Average	11.10	2.32	100.00	9.83

TABLE 76: LONG-TERM WEIBULL PARAMETERS AT 100 M MSL – NODE S30

Sector	A parameter [m/s]	k parameter	Frequency [%]	Mean wind speed [m/s]
N	9.11	2.38	5.90	8.08
NNE	9.24	2.65	5.86	8.21
ENE	10.03	2.75	6.94	8.93
E	9.99	2.63	6.66	8.87
ESE	9.34	2.46	4.92	8.28
SSE	9.45	2.33	4.78	8.37
S	11.81	2.37	7.66	10.46
SSW	13.39	2.63	14.41	11.90
WSW	12.87	2.54	15.86	11.42
W	11.46	2.26	10.72	10.15
WNW	10.44	2.30	8.73	9.25
NNW	10.09	2.23	7.56	8.94
Average	11.15	2.32	100.00	9.88

Wind and Energy Roses

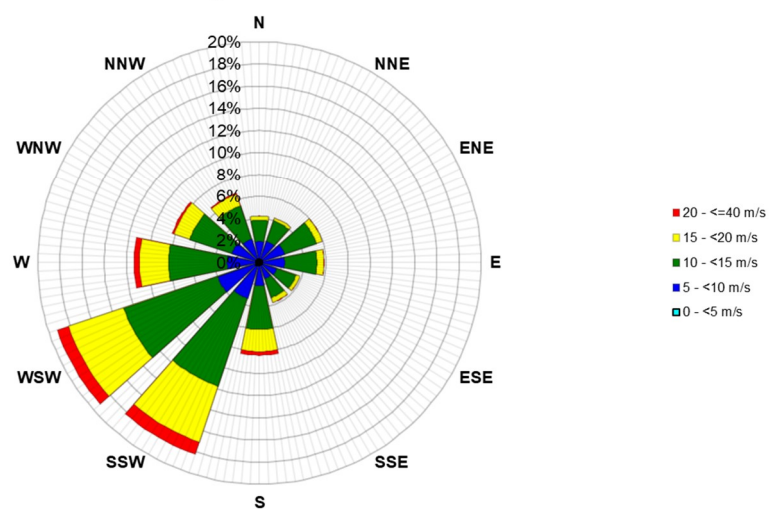
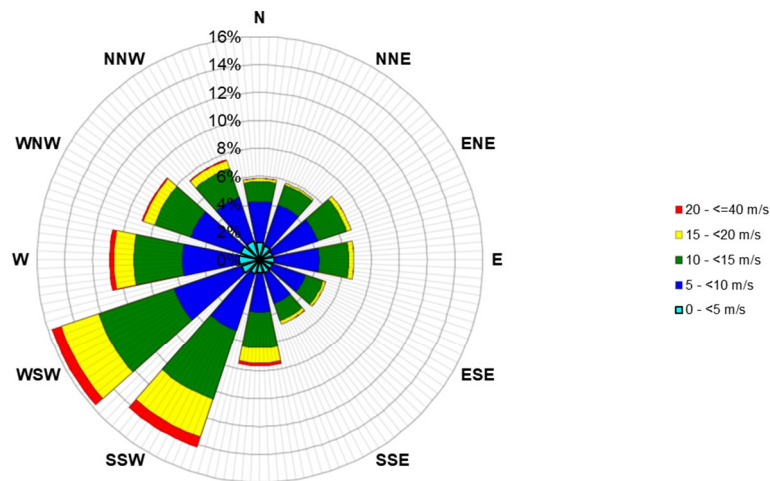
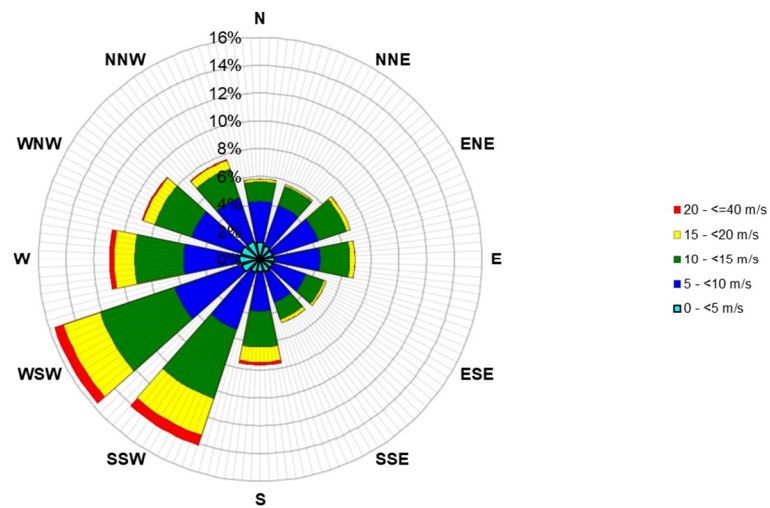


Figure 53: Frequency (top) and energy (bottom) roses at 100 m MSL – Node S2



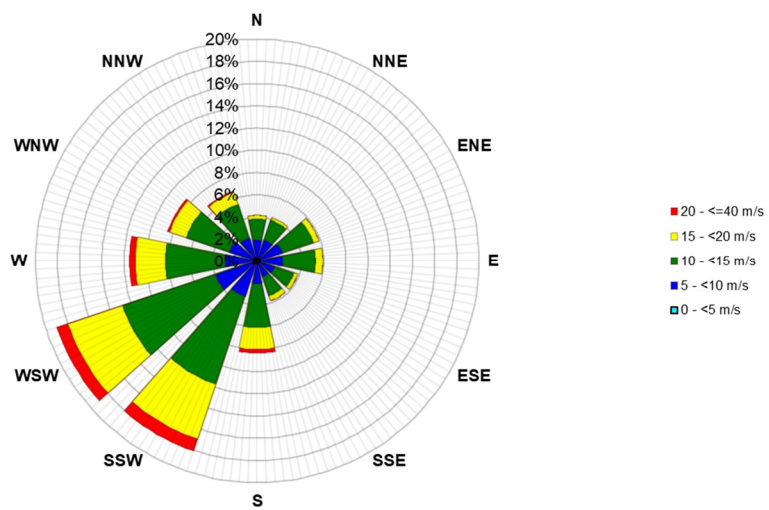


Figure 54: Frequency (top) and energy (bottom) roses at 100 m MSL – Node S22

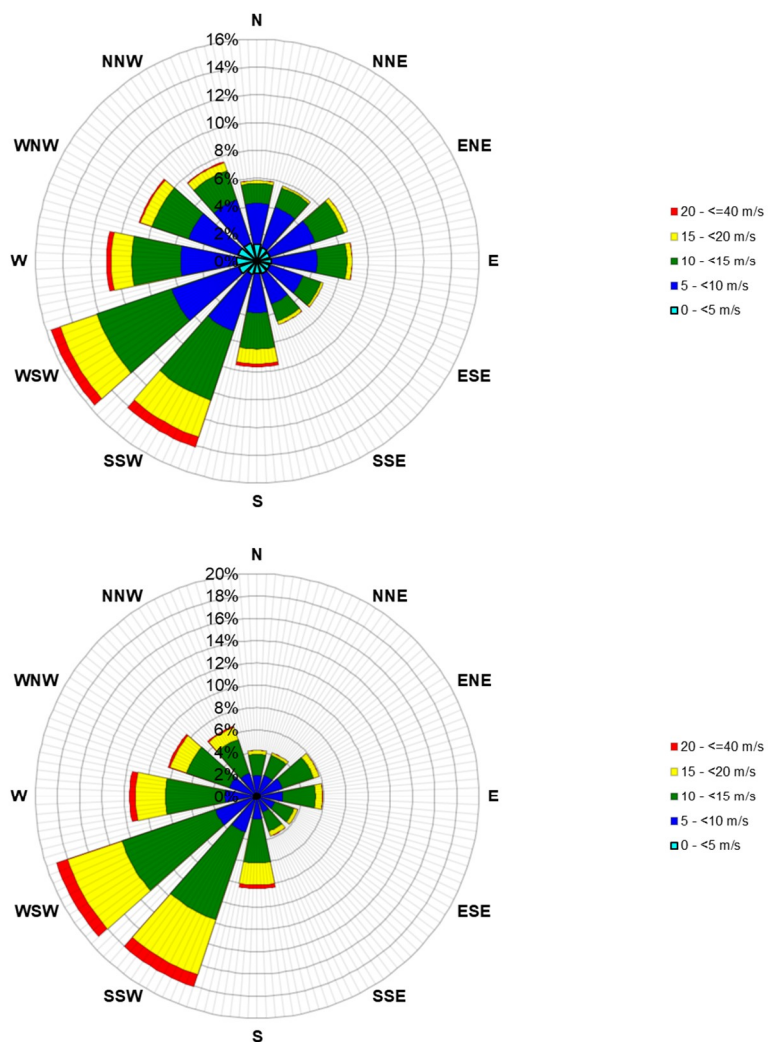


Figure 55: Frequency (top) and energy (bottom) roses at 100 m MSL – Node S23

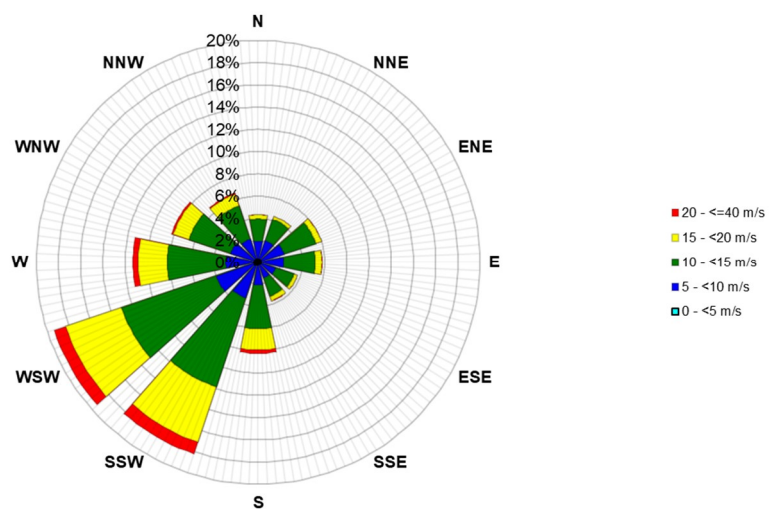
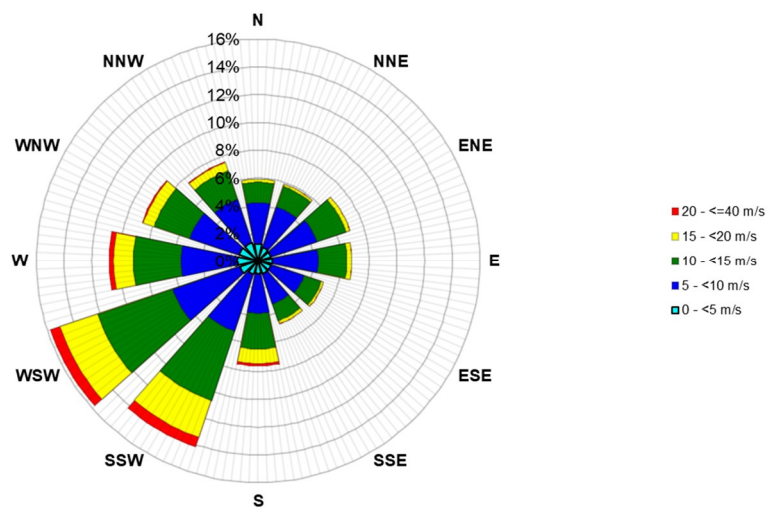
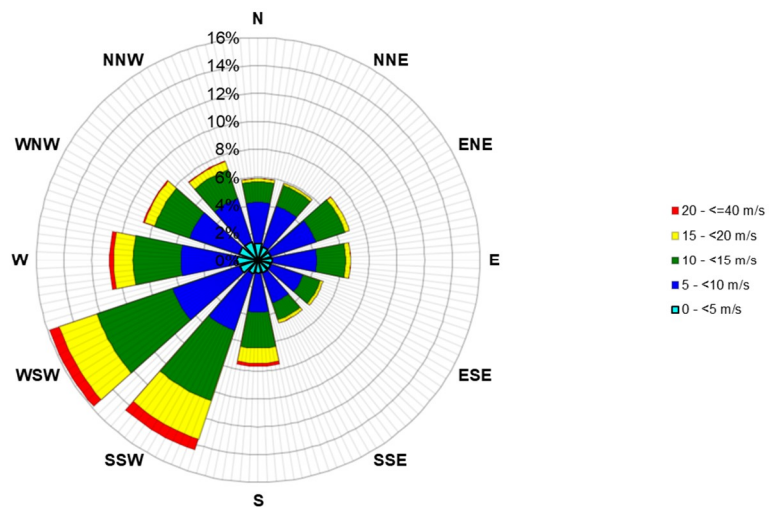


Figure 56: Frequency (top) and energy (bottom) roses at 100 m MSL – Node S24



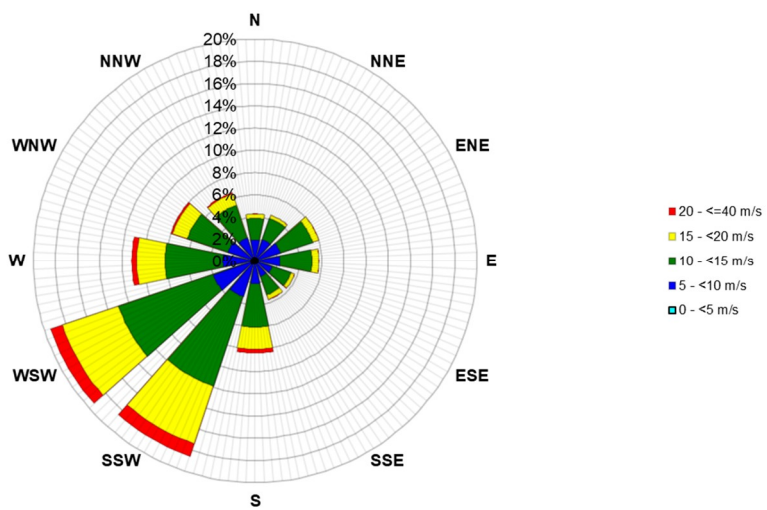


Figure 57: Frequency (top) and energy (bottom) roses at 100 m MSL – Node S30

ANNEX J : COMPARISON BETWEEN TRACTEBEL AND DHI METOCEAN DESK STUDY RESULTS

This appendix presents the results of the comparison between Tractebel's Wind Resource Assessment and DHI's metocean desk study results (in terms of wind data).

DHI was commissioned by RVO to conduct a metocean desk study while in parallel Tractebel conducted a wind resource assessment (WRA) for the Hollandse Kust (west) offshore wind farm zone (HKWWFZ). To ensure the alignment and the quality of the wind models implemented for the HKWWFZ, a joint comparison between the results provided by Tractebel and DHI was conducted. Tractebel and DHI communicated on a regular basis discussing and exchanging datasets for the preparation of this comparison.

Note that the alignment was carried out with data from the 9 and 12 months measurement campaigns only. Wind climate at the 6 nodes of the Hollandse Kust (west) offshore wind farm zone from the 24 months measurement campaign was then validated through direct comparison with wind climates from the 12 months measurement campaign.

Dataset

Two separate datasets were used in the two studies. The first dataset, produced by Tractebel, is based on Lidar measurements from the HKWWFZ buoys A, B and C, and mast measurements from the IJmuiden and OWEZ met masts that were long-term corrected using ERA5 reanalysis data, and extrapolated over the HKWWFZ using the Dutch Offshore Wind Atlas (DOWA) mesoscale model.

The second dataset, produced by DHI, is based on the CFSR reanalysis data (see Section 3.3 describing the wind fields in the HKW metocean desk study report). Both datasets are considered independent from each other as they are based on two different atmospheric models and serve two different purpose.

The Tractebel dataset is herein referred as H-KWBC+IJM+OWEZ+ERA5 when the 9-months dataset is implemented, and as HKWABC+ IJM+OWEZ+ERA5 for the 12-months dataset, while the naming CFSR is adopted for DHI's dataset.

The comparison of the mean wind speed was performed on the 100 m above mean sea level (mMSL) wind data at six (6) locations (herein referred as nodes) shown in Figure 57 for a period of 20 years between 01.11.1999 and 31.10.2019.

Please note that an update of the comparison has been carried out at the location HKW LiDAR after reception of the 12-months wind observations at HKWA, HKWB and HKWC. HKW LIDAR is therefore the geographical centre of the aggregated data acquired from the three measurement locations over the 12-month campaign.

The coordinates of the nodes are given in the table below. Main alignment items such as the metrics, agreed level of difference and details on the considered time period are summarised in Table 76.

TABLE 77: NAMING AND COORDINATES EPSG 25831 AND WGS84 OF THE SIX NODES USED IN THIS COMPARISON STUDY

Node name	Easting EPSG 25831	Northing EPSG 25831	Longitude WGS84	Latitude WGS84
HKW LiDAR	549250	5824678	3.7266708	52.5699251
S30	540612	5830154	3.5998997	52.6198654
S2	548886	5840067	3.7235796	52.7082938
S22	558354	5851409	3.8657222	52.8093065
S23	559589	5849713	3.8837328	52.7939267
S24	556675	5834446	3.8378874	52.6570073

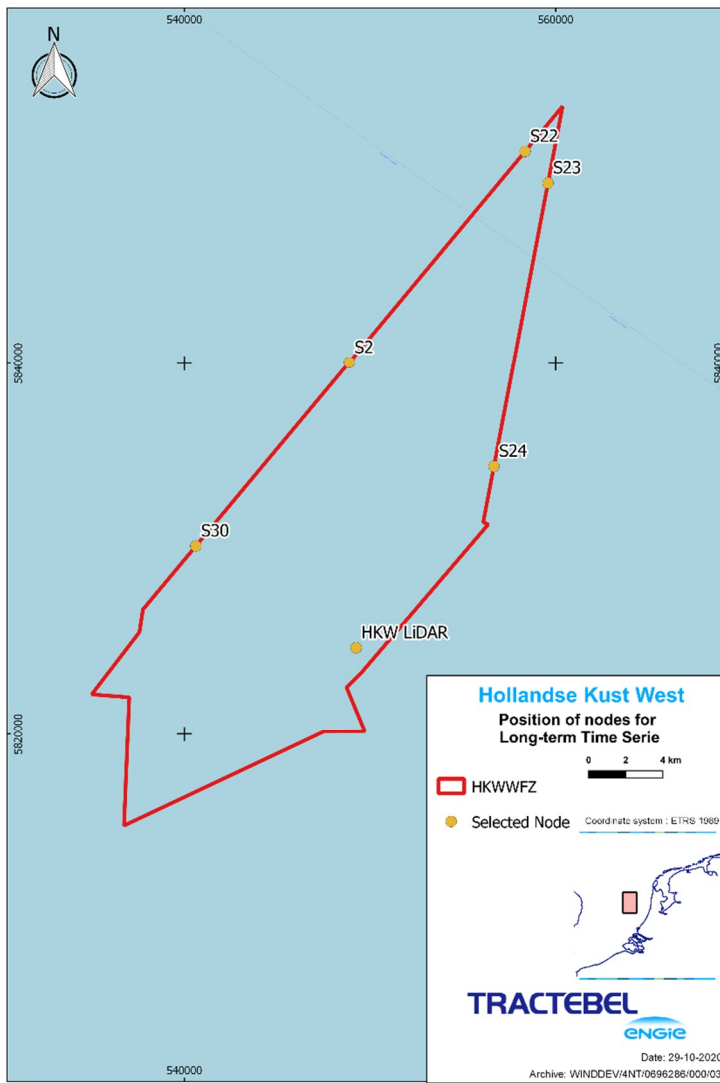


Figure 58: Location of the six nodes (yellow circles) selected by Tractebel for comparison with the DHI metocean desk study (source: Tractebel)

TABLE 78: ALIGNMENT TABLE USING 9- AND 12-MONTHS MEASUREMENTS AT HKW IN THE REFERENCE DATASET

Description	Value
Agreed metric	Mean wind speed
Agreed level	0.1 m/s
Reference dataset	Measurements from HKW Buoys B+C, IJmuiden and OWEZ masts long-term corrected using ERA-5
DHI dataset	CFSR corrected along the coasts
Length of reference time series	20 years for the 9-months dataset [1/11/1999-31/10/2019] 20 years for the 12-months dataset [1/11/1999-31/10/2019]
Length of DHI time series dataset	20 years [1/11/1999-31/10/2019]
Start/End time comparison	1/11/1999 to 31/10/2019 for the 9-months dataset (all six nodes) 1/11/1999 to 31/10/2019 for the 12-months dataset (only at the node HKW LiDAR)
Alignment height	100 m above Mean Sea Level
Time step	1 h

As described in the metocean desk study, CFSR tends to underestimate the wind speeds along the shoreline of the Hollandse Kust (west) Offshore Wind Farm zone (HKW) domain as a result of the coarse resolution (0.3° and 0.2°). DHI corrected the CFSR data directionally, using the measured data at OWEZ (the full measurement period from 01.07.2005 to 31.12.2010 was considered). In order to account for the influence of neighboured offshore wind farms, the OWEZ met mast data was filtered to keep only undisturbed periods (61). The wind speeds were corrected for 12 directions between 0° and 360° applying scaling coefficients obtained from the comparisons at the OWEZ met mast. Additionally, the shift of cells from offshore to nearshore applied during the HKN study that aimed avoiding sharp changes of wind speed due to land/sea mask effects is not affecting the CFSR cells over HKW as this OWF area is located more offshore. The 10 m CFSR wind fields were then extrapolated to 100 m MSL using the empirical wind profile described in metocean desk study report (Section 3.3.5). The values and figures presented in the current alignment note are based on discrete extractions within the CFSR original grid (0.3° for the period prior to 2011 and 0.2° after 2011). However, the wind data provided on the web-based database⁴ in Hollandse Kust (west) are interpolated values of CFSR onto the grid of the numerical wave model. The interpolation has led to slightly different numbers (within 0.1 m/s). The mean wind speed and bias values corresponding to the interpolated CFSR dataset are provided in Table 77 below as well. The difference is due to the fact that the interpolation is done between grid cells offshore and those closer to shore (east). The latter has on average lower wind speeds and thus result in slight differences between the centre of the grid cell which is located further offshore.

⁴ <https://www.metocean-on-demand.com/>

As described in the wind resource assessment study, Tractebel combined three sources of measurements in order to reduce uncertainties on the predicted wind climate over the HKWWFZ. These three main sources were selected among all available datasets in the vicinity of the HKWWFZ for their combined uncertainty to minimise the overall uncertainty on the wind climate. This resulted in the selection of the IJmuiden and OWEZ met mast measurements in addition to the Lidars measurements at the HKWWFZ. These three datasets were extrapolated to 100 m MSL (where needed) before being long-term corrected using a neural network approach and 20 years ERA5 reanalysis time series ranging from the 01.11.1999 to the 31.10.2019 at the time where the 9-months Lidars measurements were delivered. These time series have been reprocessed after delivery of the 12-months Lidars measurements at HKWWFZ though the same time range was used to enable to align with the metocean desk study (01.11.1999 to the 31.10.2019). The choice of MCP parameters (reanalysis dataset, long-term extrapolation method, long-term range) is further justified in this report. Long-term time series at the three reference locations were then extrapolated horizontally using the DOWA mesoscale model, which was selected among several other available wind flow models through an extensive comparison involving the most relevant measurements available in the vicinity of the HKWWFZ. This led to three long-term time series at each node location which were finally combined, using weights based on relative uncertainties of the three main sources of measurements, to yield a single long-term time-series at each node location.

Analysis

The figures presented below are generated by DHI and are shown in the form of scatter plots, where CFSR wind speeds are given on the x-axis and the Tractebels' time series of wind speed (based on HKWBC+IJM+OWEZ+ERA5 for the 9-months dataset and based on HKWABC+IJM+OWEZ+ERA5 for the 12-months dataset) on the y-axis. When not mentioned in the legend, the comparisons are based on the 9-months dataset. Wind roses are further presented. All statistics are based on hourly data.

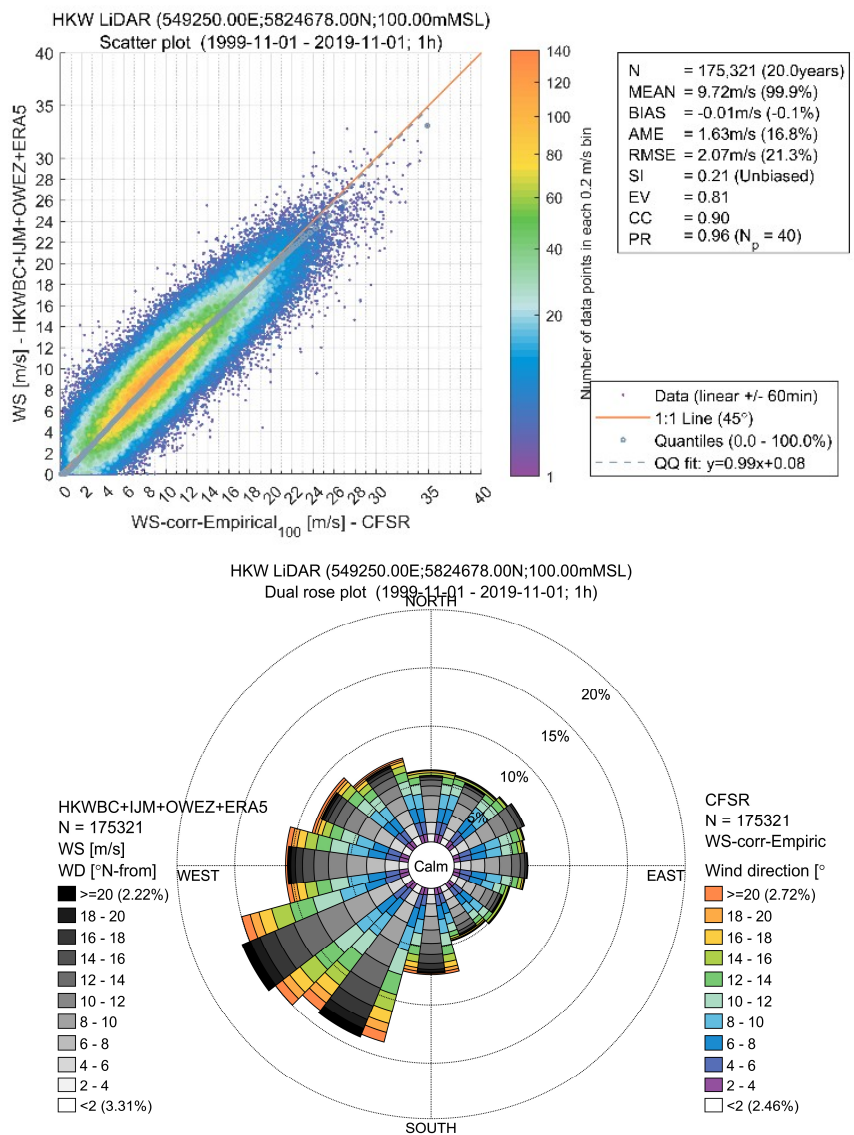


Figure 59: Comparison between CFSR and HKWBC+IJM+OWEZ+ERA5 hourly mean wind speeds at 100 m at HKW LiDAR: scatter plot (upper panel) and wind rose (bottom panel) [11.1999-11.2019]

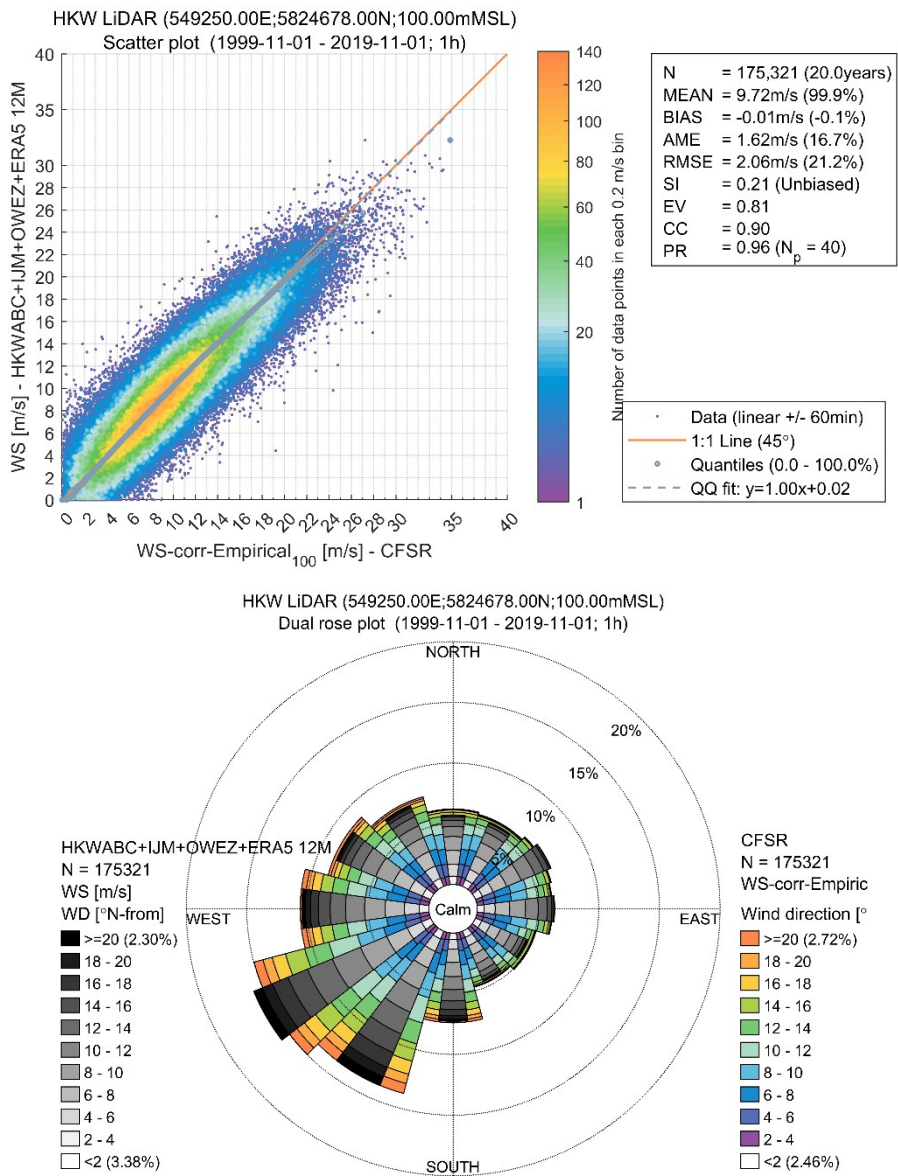


Figure 60: Comparison between CFSR and HKWABC+IJM+OWEZ+ERA5 based on **12-months** measurements hourly mean wind speeds at 100 m MSL at HKW LiDAR: scatter plot (left) and wind rose (right) [11.1999-11.2019]

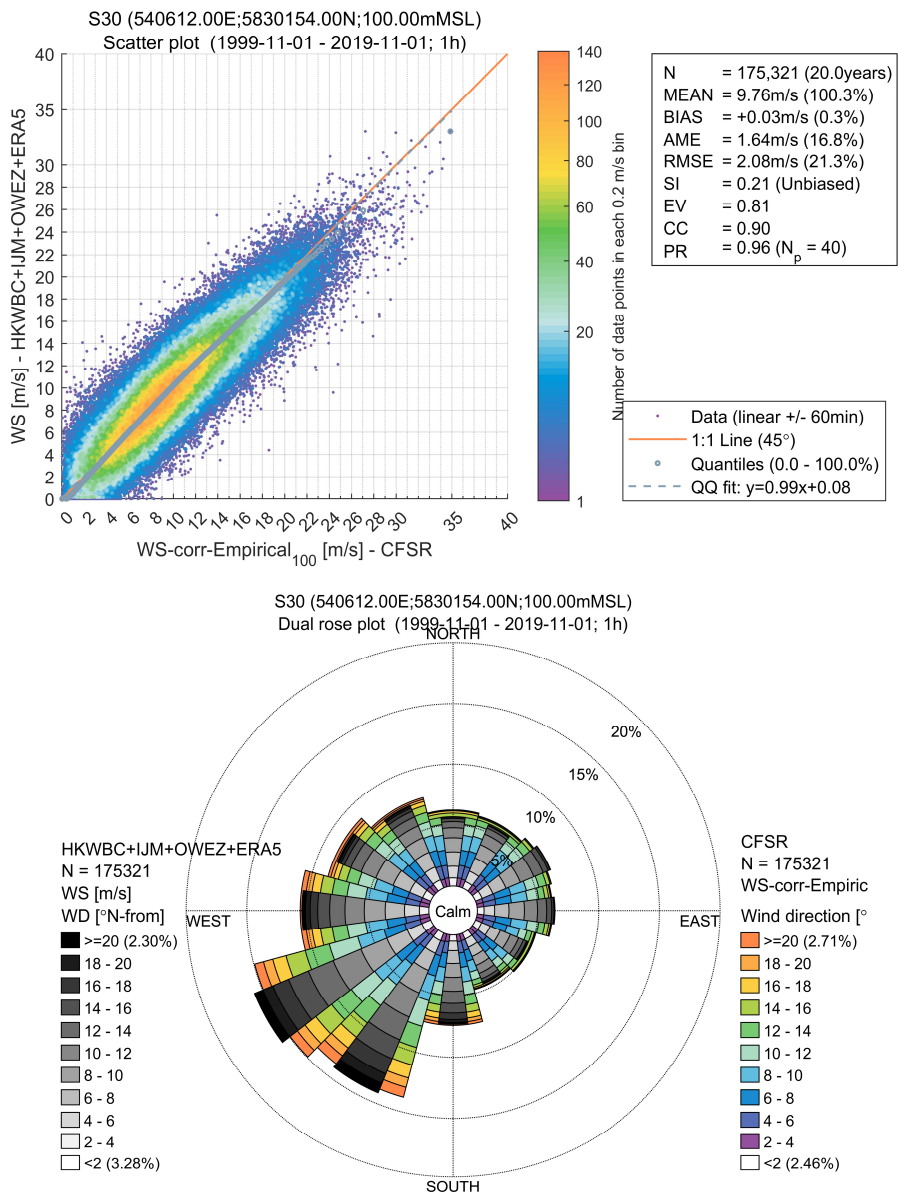


Figure 61: Comparison between CFSR and HKWBC+IJM+OWEZ+ERA5 hourly mean wind speeds at 100 m at S30: scatter plot (upper panel) and wind rose (bottom panel) [11.1999-11.2019]

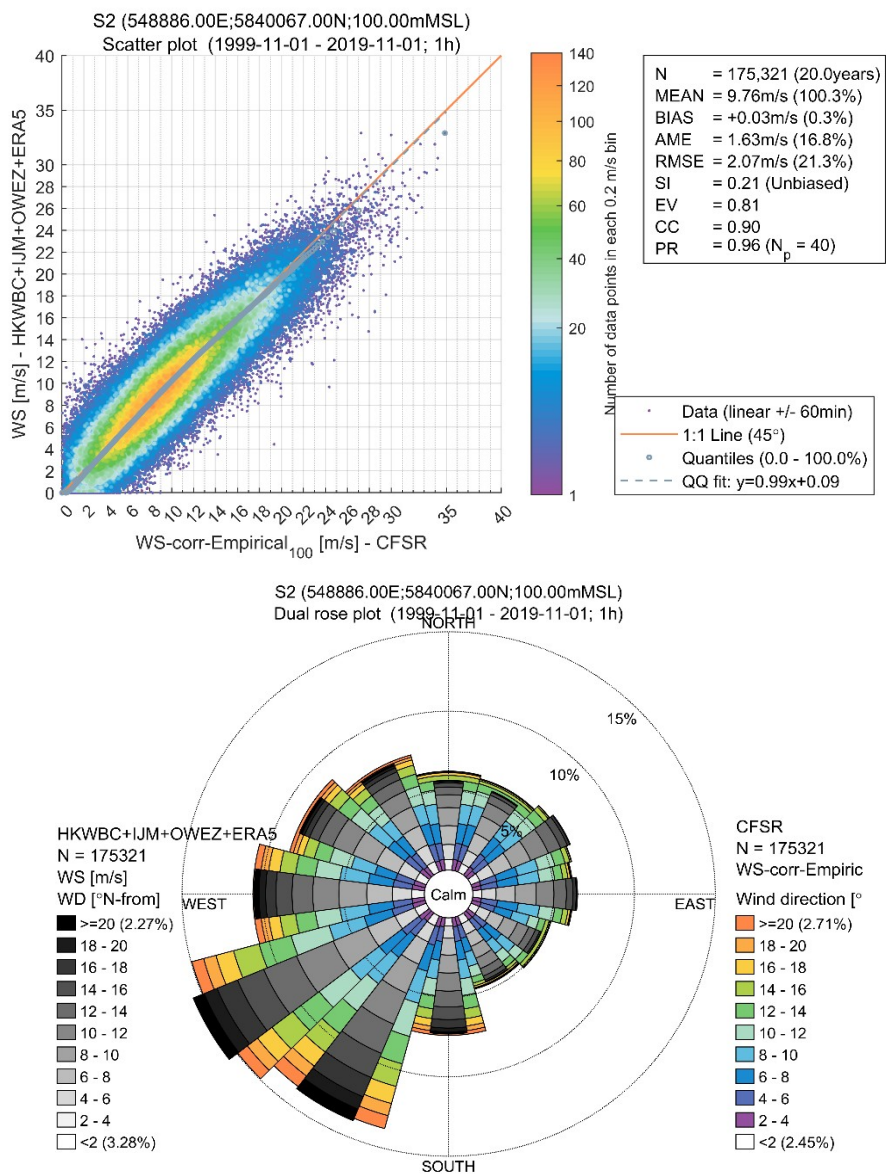


Figure 62: Comparison between CFSR and HKWBC+IJM+OWEZ+ERA5 hourly mean wind speeds at 100 m at S2: scatter plot (upper panel) and wind rose (bottom panel) [11.1999-11.2019]

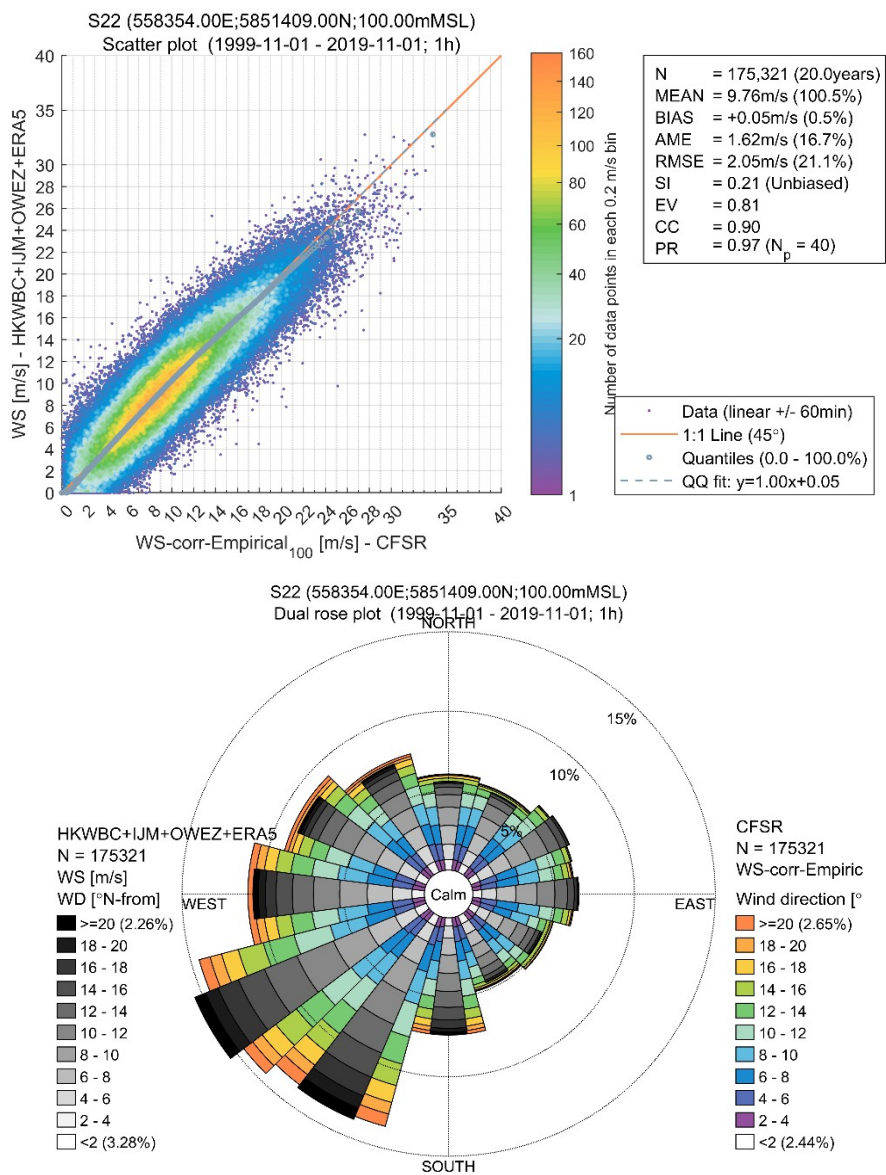


Figure 63: Comparison between CFSR and HKWBC+IJM+OWEZ+ERA5 hourly mean wind speeds at 100 m at S22: scatter plot (upper panel) and wind rose (bottom panel) [11.1999-11.2019]

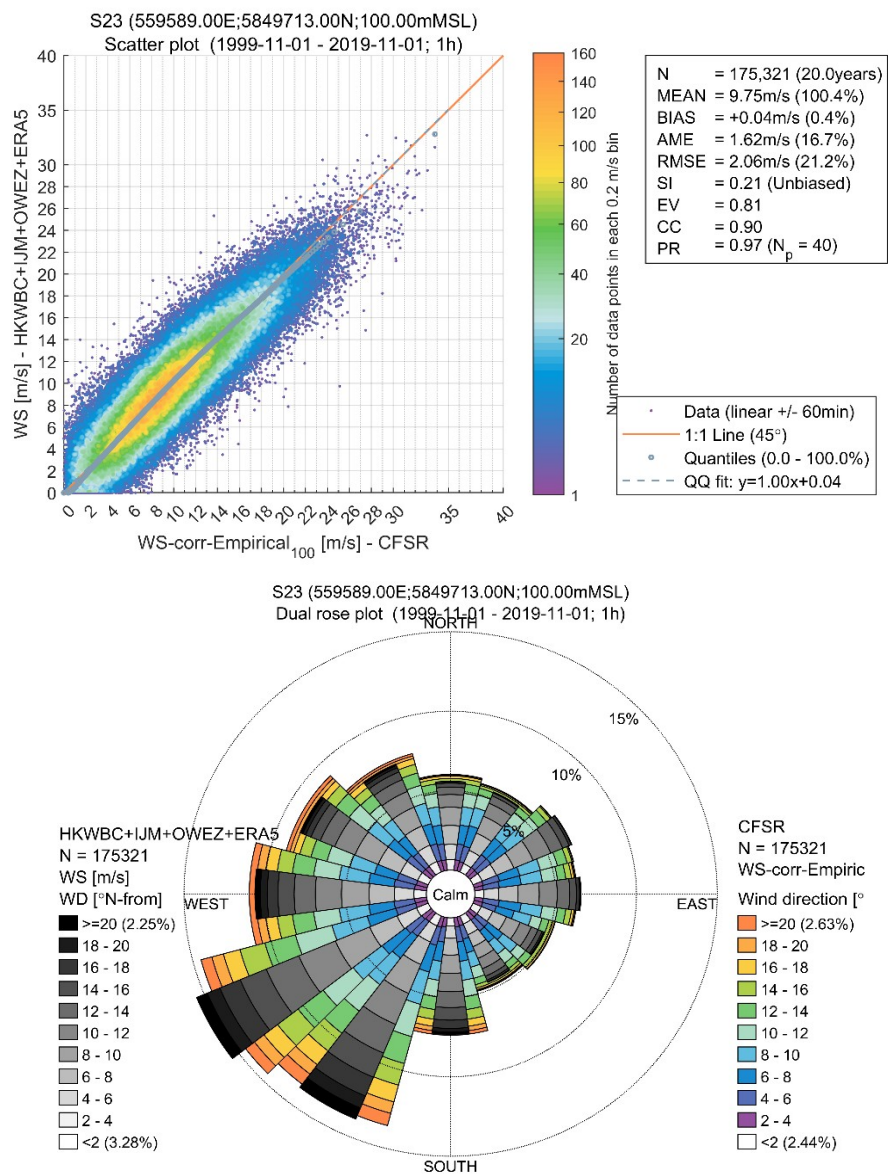


Figure 64: Comparison between CFSR and HKWBC+IJM+OWEZ+ERA5 hourly mean wind speeds at 100 m at S23: scatter plot (upper panel) and wind rose (bottom panel) [11.1999-11.2019]

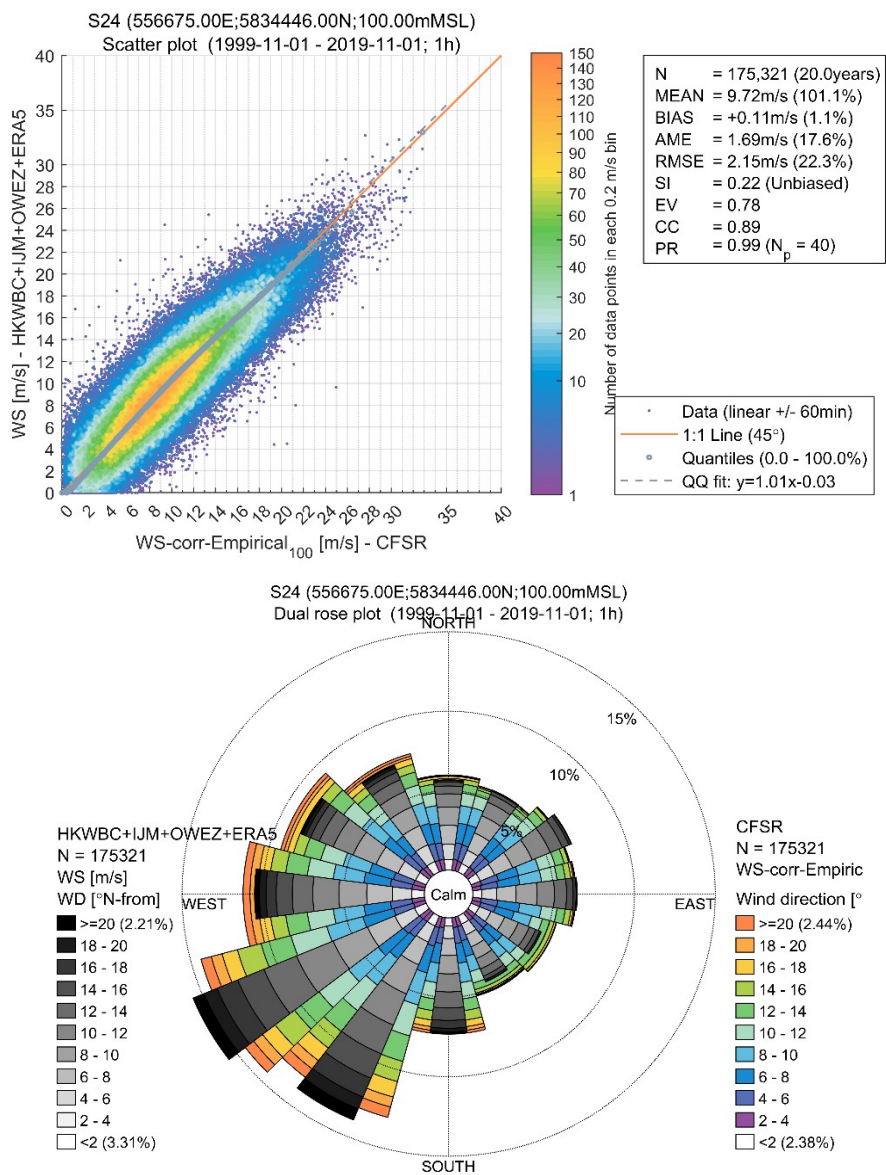


Figure 65: Comparison between CFSR and HKWBC+IJM+OWEZ+ERA5 hourly mean wind speeds at 100 m at S24: scatter plot (upper panel) and wind rose (bottom panel) [11.1999-11.2019]

The mean wind speeds and statistics of the two datasets are summarised in the table below.

TABLE 79: SUMMARY OF THE 20 YEAR MEAN WIND SPEEDS (ROUNDED TO TWO DECIMALS, PERIOD 01.11.1999 TO 31.10.2019) AT THE SIX NODES FOR THE 9-MONTHS DATASET AND AT THE NODE HKW LiDAR FOR THE 12-MONTHS DATASET FOR CFSR AND HKWBC (HKWABC)+IJM+OWEZ+ERA5 NUMBERS ARE GIVEN FOR BOTH, DISCRETE AND INTERPOLATED VALUES OF CFSR

Parameters Node	HKW LiDAR	S30	S2	S22	S23	S24
Height [mMSL]	100	100	100	100	100	100
Mean wind speed HKWBC+IJM+OWEZ+ERA5 [m/s] 9-months dataset	9.72	9.76	9.76	9.76	9.75	9.72
Mean wind speed HKWABC+IJM+OWEZ+ERA5 [m/s] 12-months dataset	9.73	-	-	-	-	-
Mean wind speed [m/s] CFSR – discrete values	9.73	9.73	9.73	9.73	9.71	9.61
Mean wind speed [m/s] CFSR – interpolated values	9.63	9.75	9.70	9.69	9.67	9.61
Bias [m/s] 9-months dataset CFSR – discrete values	-0.01	0.03	0.03	0.05	0.04	0.11
Bias [m/s] 12-months dataset CFSR – discrete values	0.01	-	-	-	-	-
Bias [m/s] 9-months dataset CFSR – interpolated values	0.11	0.02	0.06	0.07	0.08	0.11
Bias [m/s] 12-months dataset CFSR – interpolated values	0.10	-	-	-	-	-

Disclaimer

Please note that the numbers presented in the table above for CFSR are based on two extraction methods. The wind data used for the present alignment are discrete extracts from the CFSR original grid (0.3° for the period prior to 2011 and 0.2° after 2011) while the wind data available in the web-based database are interpolated values of the CFSR original grid onto the grid of the numerical wave model used in the Metocean Desk Study (around 300 m to 400 m resolution).

Conclusions

The comparison between the HKWBC+IJM+OWEZ+ERA5 and the CFSR mean wind speeds at 100 m shows that the wind climate at Hollandse Kust (west) wind farm zone from Tractebel's wind resource assessment and DHI's metocean desk study (discrete extractions from CFSR) are in good agreement. The mean wind speed of both studies is within 0.1 m/s of each other at 100 m above mean sea level. The update of the HKWBC+IJM+OWEZ+ERA5 based on 9 months to 12 months wind observations at the HKWB and HKWC did not increase the bias with the DHI dataset. The resulted mean wind speed at 100 m MSL using the updated reference dataset increased by 0.03 m/s for Tractebel's dataset and by 0.01 m/s for DHI's dataset as the comparison includes additional winter months. Based on the updated and longer reference dataset, following mean wind speed at 100 m MSL have been calculated:

Tractebel=9.75 m/s and **DHI=9.74 m/s** (against **Tractebel=9.72 m/s** and **DHI=9.73 m/s** for the previous version using 9-months wind observations) at the node representative of HKW, i.e. HKW LiDAR.

A mean wind speed of 9.63 m/s is obtained using the interpolated values of CFSR. Though the bias between Tractebel's and DHI's datasets increased slightly increased, a bias value of 0.11 m/s at HKW LiDAR is considered to be acceptable for alignment,

Both reports provide additional wind climate information beyond the average wind conditions. Each study is determined by its scope which is clearly defined by RVO.

The report by Tractebel describes the mean wind climate at 100 m MSL. This information is intended for wind farm modelling, yield assessment and business case calculation.

On the other side, the report by DHI described the normal and extreme wind conditions. This includes wind speed turbulence intensity, extreme wind speeds and wind shear, all of which are intended for wind farm design.

ANNEX K : WTG COORDINATES HKWWFZ

TABLE 80: LAYOUT 1 – 107 X 13 MW WIND TURBINES

107 x 13MW @ 138m hub height

Turbine	Easting [m]	Northing [m]	Turbine	Easting [m]	Northing [m]	Turbine	Easting [m]	Northing [m]
1	540 841	5 830 291	37	548 841	5 836	73	555 578	5 837 090
2	557 678	5 850 390	38	556 178	5 848	74	549 641	5 831 191
3	558 778	5 846 390	39	550 478	5 834	75	556 578	5 843 190
4	555 278	5 847 390	40	551 841	5 829	76	552 641	5 830 791
5	558 778	5 850 090	41	553 341	5 828	77	544 441	5 830 191
6	541 641	5 829 491	42	549 978	5 839	78	545 641	5 834 591
7	557 578	5 840 390	43	557 678	5 848	79	552 678	5 839 190
8	559 378	5 849 290	44	551 241	5 837	80	554 141	5 831 891
9	545 441	5 826 591	45	541 741	5 831	81	554 178	5 837 990
10	555 778	5 845 290	46	551 641	5 835	82	546 941	5 830 691
11	544 241	5 834 091	47	553 441	5 829	83	551 341	5 827 391
12	557 778	5 843 290	48	557 378	5 844	84	554 978	5 840 890
13	555 578	5 843 990	49	552 941	5 831	85	553 041	5 833 191
14	547 341	5 834 891	50	557 678	5 847	86	546 741	5 837 291
15	546 241	5 825 591	51	552 578	5 837	87	548 341	5 832 191
16	544 141	5 828 791	52	553 278	5 834	88	554 041	5 834 291
17	555 878	5 846 590	53	554 541	5 830	89	549 778	5 837 790
18	546 041	5 836 191	54	554 478	5 839	90	550 041	5 827 991
19	548 078	5 838 890	55	557 478	5 846	91	553 778	5 840 590
20	551 878	5 839 890	56	543 141	5 829	92	543 941	5 827 591
21	556 078	5 834 790	57	553 741	5 836	93	550 141	5 830 191
22	556 778	5 837 290	58	556 678	5 842	94	545 341	5 833 191
23	559 078	5 847 790	59	542 741	5 832	95	549 478	5 835 590
24	545 941	5 828 291	60	546 741	5 827	96	550 041	5 832 391
25	557 478	5 841 490	61	555 778	5 838	97	554 278	5 841 790
26	548 841	5 827 491	62	554 641	5 833	98	547 241	5 836 391
27	555 578	5 832 690	63	556 178	5 840	99	550 841	5 831 491
28	558 378	5 844 490	64	547 941	5 829	100	550 778	5 838 690
29	547 041	5 832 491	65	555 078	5 835	101	552 041	5 834 691
30	557 078	5 838 490	66	543 641	5 831	102	550 641	5 829 291
31	552 341	5 827 091	67	548 678	5 838	103	545 141	5 831 991
32	548 978	5 839 890	68	552 778	5 840	104	551 341	5 830 591
33	548 441	5 831 091	69	542 841	5 828	105	551 041	5 833 491
34	556 778	5 835 890	70	549 041	5 828	106	547 741	5 826 791
35	547 741	5 833 791	71	555 378	5 842	107	545 341	5 829 091
36	552 041	5 828 491	72	543 941	5 832			

TABLE 81: WIND TURBINE CHARACTERISTICS OF WT-TYPE 1

Nominal Power (MW)	Rotor Diameter (m)	Hub height (m)	Tip Height (m)
13.0	220	138.	248

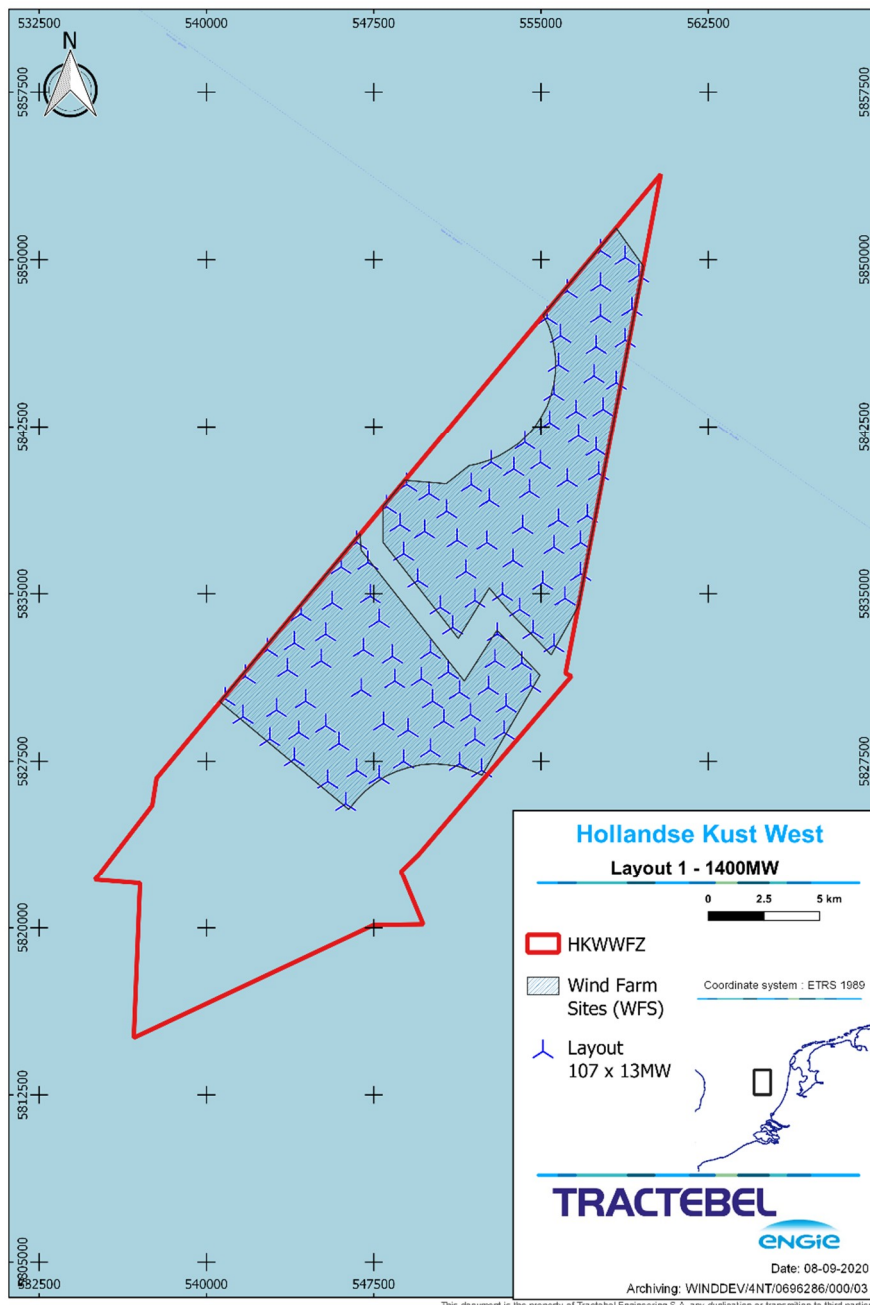


Figure 66: Illustration of the optimized layout using WT-type 1. The red polygon delimits the Hollandse Kust (west) wind farm site. Blue marks show turbine locations. Please note that the contours of the Wind Farm Sites within the HKWWFZ are preliminary only and no rights can be derived from it

TABLE 82: LAYOUT 2 – 140 X 10 MW WIND TURBINES

140 x 10 MW @ 125 m hub height

#	Easting [m]	Northing [m]	#	Easting [m]	Northing [m]	#	Easting [m]	Northing [m]	#	Easting [m]	Northing [m]
1	540 841	5 830 291	36	556 878	5 849 390	71	557 078	5 846 890	106	555 078	5 838 890
2	546 741	5 831 491	37	549 978	5 839 890	72	554 541	5 833 791	107	555 578	5 840 790
3	558 078	5 850 890	38	552 041	5 828 291	73	543 641	5 833 491	108	549 441	5 833 591
4	555 278	5 847 490	39	557 978	5 847 990	74	554 478	5 839 490	109	550 341	5 832 391
5	558 378	5 849 790	40	550 041	5 835 891	75	544 841	5 827 191	110	556 078	5 839 890
6	559 378	5 849 490	41	550 478	5 838 390	76	556 778	5 842 090	111	555 078	5 835 390
7	548 341	5 837 491	42	542 641	5 828 691	77	544 541	5 832 291	112	555 778	5 841 890
8	548 878	5 839 890	43	553 141	5 828 491	78	556 078	5 848 490	113	550 941	5 830 191
9	541 941	5 829 191	44	550 741	5 833 891	79	546 441	5 826 791	114	550 478	5 834 990
10	558 978	5 847 690	45	551 078	5 839 590	80	553 941	5 831 491	115	544 441	5 834 391
11	545 441	5 826 591	46	549 741	5 829 791	81	556 678	5 839 090	116	552 141	5 830 591
12	557 278	5 840 190	47	542 241	5 830 291	82	545 941	5 836 291	117	546 341	5 835 491
13	555 778	5 845 490	48	553 041	5 829 491	83	544 141	5 829 091	118	554 578	5 836 990
14	557 878	5 843 290	49	551 778	5 840 590	84	556 578	5 840 990	119	544 841	5 828 591
15	555 978	5 835 290	50	557 678	5 846 290	85	547 141	5 830 591	120	550 878	5 837 190
16	555 678	5 844 290	51	552 278	5 836 290	86	550 341	5 827 891	121	547 341	5 826 491
17	547 141	5 834 991	52	543 341	5 828 091	87	555 978	5 836 390	122	551 278	5 833 190
18	542 841	5 832 591	53	552 441	5 831 791	88	556 778	5 845 490	123	554 378	5 841 590
19	548 441	5 830 191	54	552 378	5 838 890	89	545 541	5 834 591	124	554 478	5 835 990
20	545 141	5 835 391	55	556 478	5 847 590	90	546 441	5 827 791	125	544 941	5 830 091
21	558 378	5 844 790	56	553 841	5 830 391	91	549 241	5 831 091	126	545 941	5 833 791
22	549 178	5 838 790	57	552 878	5 837 690	92	553 378	5 840 190	127	552 841	5 832 891
23	549 241	5 827 391	58	557 578	5 848 790	93	550 141	5 828 891	128	547 141	5 836 391
24	556 578	5 837 390	59	542 541	5 831 391	94	555 378	5 842 690	129	552 378	5 839 990
25	557 778	5 841 290	60	552 978	5 840 990	95	555 678	5 846 590	130	545 641	5 832 591
26	555 478	5 832 590	61	544 041	5 827 491	96	555 578	5 837 190	131	554 178	5 837 890
27	558 778	5 845 990	62	546 441	5 825 591	97	546 741	5 837 191	132	546 741	5 829 091
28	556 278	5 834 190	63	553 441	5 835 691	98	550 441	5 831 391	133	554 578	5 840 590
29	547 741	5 833 091	64	556 878	5 843 090	99	556 378	5 843 790	134	547 441	5 827 891
30	556 978	5 836 590	65	557 278	5 844 690	100	553 478	5 832 190	135	551 841	5 834 291
31	549 678	5 836 990	66	554 741	5 831 191	101	544 841	5 831 291	136	548 241	5 827 291
32	557 878	5 842 290	67	543 341	5 830 791	102	551 241	5 827 391	137	543 541	5 832 091
33	552 341	5 827 091	68	554 041	5 834 791	103	547 641	5 834 191	138	551 478	5 835 190
34	557 278	5 838 490	69	555 678	5 838 290	104	548 078	5 838 790	139	548 641	5 836 591
35	549 041	5 828 291	70	543 641	5 829 791	105	551 841	5 829 191	140	553 341	5 836 691

TABLE 83: WIND TURBINE CHARACTERISTICS OF WT-TYPE 2

Nominal Power (MW)	Rotor Diameter (m)	Hub height (m)	Tip Height (m)
10	200	125	225

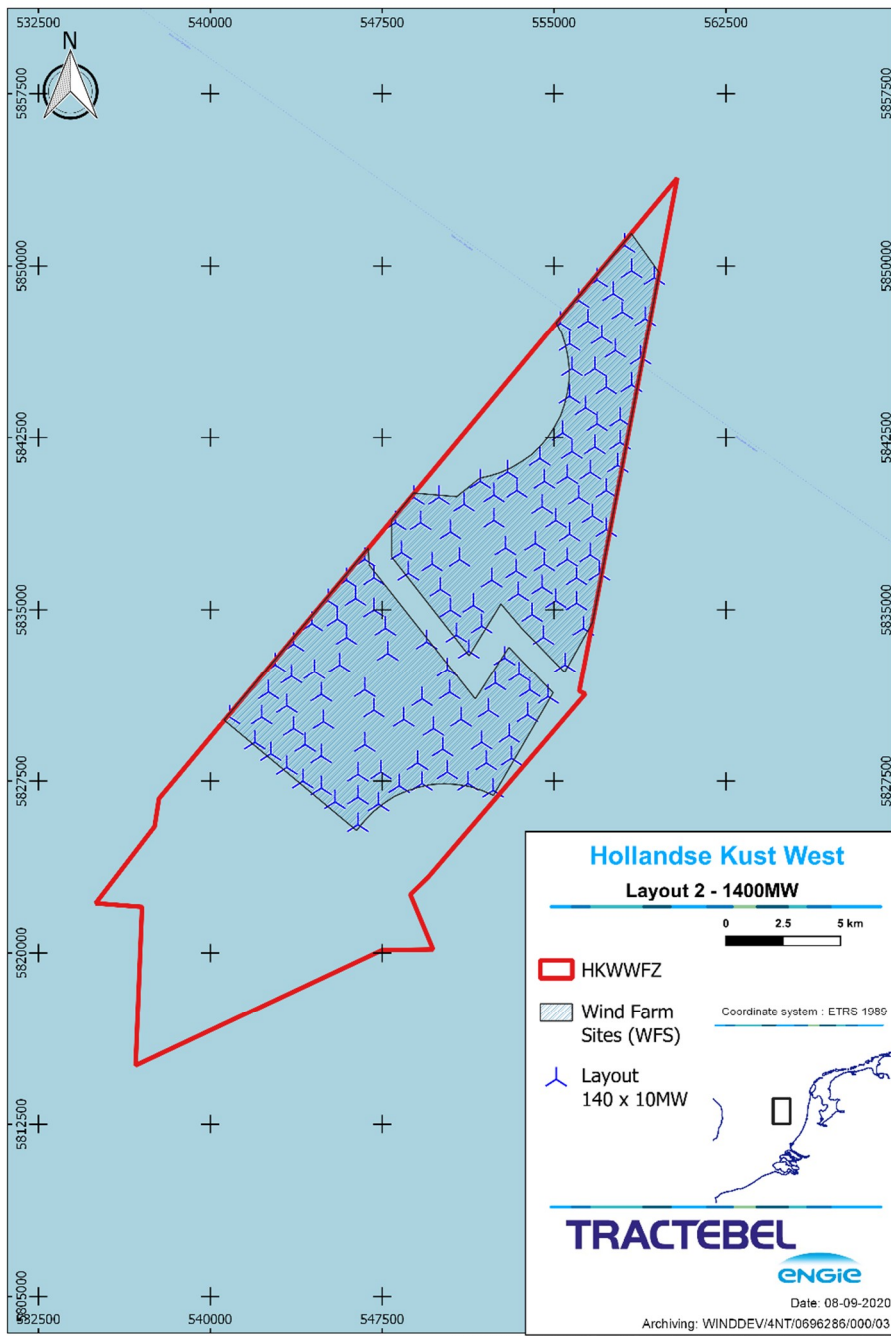


Figure 67: Illustration of the optimized layout using WT-type 2. The red polygon delimits the Hollandse Kust (west) wind farm site. Blue marks show turbine locations. Please note that the contours of the Wind Farm Sites within the HKWWFZ are preliminary only and no rights can be derived from it

TABLE 84: INDICATIVE WIND TURBINE POWER CURVE AND CT CURVE OF WT-TYPE 1 AND WT-TYPE 2

WT Type	WT Type-1		WT Type-2			
	Air density [kg/m ³]		Power [kW]	Ct	Power [kW]	Ct
				1.225		
Wind speed at hub height [m/s]	Power [kW]	Ct				
4	450	0.90	460		0.9	
5	1 180	0.86	1 000		0.86	
6	2 100	0.80	1 800		0.82	
7	3 490	0.82	2 910		0.8	
8	5 200	0.83	4 450		0.78	
9	7 450	0.81	6 350		0.77	
10	9 900	0.74	8 410		0.72	
11	12 200	0.70	9 800		0.52	
12	13 000	0.55	9 990		0.4	
13	13 000	0.35	10 000		0.3	
14	13 000	0.30	10 000		0.25	
15	13 000	0.25	10 000		0.2	
16	13 000	0.20	10 000		0.15	
17	13 000	0.15	10 000		0.12	
18	13 000	0.14	10 000		0.1	
19	13 000	0.11	10 000		0.1	
20	13 000	0.10	10 000		0.09	
21	13 000	0.08	10 000		0.07	
22	13 000	0.08	10 000		0.06	
23	13 000	0.06	10 000		0.06	
24	13 000	0.05	9 990		0.05	
25	13 000	0.05	9 450		0.04	
26	13 000	0.05	7 540		0.03	
27	13 000	0.05	5 800		0.03	
28	13 000	0.04	4 350		0.03	

ANNEX L : THREE-LAYER WAKE MODELLING, BY KUL

This section was prepared by Luca Lanzilao and reviewed by Johan Meyers from KUL.

1. Introduction

The goal of this report is to assess the power loss that the Hollandse Kust (west) (HKW) wind farm experiences due to neighbouring farms located in the North Sea. Two different HKW farm layouts are considered. Atmospheric and wind turbine data are provided by Tractebel (ENGIE).

The document is outlined as follows. Section 2 introduces the approach used for modelling farm–farm interactions. Next, Section 3 reports flow-field examples and results of related wind resource assessment (WRA). Finally, conclusions are drawn in Section 4.

2. Methodology

A mesoscale perturbation model is used for performing a WRA for the HKW wind farm. This model divides the vertical structure of the atmosphere into three layers – (thus, the name three-layer model (TLM)). The atmospheric boundary layer (ABL) is divided into two regions: the wind-farm layer which simulates the lowest region of the atmosphere, where the wind turbine forces are felt directly, and an upper layer which is only indirectly affected by the wind farm through vertical turbulent transport of momentum. The third layer accounts for the free atmosphere aloft the ABL. For further details about the TLM see Allaerts and Meyers (2019).

The Gaussian wake model (GWM) (Niayifar and Porté-Agel, 2016), which is an analytical wake merging model, is used to account for turbine wake interactions. The inputs of this model are the turbine location, turbine rotor diameter, turbine hub height and the thrust curve. The turbine data are provided by Tractebel (ENGIE). The GWM accounts for turbine wake interactions but underpredicts farm–farm interactions (i.e, when the distance between turbines is greater than several kilometres). Thus, a two-way coupling between the TLM and the wake model is established (see Allaerts and Meyers (2019)), connecting local turbine inflow velocities to global height average TLM velocities. The resulting model (GWM+TLM) accounts for turbine–turbine interactions, wind-farm wakes and gravity-wave effects. The two different HKW farm layouts and the neighbouring farms are shown in Figure 68.

Vertical profiles of wind speed and virtual potential temperature (up to 5 km) together with friction velocity, boundary layer height, surface latent heat and air density are provided by Tractebel (ENGIE). The atmospheric data are given from 23.06.2001 to 23.06.2002, with hourly resolution. The TLM is a depth-averaged model, meaning that the wind speed vertical profiles are averaged over the height of the three layers. The fitting model proposed by Rampanelli and Zardi (2004) is used for evaluating the ABL height, the lapse rate in the free atmosphere and the strength and depth of the capping inversion. A virtual potential temperature profile is the only input of this model. A maximum capping inversion depth of 300 m is chosen similarly to Allaerts et al. (2018). Finally, vertical shear stress and eddy-viscosity profiles are derived using the parametrizations proposed by Nieuwstadt (1983). An example of vertical profiles and TLM fitting is illustrated in Figure 69.

The TLM equations are discretized using a Fourier-Galerkin spectral technique, hence periodic boundary conditions at the edges of the computational domain are used. The computational domain has dimension $1000 \times 1000 \text{ km}^2$ so that perturbations die out before being recycled. A grid resolution of 500 m is adopted, which corresponds to 4×10^6 degrees of freedom per layer. The TLM solution has been proved to be grid-independent (Allaerts and Meyers, 2019), hence no benefit would be provided by finer grids. A total of 35136 simulations are performed, that is one per hour of the year with 4 different configurations (layout 1 and 2 with and without neighbouring farms). Note that the TLM has been verified against LES results by Allaerts and Meyers (2019), but no formal validation against experimental data has been performed as of to date. Therefore, results should be interpreted with care, and are only indicative of expected trends rather than precise estimates of overall losses.

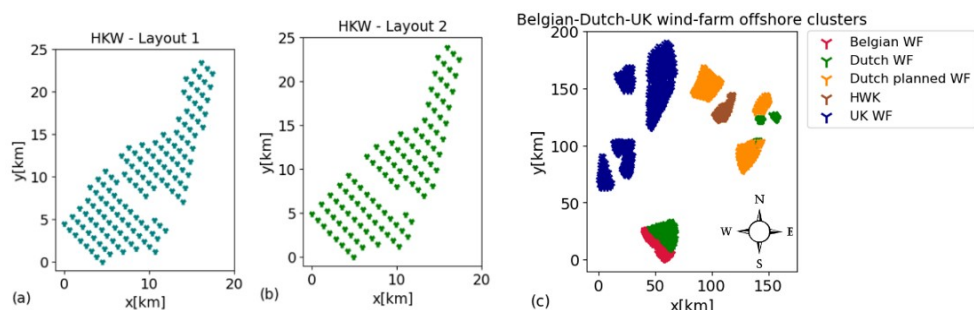


Figure 68: (a) HKW wind farm layout 1 (140 x 10 MW), (b) HKW wind farm layout 2 (107 x 13 MW) and (c) Belgian–Dutch–UK wind-farm offshore clusters

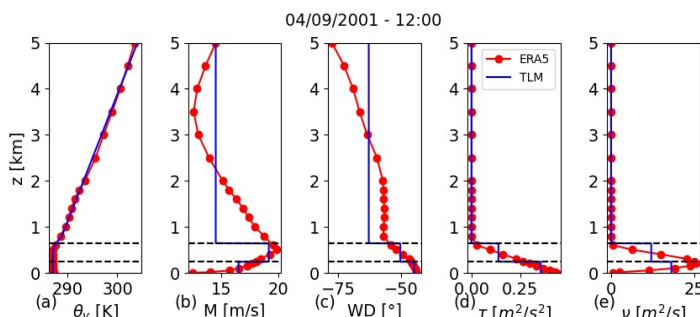


Figure 69: Vertical profiles of (a) virtual potential temperature, (b) velocity magnitude, (c) wind direction, (d) shear stress and (e) eddy viscosity. The blue profiles define the input parameters of the TLM. The horizontal dashed black lines denote the wind-farm layer and ABL height

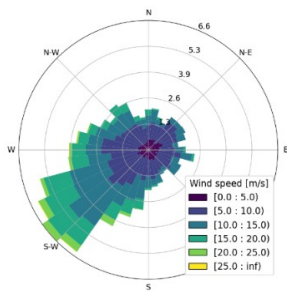


Figure 70: Wind rose plot of the height-averaged winds in the wind-farm layer

3. Results

Figure 70 illustrates the distribution of the height-averaged wind speed and direction in the wind-farm layer. Westerly and Southwesterly winds are dominant, with a probability of 32 %. Moreover, the height-averaged wind speed is less than 13.1 m/s (which is the average rated wind speed) in about 77 % of the year and rarely exceeds 20 m/s. Finally, the atmosphere is stable in about 33 % of the year and unstable in the remaining hours.

Figure 71 displays a planform view of the relative velocity reduction in the wind-farm layer. Figure 68 (a-c) show the velocity fields for different wind directions under a stable atmosphere with strong capping inversion (6.8 K) and with an upstream velocity of 10.8 m/s. Gravity waves are triggered, which modifies the velocity several kilometres upstream of the farms and further propagate downstream. A weaker capping inversion (3 K) is used in Figure 68 (d-f). The velocity oscillations in the farms' wake are reduced due to weaker buoyant forces. Also, the blockage in the farms' induction region is reduced since gravity waves cannot travel upstream in these conditions (Allaerts and Meyers, 2019). In both configurations, wind-farm wakes propagate several kilometres downwind. Moreover, high-speed channels develop between farms. Finally, Figure 68 .(g-i) illustrate velocity fields in neutral atmospheric conditions (hence, no gravity-wave effects) under different upstream velocity. An upstream velocity of 9.8 m/s is used in Figure 68 (g). The high turbine set-point values induce large flow perturbations and velocity reductions above 20 % are observed over the farms' area. For higher upstream velocity (12.8 and 18 m/s) the turbines become increasingly transparent to the flow (low set-point values) and both relative velocity reductions and wake lengths decrease (see Figure 68 (h,i)). Depending on the wind direction, the HKW farm could be located in the wakes of upstream farms or in high-speed channels. Hence, neighbouring farms could induce both power loss and power gain.

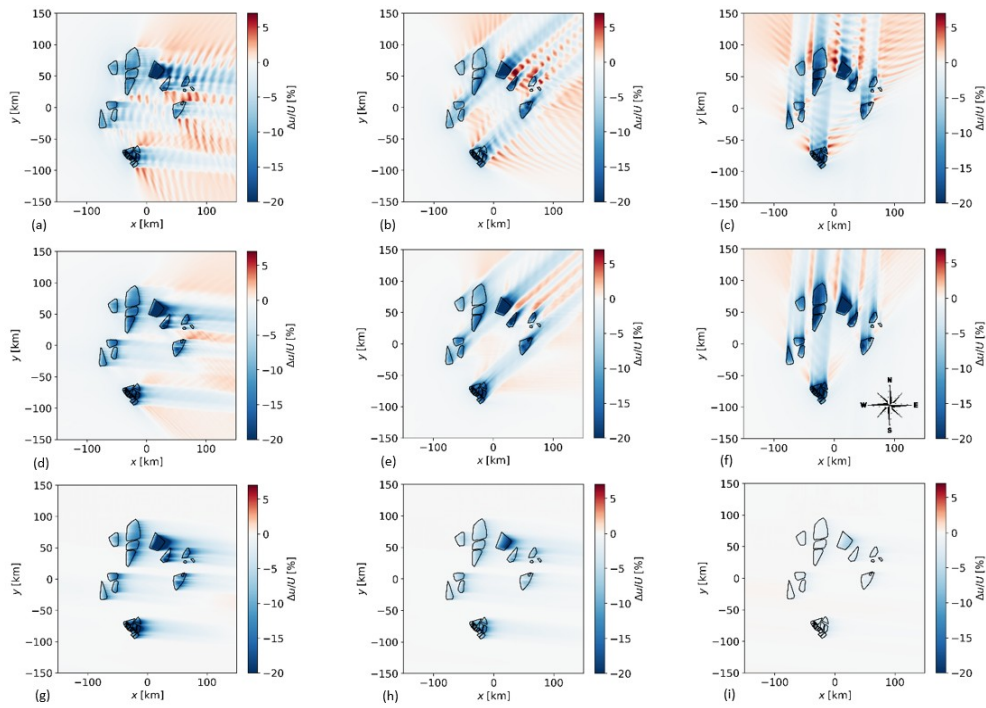


Figure 71: Planform view of the relative velocity reduction in the wind-farm layer. Stable atmosphere with capping inversion strength of 6.8 K (a-c) and 3 K (d-f) for different wind directions with upstream velocity of 10.8 m/s. Neutral atmosphere (g-i) with upstream velocity of 9.8, 12.8 and 18 m/s (from left to right)

Thus, two different simulations are performed under identical yearly atmospheric distributions. The computational domain of the first simulation contains the HKW farm only while the second one considers the whole Belgian–Dutch–UK wind-farm offshore clusters (see Figure 68c). The HKW farm power loss is evaluated as

$$\text{Power loss} = \frac{P^{\text{wt}} - P^{\text{w}}}{P_{\text{rated}}}$$

where P^{w} and P^{wt} denote the power extracted by the HKW farm with and without neighbouring farms, respectively. P_{rated} indicates the HKW farm rated power. Hence, we set P_{rated} to 1.4 GW for layout 1 and to 1.391 GW for layout 2. Note that a negative power loss corresponds to a power gain.

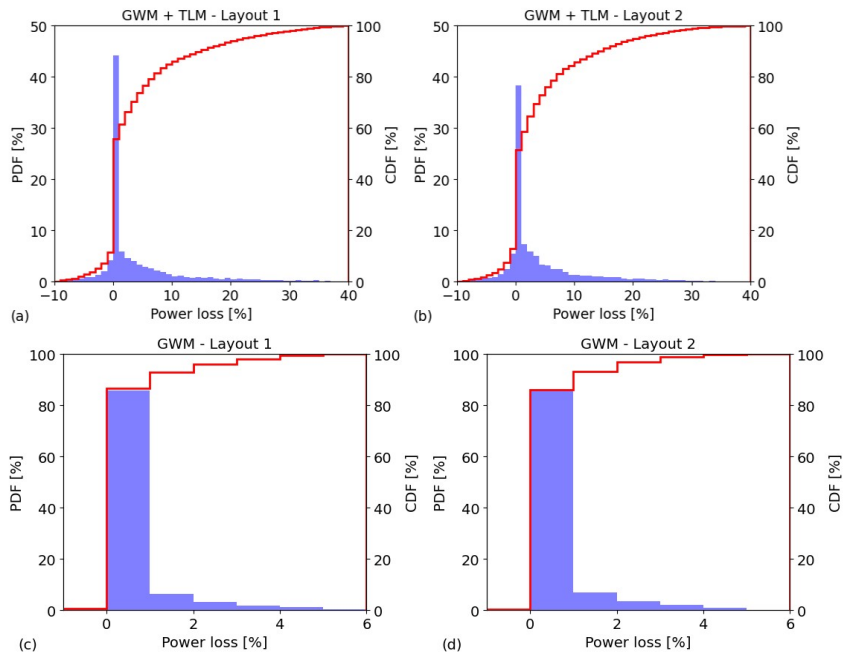


Figure 72: Probability density function (PDF) and cumulative density function (CDF) of the HKW farm power loss computed with the GWM+TLM (a,b) and with the GWM (c,d).

Figure 72 (a,b) illustrates the probability density function (PDF) and cumulative density function (CDF) of the power loss computed with the GWM+TLM for the HKW farm with layout 1 and 2. Figure 72 (a) shows that the power loss is less than 1 % in about 44 % of the cases and it exceeds the 20 % only in about 10 % of the year. A similar trend is observed in Figure 72 (b). However, higher PDF values are found for power losses in the range of 1 to 10 %. Both configurations experience a power gain in about 10 % of the cases, indicating that the wind is accelerating in front of the farm. This is due to the high-speed channels which develop around and between farms. The HKW farm is located in these regions when the wind blows toward the North (see Figure 71 (f)) and the Southwest (see below). Integrated over the year, the annual energy production (AEP) of the HKW farm computed with the GWM+TLM is 4.03 and 3.92 % lower due to wake and gravity-wave effects induced by neighbouring farms for the layout 1 and 2, respectively. The higher annual energy loss observed with layout 1 may be due to the higher gradient that the 10 MW power curve has in region 2 compared with the 13 MW (see Figure 73). The power loss distribution computed with the GWM is displayed in Figure 72 (c,d). As mentioned above, the GWM performs poorly in accounting for farm–farm interactions and it does not consider gravity-wave effects. Consequently, the power loss is considerably lower compared with Figure 72 (a,b). In fact, the predicted power loss is less than 1 % in about 83 % of the cases and it rarely exceeds 2 % for both HKW farm configurations. Moreover, very limited power gains are witnessed. Integrated over the year, the annual power loss is 0.45 and 0.44 % for layout 1 and 2, respectively. The results are summarised in .

TABLE 85: ANNUAL POWER LOSS CAUSED BY NEIGHBOURING FARMS

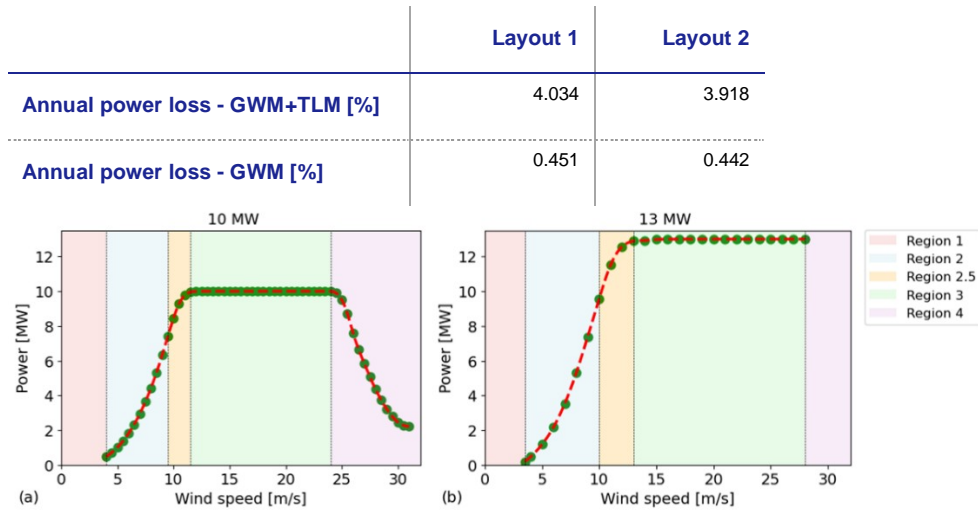


Figure 73: Power curve of the (a) 10 MW and (b) 13 MW wind turbines. The background colours mark the different operating regimes.

Figure 73 illustrates the power curve of the 10 MW and 13 MW turbines. These turbines are used in the HKW farm layout 1 and 2, respectively. The cut-in wind speed is similar for both turbines. However, the 10 MW has a rated wind speed of 11.5 m/s and operates in nominal regime up to a speed of 24 m/s, after which the power drops. The cut-out wind speed is 31 m/s. On the other hand, the rated and cut-out wind speed of the 13 MW turbine used in the current report, are 13 and 28 m/s, respectively. Moreover, the power curve does not decrease gradually in region 4. These differences are relevant in comparing the power loss as a function of wind direction and wind speed for the two different HKW farm layouts (see Figure 75).

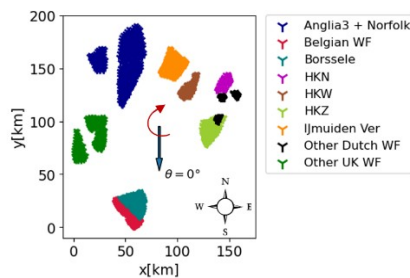


Figure 74: Belgian–Dutch–UK wind-farm offshore clusters. The South direction corresponds to 0° and positive wind directions are found clockwise

The Belgian–Dutch–UK wind-farm offshore clusters are displayed in Figure 74. Wind blowing towards the South in the wind-farm layer is assumed to have wind direction of 0° , while positive wind directions are found clockwise. Following this convention, Figure 75 illustrates the power loss computed with the GWM+TLM and with the GWM only, as a function of wind speed and wind direction. The power loss computed with the GWM+TLM as a function of the wind direction has a similar pattern for both HKW farm configurations (see Figure 75 (a,b)). Power losses of about 20 % are observed for wind directions between 90 and 150° since the HKW farm operates in the wake of the HKN and HKZ farm. High power losses are also seen for wind directions between 230 and 300° . In fact, the HKW farm is strongly influenced by the Anglia 3, Norfolk and IJmuiden Ver farms, which are located upstream. Although the HKW farm is operating in the wake of IJmuiden Ver for wind directions between 300 and 360° , power losses of only 5-10 % are observed. As mentioned above, the HKW farm experiences power gains for wind directions between 170 and 190° . The observed power gains are due to flow speed-up, which takes place around the HKZ farm as shown in Figure 71 (f). Moreover, power gains are also witnessed for wind directions between 20 and 60° , since the HKW farm is located in a high-speed channel which develops between IJmuiden Ver and HKN. The power loss computed with the GWM+TLM as a function of the wind speed has a slightly different pattern for HKW farm layout 1 and 2 due to the different power curve of the turbines used in the two configurations. In both cases, power losses are persistent in region 2 and 2.5 of the power curve, that is between the cut-in and rated wind speed. Farm wakes and induced gravity waves do not affect power production if the velocity is above the rated wind speed, since turbines operate in the nominal regime. However, Figure 75 (a) shows power gains for wind speed higher than 24 m/s. This is due to the power drop observed in region 4 of the 10 MW power curve (see Figure 73 (a)). Indeed, turbine–turbine and farm–farm interactions reduce the turbine inflow velocity, allowing for waked turbines to operated in region 3 instead of region 4, therefore increasing the HKW farm power output.

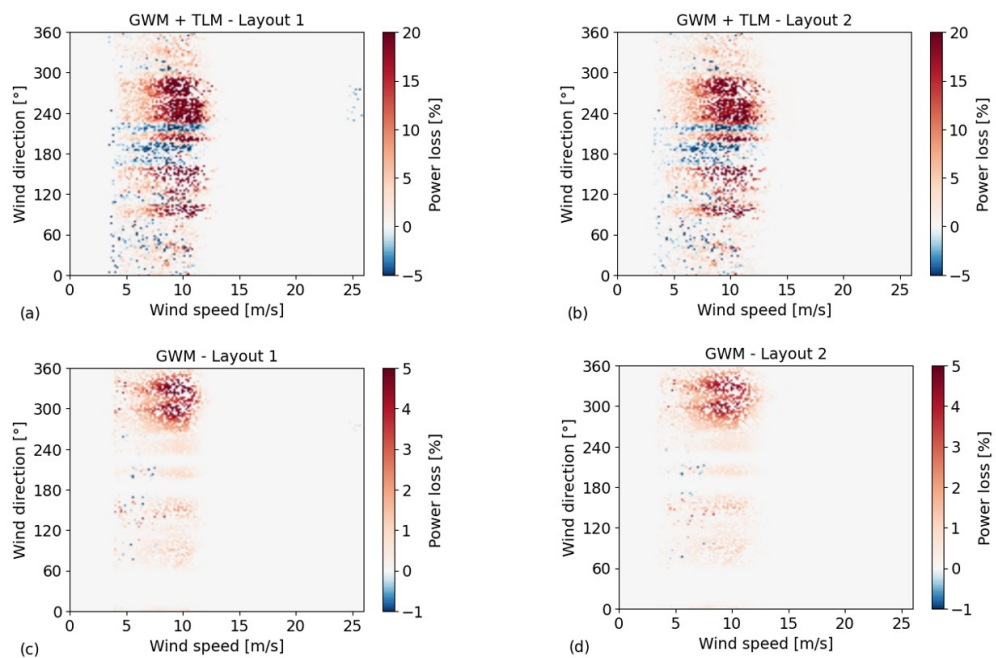


Figure 75: HKW farm power loss computed with the GWM+TLM (a,b) and with the GWM (c,d) as a function of wind speed and wind direction in the wind-farm layer. The South direction corresponds to 0° and positive wind directions are found clockwise

Figure 75 (c,d) illustrates the power loss computed with the GWM only as a function of wind speed and wind direction. As mentioned above, the GWM does not account for gravity-wave effects and underpredicts farm–farm interactions. Consequently, lower power losses are observed compared with Figure 75 (a,b). For wind directions between 0 and 260° , all HKW neighbouring farms are several kilometres away, hence power losses are below 1 %. Only for wind directions between 270 and 360° the power loss increases, due to the IJmuiden Ver wake, but remains below 3-4 %.

4. Conclusions

A WRA has been performed over the HKW wind farm zone for two different farm layouts. Atmospheric and wind turbine data were provided by Tractebel (ENGIE). The GWM coupled with the TLM was used for performing the AEP study over the year 2001–2002. The annual energy loss due to wake and gravity-wave effects induced by neighbouring farms is 4.03 and 3.92 % for layout 1 and 2, respectively. High power losses for both configurations were observed for wind directions between 90 and 150° and between 230 and 300° . Power gains due to high-speed channels which develop between farms, were also observed. Moreover, all power losses were located in region 2 and 2.5 of the respective wind turbine types while power gains were also observed in region 4. Results provided by the GWM only, were also discussed. However, the GWM does not account for gravity-wave effects and underpredicts farm–farm interactions, hence lower (and underestimated) power losses were witnessed.

5. References

- Allaerts, D. and Meyers, J. (2019), Sensitivity and feedback of wind-farm induced gravity waves, *J. Fluid Mech.*, 862, 990–1028.
- Allaerts, D., Vanden Broucke, S., Van Lipzig, N., and Meyers, J. (2018), Annual impact of wind-farm gravity waves on the Belgian-Dutch offshore wind-farm cluster, *J. Phys.: Conf. Ser.*, 1037, 072 006.
- Niayifar, A. and Porté-Agel, F. (2016), Analytical modeling of wind farms: A new approach for power prediction, *Energies*, 9, 741.
- Nieuwstadt, F. (1983), On the solution of the stationary, baroclinic Ekman-layer equations with a finite boundary-layer height, *Boundary-Layer Meteorol.*, 26, 377–390.
- Rampanelli, G. and Zardi D. (2004). A Method to Determine the Capping Inversion of the Convective Boundary Layer. *Journal of Applied Meteorology* 43, 925–933.



The creative commons license terms 4.0 CC BY apply to this material.
Please take notice of the general terms "Creative Commons Attribution 4.0 International public License" before starting to use the license. These terms can be accessed by clicking on this link <https://creativecommons.org/licenses/>

This investigation was carried out by Tractebel Engie, commissioned by RVO, an agency of the Ministry of Economic Affairs and Climate Policy.

Whilst a great deal of care has been taken in compiling the contents of this investigation, RVO can not be held liable for any damages resulting from any inaccuracies and/or outdated information.

The information in this document is valid at the time of publishing (see month/year). Updates will be published on the website <https://offshorewind.rvo.nl/> at the relevant Wind Farm Site, General Information, submap Revision Log and Q & A. In the Revision Log is indicated which versions are the latest and what the changes are in relation to previous versions. The documents can be found at the relevant sites, indicated in the List of all reports and deliverables.

Contacts

Netherlands Enterprise Agency (RVO)
Croeselaan 15 | 3521 BJ | Utrecht
P.O. Box 8242 | 3503 RE | Utrecht
www.rvo.nl / <https://english.rvo.nl>